OPERATIVE DENTISTRY

Nov/Dec 2018
Volume 43
Number 6
563–676

Academy of Operative Dentistry • American Academy of Gold Foil Operators • Academy of R.V. Tucker Study Clubs

OPERATIVE DENTISTRY

Volume 43 / Number 6
November/December 2018

www.jopdent.org

Aim and Scope

Operative Dentistry publishes articles that advance the practice of operative dentistry. The scope of the journal includes conservation and restoration of teeth; the scientific foundation of operative dental therapy; dental materials; dental education; and the social, political, and economic aspects of dental practice. Review papers, book reviews, letters and classified ads for faculty positions are also published.

Subscriptions: Fax 317-852-3162

Current pricing for individual, institutional, and dental student subscriptions (both USA and all other countries) can be found at our website: www.jopdent.org, or by contacting our subscription manager via email at editor@jopdent.org. Payment must be in USD and accompany orders. Online payment by credit card (American Express, Discover, Mastercard, and Visa) is available on our website.

Operative Dentistry (ISSN 0361-7734) is published bimonthly by Operative Dentistry, Inc, Indiana University School of Dentistry, Room S411, 1121 West Michigan Street, Indianapolis, IN 46202-5186. Periodicals postage paid at Indianapolis, IN and additional mailing offices. Postmaster: Send address changes to: Operative Dentistry, Indiana University School of Dentistry, Room S411, 1121 West Michigan Street, Indianapolis, IN 46202-5186.

Author Instructions

Please refer to author instructions at www.jopdent.org in the preparation of manuscript submissions and for journal policies.

Journal Policies

The Operative Dentistry Policy Manual which details journal policies, including late fees and claims, is available online at:

https://www.jopdent.com/journal/policies.pdf

Permissions

For permission to reproduce material from Operative Dentistry please apply to Operative Dentistry at the Editorial Office address or via email at editor@jopdent.org.

Online Access

Register for online access, manage subscriptions, save favorite articles and searches, get email alerts, and more at:

http://www.jopdentonline.org/action/registration

Editorial Board

Reviewer names available at: www.jopdent.com/journal/editorial_board.html

We thank all our reviewers for their time and dedication to Operative Dentistry.

On The Cover

"Winter on the Savannah" River Island, Evans, GA USA. Photo provided by Jacqueline Delash of Evans, Georgia. Photo taken with an Olympus OM-D E-M5 Mark II; Zuiko 14-42mm f/3.5-5.6 EZ © Operative Dentistry, Inc.

We welcome the submission of pictures for consideration for use on the cover of Operative Dentistry! All photographs should be submitted via the forms at:

https://www.jopdent.com/journal/journal.html

Editorial Office

The views expressed in Operative Dentistry do not necessarily represent those of the academies or the editors.

Operative Dentistry
Indiana University School of Dentistry, Room S411
1121 West Michigan Street, Indianapolis, IN 46202-5186
Phone 317-350-4371, Fax: 317-852-3162
http://www.jopdent.org

Editorial Staff

©Operative Dentistry, 2018, **43-6,** 563-565

2018 Reviewer Recognition

Operative Dentistry, Inc. would like to thank our conscientious team of Reviewers for their hard work, tenacity, and dedication in the furthering of operative dentistry around the word. These individuals dedicate innumerable hours in reading, re-reading, and critiquing manuscripts. Submitted articles, accepted for publication or not, all benefit from these reviewers who help authors present their hard work, as well as verifying that the work we publish is scientifically accurate, clinically relevant, and professionally uplifting. We cannot thank these individuals enough for their contributions, but we do want to publically recognize them.

Be it known here, and throughout the world, that the following named individuals have contributed real and invaluable service to the profession of Dentistry by volunteering their time and talents to the cause of peer-review for Operative Dentistry, Inc.

The time of service listed below is for the 2018 publication year.

Eva Eleni Achilleos — University of Athens
Fatima Aguilera — University of Granada
Laila Al Dehailan — Imam Abdulrahman Bin Faisal University
Hend Al Nahedh — King Saud University
Maan AlShaafi — King Saud University
Afnan AlZain — King Abdulaziz University
Masatoshi Ando — Indiana University
Watcharaphong Ariyakriangkai — Chiang Mai University
Cesar Arrais — State University of Ponta Grossa
Clifton Bailey — United States Air Force
Elizabeth Bakeman — Kois Center, Inc
David Bardwell — Tufts University
Wayne Barkmeier — Creighton University
Mark Beatty — University of Nebraska
Cristina Benavides-Reyes — University of Granada
David Berzins — Marquette University
Atul Bidarkar — University of Iowa
Lawrence Blank — University of Maryland
Igor Blum — University of Bristol
Uwe Blunck — Charité - Universitätsmedizin Berlin
Alessandra Borges — São Paulo State University
Gilberto Borges — University of Uberaba
Martha Brackett — Augusta University
Roberto Braga — University of São Paulo
James Broome — University of Alabama
Paul Brunton — University of Leeds
Richard Buck — United States Air Force
Michael Burrow — University of Hong Kong
Oriana Capin — Indiana University
Fred Certosimo — Virginia Commonwealth University
Yada Chaiyabutr — University of Washington
Daniel Chan — University of Washington
Jenn Chen — Texas A&M Health Science Center - Baylor
Liang Chen — Bisco Inc
Sopanis Cho — Indiana University
Tien-Min Gabriel Chu — Indiana University
Supattriya Chutinan — Harvard University
Joshua Cohen — University of Iowa
Adriana Cruz — Fluminense Federal University
Tracy Dantonio — United States Navy
Mario De Goes — University of Campinas
Tracy De Peralta — University of Michigan
Alex Delgado — University of Florida
Joseph Dennison — University of Michigan
Kim Diefenderfer — Indiana University
Marcelo Durski — University of Louisville
Elisabeth Dursun — Paris Descartes University
Nicholas DuVall — United States Air Force
Fred Eichmiller — Delta Dental of Wisconsin
Hatem El-Damanhoury — University of Sharjah
Heba Elkassaby — Rutgers University
Omar El-Mowafy — University of Toronto
Kristi Erickson — United States Navy
Sofia Espinosa — Universidad Intercontinental
Nels Ewoldsen — Conservative Dental Solutions
Andre Faria-e-Silva — Federal University of Sergipe
Dennis Fasbinder — University of Michigan
Sabrina Feitosa — Indiana University
Eduardo Fernandez — Instituto de Ciencias Biomédicas
Jack Ferracane — Oregon Health & Science University
Simon Flury — University of Bern
Richard Foxton — King's College London
Kevin Frazier — Augusta University
Jessica Fugaro — Bainbridge, WA USA
Orlando Fugaro — Bainbridge, WA USA
Alan Furness — Augusta University
Adilson Furuse — University of São Paulo
Maria Gaintantzopoulou — University of Athens
Gianni Gallusi — Università degli Studi di Roma Tor Vergata

©Operative Dentistry, 2018, **43-6,** 566-572

Clinical Technique/Case Report

Mini Fiberglass Post for Ankylosed Tooth Reconstruction: A Clinical Technique

AV Martins • RC Albuquerque • LFSA Morgan • NRFA Silva
AF Drummond • RR Silveira • CS Magalhães • AN Moreira

Clinical Relevance

Ankylosed posterior teeth impede tooth stability in the arch. The literature does not offer evidence regarding the predictability of ankylosed tooth restorations. Additional retention through mini fiberglass posts for composites may be indicated to improve the long-term prognosis.

SUMMARY

It was possible to restore the shape and function of a severely ankylosed tooth by fabricating a ceramic crown for placement on a resin reconstruction supported by mini fiberglass posts. By increasing the retention of the morphological reconstruction for the future support of indirect restorations, cementable intradentinal fiberglass posts enhance the longevity of these restorations. Ultimately, all proposals that seek to improve the long-term prognosis of restorations on ankylosed teeth, especially severely impacted ones, are of extreme clinical relevance.

*Adriana Vieira Martin, DDS, MSc, PhD, professor, Department of Restorative Dentistry, School of Dentistry, Federal University of Minas Gerais, Minas Gerais, Brazil

Rodrigo C Albuquerque, DDS, MSc, PhD, associate profesor, Department of Restorative Dentistry, School of Dentistry, Federal University of Minas Gerais, Minas Gerais, Brazil

Luis Fernando dos Santos Alves Morgan, DDS, MSc, PhD, professor, Department of Restorative Dentistry, Newton School of Dentistry, Minas Gerais, Brazil

Nelson Renato França Alves Silva, DDS, MSc, PhD, adjunct professor, Department of Restorative Dentistry, School of Dentistry, Federal University of Minas Gerais, Minas Gerais, Brazil

Alexandre Fortes Drummond, DDS, MSc, PhD, associate professor, Department of Restorative Dentistry, School of Dentistry, Federal University of Minas Gerais, Minas Gerais, Brazil

Rodrigo Richard da Silveira, DDS, MSc, PhD, adjunct professor, Department of Restorative Dentistry, School of Dentistry, Federal University of Minas Gerais, Minas Gerais, Brazil

Cláudia Silami Magalhães, DDS, MSc, PhD, titular professor, Department of Restorative Dentistry, School of Dentistry, Federal University of Minas Gerais, Minas Gerais, Brazil

Allyson Nogueira Moreira, DDS, MSc, PhD, titular professor, Department of Restorative Dentistry, School of Dentistry, Federal University of Minas Gerais, Minas Gerais, Brazil

*Corresponding author: Avenue Antônio Carlos, 6627, Bairro Pampulha, Caixa Postal 702, 30.123.970, Belo Horizonte, Minas Gerais, Brazil; e-mail: adrianavieiramartins@uol.com.br

DOI: 10.2341/17-203-T

INTRODUCTION

Dental ankylosis is caused by intimate contact between the root cementum and the alveolar bone as a result of the absence of the periodontal ligament between these tissues. This anomaly prevents the affected tooth from erupting and thus serving its functional role within the mouth.[1-4]

The restorative planning relative to ankylosed teeth is determined mainly by the patient's age, the remnant's degree of infraocclusion, and the relationship between the remnant and the alveolar ridge.[3,4]

Full crown reconstruction with direct composite resin is commonly used to restore the shape and consequently the function of ankylosed deciduous teeth. For permanent teeth, core build-up with composite resin aims to assist the retention of indirect restorations.[5,6] However, the literature does not offer evidence regarding the predictability of ankylosed tooth restorations.[7] Thus, it is prudent to consider the requirements of each case, which will influence the choice of restorative technique and indicate additional means of retention.[8]

The objective of this work was to review the clinical technique regarding the predictability of ankylosed tooth restorations and to describe the core build-up technique retained by mini fiberglass posts (MFPs) for composites in posterior teeth.

CLINICAL TECHNIQUE

Patient LKBL was an 18-year-old male in good general health. His first mandibular right molar (tooth 30) was affected by severe dental ankylosis. The diagnosis of severe ankylosis was determined through clinical and radiographic examinations. The patient also had a cross-bite and a posterior open bite on the same side as the ankylosed tooth (Figure 1A). The patient was under orthodontic treatment, which was partially interrupted to enable the reconstruction of tooth 30 through restorative techniques because it could not be reestablished through orthodontic treatment. A provisional restoration was initially requested so that the orthodontic treatment could be completed, after which a ceramic crown would be placed. The occlusal surface of the tooth was flush with the gingival tissue (Figure 1B). Periapical radiographic examination showed that the mesial uppermost portion of the crown was below the bone crest. The right mandibular premolar (tooth 29) was slightly distalized (Figure 1C).

The treatment plan comprised surgical crown lengthening, transsurgical morphological restoration with composite resin supported by MFPs, and

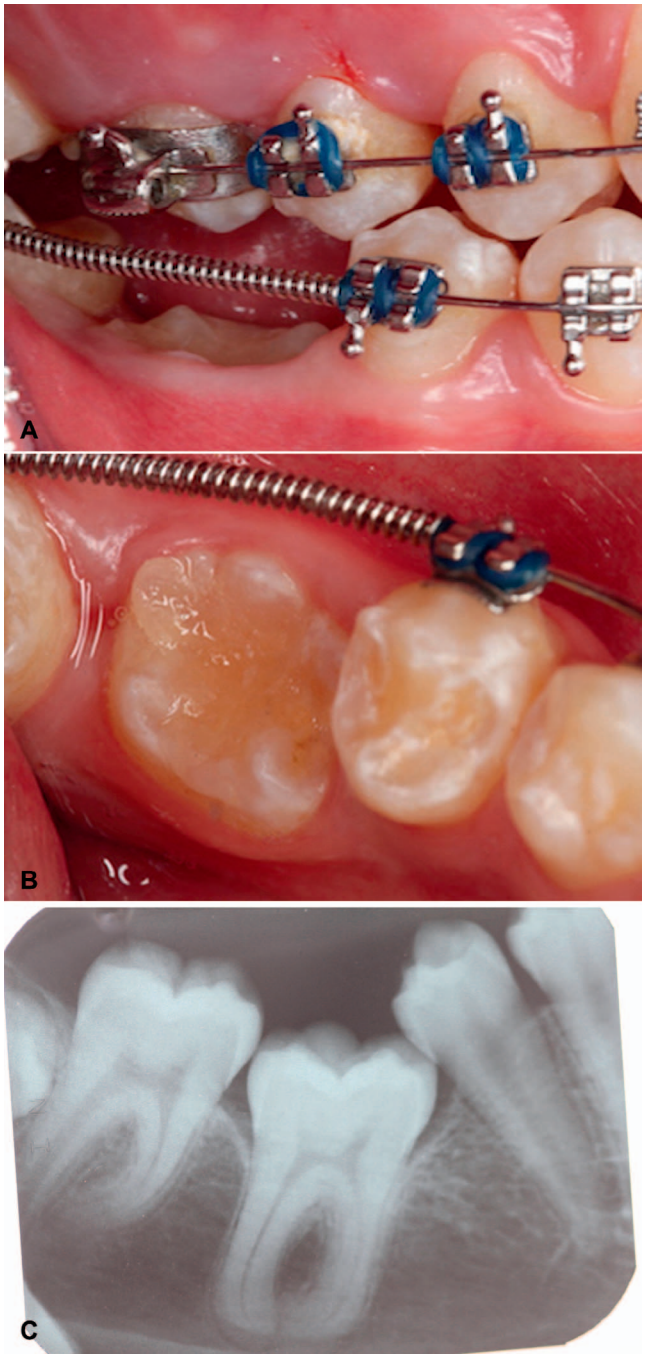

Figure 1. *(A) Initial condition: Side view of the first right lower molar flush with the upper margin of the gingival sulcus. (B) Initial condition: Occlusal view of ankylosed right mandibular first molar (severe ankylosis). (C) X-ray image of the right mandibular first molar flush with the mesial bone crest.*

provisional crown fabrication using the direct technique.

Once the occlusal level of the remnant relative to the bone crest was assessed, a partial periodontal flap was raised, and 3 mm of the mesial bone crest

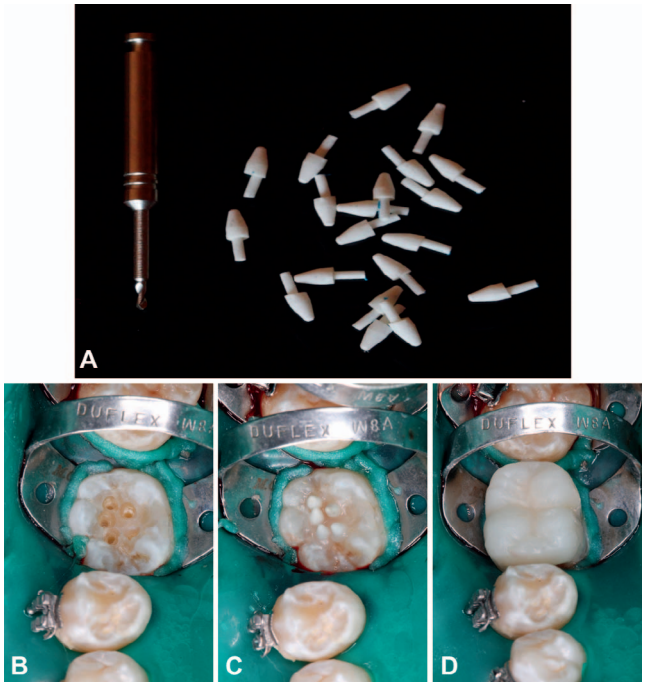

Figure 2. *(A) Mini fiberglass posts for composites and spiral bur for preparation. (B) Preparations performed in correspondence with each of the five cusps. (C) Cemented mini posts. (D) Reconstructed clinical crown using composite resin.*

was removed to restore the biological widths and to favor the absolute isolation of the operative field. After absolute isolation, a spiral bur that was included in the fiberglass post kit (Figure 2A) was used to make five perforations spaced at least 1 mm apart in the central portion of tooth 30, corresponding to its cusps (Figure 2B). A 0.65-mm–diameter and 2.0-mm–deep pin-hole parallel to the outer surface of the tooth was placed in the dentin 0.5 mm from the enamel/dentin junction with a twist drill (Angelus) in a slow-speed handpiece. An MFP was placed into the pin hole to evaluate adequate inclination and occlusal clearance. The portion of the MFP inserted into the dental substrate was 0.63 mm in diameter and 2.0 mm in length, and the coronal aspect had a conical shape of 1.3 mm in diameter at the base of the cone and 0.65 mm in diameter at the tip of the cone and was 2.5 mm in length. Taking into account the active length of the intradentinal portion of the pin, one can expect a practically limited preparation to the enamel substrate, thereby ensuring a safe distance from the pulp chamber.

The posts had been previously etched for one minute with 37% phosphoric acid (FGM, Joinville, SC, Brazil), washed abundantly with a water/air jet, and dried vigorously. Subsequently, a silane agent (Silano-Angelus, Londrina, PR, Brazil) was applied. After silanization, a hot air jet was used to fully dry the silane and to apply an adhesive layer (Adper™ Single Bond 2, 3M ESPE, St Paul, MN, USA). The enamel of the entire tooth was etched with 37% phosphoric acid (FGM) for 30 seconds and then washed and dried vigorously. As a result of the difficulty of hybridizing the prepared hole for post insertion, self-adhesive resin cement (Rely-X Unicem, 3M ESPE) was used. This cement was mechanically activated in a suitable device (Ultramat, SDI, Victoria, Australia), as recommended by the manufacturer. Then the cementing agent was introduced into the holes using an exploratory probe, and the intradentinal portion of the MFPs was simultaneously embedded in the cementing agent. One by one, the MFPs were placed into the holes using forceps specially designed for this task. Excess cement was removed using a microbrush (Cavibrush Fine, FGM), and photoactivation (Demetron Optilux 500; Kerr GmbH, Karlsruhe, Germany) was performed by focusing the light perpendicular to the long axis of the tooth (Figure 2C). After the chemical setting time had passed, the adhesive procedures were started in the enamel and in the extradental portion of the post.

Two adhesive layers (Adper Single Bond 2, 3M ESPE) were applied to the entire occlusal surface, and the last layer was light-cured for 20 seconds. Soon after, small increments of light-curing composite resin (Z350 XT, 3M ESPE) were inserted between the posts and into the occlusal portion until fine anatomy was obtained. Additional light-curing was performed for 60 seconds on all sides of the composite resin crown (Figure 2D). The rubber dam was removed, and the flap was repositioned and sutured (Figure 3). After 10 postoperative days, the sutures were removed.

At 120 days after surgery, the tooth was prepared to receive a full crown (diamond burs 3216 and 4138, KG Sorensen). A 2-mm–thick bevel was performed throughout the cervical extension at the gingival level, and the bevel was on the tooth structure. The occlusal reduction considered the crown height of adjacent teeth due to the open bite on this side. All internal angles were rounded. Finishing procedures were performed with a multilaminated bur (9642 Jet, Labordental, São Paulo, SP, Brazil), and the margins were finished with manual cutting instruments (Figure 4). The characteristics of the cavity preparation were in accordance with the prerequisites for preparation for CAD/CAM restoration.

Next, the color of the acrylic resin was chosen. Using the casting technique, an immediate provi-

Figure 3. *Completed transsurgical reconstruction.*
Figure 4. *Occlusal view of the preparation for full crown.*

sional restoration was fabricated. The restoration was used to keep the gingival margins in position, to protect the exposed dentin in the preparation margins, to maintain the position of the adjacent teeth, and to restore dental function. Accommodation for tooth wear was checked by measuring the thickness of the provisional restoration using a thickness gauge. Subsequently, the provisional restoration was cemented.

The patient resumed orthodontic therapy and, as the uprighting of the tooth 29 occurred, relapse measures of the temporary restoration were performed in order to prevent food impaction and to favor local hygiene.

After 12 months, when the fixed orthodontic appliance was removed, the patient returned so that the ceramic restoration could be fabricated. The provisional restoration was removed, and the cavity was cleaned and scanned using a Trios 3 scanner (3Shape; Copenhague, Denmark). At this time, the adjacent and opposing teeth were also digitized, and the upper and lower virtual models were related in maximal habitual intercuspation (Figure 5A). Based on the virtual models, the preparation margins were outlined, and the restoration was designed (Figure 5B) using Dental System software (3Shape). After the design was completed, color analysis and mapping were performed (Figure 5C,D). The information was sent as an STL file for the fabrication of the crown. A DWX-4W milling unit (Roland; Japan) was used. The material of choice for this patient was the Emax A3HT block (Ivoclar Vivadent, Schaan, Liechtenstein).

Once the crown was available in its pre-crystalized stage (Figure 6), its margins and proximal and occlusal contacts were checked. A small refinement of the occlusal contacts was necessary, and then the crown was crystalized and painted to produce a finely detailed restoration (Figure 7).

Subsequently, the intaglio portion of the lithium disilicate ceramic restoration was etched using hydrofluoric acid for 20 seconds and then washed and dried vigorously. A layer of universal primer (Monobond Plus, Ivoclar Vivadent) was applied, air jet-dried, and light-cured for solvent volatilization, and a layer of adhesive (Adper™ Single Bond 2, 3M ESPE) was applied. The prepared cavity was cleaned using pumice paste and a polishing brush and then washed thoroughly and dried. The enamel margins were etched for 30 seconds with 37% phosphoric acid (FGM) and then washed and dried vigorously. Relative isolation of the operative field was performed, aided by high-power suction. The self-etching resin cement was activated according to the manufacturer's instructions (U-200, 3M ESPE) and placed inside the crown, and the crown was then positioned. Excess cement was removed using a brush, and the margins were light-cured for 60 seconds on each side. The restoration was then left alone for six minutes to allow the cement to chemically set. At the end of the cementation process, the minimum excess cement was removed using a no. 12 scalpel blade (Lamedid Solidor, Barueri, Sao Paulo, Brazil). A periapical long cone paralleling technique radiograph was taken to ensure that excess cement was completely removed and to visualize the final adaptation of the restoration (Figure 8). Finally, the patient was referred back to orthodontics to be fit with a retainer.

The restoration was completed, and the proper shape and esthetics were reestablished in terms of the periodontal tissues and occlusal principles. This ensured that dental function would be correct after

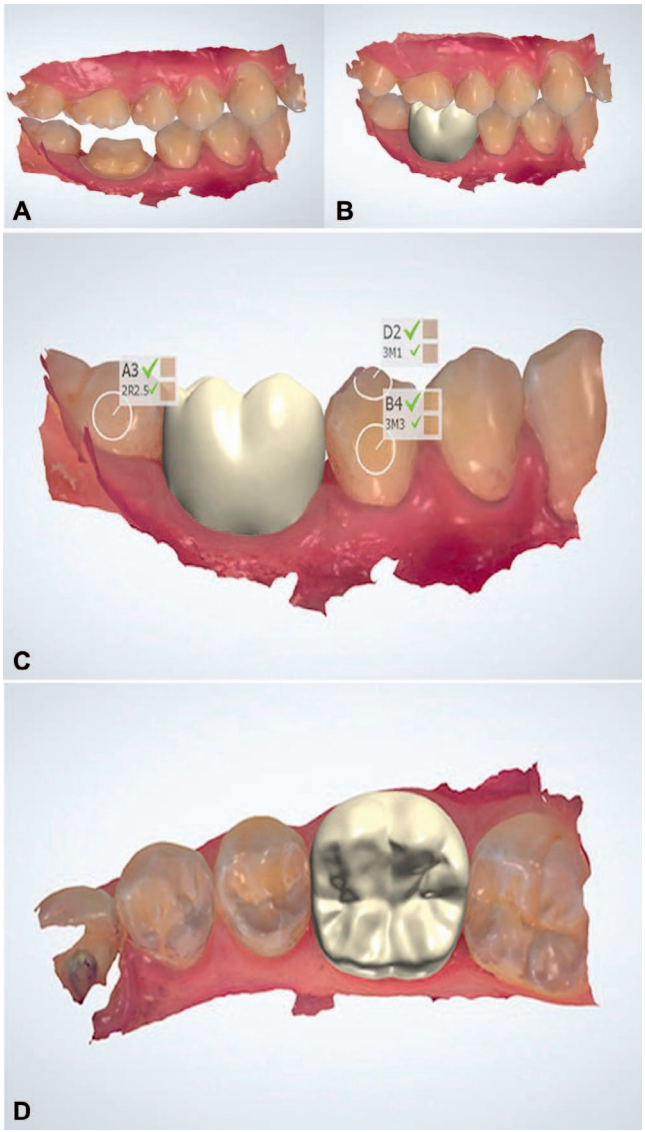

Figure 5. *(A) Sagittal view of the scanned preparation and occlusion relation. (B) Sagittal view of the crown design in position. (C) Sagittal view of the color mapping obtained after scanning and designing steps were completed. (D) Occlusal view of the final three-dimensional designed crown.*

the patient completed his orthodontic treatment. Longitudinal follow-up will be conducted to evaluate the advantages of using MFP, a novel additional retention, in posterior teeth.

DISCUSSION

Ankylosed posterior teeth impede tooth stability in the arch, which may manifest as the extrusion of the opposing tooth and the migration of adjacent teeth.[1,2,5-7] As a consequence, dental ankylosis leads to the rupture of the binomial, through which the form is responsible for the preservation of function

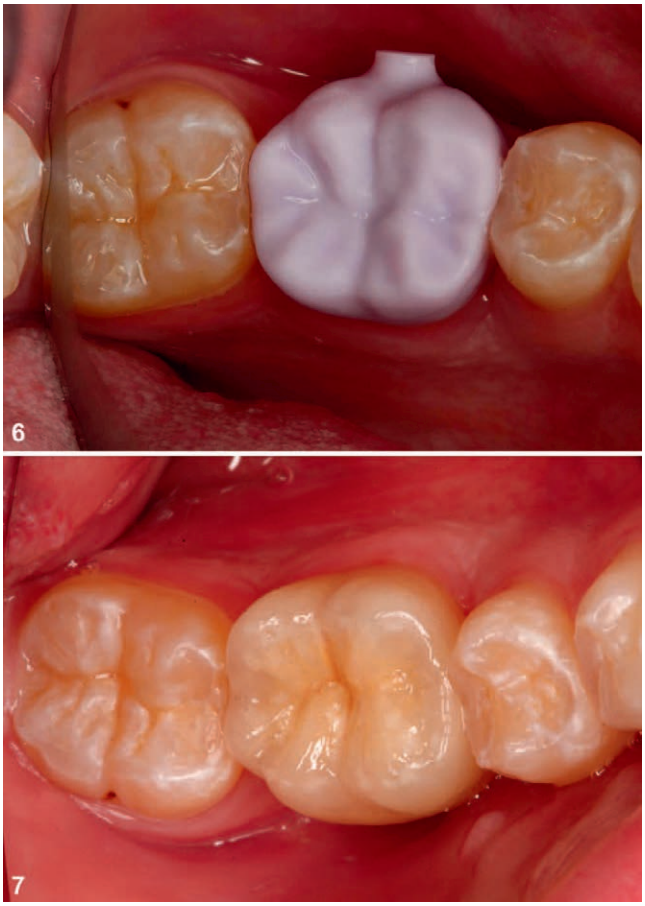

Figure 6. *Pre-crystalized crown after milling process.*
Figure 7. *Completed and cemented restoration*

and the function maintains the form.[9] Thus, it is necessary to propose a restorative therapy that can restore the crown anatomy and consequently the dental function. The earlier the patient is diagnosed and undergoes appropriate treatment, the greater the chances of reducing the complications associated with ankylosed teeth.[2-7,10]

Ideally, the restorative plan should be reconciled with orthodontic treatment and should consider the degree of infraocclusion of the tooth and the patient's age.[3,4] In addition, it should meet the main requirements for successful restorative therapy, such as periodontal health, function, and longevity of the restoration.

However, there are no studies offering long-term, predictable results for the longevity of restorations for ankylosed teeth. Thus, there is no guidance regarding the most effective form of restorative therapy. This fact was shown in 2010, when a Cochrane search confirmed that there were no randomized clinical trial data supporting a thera-

Figure 8. *Interproximal X-ray of the restoration immediately after cementing.*

peutic approach for ankylosed teeth.[7] This gap in the literature can be verified to continue through the present.

Regarding proposals for the treatment of ankylosed permanent teeth, the literature advocates both conservative and extremely invasive procedures. The conservative proposals involve completely filling the crown portion with direct composite resins and the use of a direct composite resin core build-up to support a subsequent indirect ceramic restoration. The invasive proposals include exodontia and implants, surgical repositioning with previous luxation, and osteogenic distraction.[1-3,5-7,11]

The advantages of ceramic crowns supported by composite resin reconstructions are mainly related to the possibility of maintaining the natural tooth as a pillar, thereby transmitting physiological loads to the periodontal support and allowing the tooth's dimensions to be preserved. Ceramic crowns also offer the benefits of surface smoothness, color stability, high wear resistance, and biocompatibility.[12] However, in the case of ankylosed teeth, a support must be constructed under the crown.

From the biomechanical point of view, the dental lever system developed by lateral loads is more beneficial when the resistance arm is at least twice as large as the power arm.[13] Considering this fact, the restoration of ankylosed permanent teeth is quite favorable because it has a lever system in which the resistance arm contains the root and part of the anatomical crown. The power arm, however, needs to contain material that provides the long-term retention of the filler material. In addition, restorations of posterior teeth are subjected to a tensile load.[14] Thus, improving the retention of restorations in posterior teeth is essential for successful therapy. According to Binus and others,[8] the needs presented will influence the selection of the restorative technique. Additional retention may be indicated to improve the long-term prognosis of the selected therapy.[8,15-18]

Restorative proposals that aim to improve the quality and longevity of ankylosed tooth restorations are relevant given the lack of scientific evidence. Thus, morphological reconstructions supported by additional retention, such as intradentinal posts, especially for ankylosed posterior teeth, can be planned with the aim of improving the longevity of the restoration. MFPs have recently been introduced as an alternative to threaded intradentinal metal pins.[15,16] Their greatest advantages include their low cost, their use of a simplified technique, their noninfluence on the final esthetics of the restoration for anterior teeth, for example, and the minimization of the tension imposed on dentin that they offer compared with the use of threaded intradentinal posts.[15]

To improve the retention of an intradentinal post, sufficient interocclusal and vestibular-lingual space to accommodate it inside the reconstruction material must be present. Because the present clinical case was a morphological reconstruction that was subject to occlusal wear, it was necessary to maintain the thickness of the composite resin to enable the preparation of the all-ceramic crown; this was possible because of the short height of the MFPs. In the case of direct composite resin restorations that will not require future work, which are very common in cases of ankylosis of deciduous teeth, threaded intradentinal metal pins may also be indicated. These pins have a long clinical history of success and are still used today.[18] Additional retention can be created using pins and grooves;[17,18] however, they incur greater wear of the healthy dental structure compared with the technique described herein.

Acknowledgements

Ivoclar supported this study, providing the ceramic material for the final restoration. The authors thank Renato Duarte, MDT (Belo Horizonte Brazil), for the collaboration during the final steps of the restoration fabrication. This study was supported by grant PRPq-02/2017 from the Prãreitoria de Pesquisa UFMG.

Regulatory Statement

This study was conducted in accordance with all the provisions of the local human subjects oversight committee guidelines and policies of the Federal University of Minas Gerais, Brazil.

Conflict of Interest

The authors of this manuscript certify that they have no proprietary, financial, or other personal interest of any nature or kind in any product, service, and/or company that is presented in this article.

(Accepted 13 November 2017)

REFERENCES

1. Aranha AMF, Duque C, Silva JYB, Carrara CFC, Costa B, & Gomide MR (2004) Tooth ankylosis in deciduous teeth of children with cleft lip and/or palate *Brazilian Oral Research* **18(4)** 329-332.
2. Lim WH, Kim HJ, & Chun YS (2008) Treatment of ankylosed mandibular first permanent molar *American Journal of Orthodontics and Dentofacial Orthopedics* **133(1)** 95-101.
3. Giachetti L, Bertini F, & Landi D (2005) Morphological and functional rehabilitation of severely infra-occluded primary molars in the presence of aplasia of the permanent premolar: A clinical report *Journal of Prosthetic Dentistry* **93(2)** 121-124.
4. Bertl MH, Weinberger T, Schwarz K, Gruber R, & Crismani AG (2012) Resonance frequency analysis: A new diagnostic tool for dental ankylosis *European Journal of Oral Sciences* **120(3)** 255-258.
5. Williams HA, Zwemer JD, & Hoyt DJ (1995) Treating ankylosed primary teeth in adult patients: A case report *Quintessence International* **26(3)** 161-166.
6. Tieu LD, Walker SL, Major MP, & Flores MC (2013) Management of ankylosed primary molars with premolar successors: A systematic review *Journal of the American Dental Association* **144(6)** 602-611.
7. De Souza RF, Travess H, Newton T, & Marchesan MA (2010) Interventions for treating traumatised ankylosed permanent front teeth *Cochrane Database Systematic Review* **120(1)** 1-16.
8. Binus S, Petschelt AKA, & Berthold C (2013) Restoration of endodontically treated teeth with major hard tissue loss—Bond strength of conventionally and adhesively luted fiber-reinforced composite posts *Dental Traumatology* **29(5)** 339-354.
9. Amsterdam M, & Fox L (1959) Provisional splinting—Principles and techniques *Dental Clinics of North America* **3** 73-99.
10. Becker A, Chaushu G, & Chaushu S (2010) Analysis of failure in the treatment of impacted maxillary canines *American Journal of Orthodontics and Dentofacial Orthopedics* **137(6)** 743-754.
11. Schott T, Engel E, & Goz G (2012) Spontaneous re-eruption of a permanent maxillary central incisor after 15 years of ankylosis: A case report *Dental Traumatology* **28(3)** 243-246.
12. Sarigag S, Sevimay M, & Pekkan G (2013) Fracture resistance of teeth restored with all-ceramic inlays and onlays: An in vitro study *Operative Dentistry* **38(6)** 626-634.
13. Lindhe J (1988) Technical and biophysical aspects of crowns and bridges: Therapy in patients with reduced amounts of supporting periodontal tissue In: Lindhe J (ed) *Clinical Periodontology Treatment (Tratado de Periodontologia Clínica)* Guanabara Ed Rio de Janeiro, Brazil 385-396.
14. Smith DC (1971) Dental cements *Dental Clinics of North America* **15** 3-31.
15. Morgan LFSA, Martins AV, Albuquerque RC, Silveira RR, Silva NRFA, & Moreira AN (2016) Mini fiberglass post for composite resin restorations: A clinical report *Journal of Prosthetic Dentistry* **115(6)** 654-657.
16. Villavicencio CA, Narimatsu MH, Mondelli RFL, Furuse AY, & Mondelli J (2016) Micropin: Alternative method to restore anterior teeth with extensive coronary fracture *Revista de Operatoria Dental y Biomateriales* **5(3)** 1-7.
17. Marlkey MR (1966) Pin-retained and pin-reinforced amalgam *Journal of the American Dentistry Associaton* **73(6)** 1295-1300.
18. Papa J, Wilson PR, & Tyas MJ (1993) Pins for direct restorations *Journal of Dentistry* **21(5)** 259-264.

©Operative Dentistry, 2018, **43-6,** 573-580

Clinical Research

Accuracy of Buccal Scan Procedures for the Registration of Habitual Intercuspation

M Zimmermann • A Ender • T Attin • A Mehl

Clinical Relevance

Accurate reproduction of the jaw relationship is important in many fields of dentistry. Maximum intercuspation can be registered with digital buccal scan procedures implemented in the workflow of many intraoral scanning systems.

SUMMARY

Clinical Relevance: Accurate reproduction of the jaw relationship is important in many fields of dentistry. Maximum intercuspation can be registered with digital buccal scan procedures implemented in the workflow of many intraoral scanning systems.

Objective: The aim of this study was to investigate the accuracy of buccal scan procedures with intraoral scanning devices for the registration of habitual intercuspation *in vivo*. The hypothesis was that there is no statistically significant difference for buccal scan procedures compared to registration methods with poured model casts.

Methods and Materials: Ten individuals (full dentition, no dental rehabilitations) were subjects for five different habitual intercuspation registration methods: (CI) poured model casts, manual hand registration, buccal scan with inEOS X5; (BC) intraoral scan, buccal scan with CEREC Bluecam; (OC4.2) intraoral scan, buccal scan with CEREC Omnicam software version 4.2; (OC4.5β) intraoral scan, buccal scan with CEREC Omnicam version 4.5β; and (TR) intraoral scan, buccal scan with Trios 3. Buccal scan was repeated three times. Analysis of rotation (Rot) and translation (Trans) parameters was performed with difference analysis software (OraCheck). Statistical analysis was performed with one-way analysis of variance and the *post hoc* Scheffé test ($p<0.05$).

Results: Statistical analysis showed no significant ($p>0.05$) differences in terms of translation between groups CI_Trans (98.74±112.01 μm), BC_Trans (84.12±64.95 μm), OC4.2_Trans (60.70±35.08 μm), OC4.5β_Trans (68.36±36.67 μm), and TR_Trans (66.60±64.39 μm). For rotation, there were no significant differences ($p>0.05$) for groups CI_Rot (0.23±0.25°),

*Moritz Zimmermann, Dr. med. dent., Center of Dental Medicine, Department of Computerized Restorative Dentistry, University of Zurich, Zurich, Switzerland

Andreas Ender, Dr. med. dent., Center of Dental Medicine, Department of Computerized Restorative Dentistry, University of Zurich, Zurich, Switzerland

Thomas Attin, Prof. Dr. med. dent., Center of Dental Medicine, Clinic of Preventive Dentistry, Periodontology and Cariology, University of Zurich, Zurich, Switzerland

Albert Mehl, Prof. Dr. rer. nat. Dr. med. dent., Center of Dental Medicine, Department of Computerized Restorative Dentistry, University of Zurich, Zurich, Switzerland

*Corresponding author: Plattenstrasse 11, Zurich CH-8032, Switzerland; e-mail: moritz.zimmermann@zzm.uzh.ch

DOI: 10.2341/17-272-C

BC_Rot (0.73±0.52°), OC4.2_Rot (0.45±0.31°), OC4.5β_Rot (0.50±0.36°), and TR_Rot (0.47±0.65°).

Conclusions: Intraoral scanning devices allow the reproduction of the static relationship of the maxillary and mandibular teeth with the same accuracy as registration methods with poured model casts.

INTRODUCTION

Accurate reproduction of the jaw relationship is important in many fields of dentistry. Jaw relations can be determined either by means of occlusal morphology (ie, maximum intercuspation) or by means of locating the mandibular position (eg, with respect to the position of the centric condyles).[1] Habitual intercuspation or occlusion describes the jaw position that the patient acquires when asked to close the mouth without any deflection caused by external factors, such as tooth contacts. Maximum intercuspation describes the jaw position that the patient acquires when asked to close the mouth with a focus on maximum tooth contact of teeth of the upper and lower jaws. Habitual intercuspation and maximum intercuspation normally describe identical jaw positions as far as there are no premature tooth contacts or relieving postures that the patient is forced to acquire (eg, in the case of craniomandibular dysfunction). Maximum intercuspation can be registered with digital procedures, such as the buccal scan procedure implemented in the workflow of many intraoral scanning systems.[2]

For the registration of habitual intercuspation and its transfer to poured model casts, first impressions of the upper and lower arches are taken and model casts poured. Maximum intercuspation position is taken individually by the patient or can be achieved per hand guidance of the operator.[1] The habitual intercuspation position can be additionally encoded by the use of interocclusal recording materials.[3] Poured model casts are finally mounted into the articulator with respect to the maximum intercuspation taken by the patient *in vivo*. In the literature, several aspects of this *in vitro* registration process for the registration of habitual intercuspation have been described that might be the reason for an inaccurate registration of the jaw relationship.[4,5] The exact determination of the patient's arbitrary hinge axis has been described to be the reason for difficulties.[6] Interocclusal recording materials might result in inaccurate encoding of the maximum intercuspation as a result of specific material characteristics, such as material shrinkage.[7] Hand-guided procedures may be distinctly influenced by the operator's clinical skills and experiences and could be an additional factor for inaccuracies in the registration process.[8]

Maximum intercuspation can be registered with digital buccal scan procedures with intraoral scanning devices with no need for poured plaster models.[2] Buccal scans are defined as intraoral digital scans capturing the buccal surface of approximately three teeth of both upper and lower arches while the patient's jaws rest in maximum intercuspation.[2] By a subsequent software matching process of both buccal scan and intraoral scan of the upper and lower arches, both jaws are automatically aligned, thus representing the exact jaw relationship in the form of the *in vivo* maximum intercuspation.[9,10]

To date, there is no clinical study referring to the accuracy of the buccal scan registration method with intraoral scanning devices in comparison to registration procedures with poured model casts. The aim of this study was to investigate the accuracy of habitual intercuspation registration with intraoral scanning devices on the hypothesis that there is no statistically significant difference compared to conventional registration methods with poured model casts.

METHODS AND MATERIALS

Ten individuals were randomly selected from the clinical staff personnel of the Center of Dental Medicine of the University of Zurich. All participants had full dentition without dental rehabilitation and a good general health status (ASA criteria 1). Individuals suffered from neither periodontitis nor temporomandibular joint dysfunctions. All procedures performed in this study involving human participants were in accordance with the ethical standards of the institutional and/or national research committee and with the 1964 Helsinki Declaration and its later amendments or comparable ethical standards. The study was conducted as part of an established ethical protocol accepted by the ethical committee of the University of Zurich. Estimation of total sample size for the respective study setup with five test groups, each with 10 individuals, based on a significance level of $\alpha = 0.05$ was performed by means of a power analysis with the statistical power analysis program G*Power version 3.1 (open source; Heinrich-Heine-Universität, Düsseldorf, Germany) with respect to an estimated effect size of 0.3 and an observed power of 0.85.

Habitual Intercuspation Registration With Poured Model Casts

Full-arch impressions of the upper and lower arches were taken with vinylsiloxanether material (Identium, Kettenbach, Eschenbach, Germany) for each patient. Standard metal stock trays (ASA Perma-Lock, ASA Dental, Bozzano, Italy) were used. Impressions were poured after eight hours with scanable Type IV gypsum dental stone (Fujirock EP, GC, Tokyo, Japan). Poured stone models were stored at room temperature for 48 hours and left unmodified. *In vivo* habitual intercuspation for each patient was reproduced on the poured model casts via hand guidance by seating lower and upper arch models into maximum intercuspation. The accuracy of this registration method of maximum intercuspation with poured model casts was analyzed digitally with special software tools and a lab scanner (inEOS X5, Dentsply Sirona, York, PA USA). Scanning accuracy for the inEOS X5 scanner is reported to be less than 5 μm according to the DIN EN ISO 12836 standard. First, poured upper and lower arch models were digitized with the lab scanner (inEOS X5). Second, habitual intercuspation registration was performed by manually seating the poured models into maximum intercuspation with no further manipulation. Third, three teeth of the lower and upper arches were scanned by means of a buccal scan with the lab scanner in the region of the second premolar (inEOS X5). This procedure was repeated three times for each patient.

Habitual Intercuspation Registration With Intraoral Scanning Devices

Registration of habitual intercuspation was performed using the principle of buccal scan with three different intraoral scanning devices: CEREC Bluecam (Dentsply Sirona), CEREC Omnicam (Dentsply Sirona), and Trios3 (3Shape, Copenhagen, Denmark). Four different groups were established: CEREC Bluecam, software version 4.2 (BC); CEREC Omnicam, software version 4.2 (OC4.2); CEREC Omnicam, software version 4.5β (OC4.5β) (beta version); and Trios3 (TR). The buccal scan procedure was identical in each group. First, patients were seated in a comfortable upright position. Second, quadrant scans of the upper and lower arches were taken with respect to actual principles of scanning strategy.[11] Third, patients were asked to individually take their habitual, maximum intercuspation without any further manipulation. Fourth, a buccal scan involving three teeth of the upper and lower arches, ranging from the first molar to the first premolar, was performed. Dusting of tooth surfaces with scan spray was performed prior to scans for group BC with scan spray (VITA Scan Spray, VITA, Bad Säckingen, Germany). Three buccal bite registrations were taken for each patient.

Analysis of Accuracy of Habitual Intercuspation Registration

In this study, the accuracy of the registration of habitual intercuspation was analyzed by means of the relative jaw displacement of the lower jaw. The analysis was performed by determining the relative position of the lower jaw in reference to the upper jaw described by the two parameters, rotation (Rot) and translation (Trans), with special software tools.

First, digital data sets for the upper arch had to be aligned and be transferred to an identical coordinate system. This procedure comprised several steps, all executed with Geomagic Qualify software (version 24, 3D Systems, Rock Hill, USA). First, superimposition of two upper arch data sets was performed via a best-fit algorithm. Second, the transformation matrix generated by this superimposition was applied to the respective lower arch data set. By these means, the two upper arch data sets were positioned within the identical coordinate system, whereas the position of the lower arch data sets differed as a result of the jaw displacement caused by different habitual intercuspation registration procedures. Third, STL data files were exported from Geomagic Qualify software to the 3D difference analysis software OraCheck (Cyfex AG, Zurich, Switzerland) to allow quantitative difference analysis of 3D data sets.

The principle of the OraCheck software tool has recently been described in the literature.[12] First, the origin of the coordinate system was determined by moving the center of gravity of the coordinate system to the lower first molar of the baseline data set (OraCheck software tool "eBIT_ToolOrigin"). Second, baseline and follow-up data sets of the lower arch were superimposed. The relative jaw displacements between baseline and follow-up data sets of the lower jaw represented a quantitative measure for the accuracy of the registration of habitual intercuspation. Quantitative analysis in terms of parameters translation (Trans) and rotation (Rot) was performed by using well-known mathematical procedures.

First, a CSV data file comprising a 4×4 transformation matrix was exported from OraCheck software. On the basis of this transformation matrix, the rotation angle and the all-total translation as the

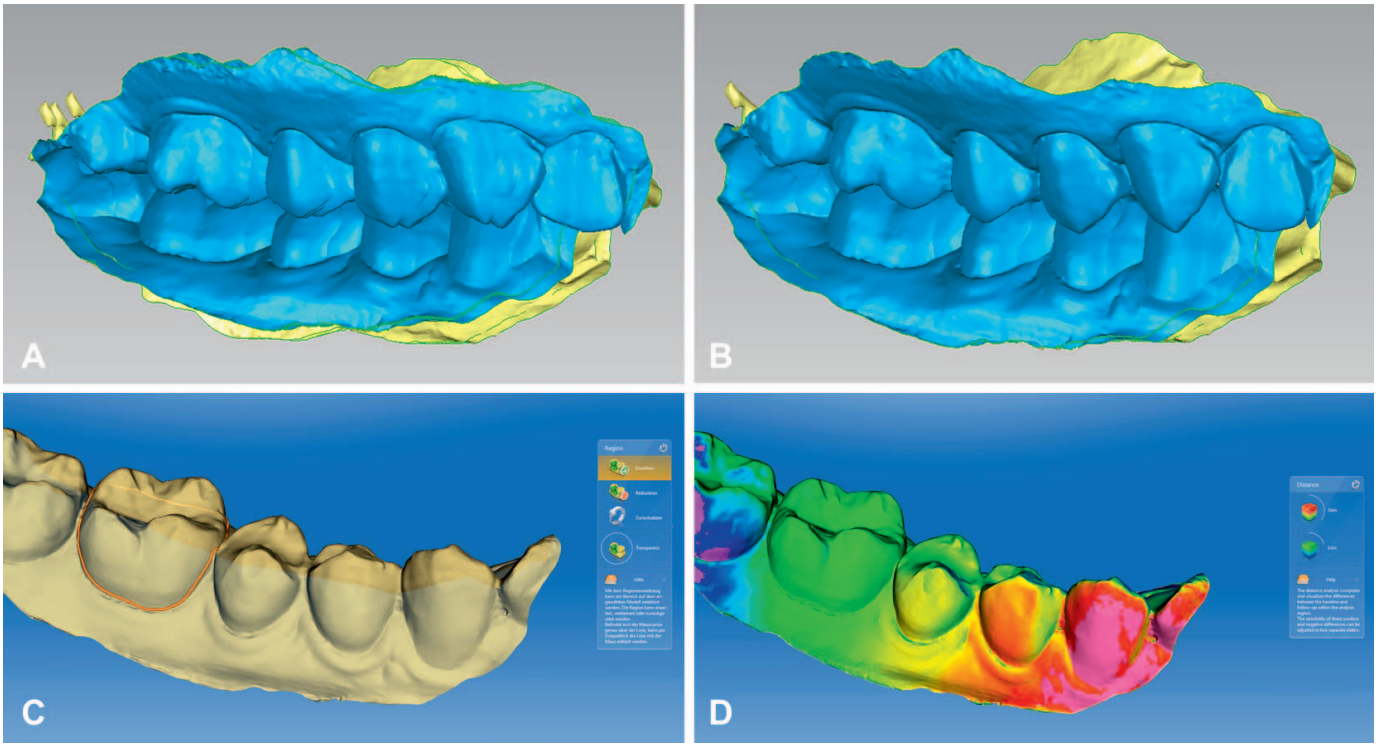

Figure 1. *Step-by-step procedure for the determination of translation and rotation parameters with Geomagic and OraCheck software; example shown for group OC4.2. (1A): Situation after import of STL data files (quadrant scans upper and lower arches) into Geomagic software, displacements of upper arch as a result of nonidentical coordinate system, and displacements of lower arch as a result of different buccal scan registrations in reference to upper arch scans. Three buccal scans were performed in each individual after scanning upper and lower arch quadrants. (1B): Situation after best-fit matching of upper arch quadrant scans. All three quadrants are in the same coordinate system, and respective lower arch quadrant scans were transformed using the transform matrix function of Geomagic software. (1C): Import of STL data files into OraCheck software and selection of the lower first molar in the baseline scan as center of origin for rotation and translation analysis. Three difference analyses were performed in each individual as baseline follow-up difference analysis (data set 1 - data set 2, data set 1 - data set 3, data set 2 - data set 3). (1D): Qualitative analysis of the displacement of the lower jaw as a result of different buccal scan registrations. Differences are color coded with respect to an adjustable scale with green showing the least differences. Quantitative analysis was performed by export of a 4 × 4 matrix and by well-known linear algebra formulas.*

square root of the squared sum of the x-, y-, and z-shifts were extracted by well-known linear algebra formulas.[12,13] Three analyses were performed for each patient in each test group and pooled (data set 1 - data set 2, data set 1 - data set 3, data set 2 - data set 3). The whole procedure is illustrated in Figure 1A-D.

Descriptive statistical analysis of translation (Trans) and rotation (Rot) was performed with SPSS Statistics 22 (IBM Statistics, Armonk, NY, USA), and one-way analysis of variance and the *post hoc* Scheffé test were used for statistical significance analysis ($p<0.05$) after pooling the data for one participant (calculation of the mean).

Table 1: *Values for Parameter Translation (Trans; in μm). Groups: Conventional Impression (CI), CEREC Bluecam (BC), CEREC Omnicam Version 4.2 (OC4.2), CEREC Omnicam Version 4.5β (OC4.5β), and Trios3 (TR). Three Scans per Individual Were Performed (n=30). No Statistically Significant Difference (One-Way Analysis of Variance and* Post Hoc *Scheffé Test,* p>*0.05)*

	n	Mean	SD	Min	Max	95% Confidence Interval	
						Lower	Upper
CI_Trans	30	98.74	112.01	5.28	365.33	56.91	140.57
BC_Trans	30	84.12	64.95	20.53	162.61	59.87	108.37
OC4.2_Trans	30	60.70	35.08	16.77	104.15	47.60	73.80
OC4.5β_Trans	30	68.36	36.67	32.83	117.76	54.67	82.06
TR_Trans	30	66.60	64.39	35.22	203.07	42.56	90.64

Table 2: *Values for Parameter Rotation (Rot; in °); Groups: Conventional Impression (CI), CEREC Bluecam (BC), CEREC Omnicam Version 4.2 (OC4.2), CEREC Omnicam Version 4.5β (OC4.5β), and Trios3 (TR). Three Scans per Individual Were Performed (n=30). No Statistically Significant Difference (One-Way Analysis of Variance and* Post Hoc *Scheffé Test,* p>*0.05)*

	n	Mean	SD	Min	Max	95% Confidence Interval	
						Lower	Upper
CI_Rot	30	0.23	0.25	0.07	0.84	0.14	0.32
BC_Rot	30	0.73	0.52	0.13	1.29	0.53	0.92
OC4.2_Rot	30	0.45	0.31	0.08	0.75	0.34	0.57
OC4.5β_Rot	30	0.50	0.36	0.17	1.00	0.37	0.64
TR_Rot	30	0.47	0.65	0.09	1.94	0.22	0.71

RESULTS

Translation of the lower jaw was found to be 98.74 ± 112.01 μm for the conventional habitual intercuspation registration method with poured model casts (CI_Trans). For digital buccal scan registration methods with intraoral scanning devices, the values for translation varied, depending on the intraoral scanning device used. Translation was found to be 84.12 ± 64.95 μm for CEREC Bluecam (BC_Trans), 60.70 ± 35.08 μm for CEREC Omnicam with software version 4.2 (OC4.2_Trans), 68.36 ± 36.67 μm for CEREC Omnicam with software version 4.5β (OC4.5β_Trans), and 66.60 ± 64.39 μm for Trios3 (TR_Trans). Statistical analysis with one-way analysis of variance and the *post hoc* Scheffé test showed no significant differences ($p>0.05$) between all the test groups. Results for translation mean, minimum, and maximum values are shown in Table 1.

Rotation analysis showed no statistically significant different results between different test groups. Rotation was found to be 0.23 ± 0.25° for the conventional habitual intercuspation registration method with poured model casts (CI_Rot). Results for rotation differed, depending on the intraoral scanning device used for the intraoral buccal scan. Rotation was 0.73 ± 0.52° for CEREC Bluecam (BC_Rot), 0.45 ± 0.31° for CEREC Omnicam with software version 4.2 (OC4.2_Rot), 0.50 ± 0.36° for CEREC Omnicam with software version 4.5β (OC4.5β_Rot), and 0.47 ± 0.65° for Trios3 (TR_Rot). Results for rotation mean, minimum, and maximum values are shown in Table 2.

DISCUSSION

The aim of this study was to investigate the accuracy of habitual intercuspation registration with intraoral scanning devices in comparison to conventional methods with poured model casts. The hypothesis was that there is no statistical significant difference between different methods applied for habitual intercuspation registration. Displacements of the relative position of the mandibular arch in reference to the maxillary arch were determined in terms of rotation (Rot) and translation (Trans) parameters with special 3D difference analysis software.

No significant differences were found in terms of translation for all test groups ($p>0.05$). The parameter translation is defined as the position shift of a certain object in the x-, y-, and z-axes, whereas the parameter rotation is defined as the tilt within a defined origin center. In terms of rotation, there were also no statistically significant differences between different test groups ($p>0.05$). Mean values for digital test groups ranged from best 0.50° (OC4.5β_Rot) to worst 0.73° (BC_Rot). The mean value for the conventional method was 0.23° (CI_Rot). Thus, both powder-based and powder-free scanning systems might be able to reproduce habitual intercuspation registration with the same accuracy as conventional habitual registration methods with poured model casts.

Several aspects need to be discussed. First, powder-based intraoral scanning systems require the dusting of buccal tooth surfaces. In order to perform intraoral buccal scans for the registration of habitual intercuspation, at least three single images are needed. If the intraoral scanner is not handled properly, the dust layer is likely to get altered during this procedure. This might lead to inaccuracies in the procedure of habitual intercuspation registration. Second, the data capturing mode and the size of the scanning tip might influence the precision of intraoral habitual intercuspation registration. During the process of habitual intercuspation registration with buccal scans, it is crucial that there are no jaw movements and that single images are matched correctly. If there is any movement of the patient, single images are matched poorly, and the registration process will be inaccurate. This effect might be

more crucial if only a few images, such as for the powder-based intraoral scanning system used in this study, are matched. Additionally, if the tip of the intraoral scanner is placed too far distally, artificial involuntary jaw movements of the patient might be more likely to occur. The tip of the CEREC Bluecam powder system is slightly larger than those of the other intraoral scanning systems used in this study. These aspects might explain why the worst results both for parameter rotation (Rot) and for translation (Trans) were found for the powder-based scanning device used in this study (CEREC Bluecam).

In this study, the worst results for the parameter translation were found for group CI with mean 98.74 ± 112.01 μm. The standard deviation was also to be found twice as high for group CI_Trans than for the other test groups. There might be several reasons for this observation. Conventional methods of habitual intercuspation registration may be inaccurate because of alterations in the plaster model, such as bubbles that might occur during the process of model fabrication. In contrast, intraoral buccal scans are directly taken from the patient. Provided that the proper scanning strategy is used, digital models are thus less susceptible to model defects, and buccal scans might lead to a more accurate habitual intercuspation registration of the digital models.

Within the limitations of this study, several aspects need to be discussed. First, there might be the question about the accuracy of intraoral scanning devices. Several published studies show that the intraoral scanning systems used in this study perform with high accuracy. For full-arch digital impressions, our group found an *in vitro* trueness of 56.4 ± 15.3 μm for CEREC Bluecam and 46.1 ± 10.4 μm for CEREC Omnicam.[14] In this study, quadrant scans for the upper and lower arches comprising four to five teeth were performed prior to the buccal scan so that accuracy values for all three scanning systems might in fact be superior. However, scanning artifacts would result in inaccurate model data and thus in a poor buccal bite registration. Scanning artifacts should be cut prior to buccal scan registration with intraoral scanning devices.

In this study, the laboratory benchtop scanner inEOS X5 was used to digitize the plaster models. Scanning accuracy for the inEOS X5 scanner is reported to be less than 5 μm according to the DIN EN ISO 12836 standard. It is important to mention that for ISO standard procedures, standardized geometrical objects and no tooth geometries are used. In terms of optical digitalization processes, however, surface morphology, textural information, and angulation of surface imaging are important. This is why there might be the assumption that scanning accuracy for tooth geometries might be inferior to the ISO standard values. There are no actual studies available addressing the accuracy of the inEOS X5 scanner for tooth geometries. Internal data (not yet published) and pilot tests performed previous to this study revealed the precision of the inEOS X5 scanner to be within a 5- to 10-μm range for full-arch plaster models. It is important to understand that the technical configuration of lab scanners includes an optical imaging from specific, predefined camera positions and model angulations. This is the main reason why the matching process of single images to obtain the final digital model performs better for lab scanners than for intraoral scanners, resulting in a higher accuracy.

There are studies reporting difficulties using digital buccal scan registration procedures.[15,16] One study reports digital model contacts and real model contacts of a full-arch model cast having an accordance for contact distribution of only 30% to 40%. Inaccuracies of the registration occurred mainly at the contralateral side of where the buccal scan registration was performed.[16] This observation might derive from the fact that no ideal scanning strategy had been used and that model deformations might have occurred, resulting in habitual intercuspation inaccuracies. The importance of scanning strategy for the accuracy of digital full-arch impressions has recently been described,[11] although intraoral buccal scans on both sides of the jaw might be beneficial in order to improve the accuracy of habitual intercuspation registration for full-arch scans. In this study, the focus was on the registration of quadrant scan models. A further study might investigate the registration accuracy of full-arch scans.

The disadvantage for conventional habitual intercuspation registration methods might be the manual seating of poured model casts with maximum intercuspation into the articulator. This procedure is reported to be highly dependent on the experience of the dental technician.[17] Boyarksy and others[17] reported that the occlusal refinement of mounted casts before the fabrication of indirect restorations significantly decreased the time needed to adjust the occlusion of the seated restoration. Digital methods such as intraoral buccal scan registrations might be consequently less technique sensitive and more reliable for both the clinician and the dental technician.

In this study, procedures for buccal scans were repeated three times for each patient. For groups BC, OC4.2, OC4.5β, and TR, patients were asked to individually take their habitual, maximum intercuspation three times. For group CI, manual seating of the poured models was repeated three times. For all groups, there might thus be the possibility of some sort of reproducible error. Previous studies that we conducted using a different protocol demonstrated that the mean ± SD value for the location of the habitual intercuspation was 42 ± 34 μm, ranging from 22 ± 9 μm to 77 ± 58 μm for single individuals.[10] In this study, we tried to minimize the reproducible error as much as possible and below the threshold previously observed by systematically standardizing the procedure of determining the maximum intercuspation for patients, such as by defining a specific seating position and exact procedure of intraoral scanning but also by performing the manual seating of plaster models by only a single operator.

Digital procedures for the intraoral habitual intercuspation registration are highly promising, as they might not be limited to reproducing only the static occlusion. In the future, it might be possible to extend the application of the buccal scan registration and simultaneously capture, for example, dynamic movements of the jaw. First attempts to integrate dynamic occlusion into the digital workflow have recently been described.[18,19]

CONCLUSIONS

Intraoral scanning systems with buccal scan procedures allow practitioners to reproduce the static relationship of the maxillary and mandibular teeth with the same accuracy as conventional registration methods with poured model casts. Intraoral scanning devices with different imaging technologies did not show any statistically significant differences for the reproduction of the static relationship. Compared to conventional methods, digital buccal scan registration methods might be less susceptible to errors and be performed more easily and reliably for the determination of habitual intercuspation.

Regulatory Statement

This study was conducted in accordance with all the provisions of the local human subjects oversight committee guidelines and policies of the national research committee and with the 1964 Helsinki Declaration and its later amendments or comparable ethical standards.

Conflict of Interest

The authors of this article certify that they have no proprietary, financial, or other personal interest of any nature or kind in any product, service, and/or company that is presented in this article.

(Accepted 21 December 2017)

REFERENCES

1. Murray MC, Smith PW, Watts DC, & Wilson NF (1999) Occlusal registration: Science or art? *International Dental Journal* **49(1)** 41-46.
2. Muller HC (2010) Registration of occlusion by buccal scan in Cerec software version 3.80. *International Journal of Computerized Dentistry* **13(3)** 265-273.
3. Ghazal M, & Kern M (2008) Mounting casts on an articulator using interocclusal records *Journal of Prosthetic Dentistry* **100(5)** 408-409.
4. Utz KH, Muller F, Luckerath W, Schwarting P, Noethlichs W, Buttner R, Fuss E, Gruner M, & Koeck B (2007) The lateral leeway in the habitual intercuspation: Experimental studies and literature review *Journal of Oral Rehabilitation* **34(6)** 406-413.
5. Eriksson A, Ockert-Eriksson G, Lockowandt P, & Eriksson O (2002) Clinical factors and clinical variation influencing the reproducibility of interocclusal recording methods *British Dental Journal* **192(7)** 395-400; discussion 391.
6. Morneburg TR, & Proschel PA (2011) Impact of arbitrary and mean transfer of dental casts to the articulator on centric occlusal errors *Clinical Oral Investigations* **15(3)** 427-434.
7. Ghazal M, & Kern M (2010) Influence of loading forces on the vertical accuracy of interocclusal records *Quintessence International* **41(2)** e31-e5.
8. Yamashita S, Igarashi Y, & Ai M (2003) Tooth contacts at the mandibular retruded position, influence of operator's skill on bite registration *Journal of Oral Rehabilitation* **30(3)** 318-323.
9. Frank E, & Frank S (2012) Bite registration in Cerec and in lab *International Journal of Computerized Dentistry* **15(2)** 149-158.
10. Jaschouz S, & Mehl A (2014) Reproducibility of habitual intercuspation in vivo *Journal of Dentistry* **42(2)** 210-218.
11. Ender A, & Mehl A (2013) Influence of scanning strategies on the accuracy of digital intraoral scanning systems *International Journal of Computerized Dentistry* **16(1)** 11-21.
12. Mehl A, Koch R, Zaruba M, & Ender A (2013) 3D monitoring and quality control using intraoral optical camera systems *International Journal of Computerized Dentistry* **16(1)** 23-36.
13. Robertson G, Hamill J, Kamen G, & Whittlesey S (2004) *Research Methods in Biomechanics* Human Kinetics, Champaign, IL 47-51.
14. Ender A, & Mehl A (2015) In-vitro evaluation of the accuracy of conventional and digital methods of obtaining full-arch dental impressions *Quintessence International* **46(1)** 9-17.
15. Fasbinder DJ, & Poticny DJ (2010) Accuracy of occlusal contacts for crowns with chairside CAD/CAM techniques

International Journal of Computerized Dentistry **13(4)** 303-316.

16. Nemli SK, Wolfart S, & Reich S (2012) InLab and Cerec Connect: Virtual contacts in maximum intercuspation compared with original contacts—An in vitro study *International Journal of Computerized Dentistry* **15(1)** 23-31.
17. Boyarsky HP, Loos LG, & Leknius C (1999) Occlusal refinement of mounted casts before crown fabrication to decrease clinical time required to adjust occlusion *Journal of Prosthetic Dentistry* **82(5)** 591-594.
18. Mehl A (2012) A new concept for the integration of dynamic occlusion in the digital construction process *International Journal of Computerized Dentistry* **15(2)** 109-123.
19. Solaberrieta E, Minguez R, Etxaniz O, & Barrenetxea L (2013) Improving the digital workflow: Direct transfer from patient to virtual articulator *International Journal of Computerized Dentistry* **16(4)** 285-292.

©Operative Dentistry, 2018, **43-6,** 581-592

Clinical Effectiveness of a Resin-modified Glass Ionomer Cement and a Mild One-step Self-etch Adhesive Applied Actively and Passively in Noncarious Cervical Lesions: An 18-Month Clinical Trial

M Jassal • S Mittal • S Tewari

Clinical Relevance

Mild one-step self-etch adhesive can be an alternative to resin-modified glass ionomer cement with similar retention and improved esthetics in noncarious cervical lesions.

SUMMARY

Objectives: To evaluate the clinical effectiveness of two methods of application of a mild one-step self-etch adhesive and composite resin as compared with a resin-modified glass ionomer cement (RMGIC) control restoration in noncarious cervical lesions (NCCLs).

Methods: A total of 294 restorations were placed in 56 patients, 98 in each one of the following groups: 1) G-Bond active application combined with Solare-X composite resin (A-1SEA), 2) G-Bond passive application combined with Solare-X composite resin (P-1SEA), and 3) GC II LC RMGIC. The restorations were evaluated at baseline and after six, 12, and 18 months according to the FDI criteria for fractures/retention, marginal adaptation, marginal staining, postoperative sensitivity, and secondary caries. Cumulative failure rates were calculated for each criterion at each recall period. The effect of adhesive, method of application, and recall period were assessed. The Kruskal-Wallis test for intergroup comparison and Friedman and Wilcoxon signed ranks tests for intragroup comparison were used for each criterion (α=0.05).

Results: The retention rates at 18 months were 93.26% for the A-1SEA group, 86.21% for the P-

Monika Jassal, MDS, Department of Conservative Dentistry & Endodontics, Post Graduate Institute of Dental Sciences, Rohtak, Haryana, India

*Shweta Mittal, MDS, Department of Conservative Dentistry & Endodontics, Post Graduate Institute of Dental Sciences, Rohtak, Haryana, India

Sanjay Tewari, MDS, Department of Conservative Dentistry & Endodontics, Post Graduate Institute of Dental Sciences, Rohtak, Haryana, India

*Corresponding author: associate professor, Department of Conservative Dentistry & Endodontics, PGIDS, Rohtak, Haryana 124001, India; e-mail: shwetagoelendo@gmail.com

DOI: 10.2341/17-147-C

1SEA group, and 90.91% for the RMGIC group. The active application improved the retention rates compared with the passive application of mild one-step self-etch adhesive; however, no statistically significant difference was observed between the groups. Marginal staining was observed in 13 restorations (1 in A-1SEA, 4 in P-1SEA, and 8 in RMGIC) with no significant difference between the groups. The RMGIC group showed a significant increase in marginal staining at 12 and 18 months from the baseline. There was no significant difference between the groups for marginal adaptation, secondary caries, or postoperative sensitivity.

Conclusion: Within the limitations of the study, we can conclude that mild one-step self-etch adhesive followed by a resin composite restoration can be an alternative to RMGIC with similar retention and improved esthetics in restoration of NCCLs. Agitation could possibly benefit the clinical performance of mild one-step self-etch adhesives, but this study did not confirm that the observed benefit was statistically significant.

INTRODUCTION

Noncarious cervical lesions (NCCLs) have become a well-known clinical entity presenting as noncarious loss of tooth substance with multifactorial etiology.[1] Restoration of such lesions becomes necessary in cases of sensitivity, esthetics, and plaque retention and where the tooth has to serve as an abutment for a removable partial denture. A variety of tooth-colored adhesives have been used in the past for restoration of NCCLs, such as glass ionomer cements (GICs), resin-based composite systems, and compomers.[2] With the development of resin-based adhesives, a number of materials have been tried from the conventional three-step etch-and-rinse to the most recent self-etch systems. The self-etch approach involves either a one-step or a two-step application procedure and can be further divided into "strong" with pH about 1 or below and "mild" with pH about 2 or greater.[3]

One-step self-etch adhesive systems have evolved as simplified adhesive systems with less technique sensitivity and shorter application time.[3,4] However, some studies have reported poor bond strength values, hydrolytic instability with time, and inferior marginal adaptation of one-step self-etch adhesives to enamel and dentin when compared with the two-step self-etch or etch-and-rinse systems.[4-9] On the other hand, some recent studies showed their satisfactory clinical performance.[10-16] This may be because of the development of new versions of one-step self-etch systems, especially the milder ones, which show bonding performance, almost comparable to the multistep gold standard approaches.[17]

In the past decade, some *in vitro* studies reported that by active application (agitation) of primer/adhesive, the bond strength of self-etch adhesives to enamel[18-20] and dentin[20-26] can be improved. This might be because of the active primer application that improves the smear layer dissolution, micromechanical interlocking, and chemical interaction with the dentin.[7,26,27]

In an *in vivo* study, Tewari and Goel[28] evaluated the effect of agitation and drying time of a mild two-step self-etch system on dentin bond strength. Agitation of primer along with adequate drying time improved the shear bond strength of adhesive to the dentin. However, clinical trials are necessary to verify the effectiveness of adhesive application methods in the oral environment over a period of time.

To our knowledge, there are only two studies that have evaluated the effect of active application of adhesive systems in a clinical scenario. Loguercio and others,[29] in a two-year clinical study showed that the application of a two-step etch-and-rinse system in a vigorously rubbing motion improved the retention of restorations in NCCLs. Similarly, in a recent clinical trial by Zander-Grande and others,[30] active application of two strong one-step self-etch adhesives improved the retention rates of cervical restorations compared with the passive application at a two year recall. However, no study has yet clinically evaluated the effect of agitation using mild one-step self-etch adhesives in restoration of NCCLs.

In a recent literature review of contemporary adhesives,[17] GICs showed the best clinical results in terms of retention in restoration of NCCLs when compared with the other adhesive categories. Despite this, glass ionomers commonly present with lower esthetic features (higher surface roughness, lower color stability, and lower wear resistance) and inferior mechanical properties when compared with the resin-based restorative materials.[31]

Besides micromechanical interlocking through hybridization, the chemical interaction between functional monomer and tooth substrate has an added advantage in improving the bonding potential of the adhesives.[32] The functional monomers in mild

self-etch systems result in superficial demineralization, keeping residual hydroxyapatite still attached to the collagen, and they have the potential to chemically interact with the hydroxyapatite.[3,17,27] Although the chemical bonding mechanism and one-step procedure of RMGIC is similar to mild one-step self-etch adhesives, there is a void in the literature as to the clinical comparison of these two materials. We could speculate that the new versions of mild one-step self-etch adhesives with a resin composite restoration would provide bonding performance comparable with GIC and with the esthetics of resin composites.

Thus, the aim of this randomized clinical study was to evaluate the influence of the application method of a mild one-step self-etch adhesive in restoration of NCCLs and also to compare it with a resin-modified GIC. The null hypothesis was that the clinical performance of both the materials is similar after 18 months of clinical service regardless of the method of application.

METHODS AND MATERIALS

Study Design and Participant Selection

The experimental design of our study followed the CONSORT statement. This randomized double-blind clinical trial was approved by the institutional ethical committee (PGIDS/IEC/2015/62). Written and informed consent was obtained from each patient after explaining the study procedure in his or her own language.

Inclusion and Exclusion Criteria

The study population included patients referred for the treatment of noncarious cervical lesions. These patients were screened by an experienced and calibrated examiner for noncarious cervical lesions to be included in the study as per specified inclusion and exclusion criteria. Healthy patients with an acceptable oral hygiene and age greater than 18 years who were willing to participate in the study and had at least 20 teeth in occlusion were included. Each patient had at least three noncarious cervical lesions to be restored in three different teeth. Lesions had to be noncarious, nonretentive, and $\geq$1 mm in depth and have a cavosurface margin not involving >50% of enamel. Lesions had to involve both enamel and dentin of vital teeth without mobility. Patients with extremely poor oral hygiene, severe periodontal disease, rampant caries, or a heavy bruxism habit were excluded.

Sample Size Calculation

The retention rate of a mild one-step self-etch adhesive, G-Bond, was reported to be 98%[13] after 1 year of clinical service. With an α of 0.05, a power of 80%, and a two-sided test, the minimal sample size of 98 restorations per group was calculated to detect a difference of 10% among the tested groups.[33]

Randomization

Randomization was carried out to balance the distribution of restorative treatment among the groups. The lesions were randomly, but consecutively, restored with each of the materials until 294 restorations were placed. When a patient presented, the teeth were restored starting from the upper right quadrant followed by upper left, lower left, and finally lower right quadrant using FDI notation for tooth identification. For a new patient, the material used to restore the first tooth was taken from the list for the next restoration. Each patient received at least three restorations, one from each of the three study groups. In some cases, more lesions were restored but not always in equal numbers.[34]

Restorative Procedure

All patients were given oral hygiene instructions before starting the operative treatment. Preoperative photograph of the lesions were taken. Before starting the treatment, some features of NCCLs were recorded as described in Table 1. The cavity dimensions in millimeters (cervicoincisal height and buccolingual depth), the geometry of the cavity (evaluated by adapting a wire along the inner walls of the cavity and then measuring the angle as <90°, 90-135°, and >135°) and presence of antagonist were recorded. The preoperative sensitivity was also evaluated by applying air from a dental syringe placed 2 cm from the tooth surface. Degree of sclerotic dentin of the lesions was measured according to the criteria described by Swift and others.[34] Lesions were then cleaned with a slurry of pumice and water on a slow rotating rubber cup in a slow-speed hand piece, rinsed, and dried. The appropriate shade of the resin composite was determined. Isolation was performed with cotton rolls and gingival retraction cord. No additional retention or bevel was given as per the guidelines recommended by the American Dental Association (ADA).[36] A mild one-step self-etch adhesive (G Bond, GC, Tokyo, Japan) with a resin composite (Solare-X, GC, Tokyo, Japan) or a resin-modified GIC (GC II LC Gold Label, GC, Tokyo, Japan) was used for restoration of the lesions. Teeth were then

Table 1: *Demographic Characteristics of Research Subjects and Characteristics and Distribution of Noncarious Cervical Lesions*

Characteristic	No. of Patients		
Gender distribution			
Male	44		
Female	12		
Age distribution, y			
30-39	4		
40-49	12		
50-59	14		
60-69	21		
70-79	5		
	Characteristics and Distribution of Noncarious Cervical Lesions		
	Group 1 (A-1SEA)	Group 2 (P-1SEA)	Group 3 (RMGIC)
Tooth distribution			
Incisors	15	13	14
Canines	20	10	10
Premolars	48	58	60
Molars	15	17	14
Shape/degree of angle			
<90	87	92	93
90-135	11	6	5
>135	0	0	0
Cervicoincisal height			
<1.5	10	11	7
1.5-2.5	51	47	47
>2.5	37	40	44
Degree of sclerotic dentin			
1	35	30	32
2	47	46	41
3	12	21	21
4	4	1	4
Buccolingual depth, mm			
1-2	86	89	95
2.1-3	12	9	3
Preoperative sensitivity			
Yes	7	5	6
No	91	93	92
Arch distribution			
Maxillary	64	57	57
Mandibular	34	41	41
Presence of antagonist			
Yes	95	96	94
No	3	2	4

randomly allocated to any of the three groups, namely, resin-modified GIC (RMGIC), mild one-step self-etch adhesive passive application (P-1SEA), and mild one-step self-etch adhesive active application (A-1SEA). The procedure for restoration placement was as per the manufacturer's instructions as follows (Table 2):

1. RMGIC group: A dentin conditioner (GC) was applied to the bonding surface for 10 seconds with a cotton pellet, washed, and dried. The RMGIC was then applied and light cured for 40 seconds. The cured restoration was then coated with a bonding agent (Tetric N-bond, Ivoclar Vivadent AG, Schaan, Liechtenstein) and light cured before and after polishing to prevent desiccation.
2. P-1SEA group: The adhesive was spread over the entire lesion surface and left undisturbed for 5-10 seconds, air dried for five seconds, and then light cured for 10 seconds.
3. A-1SEA group: The adhesive was applied rigorously for five seconds using a microbrush and left undisturbed for 5-10 seconds, air dried for five seconds, and light cured for 10 seconds.

After adhesive application in groups 2 and 3, the lesions were incrementally restored with appropriate shade of the resin composite and cured using light-emitting diode (LUX V curing light, Guilin Woodpecker Medical Instruments Co Ltd, China).

All restorations were finished and polished using abrasive discs (Super-Snap, SHOFU Inc, Kyoto, Japan) a week after placing the restorations. At this visit, baseline records of the restorations were also recorded. Clinical examination records and photographs at 1:1 magnification were taken at baseline and at every follow-up visit.[34]

Restoration Evaluation

Clinical evaluation was done by two experienced examiners who were familiar with the evaluation criteria and who were not involved in the placement of the restorations and thus were blinded to the group assignment. For training purposes, the examiners observed 10 photographs that were representative of each score for each criterion. They evaluated 10 to 15 teeth in two different clinical appointments. The intraexaminer and interexaminer agreement of at least 85% was necessary before beginning the evaluation. The restorations were evaluated at baseline and after 6, 12, and 18 months of clinical service. At each recall visit, the restorations were assessed using a dental operating microscope at 1× magnification (OPMI Pico, Carl Zeiss Surgical GmbH, Germany) according to the FDI World Dental Federation criteria described by Hickel and others.[37] The primary outcome variable evaluated was fractures/retention of the restoration. The

Table 2: *Materials, Manufacturers, Lot Number, and Application Techniques*

Material	Category	Mode of Application
G-Bond (GC, Tokyo, Japan), Lot no. 1411121	One-step self-etch adhesive with pH=2	Passive application: Apply adhesive gently over bonding surface and leave undisturbed for 5-10 s, air dry for 5 s, and light cure for 10 s
		Active application: Apply adhesive rigorously for 5 s using microbrush and leave undisturbed for 5-10 s, air dry for 5 s, and light cure for 10 s
Solare-X (GC, Tokyo, Japan), Lot no. 1309041	Light-cured resin composite	After adhesive application, resin composite was placed in 1-mm increments and cured for 20 s
GC Dentin Conditioner (GC, Tokyo, Japan), Lot no. 1401161	Polyacrylic acid conditioner	Apply to bonding surface for 10 s with a cotton pellet, wash/dry but do not desiccate, then apply light-cured GIC
GC 2 LC Gold Label Light-Cured Glass Ionomer Universal Restorative (GC, Tokyo, Japan), Lot no. 1405201	Light-cured GIC	Place dentin conditioner for 10 s, wash/dry, place RMGIC, light cure for 40 s

secondary outcome variables such as marginal staining, marginal adaptation, postoperative sensitivity, and secondary caries were also evaluated. For each evaluated criteria, scoring ranges from 1 (very good), 2 (good, after correction very good), 3 (sufficient/satisfactory, minor shortcomings), 4 (unsatisfactory, but repairable) to 5 (poor, replacement necessary). Restorations with scores 1 to 3 in each evaluated criteria were considered acceptable (success). Restorations rated 4 or 5 were classified as clinically unacceptable (failure), excluded from further assessment, and were repaired or replaced.

Statistical Analysis

Statistical analysis was performed for each criterion in IBM SPSS Statistics version 20 software. Descriptive statistics were used to describe the distributions of the evaluated criteria. The statistical analysis followed the intention-to-treat protocol, which included all teeth in their originally randomized groups, even those that were not able to be analyzed during the scheduled recall visits. In this case, the missing data are filled by carrying the last observed value of such teeth.[38] This approach is more conservative and less open to bias.

The Kruskal Wallis test was used for intergroup comparison among the three groups for each criterion, and the p-value <0.05 was considered to be statistically significant. The difference in the performance of each group at baseline and after each recall visit (6, 12, and 18 months) was assessed by Friedman and Wilcoxon signed ranks tests (α=0.05). To determine the strength of patient factors such as tooth type, location, size and shape of the lesion, and dentinal sclerosis, the logistic regression was applied on success and failure of each evaluated criteria.

The restoration failure rates were calculated for each criterion at each recall period as follows:

$$Failure\,percentage = \frac{F(previous) + F(current)}{F(previous) + N(current)} \times 100$$

whereby *F (previous)* represents the previous failures before the current recall examination, *F (current)* represents the number of failures seen in current recall, and *N (current)* represents the total number of restorations seen in the current recall.[36]

RESULTS

Initially, 80 patients were screened for the study, of which 24 were excluded (14 did not meet the inclusion criteria and 10 refused to participate). Thus, 56 patients (44 men and 12 women) with a mean age of 54 years were enrolled in the study. A total of 294 restorations were placed, 98 in each of the three groups involved in the study (Figure 1). The characteristics and distribution of NCCLs in each group are presented in Table 1. At baseline, all restorations were 100% successful with regard to the criteria evaluated (fractures/retention, marginal adaptation, marginal staining, secondary caries, and postoperative sensitivity).

The overall recall rate at 18 months was 90.81% (267 restorations out of 294). A total of nine restorations in the A-1SEA group, eight restorations in the P-1SEA group, and 10 restorations in the RMGIC group could not be evaluated as the patients moved and did not return for follow-up evaluation.

Functional Criteria

From the cumulative failure rates, the retention rates calculated for each group at 6, 12, and 18

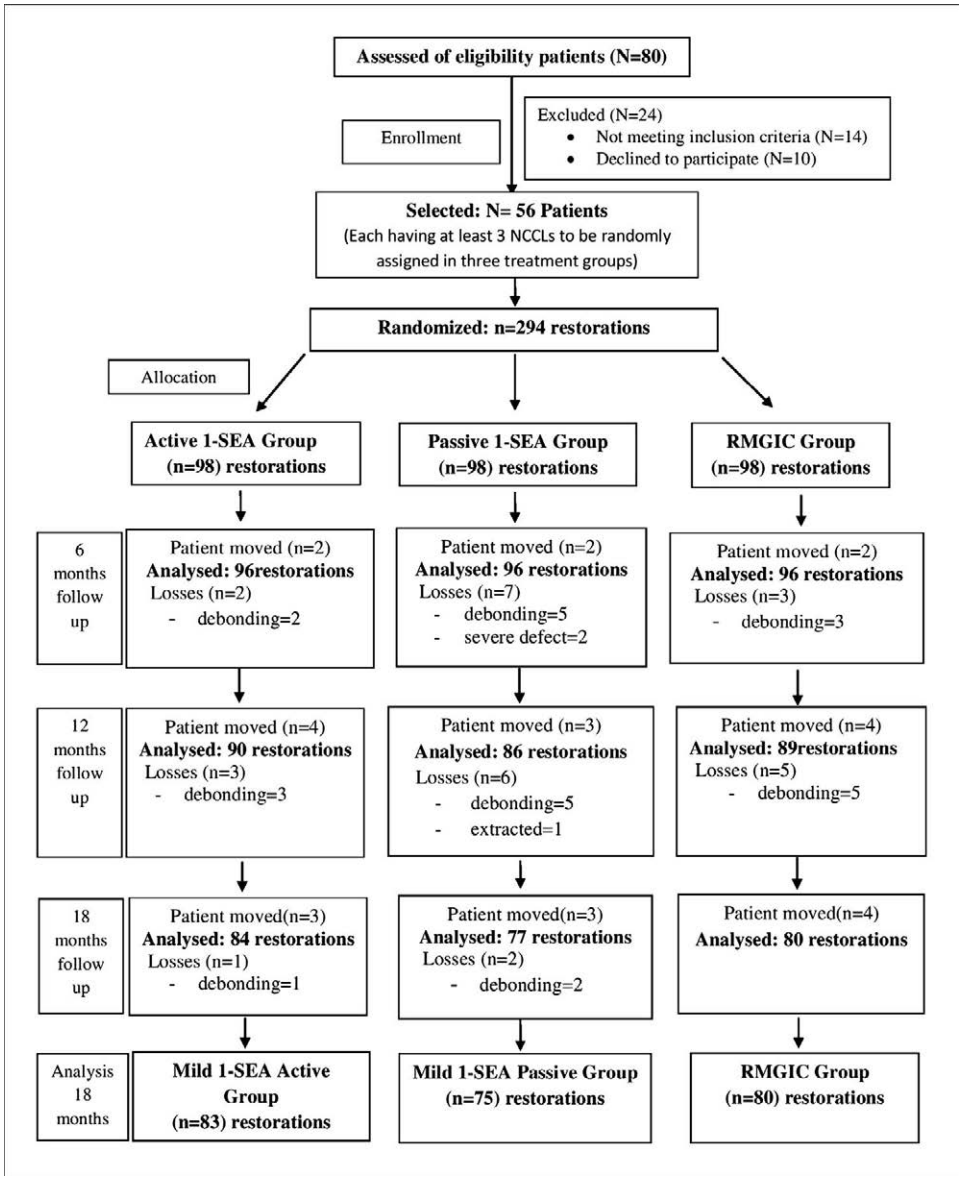

Figure 1. *Consort flow diagram of participants throughout the trial.*

months were 97.92%, 94.57%, and 93.26% for the A-1SEA group; 94.80%, 89.02%, and 86.21% for the P-1SEA group; and 96.87%, 91.31%, and 90.91% for the RMGIC group, respectively.

A total of six restorations from the A-1SEA group, 12 restorations from the P-1SEA group, and eight restorations from the RMGIC group were rated as clinically unacceptable during the 18-month follow-up period (Table 3). There was no statistically significant difference among the three groups with regard to the fractures/retention scores ($p>0.05$). However, when analyzing within the group, the factor recall period was statistically significant in all the groups at 12 and 18 months when compared with the baseline, except for the P-1SEA group, where it was significant at six months also ($p<0.05$).

With regard to the marginal adaptation, only one restoration in the P-1SEA group had clinically unacceptable results at six months, which needed to be replaced; however, the results were not statistically significant between the groups and within the groups ($p>0.05$).

Esthetic Criteria

Marginal staining was noted in one restoration of the A-1SEA group, four restorations of the P-1SEA group, and eight restorations of the RMGIC group during the 18-month follow-up period. Of these, 12 restorations were rated as clinically acceptable;

Table 3: *Number of Restorations Evaluated in Each Group at Each Recall Period According to the FDI Criteria*[37]

FDI Criteria	Score	Baseline			6 mo			12 mo			18 mo		
		A-1SEA	P-1SEA	RMGIC	A-1SEA	P-1SEA	RMGIC	A-1SEA	P-1SEA	RMGIC	A-1SEA	P-1SEA	RMGIC
Marginal Staining	VG	98	98	98	96	92	92	93	87	84	91	82	82
	GO	—	—	—	—	—	—	—	—	—	—	—	—
	SS	—	—	—	—	—	3	—	—	6	1	3	8
	UN	—	—	—	—	1	—	—	1	—	—	1	—
	PO	—	—	—	—	—	—	—	—	—	—	—	—
Fractures and retention	VG	98	98	98	96	92	95	93	87	90	92	85	90
	GO	—	—	—	—	—	—	—	—	—	—	—	—
	SS	—	—	—	—	1	—	—	1	—	—	1	—
	UN	—	—	—	—	—	—	—	—	—	—	—	—
	PO	—	—	—	2	5	3	5	10	8	6	12	8
Marginal adaptation	VG	98	98	98	96	92	95	93	87	90	92	85	90
	GO	—	—	—	—	—	—	—	—	—	—	—	—
	SS	—	—	—	—	—	—	—	—	—	—	—	—
	UN	—	—	—	—	1	—	—	1	—	—	1	—
	PO	—	—	—	—	—	—	—	—	—	—	—	—
Postoperative sensitivity	VG	98	98	98	96	93	95	93	88	90	92	86	90
	GO	—	—	—	—	—	—	—	—	—	—	—	—
	SS	—	—	—	—	—	—	—	—	—	—	—	—
	UN	—	—	—	—	—	—	—	—	—	—	—	—
	PO	—	—	—	—	—	—	—	—	—	—	—	—
Secondary caries	VG	98	98	98	96	93	95	93	88	90	92	86	90
	GO	—	—	—	—	—	—	—	—	—	—	—	—
	SS	—	—	—	—	—	—	—	—	—	—	—	—
	UN	—	—	—	—	—	—	—	—	—	—	—	—
	PO	—	—	—	—	—	—	—	—	—	—	—	—

Abbreviations: VG, clinically very good; GO, clinically good; SS, clinically sufficient/satisfactory; UN, clinically unsatisfactory; PO, clinically poor.

however, severe marginal staining was reported in one restoration of the P-1SEA group that was replaced. There was no statistically significant difference for marginal staining among the three groups tested ($p>0.05$). However, the factor recall period was statistically significant in the RMGIC group at 12 and 18 months compared with the baseline and at six months ($p<0.05$), as shown in Figure 2.

Biological Criteria

No postoperative sensitivity or secondary caries was present in any group over the period of 18 months.

Overall Analysis

Overall clinical success was not significantly different among the groups. It was 93.26% for the A-1SEA group, 84.27% for the P-1SEA group, and 90.91% for the RMGIC group (Table 4). A total of 28 restorations failed over the 18-month period (26 due to retention loss, one due to deficient margins, and one due to severe staining). Lack of retention was the main factor for overall failure of the restorations.

No correlation was found between the clinical performance of the restorations and the tooth type, location, size and shape of the lesion, and dentinal sclerosis.

DISCUSSION

NCCLs are a frequent clinical presentation with multifactorial etiology and increased prevalence with age.[39,40] In these class V cavities, the lack of macromechanical retention and small C-factor minimizes the role of material properties such as polymerization shrinkage, and thus, restoration success mainly relies on the actual bonding potential of the material. GICs are the most preferred material because of their high retention rates and ease of use.[2] However, their major shortcomings are poor surface qualities, marginal staining, and bulk discoloration.[31,41] So there is always a quest for finding a simpler, less technique sensitive material

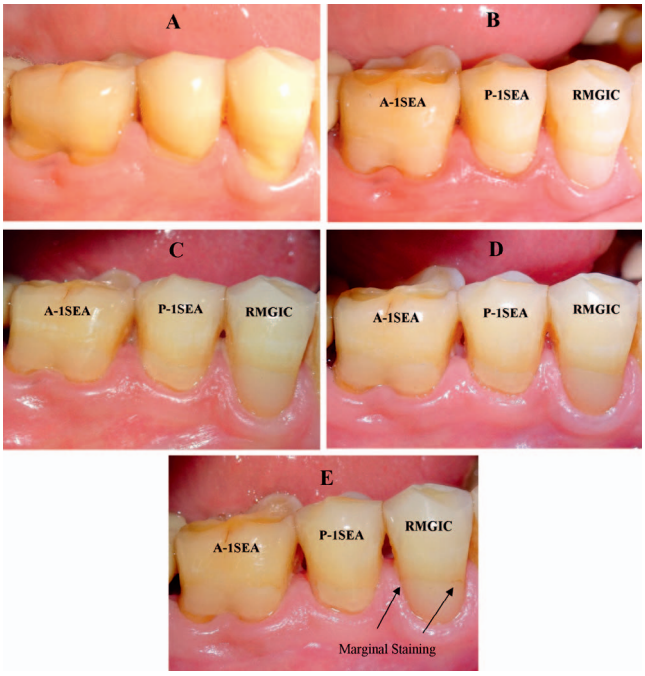

Figure 2. *(A): Preoperative view of NCCLs. (B) Postoperative view at baseline. At 6 months (C), at 12 months (D), and at 18 months (E), marginal staining was observed in the RMGIC group. Arrows points to regions of marginal discoloration.*

with durable bonding and esthetics for restoration of NCCLs.

A mild one-step self-etch adhesive was selected in the present study because in addition to its single-step procedure, better laboratory and clinical performance was observed compared with the more acidic versions.[5,42-48] G- Bond contains 4-META (4-methacryloxyethyl trimellitic acid) and a phosphate ester as functional monomers,[49,50] which are able to form a chemical bond with the hydroxyapatite of the tooth.[32] Long-term durability of adhesive-dentin bonds also depends on the chemical bonding potential of the functional monomer.[51] An RMGIC was used as a control because of its high long-term retention rates in NCCLs, as observed in a recent literature review by Peumans and others.[17]

In our study, the retention rates at 18 months for the A-1SEA, P-1SEA, and RMGIC groups were 93.26%, 86.21%, and 90.91%, respectively. The fractures/retention scores showed no statistically significant difference between the three groups tested ($p>0.05$) during the 18-month period. This may be because of the similar bonding mechanisms of both the materials to the tooth structure.[3,27,32] In addition to their micromechanical retention, both have the chemical bonding potential to the tooth.[3] Both interact superficially with dentin and do not completely dissolve hydroxyapatite crystals around the collagen, leaving them for chemical bonding. Previous clinical trials found inferior performance of one-step self-etch adhesives in terms of retention compared with the RMGICs.[52-57] These studies, however, used strong self-etch adhesives, which were observed to have low bond strength values, especially to dentin.[5,42-45] With strong self-etch adhesives, all the hydroxyapatite nearly dissolves around the collagen, and bonding primarily is diffusion based.[3]

The retention rates for G-Bond in our study were reported to be lower than in the previous studies.[12,13,58-61] Those studies placed restorations either

Table 4: *Clinical Quality of the Restorations in Percentage From Baseline to 18 Months According to FDI Criteria*[37]

Recall Period	At Baseline			At 6 mo			At 12 mo			At 18 mo		
Group	A-1SEA	P-1SEA	GIC	A-1SEA	P-1SEA	GIC	A-1SEA	P-1SEA	GIC	A-1SEA	P-1SEA	GIC
Number of restorations, n	98	98	98	96	96	96	90	86	89	84	77	80
Recall rate, %	100	100	100	97.96	97.96	97.96	93.88	94.89	93.88	90.82	91.84	89.80
Esthetic score (cumulative)												
Acceptable, %	100	100	100	100	98.96	100	100	98.85	100	100	98.72	100
Nonacceptable, %	0.0	0.0	0.0	0.0	1.04	0.0	0.0	1.15	0.0	0.0	1.28	0.0
Functional score (cumulative)												
Acceptable, %	100	100	100	97.92	93.75	96.87	94.57	88.05	91.31	93.26	85.23	90.91
Nonacceptable, %	0.0	0.0	0.0	2.08	6.25	3.13	5.43	11.95	8.69	6.74	14.77	9.09
Biological score (cumulative)												
Acceptable, %	100	100	100	100	100	100	100	100	100	100	100	100
Nonacceptable, %	0.0	0.0	0.0	0.0	0.0	0.0	0.0	0.0	0.0	0.0	0.0	0.0
Overall score (cumulative)												
Acceptable, %	100	100	100	97.92	92.71	96.87	94.57	87.1	91.31	93.26	84.27	90.91
Nonacceptable, %	0.0	0.0	0.0	2.08	7.29	3.13	5.43	12.90	8.69	6.74	15.73	9.09

after roughening the cavity surface and placing an enamel bevel or after enamel etching with phosphoric acid, which could be a factor influencing the increased retention of the mild one-step self-etch adhesive.[62] However, as per recent ADA guidelines,[36] any surface treatment in the form of roughening or enamel beveling was not done in our study.

Laboratory studies on enamel[18-20] and dentin[20-24,26] using simplified self-etch adhesives found increased bond strength values with active application of adhesive. The authors concluded that active application may improve the bonding performance by smear layer dissolution, increased solvent evaporation, and carrying fresh monomer to the basal parts of etched dentin. This was also confirmed by two recent clinical trials employing a two-step etch-and-rinse system[29] and strong one-step self-etch systems.[30] However, a laboratory study by Zhang and Wang[25] did not find a significant effect of agitation on the degree of demineralization or degree of conversion of monomer for a mild self-etch adhesive. Instead, they attributed it to the adhesive's favorable pH value and composition, as monomer acidity has a negative influence on initiating efficacy of co-initiator in self-etch adhesive systems. When applied actively, we found increased retention rates for the mild one-step self-etch adhesive compared with the passive application, although not to a statistically significant level.

With regard to the marginal adaptation, all groups showed excellent results over the 18-month period. Only one restoration of the P-1SEA group displayed a severe marginal gap of >250 μm at six months, which may be because of technical error during placement of the restoration. These clinical results suggest that both materials are strong enough to withstand intraoral chewing stresses as well as expansion and contraction stresses by thermal changes to preserve the marginal integrity.[12]

Staining at restoration margins may result either due to deficiency or excess of the restorative material. Incomplete degree of conversion of monomer is another reason observed in self-etch adhesives because of their high water and hydrophilic monomer content.[63,64] Furthermore, marginal staining is also related to patient factors such as oral microflora and dietary habits.[49,65] Marginal staining was observed in one restoration of the A-1SEA group, four restorations of the P-1SEA group, and eight restorations of the RMGIC group. Most restorations displayed esthetically acceptable results during the 18-month period, with no significant difference between the groups tested. The active application group displayed less marginal staining compared with the passive application. The active application of adhesive with a microbrush might have resulted in better smear layer removal and enhanced demineralization of the surface layer. It might have allowed better penetration of the monomer with resultant improved marginal characteristics.

The RMGIC group showed significantly progressive yet acceptable marginal staining at 18 months when compared with baseline. Our results were similar to the studies that observed an increase in marginal staining in RMGICs over the same period of time.[55,65-69] Despite the excellent retention in NCCLs, RMGICs were commonly observed to show more water sorption and lower esthetic results compared with resin-based restorative materials.[62,66] In contrast, G-Bond showed no significant increase in marginal staining over the period of 18 months. Being HEMA free, it is reported to have the advantage of decreased water sorption and hydrolytic degradation with time.[70,71]

We found no postoperative sensitivity or secondary caries in any of the groups tested. This is believed to be a result of the ability of the adhesives to seal the dentinal tubules and reduce microleakage. Other studies also reported similar results.[12,13,31] Our study found no correlation between the performance of NCCL restorations and tooth type, location, or size and shape of the lesion. Also, the degree of dentin sclerosis was not found to affect the restorations in NCCLs.

The strength of the present study was that the comparison was done between the groups within the same patient, which ruled out inter-individual variance affecting the clinical performance of the adhesives. We used the FDI criteria introduced by Hickel and others,[37] which was found to be more sensitive than the USPHS criteria for short-term clinical evaluation of restorations, as proved by recent clinical trials by Mena-Serrano and others[72] and Lopes and others.[73] However, the limitation of our study was the short evaluation period of 18 months, so further long-term studies are required to evaluate the effectiveness of different application techniques on clinical performance of mild self-etch adhesives.

CONCLUSION

Within the limitations of the study, we can conclude that a mild one-step self-etch adhesive followed by a resin composite restoration can be an alternative to

RMGIC with similar retention and improved esthetics in restoration of NCCLs. Agitation could possibly benefit the clinical performance of mild one-step self-etch adhesives, but this study did not confirm that the observed benefit was statistically significant.

Regulatory Statement

This study was conducted in accordance with all the provisions of the local human subjects oversight committee guidelines and policies of the Post Graduate Institute of Dental Sciences institutional ethical committee. The approval code for this study is PGIDS/IEC/2015/62.

Conflict of Interest

The authors of this manuscript certify that they have no proprietary, financial, or other personal interest of any nature or kind in any product, service, and/or company that is presented in this article.

(Accepted 14 December 2017)

REFERENCES

1. Osborne-Smith KL, Burke FJT, & Wilson NHF (1999) The aetiology of the non-carious cervical lesion *International Endodontic Journal* **49(3)** 139-143.
2. Pecie R, Krejci I, Garcia-Goddy F, & Bortolotto T (2011) Noncarious cervical lesions (NCCL)—a clinical concept based on the literature review. Part 2: restoration *American Journal of Dentistry* **24(3)** 183-192.
3. Van Meerbeek B, De Munck J, Yoshida Y, Inoue S, Vargas M, Vijay P, Van Landuyt K, Lambrechts P, & Vanherle GB (2003) Buonocore memorial lecture. Adhesion to enamel and dentin: current status and future challenges *Operative Dentistry* **28(3)** 215-235.
4. Peumans M, Kanumilli P, De Munck J, Van Landuyt K, Lambrechts P, & Van Meerbeek B (2005) Clinical effectiveness of contemporary adhesives: a systematic review of current clinical trials *Dental Materials* **21(9)** 864-881.
5. Inoue S, Vargas MA, Abe Y, Yoshida Y, Lambrechts P, Vanherle G, Sano H, & Van Meerbeek B (2001) Microtensile bond strength of eleven contemporary adhesives to dentin *Journal of Adhesive Dentistry* **3(3)** 237-245.
6. Frankenberger R, & Tay FR (2005) Self-etch vs etch-and-rinse adhesives: effect of thermo-mechanical fatigue loading on marginal quality of bonded resin composite restorations *Dental Materials* **21(5)** 397-412.
7. Can Say E, Nakajima M, Senawongse P, Soyman M, Ozer F, Ogata M, & Tagami J (2006) Microtensile bond strength of a filled vs unfilled adhesive to dentin using self-etch and total-etch technique *Journal of Dentistry* **34(4)** 283-291.
8. Sarr M, Kane AW, Vreven J, Mine A, Van Landuyt KL, Peumans M, Lambrechts P, Van Meerbeek B, & De Munck J (2010) Microtensile bond strength and interfacial characterization of 11 contemporary adhesives bonded to bur-cut dentin *Operative Dentistry* **35(1)** 94-104.
9. Heintze SD, Ruffieux C, & Rousson V (2010) Clinical performance of cervical restorations- a meta-analysis *Dental Materials* **26(10)** 993-1000.
10. Burgess JO, Sadid-Zadeh R, Cakir D, & Ramp LC (2013) Clinical evaluation of self-etch and total-etch adhesive systems in non-carious cervical lesions *Operative Dentistry* **38(5)** 477-487.
11. Moosavi H, Kimyai S, Forghani M, & Khodadadi R (2013) The clinical effectiveness of various adhesive systems: an 18-month evaluation *Operative Dentistry* **38(2)** 134-141.
12. Van Dijken JWV (2013) A randomized controlled 5-year prospective study of two HEMA-free adhesives, a 1-step self etching and a 3-step etch-and-rinse, in non-carious cervical lesions *Dental Materials* **29(11)** e271-e280.
13. Van Landyut KL, De Munck J, Ermis RB, Peumans M, & Van Meerbeek B (2014) Five year clinical performance of a HEMA-free one step self-etch adhesive in noncarious cervical lesions *Clinical Oral Investigations* **18(4)** 1045-1052.
14. Brackett MG, Dib A, Franco G, Estrada BE, & Brackett WW (2010) Two-year clinical performance of Clearfil SE and Clearfil S3 in restoration of unabraded non-carious class V lesions *Operative Dentistry* **35(3)** 273-278.
15. Ermis RB, Van Landuyt KL, Cardoso MV, De Munck J, Van Meerbeek B, & Peumans M (2012) Clinical effectiveness of a one-step self-etch adhesive in non-carious cervical lesions at 2 years *Clinical Oral Investigations* **16(3)** 889-897.
16. Häfer M, Jentsch H, Haak R, & Schneider H (2015) A three-year clinical evaluation of a one-step self-etch and a two-step etch-and-rinse adhesive in non-carious cervical lesions *Journal of Dentistry* **43(3)** 350-361.
17. Peumans M, De Munck J, Mine A, & Van Meerbeek B (2014) Clinical effectiveness of contemporary adhesives for the restoration of non-carious cervical lesions: a systematic review *Dental Materials* **30(10)** 1089-1103.
18. Ando S, Watanabe T, Tsubota K, Yoshida T, Irokawa A, Takamizawa T, Kurokawa H, & Miyazaki M (2008) Effect of adhesive application methods on bond strength to bovine enamel *Journal of Oral Sciences* **50(2)** 181-186.
19. Torres CR, Barcellos DC, Pucci CR, Lima G de M, Rodrigues CM, & Siviero M (2009) Influence of methods of application of self-etching adhesive systems on adhesive bond strength to enamel *Journal of Adhesive Dentistry* **11(4)** 279-286.
20. Velasquez LM, Sergent RS, Burgess JO, & Mercante DE (2006) Effect of placement agitation and placement time on the shear bond strength of 3 self-etching adhesives *Operative Dentistry* **31(4)** 426-430.
21. Amaral RC, Stanislawczuk RG, Zander-Grande C, Gagler D, Reis A, & Loguercio AD (2010) Bond strength and quality of the hybrid layer of one-step self-etch adhesives applied with agitation on dentin *Operative Dentistry* **35(2)** 211-219.
22. Amaral RC, Stanislawczuk R, Zander-Grande C, Michel MD, Reis A, & Loguercio AD (2009) Active application improves the bonding performance of self etch adhesives to dentin *Journal of Dentistry* **37(1)** 82-90.

23. Loguercio AD, Stanislawczuk R, Meena-Serrano A, & Reis A (2011) Effect of 3-year water storage on the performance of one-step self-etch adhesives applied actively on dentin *Journal of Dentistry* **39(8)** 578-587.
24. Dal-Bianco K, Pellizzaro A, Patzlaft R, de Oliveira Bauer JR, Loguercio AD, & Reis A (2006) Effects of moisture degree and rubbing action on the immediate resin-dentin bond strength *Dental Materials* **22(12)** 1150-1156.
25. Zhang Y, & Wang Y (2013) Effect of application mode on interfacial morphology and chemistry between dentin and self-etch adhesives *Journal of Dentistry* **41(3)** 231-240.
26. Miyazaki M, Platt JA, Onose H, & Moore BK (1996) Influence of dentin primer application methods on dentin bond strength *Operative Dentistry* **21(4)** 167-172.
27. Van Meerbeek B, Yoshihara K, Yoshida Y, Mine A, De Munck J, & Van Landuyt KL (2011) State the art of self-etch adhesives *Dental Materials* **27(1)** 17-28.
28. Tewari S, & Goel A (2009) Effect of placement agitation and drying time on dentin shear bond strength: an *in vivo* study *Operative Dentistry* **34(5)** 524-530.
29. Loguercio AD, Raffo J, Bassani F, Balestrini H, Santo D, do Amaral RC, & Reis A (2011) 24-month clinical evaluation in non-carious cervical lesions of a two-step etch-and-rinse adhesive applied using a rubbing motion *Clinical Oral Investigations* **15(4)** 589-596.
30. Zander-Grande C, Amaral RC, Loguercio AD, Barroso LP, & Reis A (2014) Clinical performance of one-step self-etch adhesives applied actively in cervical lesions: 24-month clinical trial *Operative Dentistry* **39(3)** 228-238.
31. Sidhu SK (2010) Clinical evaluations of resin-modified glass-ionomer restorations *Dental Materials* **26(1)** 7-12.
32. Yoshida Y, Nagakane K, Fukuda R, Nakayama Y, Okazaki M, Shintani H, Inoue S, Tagawa Y, Suzuki K, De Munck J, & Van Meerbeek B (2004) Comparative study on adhesive performance of functional monomers *Journal of Dental Research* **83(6)** 454-458.
33. Pocock SJ (1983) The size of a clinical trial. In: Pocock SJ (ed) *Clinical Trials: A Practical Approach* John Wiley & Sons, Chichester, UK 123-141.
34. Ritter AV, Heymann HO, Swift EJ Jr, Sturdevant JR, & Wilder AD Jr (2008) Clinical evaluation of an all-in-one adhesive in non-carious cervical lesions with different degrees of dentin sclerosis *Operative Dentistry* **33(4)** 370-378.
35. Burrow MF, & Tyas MJ (2007) Clinical evaluation of three adhesive systems for the restoration of non-carious cervical lesions *Operative Dentistry* **32(1)** 11-15.
36. American Dental Association Council on Scientific Affairs (2011) *Acceptance Program Guidelines: Dentin & Enamel Adhesive Materials* American Dental Association, Chicago Ill.
37. Hickel R, Roulet JF, Bayne S, Heintze SD, Mjör IA, Peters M, Rousson V, Randall R, Schmalz G, Tyas M, & Vanherle G (2007) Recommendations for conducting controlled clinical studies of dental restorative materials *Clinical Oral Investigations* **11(1)** 5-33.
38. Schulz KF, Altman DG, Moher D; CONSORT Group (2011) CONSORT 2010 Statement: updated guidelines for reporting parallel group randomized trials *International Journal of Surgery* **9(8)** 672-677.
39. Grippo JO, Simring M, & Schreiner S (2004) Attrition, abrasion, corrosion and abfraction revisited: a new perspective on tooth surface lesions *Journal of American Dental Association* **135(8)** 1109-1118.
40. Aw TC, Lepe X, Johnson GH, & Mancl L (2002) Characteristics of noncarious cervical lesions: a clinical investigation *Journal of American Dental Association* **133(6)** 725-733.
41. Gladys S, Van Meerbeek B, Lambrechts P, & Vanherle G (1999) Evaluation of esthetic parameters of resin-modified glass-ionomer materials and a polyacid-modified resin composite in Class V cervical lesions *Quintessence International* **30(9)** 607-614.
42. Inoue S, Vargas MA, Abe Y, Yoshida Y, Lambrechts P, Vanherle G, Sano H, & Van Meerbeek B (2003) Microtensile bond strength of eleven modern adhesives to enamel *American Journal of Dentistry* **16(5)** 329-334.
43. De Munck J, Van Meerbeek B, Inoue S, Vargas M, Yoshida Y, Armstrong S, Lambrechts P, & Vanherle G (2003) Micro-tensile bond strength of one- and two-step self-etch adhesives to bur-cut enamel and dentin *American Journal of Dentistry* **16(6)** 414-420.
44. De Munck J, Shirai K, Yoshida Y, Inoue S, Van Landuyt KL, Lambrechts P, Suzuki K, Shintani H, & Van Meerveek B (2006) Effect of water storage on the bonding effectiveness of six adhesives to class I cavity dentin *Operative Dentistry* **31(4)** 456-465.
45. Shirai K, De Munck J, Yoshida Y, Inoue S, Lambrechts P, Suzuki K, Shintani H, & Van Meerveek B (2005) Effect of cavity configuration and aging on the bonding effectiveness of six adhesives to dentin *Dental Materials* **21(2)** 110-124.
46. Ernst CP, Brandenbusch M, Meyer GR, Canbek K, Werling U, & Willershausen B (2007) Hybrid bond and Xeno III in cervical lesions: two year results *Journal of Dental Research* **86(Special Issue A)** Abstract 895.
47. Walter R, Swift Jr EJ, Boushell LW, Heymann H, Wilder Jr AD, Sturdevant J, Ritter AV, & Chung Y (2013) Clinical evaluation of dental adhesives of different bonding strategies *Journal of Dental Research* **92(Special Issue A)** Abstract 605.
48. Kurokawa H, Takamizawa T, Rikuta A, Tsubota K, & Miyazaki M (2012) Long term clinical evaluation of one-step self-etch adhesive systems *Journal of Dental Research* **91(Special Issue A)** Abstract 803.
49. Burrow MF, & Tyas MJ (2007) Clinical trial of G-Bond all-in-one adhesive and Gradia Direct resin composite in non-carious cervical lesions—results at 1 year *Journal of Dentistry* **35(7)** 623-625.
50. Kubo S, Yokota H, Yokota H, & Hayashi Y (2009) Two-year clinical evaluation of one-step self-etch systems in non-carious cervical lesions *Journal of Dentistry* **37(2)** 149-155.
51. Inoue S, Koshiro K, Yoshida Y, De Munck J, Nagakane K, Suzuki K, Sano H, & Van Meerbeek B (2005) Hydrolytic stability of self-etch adhesives bonded to dentin *Journal of Dental Research* **84(12)** 1160-1164.

52. Abdalla AI, & Alhadainy HA (1997) Clinical evaluation of hybrid ionomer restoratives in class V abrasion lesions: two-year results *Quintessence International* **28(4)** 255-258.

53. Gladys S, Van Meerbeek B, Lambrechts P, & Vanherle G (1998) Marginal adaptation and retention of a glass-ionomer, resin-modified glass ionomers and a polyacid-modified resin composite in cervical Class-V lesions *Dental Materials* **14(4)** 294-306.

54. Ermis RB (2002) Two year clinical evaluation of four polyacid-modified resin composites and a resin-modified glass-ionomer cement in Class V lesions *Quintessence International* **33(7)** 542-548.

55. Loguercio AD, Reis A, Barbosa AN, & Roulet JF (2003) Five-year double blind randomized clinical evaluation of a resin-modified glass ionomer and a polyacid-modified resin in noncarious cervical lesions *Journal of Adhesive Dentistry* **5(4)** 323-332.

56. Onal B, & Pamir T (2005) The two-year clinical performance of esthetic restorative materials in non-carious cervical lesions *Journal of American Dental Association* **136(11)** 1547-1555.

57. Van Dijken JW, & Pallesen U (2008) Long term dentin retention of etch-and-rinse and self-etch adhesives and a resin-modified glass ionomer cement in non-carious cervical lesions *Dental Materials* **24(7)** 915-922.

58. Van Landuyt KL, Peumans M, Fieuws S, De Munck J, Cardoso MV, Ermis RB, Lambrechts P, & Van Meerbeek B (2008) A randomized controlled clinical trial of a HEMA-free all-in-one adhesive in non-carious cervical lesions at 1 year *Journal of Dentistry* **36(10)** 847-855.

59. Van Landuyt KL, Peumans M, De Munck J, Cardoso MV, Ermis RB, & Van Meerbeek B (2011) Three year clinical performance of a HEMA-free one-step self-etch adhesive in non-carious cervical lesions *European Journal of Oral Sciences* **119(6)** 511-516.

60. Burrow MF, & Tyas MJ (2012) Clinical investigation of G-bond resin-based adhesive to non-carious cervical lesions over five years *Australian Dental Journal* **57(4)** 458-463.

61. Moretto SG, Russo EM, Carvalho RC, De Munck J, Van Landuyt K, Peumans M, Van Meerbeek B, & Cardoso MV (2013) 3-year clinical effectiveness of one-step adhesives in non-carious cervical lesions *Journal of Dentistry* **41(8)** 675-682.

62. Mahn E, Rousson V, & Heintze S (2015) Meta-analysis of the influence of bonding parameters on the clinical outcome of tooth-colored cervical restorations *Journal of Adhesive Dentistry* **17(5)** 391-403.

63. Malacarne J, Carvalho RM, de Goes MF, Svizero N, Pashley DH, Tay FR, Yiu CR, & Carrilho MR (2006) Water sorption/solubility of dental adhesive resins *Dental Materials* **22(10)** 973-980.

64. Itoh S, Nakajima M, Hosaka K, Okuma M, Takahashi M, Shinoda Y, Seki N, Ikeda M, Kishikawa R, Foxton RM, & Tagami J (2010) Dentin bond durability and water sorption/solubility of one-step self-etch adhesives *Dental Materials Journal* **29(5)** 623-630.

65. Maneenut C, & Tyas MJ (1995) Clinical evaluation of resin-modified glass ionomer restorative cements in cervical "abrasion" lesions: one year results *Quintessence International* **26(10)** 739-743.

66. Small IC, Watson TF, Chadwick AV, & Sidhu SK (1998) Water sorption in resin-modified glass-ionomer cements: an *in vitro* comparison with other materials *Biomaterials* **19(6)** 545-550.

67. Ozgunaltay G, & Onen A (2002) Three year clinical evaluation of a resin modified glass-ionomer cement and a composite resin in non-carious class V lesions *Journal of Oral Rehabilitation* **29(11)** 1037-1041.

68. Smales RJ, & Ng KK (2004) Longevity of a resin-modified glass ionomer cement and a polyacid-modified resin composite restoring non-carious cervical lesions in a general practice *Australian Dental Journal* **49(4)** 196-200.

69. Chinelatti MA, Ramos RP, Chimello DT, & Palma-Dibb RG (2004) Clinical performance of a resin-modified glass ionomer and two polyacid-modified resin composites in cervical lesions restorations: 1-year follow up *Journal of Oral Rehabilitation* **31(3)** 251-257.

70. Yiu CK, King NM, Pashley DH, Suh BI, Carvalho RM, Carrilho MR, & Tay FR (2004) Effect of resin hydrophilicity and water storage on resin strength *Biomaterials* **25(26)** 5789-5796.

71. Torkabadi S, Nakajima M, Ikeda M, Foxton RM, & Tagami J (2008) Bonding durability of HEMA-free and HEMA-containing one-step adhesives to dentine surrounded by bonded enamel *Journal of Dentistry* **36(1)** 80-86.

72. Mena-Serrano A, Kose C, De Paula EA, Tay LY, Reis A, Loguercio AD, & Perdigão J (2013) A new universal simplified adhesive: 6-month clinical evaluation *Journal of Esthetic Restorative Dentistry* **25(1)** 55-69.

73. Lopes LS, Calazans FS, Hidalco R, Buitrago LL, Guitierrez F, Reis A, Loguercio AD, & Barceleiro MO (2016) Six month follow-up of cervical composite restorations placed with a new universal adhesive system: a randomized clinical trial *Operative Dentistry* **41(5)** 465-480.

©Operative Dentistry, 2018, **43-6,** 593-601

Laboratory Research

Effects of Manufacturing and Finishing Techniques of Feldspathic Ceramics on Surface Topography, Biofilm Formation, and Cell Viability for Human Gingival Fibroblasts

LPC Contreras • AMO Dal Piva • FC Ribeiro
LC Anami • SEA Camargo • AOC Jorge • MA Bottino

Clinical Relevance

For both stratified and machined porcelains, polishing as a finishing technique promotes smoother surfaces with higher surface free energy and decreasing microorganism adhesion.

SUMMARY

Purpose: Feldspathic ceramic restorations can be obtained by different techniques (stratification or computer-aided design/computer-aided manufacturing [CAD/CAM] blocks) and finishing procedures (polishing or glaze application). This study evaluated the effects of techniques and finishing procedures on surface properties, biofilm formation, and viability of human gingival fibroblasts (FMM-1) in contact with these materials.

Methods and Materials: Ceramic specimens were obtained through a stratification technique (Vita VM9) and from CAD/CAM blocks (Vita Blocs Mark II; both Vita Zahnfabrik) and

Lisseth Patricia Claudio Contreras, DDS, MSc, Institute of Science and Technology, São Paulo State University–Unesp, Department of Dental Materials and Prosthodontics, São José dos Campos, Brazil

Amanda Maria Oliveira Dal Piva, DDS, MSc, Department of Dental Materials and Prosthodontics, São Paulo State University–Unesp, Department of Dental Materials and Prosthodontics, São José dos Campos, Brazil

Felipe de Camargo Ribeiro, MSc, Institute of Science and Technology, São Paulo State University–Unesp, Department of Biosciences and Oral Diagnosis, São José dos Campos, Brazil

Lilian Costa Anami, DDS, MSc, PhD, Universidade Santo Amaro, Department of Dentistry, São Paulo, Brazil

Samira Esteves Afonso Camargo, DDS, MSc, PhD, Institute of Science and Technology, São Paulo State University–Unesp, Department of Biosciences and Oral Diagnosis, São José dos Campos, Brazil

Antonio Olavo Cardoso Jorge, DDS, MSc, PhD, Institute of Science and Technology, São Paulo State University–Unesp, Department of Biosciences and Oral Diagnosis, São José dos Campos, Brazil

*Marco Antonio Bottino, DDS, MSc, PhD, Institute of Science and Technology, São Paulo State University–Unesp, Department of Dental Materials and Prosthodontics, São José dos Campos, Brazil

*Corresponding author: Av. Eng. Fco. José Longo, 777, São José dos Campos, 12245000, Brazil; e-mail: bottinomarcoantonio@gmail.com

DOI: 10.2341/17-126-L

their surfaces were finished by polishing (ceramisté diamond rubbers + polishing paste; "p" subgroups) or glaze spray application + sintering ("g" subgroups). Roughness (Ra and RSm parameters) and surface free energy (SFE) were measured. Early biofilm formation of *Streptococcus mutans*, *Streptococcus sanguinis*, and *Candida albicans* was evaluated by counting colony-forming units (CFU). MTT (3-[4.5-dimethyl-thiazol-2-yl-]-2.5-diphenyl tetrazolium bromide) cytotoxicity test evaluated cellular viability for the growth of FMM-1 after 24 hours and seven days of contact. Scanning electron microscopy (SEM) and three-dimensional optical profilometry were performed to qualitatively analyze the surface. Data were analyzed by analysis of variance, Tukey test, and *t*-test (all α=0.05).

Results: Polished samples presented lower roughness (Ra, p=0.015; RSm, p=0.049) and higher SFE (p=0.00). *Streptococci* had higher CFU in all groups, but the CFU of *C albicans* was lower for polished samples. Biofilm formation was influenced by the interaction of all factors (p=0.018), and the materials showed no cytotoxicity to FMM-1 growth.

Conclusions: Polishing resulted in the lowest values for surface roughness and higher SFE values. Polished ceramics showed less *C albicans* adherence while the adherence of *Streptococci* was greater than *C albicans* in all conditions.

INTRODUCTION

Feldspathic ceramics can be used to obtain partial or full restorations and for veneering metal or ceramic substructures. These restorations can be prepared by various techniques, such as conventional stratification or the computer-aided design/computer-aided manufacturing (CAD/CAM) technique, in which restorations are obtained from milling ceramic blocks. The final product may have different properties, such as porosity[1] and residual stress and grain size,[2] which influence the physical characteristics of the restorations.

Different particle sizes, porosity, and impurities present in the material can influence the surface characteristics that are in intimate contact with the periodontal tissues. For the success of rehabilitation treatment, it is essential to know the behavior of the restorative materials in relation to the microbiology of the oral environment.[3]

There is no consensus about the best surface treatment to obtain smooth feldspathic surfaces. Many ceramists advocate polishing rather than glazing, to better control the surface gloss of ceramic restorations.[4-7] There is little information about CAD/CAM ceramics.[8] Some authors have found that the initial softness of a glazed surface was superior than a polished surface.[9,10] Roughness and surface free energy (SFE) have important roles in bacterial adhesion[8-13] and consequent early biofilm formation.[14-16] Interactions between bacteria and the surfaces of the prosthetic device are thought to be based on a variety of forces, including the Lifshitz–van der Waals, electrostatic, and hydrophobic forces and various specific receptor-ligand interactions.[17] However, other studies have reported greater adherence of microorganisms on hydrophobic surfaces[18,19] and divergent results in which no significant relationship was observed between SFE and microbial adhesion are also described in the literature.[20,21] The bacterial community in the oral environment is very broad, and *in vitro* studies have revealed that interaction of *Streptococcus mutans* and *Candida albicans* may favor the formation of heterotypic biofilm.[12]

The biocompatibility of feldspathic ceramics is well accepted by dentists.[23] However, there are not enough studies on how CAD/CAM ceramics can influence fibroblast cells. These cells are responsible for creating soft tissues that can affect the esthetic result. In studies, the CAD block feldspathic ceramics demonstrated a significant decrease in cell viability in this type of cells.[24]

The good relation between feldspathic ceramic and fibroblast cells is due to Al^{+3} and K^{+} ions released upon degradation of feldspathic ceramics, which leads to lower cytotoxicity.[23] However, information on surface characteristics and formation of biofilms on materials is scarce, particularly with regard to the impact of intraoral polishing and the new spray glaze with respect to bacterial adherence and cellular viability.[8] Therefore, this study aimed to evaluate the oral biofilm formation and human gingival fibroblasts (FMM-1) viability on the surface of two feldspathic ceramics manufactured and finished by different techniques.

METHODS AND MATERIALS

Preparation of the Specimens

Vita Mark II blocks (Vita Zahnfabrik, Bad Säckingen, Germany, batch 34700) were cut into smaller blocks (4.5 × 4.5 × 1.5 mm) with a diamond disk under constant water cooling using a cutting machine. Vita VM9 stratified ceramic powder and

modeling liquid (Vita Zahnfabrik, batch 41810) were mixed following the manufacturer's recommendations and applied into a matrix. The excess liquid was removed, and the blocks were sintered in Vacumat 6000 MP (Vita Zahnfabrik). All samples were polished until reaching standardized dimensions (4.5 × 4.5 × 1.5 mm) in an automatic polisher (EcoMet/Auto Met 250, Buehler, IL, USA) with granulated sandpaper decreasing up to No. 1200 (30 seconds per sandpaper) and under water cooling. The samples were cleaned in an ultrasonic bath with isopropyl alcohol. Half of the samples received a layer of Vita AKZENT Plus–Glaze LT Spray ("g" subgroups; Vita Zahnfabrik, batch 36300). The other half was polished with Ceramisté PM ("p" subgroups; Standard, Ultra and Ultra II, Shofu Kyoto, Japan, batches 0511125, 0113203, 0113203) in three steps (standard for finishing, ultra for polishing, and ultra II for superpolishing) and then followed by diamond paste (Diamond Excel, FGM, Joinville, Brazil, batch 130616) on a felt disc (Diamond, FGM, batch 231115) using a handpiece at slow speed, for 20 seconds each. Next, the specimens were randomly divided into four groups according to the "manufacture technique" (stratification technique [ST] or CC [CAD/CAM]) and "surface finishing treatment" (p=polished or g=glazed).

Surface Roughness

For an effective evaluation of the roughness, measurement of more than one roughness parameter is recommended.[25] Ra (average roughness) and RSm (mean width of the roughness profile elements) parameters were evaluated by a surface roughness tester (SJ 400, Mitutoyo, Tokyo, Japan). A mean value was obtained for each sample (n=20) from three readings performed at the center of the samples at 0.2 mm/s speed, following ISO 4287-1997, with a Gaussian filter and a cutoff value of 0.8 mm.

Surface Free Energy

For SFE, larger samples (14 × 12 × 1.5 mm) of each group were obtained as previously described. A tensiometer (TL 1000, One Attension, Lichfield, Staffordshire, UK) was used to measure the mean contact angle in five distinct areas of each sample with the sessile drop technique, using two different liquids: water (polar liquid) and diiodomethane (dispersive liquid). The SFE was calculated using the method proposed by Owens and Wendt[26] along with the harmonic average equation (1). With the cosine of the contact angle for each liquid, we can calculate the components of surface energy of a solid surface. Replacing the known values of the liquids, starting with diiodomethane values (γ^L=50,811, $\gamma^L{}_P$=0, $\gamma^L{}_d$=50) then, water values (γ^L=72.8, $\gamma^L{}_P$=51, $\gamma^L{}_d$=21.8)[27] to obtain the γ^Sd and γ^Sp values. The SFE of the solid can be calculated by equation 2.

$$\gamma^L \cdot [\cos(\theta) + 1] = \frac{4\gamma_d^S \cdot \gamma_d^L}{\gamma_d^S + \gamma_d^L} + \frac{4\gamma_p^S \cdot \gamma_p^L}{\gamma_p^S + \gamma_p^L} \quad (1)$$

$$\gamma^{\mathbf{T}} = \gamma_{\mathbf{d}}^{\mathbf{S}} + \gamma_{\mathbf{p}}^{\mathbf{S}} \quad (2)$$

where $\gamma^{\mathbf{T}}$ corresponds to the SFE and γ_p and γ_d correspond to the polar and dispersive components, respectively.

Colony-Forming Units

Specimens were sterilized in a flow chamber under ultraviolet light (15 minutes each side). The biofilms were composed of standard strains of *Streptococcus mutans* (ATCC 35688), *Streptococcus sanguinis* (ATCC 10556), and *Candida albicans* (ATCC 18804). Standard suspensions were suspended in sterile physiological solution (0.9% NaCl), and the number of cells was calculated through a spectrophotometer (B582, Micronal, Sao Paulo, Brazil). Each sample was individually distributed on each plate from a 96-well sterile plate (Costar Corning, Corning, NY, USA) containing 150 μL of sterile BHI broth supplemented with 1% sucrose and 16.5 μL standardized suspension of each microorganism: *S mutans*, *S sanguinis*, and *C albicans*. Then, the plates were incubated at 37°C in a CO_2 chamber for 48 hours. Each specimen was washed by replacing 200 μL of the broth from each well with sterile physiological solution, and the plates were shaken for 5 minutes (Orbital Shaker, Solab, Piracicaba, Brazil). Samples of each group were individually transferred to falcon tubes with 10 mL of sterile saline solution (NaCl 0.9%) and were sonicated (Sonoplus HD 2200, 50 W, Bandelin Eletronic, Berlin, Germany) for 30 seconds to remove loose bacteria from the surface. Aliquots with dilutions of 10^{-1} to 10^{-4} were performed until *C albicans* was seeded at 10^{-3} and *Streptococcus* at 10^{-4}. Next, the suspensions were seeded in duplicate in Petri plates with a selective medium for each microorganism and then were incubated at 37°C for 16 hours. The plates containing colonies were counted, and the number of colony-forming units per milliliter (CFU/mL) was determined and transformed to log10.

Table 1: *Mean ± Standard Deviation (SD), Coefficient of Variance (CV), and Homogeneous Groups From Tukey Test of the Roughness Data According to the Ra and RSm Parameters*[a]

Groups	Ra		RSm	
	Mean ± SD, μm	CV, %	Mean ± SD, μm	CV, %
CCp	0.3 ± 0.1^{C}	43.3	108.9 ± 38.9^{B}	35.7
CCg	1.6 ± 0.7^{B}	19.2	168.6 ± 44.0^{A}	26.1
STp	0.3 ± 0.2^{C}	59.7	123.3 ± 64.5^{B}	52.3
STg	2.0 ± 0.7^{A}	35.6	135.8 ± 59.3^{AB}	43.7

Abbreviations: CCp, CAD/CAM and polished surface; CCg, CAD/CAM and glazed surface; STp, stratification technique and polished surface; STg, stratification technique and polished surface.
[a] *Different uppercase letters represent statistically significant difference within the same parameter (column).*

Cytotoxicity Assay

Human gingival fibroblasts (FMM-1) were cultured in Dulbecco's Modified Eagle Medium (DMEM high glucose, GlutaMAXTMSupplement, pyruvate, Gibco, Gaithersburg, MD, USA) supplemented with 10% fetal bovine serum (Gibco) and 1% penicillin streptomycin (LGC, Cotia, Brazil). Two sterilized samples per well (24-well plate) were placed with 1 mL of the suspensions containing 2×10^4 cells. The plates were incubated at 37°C in a humid atmosphere containing 5% CO_2 for 24 hours or seven days. After these periods, cell viability was measured by MTT assay (3-[4.5-dimethyl-thiazol-2-yl-]-2.5-diphenyl tetrazolium bromide; Sigma, St Louis, MO, USA). The supernatant from each well was discarded, and the ceramics were removed from the wells. The cell monolayers at the bottom of the wells were washed with 500 μL of phosphate-buffered saline (PBS) and 500 μL of MTT (0.5 mg/mL PBS) solution was applied to each well. The plates were incubated for one hour at 37°C in a completely dark environment. Then, the supernatant was discarded, and the wells were washed with 500 μL PBS. Next, 500 μL of DMSO was added, and the plates were incubated for 10 minutes and shook on an orbital table for 10 minutes. Then, 100 μL of the supernatant from each well was removed for further optical density reading in a spectrophotometer using 570-nm wavelength (EL808IU, Biotek, Winooski, VT, USA). Cell viability was expressed as a percentage of the control (=100%) that remained on plates without ceramic material, according to the International Organization of Standardization 10993-5:1999.[28]

Qualitative Analysis

Sample topography was evaluated by scanning electron microscopy (SEM) and optical profilometry. SEM (Inspect S50, FEI Company, Brno, Czech Republic) was performed on sterile and contaminated samples and on samples with FMM-1 cells after each evaluation period. Specimens with oral biofilm or cells were fixed in 2.5% glutaraldehyde solution for one hour and dehydrated in increasing series of ethyl alcohol baths for 30 minutes (10%, 25%, 50%, 75%, 80%, 90%, and 100%). Then, specimens were metallized with gold alloy (Emitech SC 7620, Sputter Coater, Laughton, UK) and evaluated at a magnitude of 2000× to 3000×. Profilometry was evaluated on two sterile samples from each group in the area of 301.3 × 229.2 μm (Wyko, NT 1100, Veeco, Tucson, AZ, USA).

Statistical Analysis

Surface roughness (Ra and RSm parameters) and SFE data were analyzed by two-way analysis of variance (ANOVA) followed by Tukey test. CFU and MTT assay data were analyzed by three-way ANOVA followed by Tukey test. MTT assay was also evaluated by *t*-test. All tests were performed with $\alpha = 0.05$.

RESULTS

Surface Roughness

The interaction between "Manufacture Technique × Finishing Treatment" significantly influenced both roughness parameters (Ra, $p=0.015$; RSm, $p=0.049$). Tukey test presented glazed groups showing higher mean values of Ra and RSm parameters. In summary, polished surfaces presented decreased roughness values, suggesting lower but more frequent defects (Table 1).

Surface Free Energy

Surface finishing treatment also influenced SFE ($p=0.00$), and Tukey test demonstrated that the polished groups showed higher SFE (γT). The polar component was higher than the dispersive component for all tested groups (Table 2).

Colony-Forming Units

The interaction among "Manufacture Technique × Finishing Treatment × Microorganisms" statistically influenced the adherence of microorganisms on the materials' surfaces ($p=0.018$). The adherence of *S mutans* and *S sanguinis* ranged from 6.38^{A} to 7.29^{A} CFU/mL(log10), and it was statistically similar among all tested groups and superior than Candida. Glazed samples presented higher adherence of *C albicans* than polished groups, with mean CFU

Table 2: *Mean Contact Angle Values ± Standard Deviation (SD) for Water and Diiodomethane, Dispersive (γ_d) and Polar (γ_p) Components and Respective SFE (γ_T)*[a]

Group	Mean Contact Angle		Components		
	Water Mean ± SD, °	Dioodomethane Mean ± SD, °	γ_d, mN/m	γ_p, mN/m	γ_T, mN/m
CCp	60.8 ± 6	43.1 ± 7	18.5 ± 1	46.6 ± 3	65.1 ± 6[A]
CCg	41.5 ± 6	37.5 ± 5	17.7 ± 3	38.6 ± 3	56.3 ± 4[B]
STp	66.0 ± 5	46.9 ± 5	26.8 ± 3	41.1 ± 2	67.9 ± 4[A]
STg	33.8 ± 6	36.4 ± 3	15.6 ± 3	36.8 ± 3	52.4 ± 2[B]

Abbreviations: CCp, CAD/CAM and polished surface; CCg, CAD/CAM and glazed surface; STp, stratification technique and polished surface; STg, stratification technique and polished surface.
[a] *Different uppercase letters represent statistically significant difference among experimental groups.*

adherence of 0[D] CFU/mL(log10) for CAD/CAM and polished surface (CCp), 4.78[B] CFU/mL(log10) for CAD/CAM and polished surface (CCg), 1.55[C] CFU/mL(log10) for stratification technique and glazed surface (STp), and 4.67[B] CFU/mL(log10) for CAD/CAM and polished surface (STg).

Cytotoxicity Assay

The absorbance means resulting from the MTT test in relation to the control (considered 100%) is shown in Table 3. Student *t*-test showed that polished groups for seven days were not statistically different from the control. All groups were noncytotoxic (with viability higher than 50%). Three-way ANOVA showed that the interaction of "Time × Finishing Treatment" statistically influenced viability (p=0.00), and Tukey test identified that the highest viability values occurred at 24 hours for glazed samples. Viability decreased after seven days.

Table 3: *Cell Viability Percentage in Relation to the Control, Considered 100%, and Absorbance Means ± Standard Deviation (SD), in Optical Density, and Homogeneous Groups From Tukey Test of the Interaction Between Time × Surface Effects*[a]

Group	Cell Viability, %		Absorbance	
	24 h	7 d	24 h	7 d
Polished				
CCp	85.91	86.11	0.083 ± 0.01[B]	0.069 ± 0.00[C]
STp	95.26	71.77		
Glazed				
CCg	152.00	69.11	0.143 ± 0.02[A]	0.064 ± 0.00[C]
STg	160.75	75.69		

Abbreviations: CCp, CAD/CAM and polished surface; CCg, CAD/CAM and glazed surface; STp, stratification technique and polished surface; STg, stratification technique and polished surface.
[a] *Different uppercase letters indicate statistical difference of absorbance among groups.*

Qualitative Analysis

Representative three-dimensional (3D) images of profilometry (left column) and micrographs of sterile (central column) and contaminated surfaces (right column) are presented in Figure 1. In SEM micrographs of biofilm, *C albicans* is more prevalent than the bacteria, and it is possible to identify its hyphae (Figure 1I). Figure 2 shows SEM micrographs of cell viability. FMM-1 fibroblasts grew independent of porosities. The 24-hour period (Figure 2, left column) shows the presence of fibroblasts. In the seven-day period (Figure 2, right column), there are cells adhered to the glazed surfaces arranged in multilayers and with higher extracellular matrix production (Figures 2D,H).

DISCUSSION

To improve their material properties, ceramics are subjected to treatments for smooth surfaces, as lower surface roughness is associated with improved patient comfort as well as esthetic and biological aspects.[29,30] With the Ra parameter, commonly used in the scientific literature, it is observed that different profiles can result in the same measure of average profile amplitude, that is, in the same Ra value. This parameter (or any parameter of amplitude) does not faithfully characterize a surface, and therefore, the relation with other parameters is necessary, for example, the parameter of spacing (RSm).[25] The roughness of the evaluated feldspathic ceramics was influenced by the interaction of surface finishing treatment and manufacturing techniques. Our findings are similar to those of Han and others,[18] who evaluated only the Ra parameter and observed the lowest roughness values for polished samples. For Sarikaya and Guler,[19] the roughness of polished samples varied according to the manufacturing technique (stratification and CAD/CAM). The authors evaluated porcelains obtained by different techniques (VMK 95 and Vitablocs Mark II, Vita Zahnfabrik, Bad Säckingen, Germany; Ceramco III,

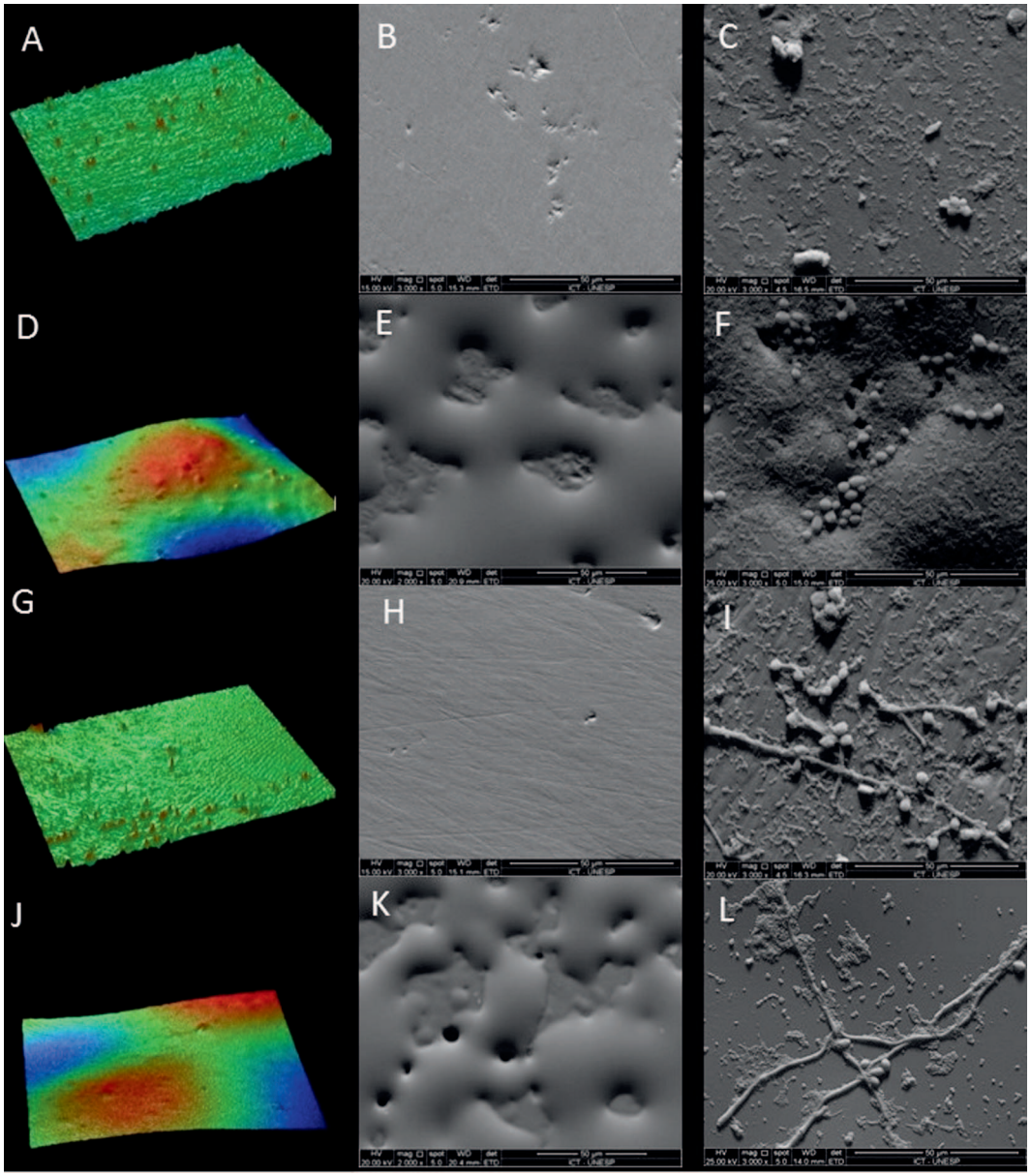

Figure 1. *Representative micrographs. Left column, three-dimensional images of optical profilometry. Central column, micrographs of sterile samples. Right column, samples contaminated with heterotypic biofilm. (A–C): CCp. (D–F): CCg. (G–I): STp. (J–L): STg.*

Degudent GmbH, York, PA, USA; Matchmaker MC, Schottlander, Letchworth, UK) and used glaze as a paste. They also verified an increase of mean roughness by applying glaze on VMII compared with some polishing techniques for this material and concluded that the evaluated polishing techniques were similar to each other because of the hardness of the ceramic blocks.[19] In the present study, the glaze spray application resulted in a higher average amplitude profile for the stratified ceramic (VM9, ST group) when compared with CAD/CAM blocks (VMII, CC group).

Glazing is not a requirement of manufacturers but rather an alternative to polishing. It is performed by applying a thin layer of ceramic paste with low melting temperature on the ceramic surface, followed by sintering at a temperature lower than the firing of ceramics.[20,21] The glaze used in this study was sprayed and thus deposited ceramic powder particles on the ceramic surface, but the distribution of material depends on the distance, pressure, and duration of the application. In theory, the glaze application should fill the surface irregularities, as it is initially a liquid material.

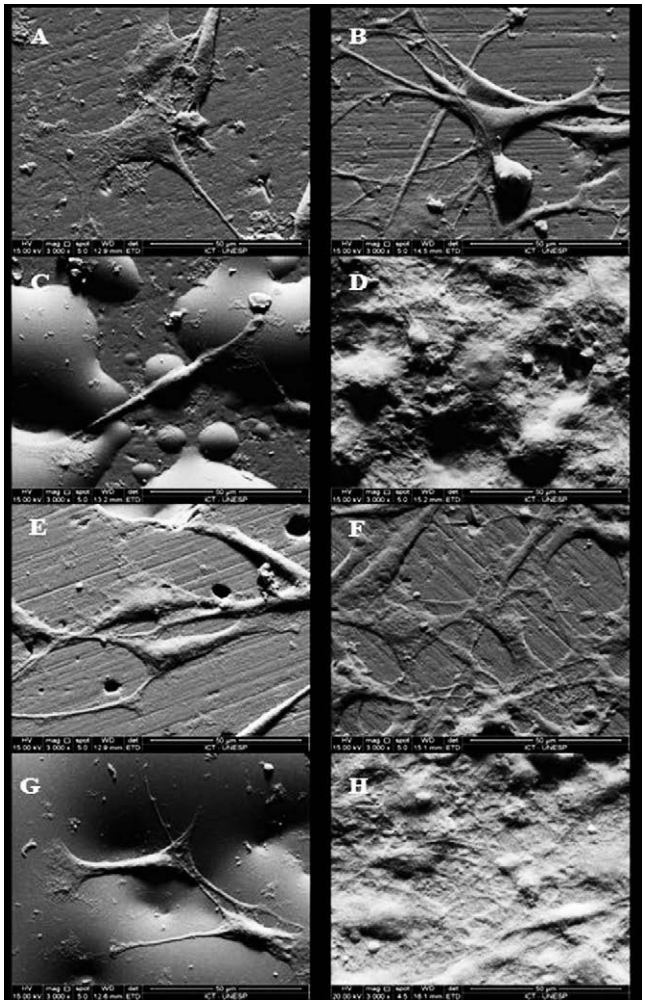

Figure 2. *Representative micrographs. Left column, 24 hours of cell growth. Right column, seven days. (A, B): CCp. (C, D): CCg. (E, F): STp. (G, H): STg.*

However, glazing does not always result in flat and smooth surfaces but in waved surfaces with numerous irregularities due to the nonhomogeneity of the application and to gaps in the ceramic's surface. In this study, topographic analysis performed by SEM and profilometry showed that polished surfaces presented fine scratches resulting from the polishing and glazed surfaces presented greater irregularities due to glaze distribution, which accumulated in "islands" on the materials. There are few studies on the glaze spraying technique applied to feldspathic ceramics or on the interaction between different glazes and materials and their subsequent performance in the oral cavity. A previous study found that glaze spraying resulted in greater roughness than the paste version but with similar final brightness.[8]

Despite the manufacturing technique not influencing SFE, surface finishing treatment was significant, and polished ceramics resulted in greater SFE.

According to the literature, the average values of SFE for *S mutans*, *S sanguinis*, and *C albicans* are, respectively, 48.4, 47.7, and 40.1 mNm; however, these values vary among different strains.[31] According to Minagi and others,[32] the closer the SFE of the material and microorganism, the greater the likelihood of adhesion. The gram-negative bacterial cells have predominantly higher SFE (35 to 65 mNm,) whereas some gram-positive bacterial cells have high (35 to 65 mNm) or low (0 to 25 mNm) values.[31] Evidence suggests that the presence of polysaccharides on the cell's surface of gram-positive bacteria, such as *S mutans* and *S sanguinis*, tends to make the bacterial cell more hydrophilic. Other studies have demonstrated that SFE has an important role in the early adhesion stages of *C albicans*, and substrates with greater SFE induce greater adherence by *C albicans*.[33] In our study, the surface energy in all groups was higher than 52.0 mN/m and was not as relevant as roughness.

Studies have found a positive relation between the roughness of the material and the amount of adhered bacteria.[15,34] Surface energy values depend primarily on the chemical composition of the interactors at each interface, and an SFE analysis can be performed on smooth or rough surfaces. The roughness tends to accentuate the wettability characteristic of the surface. It is known that roughness values less than 0.2 μm have less relation to bacterial colonization than superficial properties. On the other hand, rough surfaces provide physical protection to the bacteria, as well as increased contact area for bacterial adhesion.[11,35,36] In this study, the average roughness of polished ceramic was 0.3 μm, which probably hindered the adherence of *C. albicans*, which measured from 2 to 6 μm.[37] This might have contributed to the lower CFU number of *C albicans* on polished samples, as they probably shed from the surface of the specimens during the wash, since the presence of *C albicans* can be checked by SEM.

MTT analysis showed that all groups had no cytotoxicity. The surface finishing treatment and evaluation period had an influence on the cell viability of fibroblasts. In the 24-hour period, glazed ceramics had higher cell viability compared with the polished groups. The cell viability of glazed samples was higher than the control group in the 24-hour period, representing a good initial relationship

between material and cells.[38,39] Cell viability was reduced after seven days, but it was similar, regardless of the surface finishing treatment. The micrographics show greater cell growth on glazed samples after seven days (Figure 2D,H) when compared with polished ones (Figure 2B,F). This can be justified by the fact that fibroblasts have good affinity for rough surfaces (glazed samples, higher Ra, higher RSm), as they anchor better and proliferate more. However, this excessive proliferation represented by the provision of these cells in multilayers can culminate in cell death, and SEM fibroblast images can generate some confusion in interpretation since the MTT test showed quantification of viable cells present in the supernatant liquid where the sample had been in contact with fibroblasts, while SEM features cells (viable or nonviable) on the material's surface. The integrity of the fibroblastic cells is important for the health of the tissues and around prosthetic restorations, since these cells are responsible for tissue maintenance and offer a buffer that serves as a protective barrier.[40,41]

CONCLUSION

Based on the results of the present study, it can be concluded that polishing compared with glaze spray treatment resulted in the lowest values for surface roughness and higher SFE values. The adherence of *Streptococcus* was superior in all conditions to *C albicans*, and polished ceramics adhered even less *C albicans*. More studies are necessary to understand which properties interact with the formation of biofilm and other tests for cellular viability of human gingival fibroblasts after seven days.

Acknowledgements

The authors would like to thank FAPESP (2014/19357-9), the Coordination for the Improvement of Higher Education Personnel (CAPES) for scholarship, VITA Zahnfabrik, and Wilcos (Brazil) for donating ceramic materials.

Conflict of Interest

The authors of this article certify that they have no proprietary, financial, or other personal interest of any nature or kind in any product, service, and/or company that is presented in this article.

(Accepted 14 October 2017)

REFERENCES

1. Nakamura T, Wakabayashi K, Kawamura Y, Kinuta S, Mutobe Y, & Yatani H (2007) Analysis of internal defects in all-ceramic crowns using micro-focus X-ray computed tomography *Dental Materials Journal* **26(4)** 598-601.
2. Rueda A, Seuba J, Anglada M, & Jiménez-Piqué E (2013) Tomography of indentation cracks in feldspathic dental porcelain on zirconia *Dental Materials* **29(3)** 348-356.
3. Rashid H (2014) The effect of surface roughness on ceramics used in dentistry: a review of literature *European Journal of Dentistry* **8(4)** 571-579.
4. Rosenstiel S, Baiker M, & Johnston M (1989) Comparison of glazed and polished dental porcelain. *International Journal of Prosthodontics* **2(6)** 524-529.
5. Al-Wahadni A, & Martin DM (1998) Glazing and finishing dental porcelain: a literature review. *Journal of the Canadian Dental Association* **64(8)** 580-583.
6. Al-Marzok MI, & Al-Azzawi HJ (2009) The effect of the surface roughness of porcelain on the adhesion of oral *Streptococcus mutans Journal of Contemporary Dental Practice* **10(6)** E017-E024.
7. Sarac D, Sarac YS, Yuzbasioglu E, & Bal S (2006) The effects of porcelain polishing systems on the color and surface texture of feldspathic porcelain *Journal of Prosthetic Dentistry* **96(2)** 122-128.
8. Carrabba M, Vichi A, Vultaggio G, Pallari S, Paravina R, & Ferrari M (2016) Effect of finishing and polishing on the surface roughness and gloss of feldspathic ceramic for chairside CAD/CAM systems *Operative Dentistry* **42(2)** 175-184.
9. Klausner LH, Cartwright CB, & Charbeneau GT (1982) Polished versus autoglazed porcelain surfaces *Journal of Prosthetic Dentistry* **47(2)** 157-162.
10. Patterson CJW, Mclundie AC, Stirrups DR, & Taylor WG (1992) Efficacy of a porcelain refinishing system in restoring finish after grinding with fine and extra-fine diamond *Journal of Prosthetic Dentistry* **68(3)** 402-406.
11. Bollen CM, Lambrechts P, & Quirynen M (1977) Comparison of surface roughness of oral hard materials to the threshold surface roughness for bacterial plaque retention: a review of the literature *Dental Materials* **13(4)** 258-269.
12. Quirynen M, De Soete M, & Van Steenberghe D (2002) Infectious risks for oral implants: a review of the literature. *Clinical Oral Implants Research* **13(1)** 1-19.
13. Kantorski KZ, Scotti R, Valandro LF, Bottino MA, Koga-Ito CY, & Jorge AO (2008) Adherence of *Streptococcus mutans* to uncoated and saliva-coated glass-ceramics and composites *General Dentistry* **56(7)** 740-747.
14. Anami LC, Pereira CA, Guerra E, Assuncao e Souza RO, Jorge AO, & Bottino MA (2012) Morphology and bacterial colonisation of tooth/ceramic restoration interface after different cement excess removal techniques *Journal of Dentistry* **40(9)** 742-749.
15. Hannig C, & Hannig M (2009) The oral cavity a key system to understand substratum-dependent bioadhesion on solid surfaces in man *Clinical Oral Investigations* **13(2)** 123-139.
16. Subramani K, Jung RE, Molenberg A, & Hammerle CH (2009) Biofilm on dental implants: a review of the literature *International Journal of Oral & Maxillofacial Implants* **24(4)** 616-626.

17. Harris LG, Tosatti S, Wieland M, Textor M, & Richards RG (2004) *Staphylococcus aureus* adhesion to titanium oxide surfaces coated with non-functionalized and peptide-functionalized poly(L-lysine)-grafted-poly(ethylene glycol) copolymers. *Biomaterials* **25(18)** 4135-4148.
18. Han GJ, Kim JH, Lee M, Chae SY, Lee YH, & Cho BH (2014) Performance of a novel polishing rubber wheel in improving surface roughness of feldspathic porcelain *Dental Materials Journal* **33(6)** 739-748.
19. Sarikaya I, & Guler AU (2010) Effects of different polishing techniques on the surface roughness of dental porcelains *Journal of Applied Oral Science* **18(1)** 10-16.
20. Aksoy G, Polat H, Polat M, & Coskun G (2006) Effect of various treatment and glazing (coating) techniques on the roughness and wettability of ceramic dental restorative surfaces. *Colloids and Surfaces B: Biointerfaces* **53(2)** 254-259.
21. Hahnel S, Rosentritt M, Handel G, & Burgers R (2009) Surface characterization of dental ceramics and initial streptococcal adhesion *in vitro Dental Materials* **25(8)** 969-975.
22. Pereira-Cenci T, Cury AA, Cenci MS, & Rodrigues-Garcia RC (2007) *In vitro* Candida colonization on acrylic resins and denture liners: influence of surface free energy, roughness, saliva, and adhering bacteria *International Journal of Prosthodontics* **20(3)** 308-310.
23. Elshahawy WM, Watanabe I, & Kramer P (2009) *In vitro* cytotoxicity evaluation of elemental ions released from different prosthodontic materials *Dental Materials* **25(12)** 1551-1555.
24. Pabst AM, Walter C, & Grassmann L (2014) Influence of CAD/CAM all-ceramic materials on cell viability, migration ability and adenylate kinase release of human gingival fibroblasts and oral keratinocytes *Clinical Oral Investigations* **18(4)** 1111-1118.
25. Wennerberg A, & Albrektsson T (2000) Suggested guidelines for the topographic evaluation of implant surfaces *International Journal of Oral and Maxillofacical Implants* **15(3)** 331-344.
26. Owens DK, & Wendt RC (1969) Estimation of the surface free energy of polymers *Journal of Applied Polymer Science* **13(8)** 1741-1747.
27. Gryte KF, & Hansen F (2006) Surface modification of EPDM rubber by plasma treatment *Langmuir* **22(14)** 6109-6124.
28. International Organization for Standardization (1999) *Biological Evaluation of Medical Devices—ISO 10993, Part 5: Tests for In Vitro Cytotoxicity* Geneva, Switzerland, 1999.
29. Kawai K, Urano M, & Ebisu S (2000) Effect of surface roughness of porcelain on adhesion of bacteria and their synthesizing glucans *Journal of Prosthetic Dentistry* **83(6)** 664-667.
30. Yilmaz C, Korkmaz T, Demirkoprulu H, Ergun G, & Ozkan Y (2008) Color stability of glazed and polished dental porcelains *Journal of Prosthodontics* **17(1)** 20-24.
31. Sharma P, & Hanumantha K (2002) Analysis of different approaches for evaluation of surface energy of microbial cells by contact angle goniometry *Advances in Colloid and Interface Science* **98(5)** 341-463.
32. Minagi S, Miyake Y, Inagaki K, Tsuru H, & Suginaka H (1985) Hydrophobic interaction in *Candida albicans* and *Candida tropicalis* adherence to various denture base resin materials *Infection and Immunity* **47(1)** 11-14.
33. Al-Marzok MI, & Al-Azzawi HJ (2009) The effect of the surface roughness of porcelain on the adhesion of oral *Streptococcus mutans Journal of Contemporary Dental Practice* **10(6)** E017-E024.
34. Aykent F, Yondem I, Ozyesil AG, Gunal SK, Avunduk MC, & Ozkan S (2010) Effect of different finishing techniques for restorative materials on surface roughness and bacterial adhesion *Journal of Prosthetic Dentistry* **103(4)** 221-227.
35. Quirynen M, Bollen CM, Papaioannou W, Van Eldere J, & Van Steenberghe D (1996) The influence of titanium abutment surface roughness on plaque accumulation and gingivitis: short term observations *International Journal of Oral & Maxillofacial Implants* **11(2)** 169-178.
36. Borchers F, Tavassol H, & Schernitschek T (1999) Surface quality achieved by polishing and by varnishing of temporary crown and fixed partial denture resins *Journal of Prosthetic Dentistry* **82(5)** 550-556.
37. Goldman L, & Schafer A. *Goldman's Cecil Medicine. 24th ed*. Philadelphia, Elsevier, 2012.
38. Tete S, Zizzari VL, Borelli B, De Colli M, Zara S, Sorrentino R, Scarano A, Gherlone E, Cataldi A, & Zarone F (2014) Proliferation and adhesion capability of human gingival fibroblasts onto zirconia, lithium disilicate and feldspathic veneering ceramic *in vitro Dental Materials Journal* **33(1)** 7-15.
39. Zizzari V, Borelli B, De Colli M, Tumedei M, Di Iorio D, Zara S, Sorrentino R, Cataldi A, Gherlone EF, Zarone F, & Tetè S (2013) SEM evaluation of human gingival fibroblasts growth onto CAD/CAM zirconia and veneering ceramic for zirconia *Annali di Stomatologia* **4(3)** 244-249.
40. Linkevicius T, & Aps P (2008) Biologic width around implants: an evidence-based review *Stomatologija* **10(1)** 27-35.
41. Furuhashi A, Ayukawa Y, Atsuta I, Okawachi H, & Koyano K (2012) The difference of fibroblast behavior on titanium substratum with different surface characteristics *Odontology* **100(2)** 199-205.

©Operative Dentistry, 2018, **43-6,** 602-612

High Bond Durability of Universal Adhesives on Glass Ceramics Facilitated by Silane Pretreatment

C Yao • H Yang • J Yu • L Zhang • Y Zhu • C Huang

Clinical Relevance

Additional silane treatment prior to the application of universal adhesive is necessary to improve the bonding longevity to lithium disilicate glass ceramic.

SUMMARY

Objective: This study aimed to investigate the long-term effectiveness of ceramic–resin bonding with universal adhesives in non–silane-pretreated and silane-pretreated modes after 10,000 cycles of thermal aging.

Methods and Materials: All Bond Universal, Adhese Universal, Clearfil Universal Bond, and Single Bond Universal were selected. Etched lithium disilicate glass ceramics were prepared, randomly assigned to groups, and pretreated with or without ceramic primer containing silane coupling agent prior to the application of universal adhesive (ie, silane-pretreated or non–silane-pretreated mode). The shear bond strength (SBS), microleakage, and field-emission scanning electron microscopy images of the ceramic–resin interfaces were examined after 24 hours of water storage or 10,000 thermal cycles. Light microscopy and confocal laser scanning microscopy (CLSM) were performed to analyze marginal sealing ability.

Results: SBS and microleakage percentage were significantly affected by bonding procedure (non–silane-pretreated or silane-pretreated mode) and aging (24 hours or 10,000 thermal cycles). After the universal adhesives in the non–silane-pretreated mode were aged, SBS significantly decreased and microleakage percentage increased. By contrast, the SBS of

Chenmin Yao, PhD student, Wuhan University, The State Key Laboratory Breeding Base of Basic Science of Stomatology (Hubei-MOST) & Key Laboratory for Oral Biomedicine Ministry of Education, School & Hospital of Stomatology, Wuhan, China

Hongye Yang, MDS, PhD, Wuhan University, School & Hospital of Stomatology, Wuhan, China

Jian Yu, MSD, PhD, Wuhan University, School & Hospital of Stomatology, Wuhan, China

Lu Zhang, MSD, PhD student, Wuhan University, The State Key Laboratory Breeding Base of Basic Science of Stomatology (Hubei-MOST) & Key Laboratory for Oral Biomedicine Ministry of Education, School & Hospital of Stomatology, Wuhan, China

Yuanjing Zhu, PhD student, Wuhan University, The State Key Laboratory Breeding Base of Basic Science of Stomatology (Hubei-MOST) & Key Laboratory for Oral Biomedicine Ministry of Education, School & Hospital of Stomatology, Wuhan, China

*Cui Huang, MS, MDS, PhD, Wuhan University, The State Key Laboratory Breeding Base of Basic Science of Stomatology (Hubei-MOST) & Key Laboratory for Oral Biomedicine Ministry of Education, School & Hospital of Stomatology, Wuhan, China

*Corresponding author: 237 Luoyu Road, Wuhan, 430079 China; e-mail: huangcui@whu.edu.cn

DOI: 10.2341/17-227-L

Adhese Universal, Clearfil Universal Bond, and Single Bond Universal decreased, and the microleakage percentage of all of the adhesives increased in the silane-pretreated mode. However, after aging, the SBS of the silane-pretreated groups were higher and their microleakage percentages lower than those of the non–pretreated groups. In the non–silane-pretreated mode, adhesive failure was dominant and gaps between composite resin and the adhesive layer were significant when observed with CLSM.

Conclusions: The simplified procedure reduced the ceramic–resin bonding effectiveness of universal adhesives after aging, and additional silane pretreatment helped improve the long-term durability.

INTRODUCTION

Dental glass ceramic has gained considerable interest from both dentists and patients because of outstanding esthetics and biocompatibility. Lithium disilicate glass ceramic, which is a third-generation ceramic system, was introduced in 1998 for single- and multiple-unit frameworks[1] and is a widely used dental restorative material.[2] A glass ceramic restorative material is generally bonded to tooth substrates by using an adhesive system. Although the properties of current adhesives have been remarkably enhanced,[3-5] glass ceramic–resin bonding is limited by factors such as bulk fractures and marginal deficiencies.[6] Therefore, effective and stable bonding are key elements in the application of ceramic restorations and have been intensively explored in clinical practice.

Etching with hydrofluoric acid and application of a ceramic primer containing a silane coupling agent is an effective approach for glass ceramic bonding because of the silica base of glass ceramics.[7] The glass matrix is dissolved by the hydrofluoric acid and a porous structure for micromechanical retention is produced. Silane is an effective adhesion promoter[8] that reacts and couples with inorganic and organic materials.[9] However, the clinical application of glass ceramic treatment is impeded by time-consuming and complex steps. Thus, an efficient and simplified method must be established in the adhesive protocol, not only to maintain stable bonding, but also to reduce clinical operation time.

Universal adhesive has emerged as a promising bonding candidate because it can be applied to various substrates, such as enamel, dentin,[10,11] zirconia ceramics,[12] and glass ceramics.[13] For a simplified glass ceramic bonding procedure, some universal adhesive manufacturers claim that additional silane pretreatment is unnecessary because a silane coupling agent is incorporated in their products. Although universal adhesives have the advantage of convenient use, this material cannot guarantee the long-term clinical success of adhesive bonding for restorations. Furthermore, the durability and efficiency traits of adhesive bonding have yet to be enhanced. Therefore, in-depth *in vitro* and *in vivo* studies and clinical trials must be conducted to verify the longevity of glass ceramic–resin bonds produced by universal adhesives.

Thermal cycling with simulated intraoral temperature is commonly used to evaluate the bond durability and degradation of an adhesive system.[14,15] In particular, a widely accepted criterion is that 10,000 cycles are equivalent to the clinical physiological aging of one year.[16] To the extent of our knowledge, although numerous studies have investigated the longevity of dentin-resin bonding produced by universal adhesives,[17-19] few studies have explored the ceramic–resin bonding durability with universal adhesives. Limited reports have verified whether silane incorporated in universal adhesives is a sufficient substitute for additional silane pretreatment in long-term applications.

Therefore, this study aimed to evaluate the effect of additional silane pretreatment on the durability of ceramic–resin bonding with universal adhesives after 10,000 thermal cycles of aging. Two silane-containing and two silane-free universal adhesives were used in the present study. Our tested null hypotheses were as follows: 1) there is no significant difference in the bonding performance of universal adhesive on lithium disilicate glass ceramics between non–silane-pretreated and silane-pretreated modes and 2) there is no significant difference in ceramic–resin bonding with universal adhesive after 24 hours of water storage and after 10,000 thermal cycles.

METHODS AND MATERIALS

Specimen Preparation and Experimental Design

Two hundred forty-two lithium disilicate glass ceramic specimens (e.max CAD, Ivoclar Vivadent, Schaan, Liechtenstein) with dimensions of 8 mm × 7 mm × 2 mm were prepared by using a low-speed cutting device (Isomet, Buehler, Evanston, IL, USA). The specimens were sintered in accordance with the

manufacturer's instructions. The ceramic specimens were ground flat using silicon carbide (SiC) paper through 3000-grit and polished with a soft cloth and 0.5-μm-grit diamond paste in distilled water. The ceramics were etched with 9% hydrofluoric acid (Ultradent Products, Inc, South Jordan, UT, USA) for 90 seconds and thoroughly rinsed with water for 15 seconds.

A total of 240 etched ceramic blocks were randomly divided into four universal adhesives groups: All Bond Universal (ABU; Bisco, Schaumburg, IL, USA), Adhese Universal (ADU; Ivoclar Vivadent), Clearfil Universal Bond (CUB; Kuraray Noritake Dental, Tokyo, Japan), and Single Bond Universal (SBU; 3M ESPE, St. Paul, MN, USA). The compositions of the adhesives are listed in Table 1. The etched blocks were directly treated with adhesive (ie, non–silane-pretreated mode, eg, ABU, n=30) or pretreated with ceramic primer containing silane (RelyX ceramic primer; 3M ESPE) for 20 seconds, followed by adhesive treatment (ie, silane-pretreated mode, eg, S-ABU, n=30). The bonding procedure of adhesive systems (Table 1) was conducted strictly in accordance with the manufacturer's instruction. The adhesive was light polymerized with a high-intensity light-emitting diode curing light (1100 mW/cm^2; Ivoclar Vivadent).

Shear Bond Strength

After light polymerizing each adhesive, a Tygon tube (inner diameter: 3 mm; height: 4 mm) was placed on the ceramic surface. Then, the composite resin (Charisma, Heraeus Kulzer, Hanau, Germany) was placed into the tube with 2 layers up to a height of 4 mm. Each resin increment of 2 mm was light-polymerized for 20 seconds using a light-emitting diode curing light (1100 mW/cm^2; Ivoclar Vivadent). Prior to shear bond strength (SBS) testing, the tubes were removed to reveal the composite cylinders. Eighty etched ceramic specimens were randomly selected from each adhesive in the non–silane-pretreated (eg, ABU, n=10) and silane-pretreated modes (eg, S-ABU, n=10), and these specimens were used for SBS evaluation with storage in distilled water (37°C) for 24 hours. Another 80 specimens were randomly selected from each adhesive in the non–silane-pretreated (eg, ABU, n=10) and silane-pretreated modes (eg, S-ABU, n=10), and these specimens were treated with 10,000 thermocycles between two water baths at 5°C and 55°C, with a dwell time of 60 seconds for each temperature and an exchange time of 10 seconds between the baths (Thermo-cycler, Thermo Fisher Scientific, Waltham, MA, USA).

All specimens were placed in a steel fixture in a universal testing machine (ZY-100K, Yangzhou, Jiangsu, China) and subjected to shear stress at a constant crosshead speed of 1 mm/min.[20,21] The peak load that created a fracture was recorded. SBS (MPa) was calculated by dividing the peak load during interface failure by the adhesive bonding area.

Failure Mode Analysis

After debonding, the fractured samples were sputter coated with Au–Pd alloy (JFC-1600, JEOL, Tokyo, Japan) and analyzed by field-emission scanning electron microscopy (FESEM; Zeiss, Sigma, Germany) at 24×, 5000×, and 20,000× magnifications. The failure modes of the fractured interfaces were classified as adhesive failures on the ceramic surface or cohesive failures in the adhesive or composite resin.[22,23] Image J analysis software (National Institutes of Health Frederick, MD, USA) was used to calculate the adhesive and cohesive failure percentages of the fracture surfaces.

Microleakage Evaluation

Forty etched ceramic specimens were randomly selected from each adhesive in the non–silane-pretreated (eg, ABU, n=5) and silane-pretreated modes (eg, S-ABU, n=5), and these specimens were used for microleakage evaluation with storage in distilled water (37°C) for 24 hours. Another 40 specimens were randomly selected from each adhesive in the non–silane-pretreated (eg, ABU, n=5) and silane-pretreated modes (eg, S-ABU, n=5), and these specimens were treated with 10,000 thermocycles. After the adhesive was light polymerized, 2-mm-thick composite resin was placed onto the ceramic and polymerized for 40 seconds using a light-emitting diode curing light (1100 mW/cm^2; Ivoclar Vivadent).

The bonded specimens were sectioned longitudinally across the interface, obtaining slabs with dimensions of 7 mm × 4 mm × 1 mm. Peripheral slabs with excessive or insufficient resin amount at the interface were abandoned. Finally, 80 slabs were collected, stored in distilled water (37°C) for 24 hours or subjected to 10,000 thermocycles, coated with two consecutive nail varnish layers (except for an area of approximately 0.5 mm away from the interface), and immersed in 0.5% basic fuchsin solution[24] at 37°C for 24 hours. Afterward, the

Table 1: *Composition and Application Procedures of the Universal Adhesive Systems Used in This Study*

Universal Adhesive (Batch No.)	PH	Composition	Application Procedures
All-Bond Universal-ABU (1200006111)	3.2	Bis-GMA, HEMA, MDP, initiators, ethanol, water	Apply for 10-15 seconds, mild air dry for at least 10 seconds, light cure for 10 seconds
Adhese Universal-ADU (SS4248)	2.5-3.0	Bis-GMA, HEMA, MDP, CQ, D3MA, MCAP, highly dispersed silicon dioxide, ethanol, water	Apply for 20 seconds, mild air dry for five seconds, light cure for 10 seconds
Clearfil Universal Bond-CUB (01416)	2.3	Bis-GMA, HEMA, MDP, CQ, colloidal silica, silane coupling agent, ethanol, water, hydrophilic aliphatic dimethacrylate	Apply for 10 seconds, mild air dry for five seconds, light cure for 10 seconds
Single Bond Universal-SBU (D-82229)	2.7	HEMA, MDP, silane, filler, dimethacrylate resins, initiators, Vitrebond copolymer, ethanol, water	Mix Single Bond Universal dual cure activator with Single Bond universal in a ratio of 1-to-1, apply adhesive mixture for 20 seconds, dry gently for five seconds, light cure for 10 seconds

Abbreviations: Bis-GMA, bisphenol A diglycidylmethacrylate; CQ, camphorquinone; D3MA, decandiol dimethadrylate; HEMA, 2-hydroxyethyl methacrylate; MCAP, methacrylated carboxylic acid polymer; MDP, 10-methacryloyloxydecyl dihydrogen phosphate.

specimens were fixed on glass slides,[25] subsequently polished with SiC paper and distilled water through 5000-grit, and cleaned ultrasonically. The ceramic–resin interface was examined with light microscopy (LM; DP72, Olympus, Tokyo, Japan). Ten images with 100× magnification were randomly captured for each subgroup (eg, ABU-24h). For quantitative analysis, Image J analysis software was employed to determine the microleakage percentage at the adhesive interface.

Confocal Laser Scanning Microscopy

CUB (silane-containing universal adhesive) was evaluated. One etched ceramic block directly received CUB, whereas another block was pretreated with additional silane and then the CUB applied. Rhodamine B was added to the adhesive for confocal microscopy evaluation.[26] After application of 2-mm of composite resin, the specimens were sectioned into 7-mm × 4-mm × 1-mm slabs with a low-speed diamond saw. The peripheral slabs were discarded, and a middle slab was collected from each group. After being stored in distilled water at 37°C for 24 hours and subjected to 5000 and 10,000 thermocycles, the slabs were observed using a Fluoview Ver.4.2 confocal laser scanning microscope (CLSM; FV1000, Olympus). The same observation place was strictly implemented for each slab under the above three conditions. Emission fluorescence was conducted at 559 nm. Topographic single projection was established from the serial images obtained at a depth of 20 μm.[27] The captured images were analyzed with Imaris 7.2.3 software (v.7.2.3, Bitplane, Zurich, Switzerland). The configuration was standardized at the same level for the entire investigation.

Statistical Analysis

SBS and microleakage percentage were presented as mean and standard deviation values. SBS and microleakage percentage were separately analyzed for each universal adhesive by conducting two-way analysis of variance (ANOVA), with "bonding procedure" and "aging" as independent variables. Tukey post hoc test was applied for multiple comparisons. The significance level was set at $\alpha = 0.05$. Statistical analysis was calculated using SPSS version 23.0 (SPSS, Chicago, IL, USA).

RESULTS

SBS

Figure 1A shows the SBS results for the four different universal adhesives bonded to lithium disilicate glass ceramics. For each adhesive, two-way ANOVA revealed that the SBS was significantly affected by additional silane pretreatment and thermocycling aging ($p<0.001$). The interaction between the two factors was significant (for ABU, CUB, and SBU, $p<0.001$; for ADU, $p=0.018$). For pairwise comparisons within the factor silane pretreatment strategy, after 24 hours of water storage, the SBS of each universal adhesive in the silane-pretreated mode significantly differed from those in the non–silane-pretreated mode ($p<0.05$). After aging, the SBS of the four adhesives under silane-pretreated mode was significantly higher than those of the non–pretreated ones ($p<0.001$). For pairwise comparisons within the factor aging, the SBS of all four adhesives in the non–silane-pretreated mode significantly decreased ($p<0.001$). No significant differences were observed in S-ABU between the 24-hour soaked samples and those subjected to 10,000 thermocycling aging ($p=0.84$); by contrast,

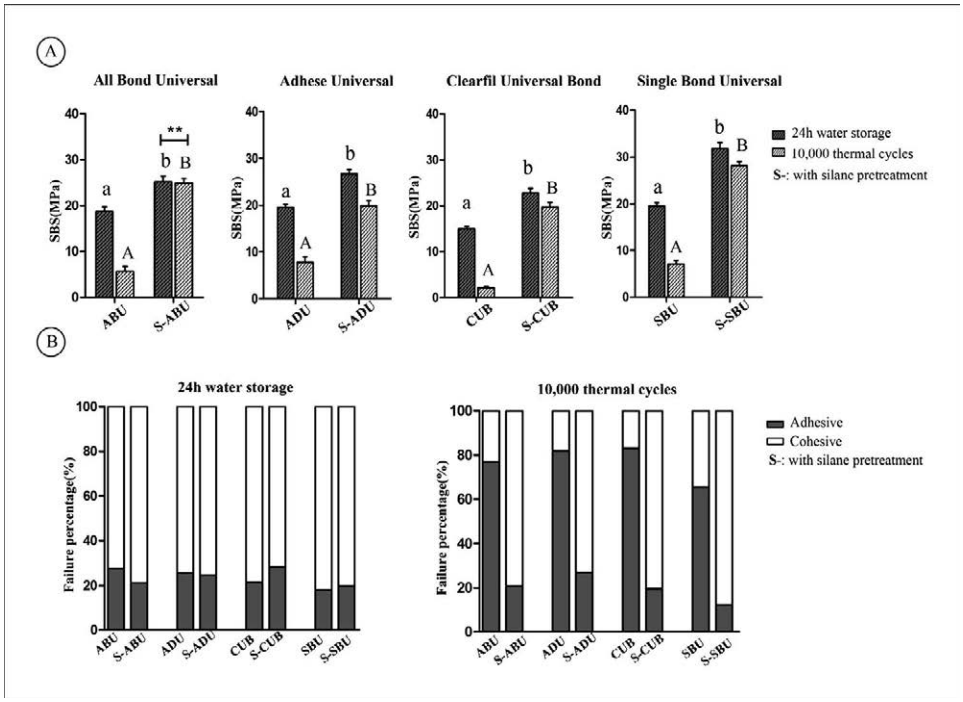

Figure 1. *Effectiveness of bonding strategy and aging on SBS of lithium disilicate glass ceramic with four universal adhesives. (A): SBS was analyzed separately for each adhesive using two-factor ANOVA. For each adhesive, columns labeled with the same lowercase letters or uppercase letters are not significantly different in pairwise comparisons within "bonding strategy" (*p*>0.05), and columns distinguished with asterisks are not significantly different in pairwise comparisons within "aging" (*p*>0.05). (B): Failure mode distribution in the study groups. Failure within the ceramic was classified as adhesive failure mode, whereas failure within the resin or the adhesive was regarded as cohesive failure mode.*

the performance of S-ADU, S-CUB, and S-SBU declined in SBS ($p<0.05$).

Failure Mode Analysis of Debonded Specimens

Figure 1B shows the failure percentage of the different groups in various modes after SBS testing. For immediate groups, the predominant failure mode of the specimens was cohesive failure, regardless of whether an additional silane pretreatment was performed or not. Nevertheless, for aging groups, adhesive failure increased for all groups in the non–silane-pretreated mode, whereas cohesive failure was the predominant mode for groups in the silane-pretreated mode.

Figure 2 provides representative FESEM images of debonded specimens in ABU, S-ABU, SBU, and S-SBU groups after 24 hours of SBS testing. An insignificant difference in morphological appearance was observed between silane-pretreated and non-pretreated groups. The debonded specimens displayed predominant cohesive failure at low magnification, and the adhesives and the composites resins were visible at high magnification.

Representative FESEM images of debonded specimens in ADU, S-ADU, CUB, and S-CUB groups after SBS testing of 10,000 runs with thermocycling are shown in Figure 3. The debonded specimens of the groups in the non–silane-pretreated mode exhibited predominant adhesive failure at low magnification. The fracture mainly exposed the ceramic crystals. Particularly, at high magnification, the crystal structures displayed a round pattern that differed from the etched ceramic surface. For groups in the silane-pretreated mode, FESEM images showed dominant cohesive failure. The bond appeared to fracture underneath the adhesives and the resins. In addition, cleavages and small voids were observed in the debonded interface of the S-CUB group at high magnification.

Microleakage

The results of microleakage percentage for the four different universal adhesives bonded to lithium disilicate glass ceramics are presented separately in Figure 4A. For each adhesive, two-way ANOVA showed that the microleakage percentage was considerably affected by silane pretreatment strategy and thermocycling aging ($p<0.001$). Nevertheless, the interaction between the two factors was insignificant ($p>0.05$). Then, experiments for main effects were conducted. During a 24-hour evaluation, the microleakage percentages of the CUB and SBU groups in the silane-pretreated mode significantly differed from those in non–silane-pretreated mode ($p<0.05$). After aging, the microleakage percentages of all universal adhesives in the silane-pretreated mode were significantly lower than those of the non–silane-pretreated ones ($p<0.05$). In addition, the percentage of all adhesives significantly increased

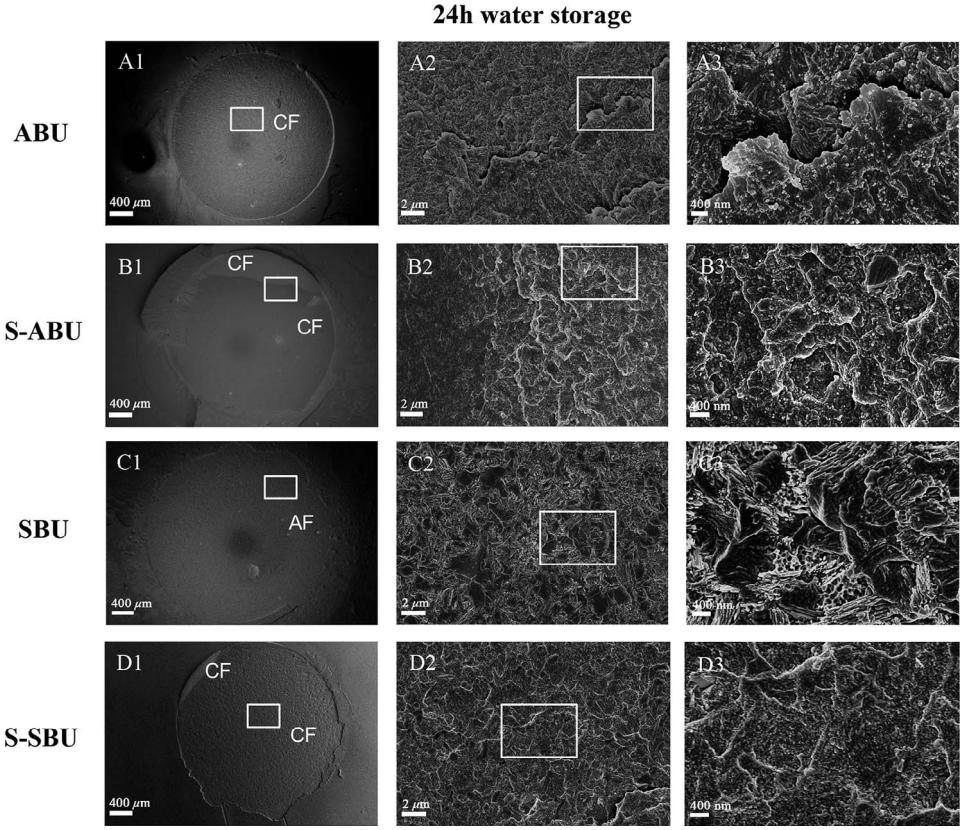

Figure 2. *Representative FESEM images of fracture surface after 24 hours of water storage. (A1): Overview (24×) in All Bond Universal (ABU in non–silane-pretreated mode). (A2-A3): High magnification (5000× and 20,000×) of the cohesive failure part. (B1): Overview in S-ABU (All Bond Universal in silane-pretreated mode). (B2-B3): High magnification of the cohesive failure part. (C1): Overview in SBU. (C2-C3): High magnification of the failure part. (D1): Overview in S-SBU. (D2-D3): High magnification of the cohesive failure part. AF, adhesive failure; CF, cohesive failure.*

after aging compared with 24-hour immediate bonding ($p<0.05$), regardless of whether silane pretreatment was implemented. For each adhesive, the subgroup in the non–silane-pretreated mode after aging (eg, ABU-10,000 thermal cycles) had the highest microleakage percentage.

Figure 4B shows the representative LM images of the ABU and S-ABU groups after 10,000 thermal cycles. Compared with the nonpretreatment group, the pretreatment group exhibited lower degrees of basic fuchsin along the ceramic–resin interface, and the ratio between the stained layer and the bond interface was less than 50%.

CLSM Images

Strong red fluorescence signals were observed in the interface between the composite resin and the lithium disilicate glass ceramic, indicating the presence of adhesive. Figure 4C shows representative CLSM images after 24 hours of soaking and 5000 or 10,000 runs of thermocycling. For the CUB group, the middle area of the adhesive layer significantly thinned after 10,000 cycles of aging compared with that after 24 hours of water storage, possibly implying a weak zone for interfacial fracture. For the S-CUB group, the adhesive layer showed only a few small cracks, cleavages, and voids after aging.

DISCUSSION

In this study, the SBS of all universal adhesives in the silane-pretreated mode was higher than that in the non–silane-pretreated mode regardless of the occurrence of immediate or durable bonding. Furthermore, the durable marginal sealing performance of these universal adhesives in the silane-pretreated mode was better than that in the nonpretreated mode. Thus, the first null hypothesis was rejected. These results suggested that additional silane pretreatment was necessary to improve the durable bonding effectiveness of universal adhesives to lithium disilicate glass ceramics. The SBS of these adhesives after aging was lower and their marginal sealing capability was less stable than those in the immediate condition regardless of the non–silane-pretreated or silane-pretreated mode, except that the SBS of S-ABU after aging was similar to that after 24 hours of water storage. Accordingly, the second null hypothesis was also rejected.

In the oral environment, chemical, thermal, and mechanical factors including saliva, temperature change, biting force, and other habits[7,28] may

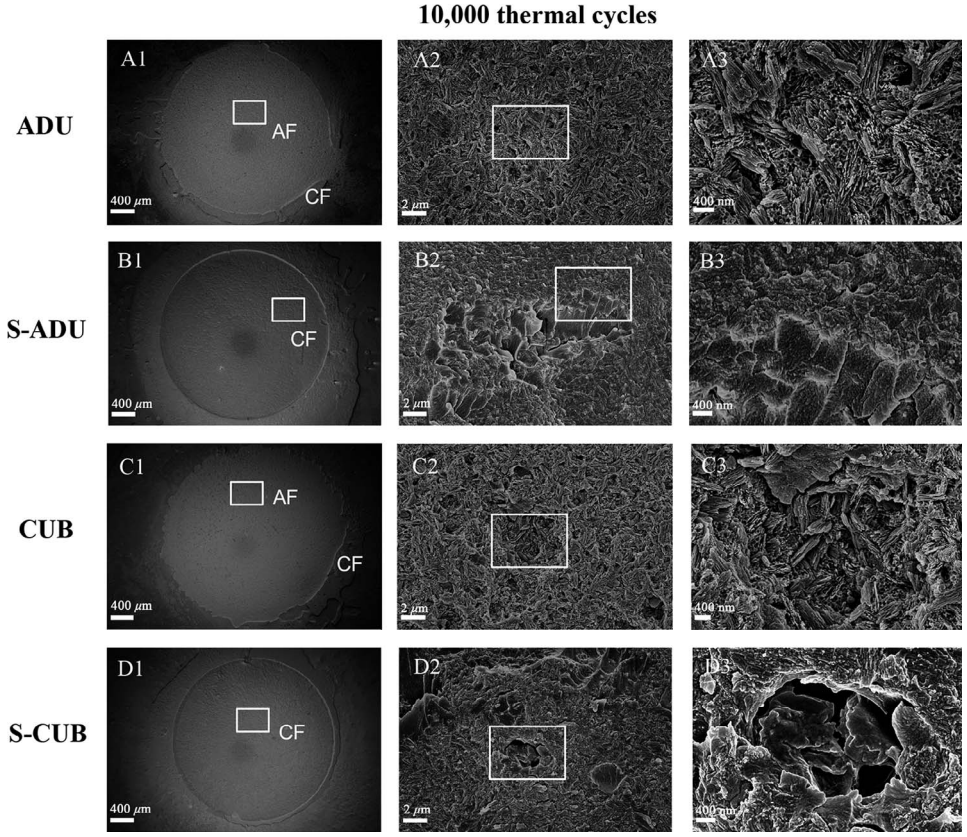

Figure 3. *Representative FESEM images of fracture surface after aging. (A1-A3): ADU group. (B1-B3): S-ADU group. (C1-C3): CUB group. (D1-D3): S-CUB group. Adhesive failure dominated in the ADU and CUB groups. Cohesive failure dominated in the S-ADU and S-CUB groups. AF, adhesive failure; CF, cohesive failure.*

influence ceramic–resin bonding stability.[29] We adopted 10,000 thermal cycles in this study to imitate 1-year clinical physiological aging[16] and to evaluate bond degradation. Our results showed that the SBS of the universal adhesives in the silane-pretreated or non–silane-pretreated mode declined after aging, indicating that thermal cycling aging negatively affected the bonding performance of universal adhesives on lithium disilicate glass ceramic. This deterioration can be explained as follows: (1) thermal cycling could produce hoop stress[30] as a result of the different thermal expansion rates of substrates in bonded interfaces[17] and consequently induce volumetric changes in adhesive layers; thus, the local ingress of water is further enhanced, thereby decreasing the physical/mechanical properties by weakening the frictional forces between polymer chains,[31] (2) the effects of aging may be exacerbated by the chemical hydrolysis of the interfacial components,[32,33] including hydrolytically susceptible groups within methacrylate adhesives, such as hydroxyl, carboxyl, ester, and urethane,[34] thus, adversely affecting durable bonding performance because of these vulnerable areas in the vicinity of the ceramic–resin interface.

However, the extent of SBS decline for adhesives in the non–silane-pretreated mode was significantly higher than that in the silane-pretreated mode, indicating that additional silane may be an efficient material to improve the long-term durability of adhesive interface bonding. This finding corroborated the results obtained by Kim and others,[13] who studied the bonding performance of universal adhesives on leucite-reinforced ceramics. A previous work also reported that optimal bonds are achieved by applying silane to etched lithium disilicate glass ceramics before Scotchbond Universal is used.[35]

Notably, the higher SBS in the silane-pretreated mode than in the non–silane-pretreated mode was possibly related to the predominant cohesive failure. The present study demonstrated that cohesive failure was dominate for all of the universal adhesives in the silane-pretreated mode after 10,000 cycles of thermal aging. Cohesive failure was recognized to increase bond strength values because a fracture propagates through the bulk of a bonded material.[29] Consistent with our findings, previous research also indicated that the bond between glass ceramic and composite resin is stronger if there is cohesive failure within composite

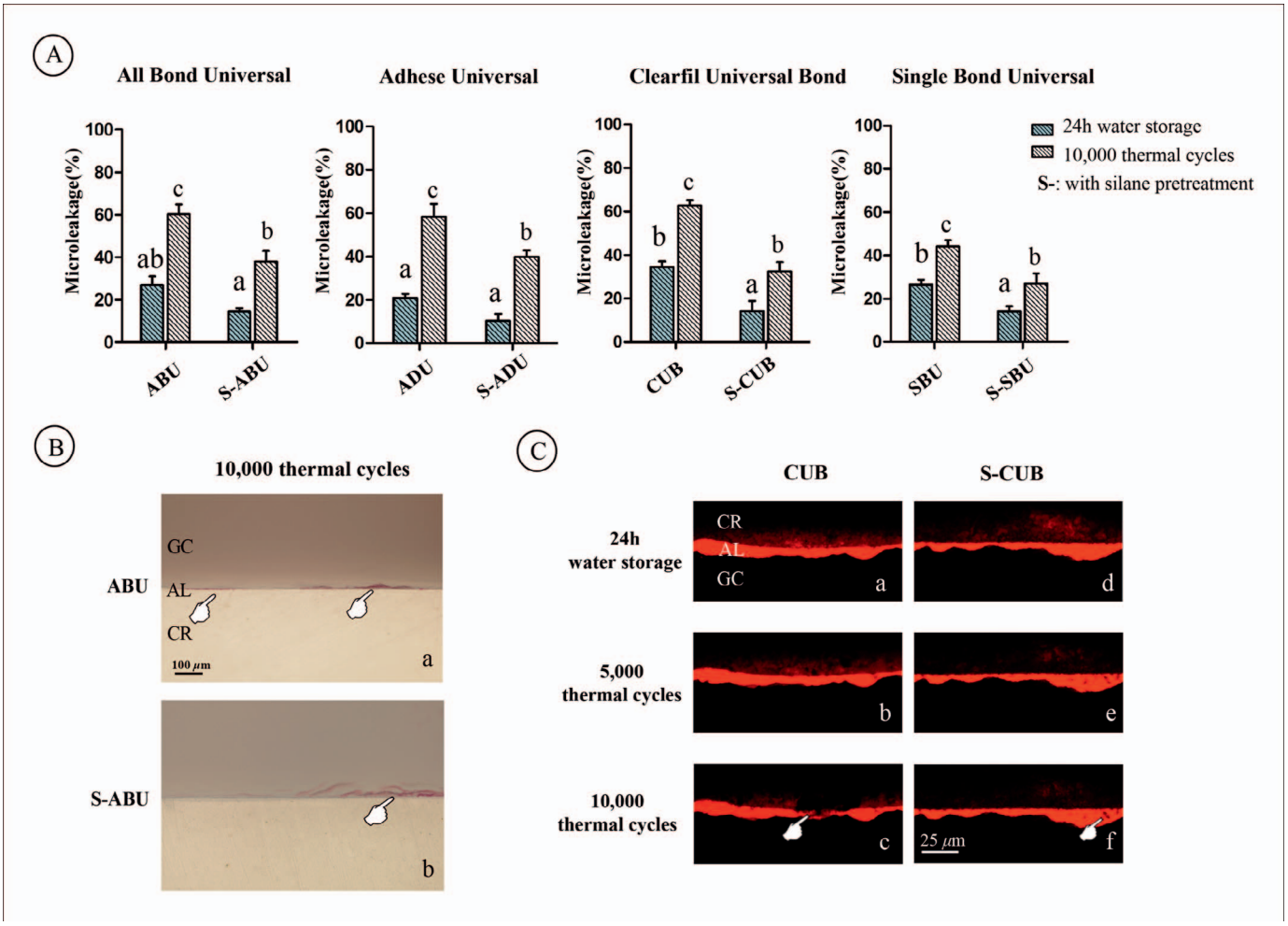

Figure 4. *Effectiveness of bonding strategy and aging on the marginal sealing ability of lithium disilicate glass ceramic with four universal adhesives. (A): Microleakage percentage was analyzed separately for each adhesive using two-factor ANOVA with the main effects. For each adhesive, columns labeled with the same lowercase letters are not significantly different in pairwise comparisons (p>0.05). (B): Representative LM images after aging. a, ABU group. b, S-ABU group. The sign indicates the area with existing microleakage. (C): Representative CLSM images after aging. The sign indicates cleavages and voids existing in the adhesive layer. AL, adhesive layer; CR, composite resin; GC, lithium disilicate glass ceramic.*

in debonded specimens, and this strong bond is attained by applying silane.[36]

Ensuring stable adhesion and tight sealing is key to evaluating the durability of adhesive systems. The mean SBS of the mechanical analysis cannot be considered the sole indicator of bond quality. Thus, an interfacial morphological evaluation may provide additional information. In this work, basic fuchsin stains were observed in the adhesive layer by using light microscopy to reveal the microleakage areas at the interface. The microleakage percentages of all of the adhesives were significantly higher after aging than those with immediate bonding regardless of the silane application mode. However, the percentages of the groups in the silane-pretreated mode (eg, S-ABU) were significantly lower than those in the non–silane-pretreated ones (eg, ABU) after aging. Similarly, the microleakage results validated that the additional silane enhanced the durability and stability of the adhesive interface.

Although aging inevitably occurred, based on the above SBS and microleakage results after aging in the silane-pretreated mode, our findings provided direct evidence that the additional silane was conducive for maintaining long-term ceramic–resin stability. Two reasons may contribute to this effect. On one hand, although the adhesive interface behaves as a permeable membrane,[37] the silanols of silane coupling agents form a direct siloxane bridge with the hydroxyls of the ceramic surface after silane pretreatment is applied. Thus, a cross-linked siloxane polymolecular layer is produced, thereby forming an interpenetrating polymer network with the composite resin.[38] In brief, a hydro-

phobic and branched three-dimensional siloxane film is produced through silanization.[39] Therefore, using a separate silane before applying an adhesive may increase the hydrophobicity of a layer and likely inhibit water uptake. Previous studies also found that degradation occurs less frequently when a more hydrophobic adhesive coating is used.[40,41] Consequently, silane pretreatment could help decrease the possibility of hydrolytic degradation of ceramic–resin bonding and increase the durable bonding quality of the adhesive interface.

On the other hand, additional silane pretreatment may increase the thickness and uniformity of the whole adhesive bonding layer because silane can form an additional layer of chemical bonds between adhesive resin and glass ceramic. In particular, methacrylate groups within adhesive resin can copolymerize with silane molecules,[36] and silanol groups produced by the corresponding methoxy groups can react with the glass ceramic surface.[25] Thus, CLSM images were observed to validate the morphological changes between the non–silane-pretreated and silane-pretreated modes after aging. In a previous study,[42] CLSM revealed that fluid moved at the junction of the adhesive resin and a hybrid layer during the flexure of a tooth and a restoration. In our study, CLSM images demonstrated that the rhodamine dye diffused through the adhesive interface. The gaps among composite resins, adhesives, and glass ceramics may be responsible for the unstable bonding. After the S-CUB was subjected to 10,000 cycles of thermal aging, the adhesive layer showed some small cracks, cleavages, and voids. By comparison, greater dimensional alterations were observed in CUB. The alterations at the interfaces were considered flaws that might expand and contract. Water would infiltrate into the flaw zones, thereby impairing the mechanical properties of the adhesive layer and accelerating deterioration. This phenomenon suggested that the relative integrity of the ceramic–resin adhesive layer created by applying additional silane was essential to bond durability.

Another notable observation was that the silane-containing universal adhesives (CUB and SBU) did not perform better than the silane-free ones (ABU and ADU) as we had expected. After aging occurred, the SBS of the silane-containing universal adhesives in the non–silane-pretreated mode significantly decreased and their microleakage percentage increased. This result shed light on the fact that the silane incorporated in universal adhesives was incapable of slowing down the aging of the ceramic–resin bonding interface, possibly because of the finite quantities and proportions of silane in universal adhesives, along with numerous other components, such as bisphenol A diglycidylmethacrylate, camphorquinone, 10-methacryloyloxydecyl dihydrogen phosphate, and solvent.[34] The efficiency and chemical stability of silane existing in universal adhesives should be further examined.

CONCLUSIONS

Four universal adhesives (two silane-containing and two silane-free) in the silane-pretreated mode exhibited an improvement in bond strengths and a reduction in microleakage percentages compared with those in the non–silane-pretreated mode after 10,000 cycles of thermal aging. Despite the enhanced ease of use of universal adhesive, the simplified bonding approach decreased the bonding quality after aging. Therefore, treatment with additional silane prior to the application of the universal adhesives (for either silane-containing or silane-free) should be clinically promoted to improve the effectiveness and longevity of ceramic–resin bonding.

Acknowledgements

This study was financially supported by grants from the National Nature Science Foundation of China (No. 81571012).

Conflict of Interest

The authors of this article certify that they have no proprietary, financial, or other personal interest of any nature or kind in any product, service, and/or company that is presented in this article.

(Accepted 4 September 2017)

REFERENCES

1. Lien W, Roberts HW, Platt JA, Vandewalle KS, Hill TJ, & Chu TM (2015) Microstructural evolution and physical behavior of a lithium disilicate glass-ceramic *Dental Materials* **31(8)** 928-940.
2. Montazerian M, & Zanotto ED (2017) Bioactive and inert dental glass-ceramics *Journal of Biomedical Materials Research. Part A* **105(2)** 619-639.
3. Song L, Ye Q, Ge X, Misra A, & Spencer P (2016) Mimicking nature: self-strengthening properties in a dental adhesive *Acta Biomaterialia* **35** 138-152.
4. Van Meerbeek B, Yoshihara K, Yoshida Y, Mine A, De Munck J, & Van Landuyt KL (2011) State of the art of self-etch adhesives *Dental Materials* **27(1)** 17-28.
5. Pashley DH, Tay FR, Breschi L, Tjaderhane L, Carvalho RM, Carrilho M, & Tezvergil-Mutluay A (2011) State of the art etch-and-rinse adhesives *Dental Materials* **27(1)** 1-16.
6. Kramer N, & Frankenberger R (2005) Clinical performance of bonded leucite-reinforced glass ceramic inlays

and onlays after eight years *Dental Materials* **21(3)** 262-271.

7. Tian T, Tsoi JK, Matinlinna JP, & Burrow MF (2014) Aspects of bonding between resin luting cements and glass ceramic materials *Dental Materials* **30(7)** e147-e162.
8. Brentel AS, Ozcan M, Valandro LF, Alarca LG, Amaral R, & Bottino MA (2007) Microtensile bond strength of a resin cement to feldpathic ceramic after different etching and silanization regimens in dry and aged conditions *Dental Materials* **23(11)** 1323-1331.
9. Zaghloul H, Elkassas DW, & Haridy MF (2014) Effect of incorporation of silane in the bonding agent on the repair potential of machinable esthetic blocks *European Journal of Dentistry* **8(1)** 44-52.
10. Gregoire G, Sharrock P, & Prigent Y (2016) Performance of a universal adhesive on etched and non-etched surfaces: do the results match the expectations? *Materials Science & Engineering. C, Materials for Biological Applications* **66(1 September)** 199-205.
11. Luque-Martinez IV, Perdigao J, Munoz MA, Sezinando A, Reis A, & Loguercio AD (2014) Effects of solvent evaporation time on immediate adhesive properties of universal adhesives to dentin *Dental Materials* **30(10)** 1126-1135.
12. Passia N, Mitsias M, Lehmann F, & Kern M (2016) Bond strength of a new generation of universal bonding systems to zirconia ceramic *Journal of the Mechanical Behavior of Biomedical Materials* **62(September)** 268-274.
13. Kim RJ, Woo JS, Lee IB, Yi YA, Hwang JY, & Seo DG (2015) Performance of universal adhesives on bonding to leucite-reinforced ceramic *Biomaterials Research* **19(1)** 11.
14. Deng D, Yang H, Guo J, Chen X, Zhang W, & Huang C (2014) Effects of different artificial aging methods on the degradation of adhesive-dentine interfaces *Journal of Dentistry* **42(12)** 1577-1585.
15. Price RB, Derand T, Andreou P, & Murphy D (2003) The effect of two configuration factors, time, and thermal cycling on resin to dentin bond strengths *Biomaterials* **24(6)** 1013-1021.
16. Gale MS, & Darvell BW (1999) Thermal cycling procedures for laboratory testing of dental restorations *Journal of Dentistry* **27(2)** 89-99.
17. Sai K, Shimamura Y, Takamizawa T, Tsujimoto A, Imai A, Endo H, Barkmeier WW, Latta MA, & Miyazaki M (2016) Influence of degradation conditions on dentin bonding durability of three universal adhesives *Journal of Dentistry* **54(November)** 56-61.
18. Sezinando A, Luque-Martinez I, Munoz MA, Reis A, Loguercio AD, & Perdigao J (2015) Influence of a hydrophobic resin coating on the immediate and 6-month dentin bonding of three universal adhesives *Dental Materials* **31(10)** e236-e246.
19. Perdigao J, Kose C, Mena-Serrano AP, De Paula EA, Tay LY, Reis A, & Loguercio AD (2014) A new universal simplified adhesive: 18-month clinical evaluation *Operative Dentistry* **39(2)** 113-127.
20. Queiroz JRC, Nogueira Junior L, Massi M, Silva AdM, Bottino MA, Sobrinho ASdS & Özcan M (2013) Si-based thin film coating on Y-TZP: nfluence of deposition parameters on adhesion of resin cement *Applied Surface Science* **282(1 October)** 245-252.
21. Lung CY, Botelho MG, Heinonen M, & Matinlinna JP (2012) Resin zirconia bonding promotion with some novel coupling agents *Dental Materials* **28(8)** 863-872.
22. Wang C, Niu LN, Wang YJ, Jiao K, Liu Y, Zhou W, Shen LJ, Fang M, Li M, Zhang X, Tay FR, & Chen JH (2014) Bonding of resin cement to zirconia with high pressure primer coating *PLoS One* **9(7)** e101174.
23. Kern M, Barloi A, & Yang B (2009) Surface conditioning influences zirconia ceramic bonding *Journal of Dental Research* **88(9)** 817-822.
24. Aschenbrenner CM, Lang R, Handel G, & Behr M (2011) Analysis of marginal adaptation and sealing to enamel and dentin of four self-adhesive resin cements *Clinical Oral Investigations* **16(1)** 191-200.
25. Yao C, Zhou L, Yang H, Wang Y, Sun H, Guo J, & Huang C (2017) Effect of silane pretreatment on the immediate bonding of universal adhesives to computer-aided design/computer-aided manufacturing lithium disilicate glass ceramics *European Journal of Oral Sciences* **125(2)** 173-180.
26. Yang H, Guo J, Guo J, Chen H, Somar M, Yue J, & Huang C (2015) Nanoleakage evaluation at adhesive-dentin interfaces by different observation methods *Dental Materials Journal* **34(5)** 654-662.
27. Sauro S, Watson TF, Thompson I, & Banerjee A (2012) One-bottle self-etching adhesives applied to dentine air-abraded using bioactive glasses containing polyacrylic acid: an *in vitro* microtensile bond strength and confocal microscopy study *Journal of Dentistry* **40(11)** 896-905.
28. Peumans M, Hikita K, De Munck J, Van Landuyt K, Poitevin A, Lambrechts P, & Van Meerbeek B (2007) Bond durability of composite luting agents to ceramic when exposed to long-term thermocycling *OperativeDentistry* **32(4)** 372-379.
29. AlJehani YA, Baskaradoss JK, Geevarghese A, AlShehry MA, & Vallittu PK (2015) Shear bond strength between alumina substrate and prosthodontic resin composites with various adhesive resin systems *BMC Oral Health* **15(May 2)** 55.
30. Crim GA, Swartz ML, & Phillips RW (1985) Comparison of four thermocycling techniques *Journal of Prosthetic Dentistry* **53(1)** 50-53.
31. Buruiana T, Melinte V, Aldea H, Pelin IM, & Buruiana EC (2016) A new fluorinated urethane dimethacrylate with carboxylic groups for use in dental adhesive compositions *Materials Science & Engineering. C, Materials for Biological Applications* **62(May 1)** 96-104.
32. De Munck J, Van Landuyt K, Peumans M, Poitevin A, Lambrechts P, Braem M, & Van Meerbeek B (2005) A critical review of the durability of adhesion to tooth tissue: methods and results *Journal of Dental Research* **84(2)** 118-132.
33. Ferracane JL (2006) Hygroscopic and hydrolytic effects in dental polymer networks *Dental Materials* **22(3)** 211-222.

34. Van Landuyt KL, Snauwaert J, De Munck J, Peumans M, Yoshida Y, Poitevin A, Coutinho E, Suzuki K, Lambrechts P, & Van Meerbeek B (2007) Systematic review of the chemical composition of contemporary dental adhesives *Biomaterials* **28(26)** 3757-3785.

35. Kalavacharla VK, Lawson NC, Ramp LC, & Burgess JO (2015) Influence of etching protocol and silane treatment with a universal adhesive on lithium disilicate bond strength *Operative Dentistry* **40(4)** 372-378.

36. Shen C, Oh WS, & Williams JR (2004) Effect of post-silanization drying on the bond strength of composite to ceramic *Journal of Prosthetic Dentistry* **91(5)** 453-458.

37. Tay FR, Pashley DH, Suh BI, Carvalho RM, & Itthagarun A (2002) Single-step adhesives are permeable membranes *Journal of Dentistry* **30(7-8)** 371-382.

38. Matinlinna JP, Lassila LV, Ozcan M, Yli-Urpo A, & PK V (2004) An introduction to silane and their clinical applications in dentistry *International Journal of Prosthodontics* **17(2)** 155-164.

39. Matinlinna JP, & Vallittu PK (2007) Bonding of resin composites to etchable ceramic surfaces—an insight review of the chemical aspects on surface conditioning *Journal of Oral Rehabilitation* **34(8)** 622-630.

40. Abdalla AI, & Feilzer AJ (2008) Four-year water degradation of a total-etch and two self-etching adhesives bonded to dentin *Journal of Dentistry* **36(8)** 611-617.

41. Gamborgi GP, Loguercio AD, & Reis A (2007) Influence of enamel border and regional variability on durability of resin-dentin bonds *Journal of Dentistry* **35(5)** 371-376.

42. Dorfer CE, Staehle HJ, Wurst MW, Duschner H, & Pioch T (2000) The nanoleakage phenomenon: influence of different dentin bonding agents, thermocycling and etching time *European Journal of Oral Sciences* **108(4)** 346-351.

©Operative Dentistry, 2018, **43-6,** 613-618

Effect of Various Bleaching Agents on the Surface Composition and Bond Strength of a Calcium Silicate-based Cement

S Kucukkaya Eren • H Aksel • O Uyanık • E Nagas

Clinical Relevance

We recommend the use of calcium silicate-based cement as a cervical barrier when performing intracoronal bleaching using a mixture of sodium perborate with water or 3% hydrogen peroxide.

ABSTRACT

This study aimed to evaluate the morphological and elemental changes that occur on the surface of calcium silicate–based cement (CSC) and to analyze the bond strength of composite resin to CSC after application of various bleaching agents. One hundred twenty-five CSC blocks (Biodentine) were prepared and randomly divided into five groups according to the bleaching agent applied over the material surface (n=25): SP-DW (sodium perborate–distilled water mixture), SP-HP (sodium perborate–3% hydrogen peroxide [H_2O_2] mixture), CP (37% carbamide peroxide gel), HP (35% H_2O_2 gel), and a control group (no bleaching agent). After 1 week, scanning electron microscopy provided an analysis of the surface morphology and elemental composition for 10 specimens from each group. Composite resin was placed at the center of each cement surface in the remaining specimens (n=15). A universal testing machine determined shear bond strength (SBS) and fracture patterns were identified with a dental operating microscope. Data were analyzed using one-way analysis of variance and Tukey HSD tests. The cement surface in the CP and HP groups presented changes in structure and elemental distribution compared with the remaining groups. The former groups exhibited a decrease in the calcium level and an increase in the silicon level and presented significantly fewer SBS values than the remaining groups ($p<0.05$). Most failures were adhesive in the CP and HP groups, while they were predominantly cohesive in the remaining groups. The bleaching agents with higher concentration induced deterioration of the cement surface

*Selen Kucukkaya Eren, DDS, PhD, Hacettepe University, Department of Endodontics, Faculty of Dentistry, Sıhhiye, Ankara, Turkey

Hacer Aksel, DDS, PhD, Hacettepe University, Department of Endodontics, Faculty of Dentistry, Ankara, Turkey

Ozgur Uyanık, DDS, PhD, Hacettepe University, Department of Endodontics, Faculty of Dentistry, Ankara, Turkey

Emre Nagas, DDS, PhD, Hacettepe University, Endodontics, Faculty of Dentistry, Sıhhiye, Ankara, Turkey

*Corresponding author: Hacettepe University, Sıhhiye, Ankara, 06100, Turkey; e-mail: selenkkkaya@yahoo.com

DOI: 10.2341/17-188-L

and negatively affected the bond strength of the composite resin to CSC. The use of CSC is recommended as a cervical barrier when intracoronal bleaching is performed with a mixture of sodium perborate with water or 3% H_2O_2.

INTRODUCTION

Intracoronal bleaching is a conservative and cost-effective procedure to improve the esthetics of discolored endodontically treated teeth.[1] It involves insertion of a bleaching agent into the pulp chamber, which is then sealed using a temporary restoration between visits.[1]

Several bleaching agents are used for intracoronal bleaching, including a mixture of sodium perborate and water, carbamide peroxide, hydrogen peroxide (H_2O_2), or a combination of sodium perborate and H_2O_2.[1] These agents typically accomplish bleaching through the release of H_2O_2 and diffusion of reactive oxygen through dentinal tubules, which then oxidizes the pigments and reverses the chromatic alteration of dental tissues.[2] However, H_2O_2 has the capacity to denature dentin, which leads to a slightly acidic environment that may induce osteoclastic activity and invasive cervical resorption.[1] To prevent such occurrences, the placement of a cervical barrier before intracoronal bleaching is recommended.[1]

The cervical barrier should be impermeable in order to prevent intraradicular and extraradicular diffusion of the peroxides.[1] Recently, mineral trioxide aggregate (MTA), a calcium silicate–based cement (CSC), has been evaluated as a cervical barrier during intracoronal bleaching procedures.[3] Despite possessing several desirable properties such as superior sealing ability, good mechanical properties, and biocompatibility, MTA presents certain notable shortcomings such as a long setting time and tooth discoloration.[4] In recent years, another CSC, Biodentine, has drawn attention because of its good mechanical properties, high biocompatibility and bioactivity.[5,6] And owing to its color stability, this cement is recommended for use as a dentin substitute under composite resin restorations[7,8] and in esthetically sensitive areas.[9]

There is no available data on the use of Biodentine as a cervical barrier during intracoronal bleaching. The effects of bleaching agents on the Biodentine surface and adhesion between Biodentine and a composite resin restoration warrant further investigation. Therefore, the aim of this study was to evaluate the morphological and elemental changes that occur on the Biodentine surface and to analyze the bond strength of composite resin to Biodentine after application of various bleaching agents.

METHODS AND MATERIALS

Specimen Preparation

One hundred twenty-five acrylic blocks were prepared in silicone having an internal diameter of 5 mm and height of 7 mm. To obtain the blocks, autopolymerizing acrylic resin (Meliodent, Heraeus Kulzer, Armonk, NY, USA) was mixed according to the manufacturer's instructions and placed in the silicone tubes. After polymerization, a cavity with a diameter of 3 mm and height of 1.5 mm was prepared with a fissure bur (Dentsply Maillefer, Ballaigues, Switzerland) at the center of each acrylic block. Biodentine (Septodont, St-Maur-des-Fossés, France) was mixed according to the manufacturer's instructions and placed in the cavities using a spatula.

The specimens were stored for 72 hours at 37°C and 100% humidity. All prepared surfaces were polished with a 400-grit silicone carbide abrasive disc (Buehler, Lake Bluff, IL, USA) using a polishing device (Mecapol P230, Presi, France) for 60 seconds to create a standard layer. The specimens were randomly divided into five groups (n=25) according to the bleaching agent, applied to the surface of the cement as follows (from lower to higher H_2O_2 release):

Control group—No treatment

SP-DW group—Sodium perborate powder mixed with distilled water in a ratio of 2:1 g/mL

SP-HP group—Sodium perborate powder mixed with 3% H_2O_2 solution in a ratio of 2:1 g/mL

CP group—37% carbamide peroxide gel (Whiteness Super-Endo, FGM Products, Joinville, SC, Brazil).

HP Group—35% H_2O_2 gel (Opalescence Endo, Ultradent Products, South Jordan, UT, USA)

Following the preparation, the bleaching agents were placed in silicone tubes with an internal diameter of 5 mm and height of 2 mm. Then, the tubes with the bleaching agents were placed on the cement surfaces. The top surface of each bleaching agent was covered with a cotton pellet and a temporary filling material (Cavit-W, 3M ESPE, Seefeld, Germany). Each tube with the bleaching agent and block with CSC were taped together to prevent separation during storage. All specimens were stored for 1 week at 37°C and 100% humidity.

Thereafter, each tube with the bleaching agent was removed and the cement surface was cleaned with distilled water for 1 minute and air-dried.

Scanning Electron Microscopy Analysis

Ten specimens from each group were coated with gold using a vacuum evaporator (JEE-400; JEOL Ltd, Tokyo, Japan) and examined with a scanning electron microscope (SEM) (JEOL 6400, JEOL Corp, Tokyo, Japan) fitted with an energy dispersive spectroscopy (EDS) system (EMAX-7000 Type S; Horiba Ltd, Kyoto, Japan) to characterize the microstructural surface morphology and to calculate the weight percentages of the elements Ca, Si, Mg, Na, K, Al, Zr, and P. To standardize the examined area of each sample, the central beam of the SEM was directed to the center of the specimen under 10× magnification, which was gradually increased to 1000×.

Placement of Restorative Material

A composite resin system (Ice, SDI, Bayswater, Victoria, Australia) was applied over the remaining samples (n=15) according to the manufacturer's instructions. Initially, each cement surface was etched with 37% phosphoric acid (Super Etch, SDI) for 20 seconds and washed with water for 15 seconds. Then, the surfaces were dried with an oil-free air spray to remove excess water. The bonding agent (Stae, SDI) was applied with a microbrush to the surfaces, which were then air-dried for 5 seconds. The bonding agent was cured using a light-emitting diode light-curing unit (Mini LED, Acteon, Mount Laurel, NJ, USA) with an output of 1000 mW/cm^2 for 10 seconds. Cylindrically shaped plastic tubes, with a 2-mm internal diameter and 2-mm height, were placed at the center of the cement surface, and composite resin was condensed into each tube and polymerized for 40 seconds with the light-curing unit. After the polymerization process, the tubes were cut with a scalpel and carefully removed. The specimens were stored at 37°C in 100% humidity for 24 hours.

In this study, a single operator performed the preparation and placement of the CSC and bleaching agents; a second operator, who was blinded to the groups, placed the restorative material.

Shear Bond Strength Test

The shear bond strength (SBS) test was performed using a knife-edge blade in a universal testing machine (Instron, Model 1334, Instron, Canton, MA, USA) with a crosshead speed of 1 mm/min. The load at failure was recorded in newtons, and the bond strength was calculated in megapascals (MPa) by dividing the load at failure by the adhesive surface area. Failure modes were evaluated under a dental operating microscope at 20× magnification and categorized into one of three failure types: adhesive failure at the CSC and composite resin interface, cohesive failure within the CSC or composite resin, or mixed failure composed of adhesive and cohesive failure of the materials (Figure 1a-c).

Statistical Analysis

Data were analyzed using one-way analysis of variance and Tukey HSD tests. The level of significance was set at α=0.05.

RESULTS

In the SEM examination, platelike, globular, and rodlike structures were observed on the surface of the control group (Figure 2a). The SP-DW group showed clusters of globular and cubic crystals with air bubbles in some places (Figure 2b). In the SP-HP group, globular and rodlike structures were observed with air bubbles throughout the surface (Figure 2c). There were numerous crack lines and "woodpecker holes" on the cement surface in the CP (Figure 2d) and HP groups (Figure 2e).

Table 1 shows the results of element analysis detected in each group. The Ca and Si values of the SP-DW and SP-HP groups were similar to those of the control group ($p>0.05$). The Ca values of the CP and HP groups were significantly lower, while the Si values were higher than were the remaining groups ($p<0.05$).

The mean (±SDs) of the SBS values of the groups and the modes of failure of the specimens after the SBS test are presented in Table 2. There was no statistically significant difference between the CP and HP groups ($p>0.05$), while they showed significantly lower SBS values than did the remaining groups ($p<0.05$). The SP-DW, SP-HP, and control groups presented similar SBS values ($p>0.05$). Inspection of the samples revealed the bond failure to be predominantly cohesive for the SP-DW, SP-HP, and control groups and adhesive for the CP and HP groups.

DISCUSSION

Numerous clinical reports using several bleaching agents have revealed that there is no ideal protocol for intracoronal bleaching of endodontically treated

Table 1: *Quantitative SEM/EDS Analysis of the Element Proportion of CSC Surface in Groups (Weight %)*[a]

Element	Control	Groups			
		SP-DW	SP-HP	CP	HP
Ca	86.59 ± 7.12	82.11 ± 5.33	85.29 ± 7.91	60.75 ± 7.97	65.77 ± 9.61
Si	13.09 ± 7.07	12.94 ± 7.01	11.37 ± 5.69	33.71 ± 3.92	23.88 ± 7.48
Mg	0.32 ± 0.12	1.32 ± 0.82	0.44 ± 0.25		
Na		2.58 ± 1.92	2.12 ± 1.55	0.25 ± 0.06	0.97 ± 0.64
K		1.05 ± 0.39	0.78 ± 0.29	0.97 ± 0.41	0.49 ± 0.21
Al				2.08 ± 1.01	
Zr				2.24 ± 1.79	
P					8.89 ± 3.99

[a] *Data are expressed as mean ± SD.*

teeth.[10-12] However, it is clear that the aim should be to maximize bleaching efficacy while minimizing damage to adjacent tissues.[13] Sodium perborate with water has been reported as the safest bleaching agent owing to its low hydroxyl radical diffusion.[13] However, in case of severe discoloration, the use of bleaching agents that generate greater hydroxyl radical penetration may be indicated.[1,13] In this regard, a balance might be achieved by decreasing the change frequency or application time of the bleaching agent while increasing the concentration.[13] Considering that the use of each agent may have a clinical indication, bleaching agents that release H_2O_2 at varying concentrations were tested in the present study.

SEM images obtained in the present study indicate that the effects of a bleaching agent on the surface morphology of CSC were concentration dependent. The cement surface presented various defects such as cracks and holes after application of 37% carbamide peroxide and 35% H_2O_2. On the other hand, the cement surface in the SP-DW and SP-HP groups presented mainly platelike, globular, cubic, and rodlike structures as in the control group. These findings are consistent with those of a previous study wherein MTA was used as a cervical barrier.[3] H_2O_2 may produce bubbling when in contact with the surface of CSC; this oxygen bubbling could be the reason for the more porous surface in the SP-HP group compared with the control and SP-DW groups. When in contact with moisture, carbamide peroxide decomposes into one-third H_2O_2 and two-thirds urea.[2] Accordingly, approximately 10%-15% H_2O_2 was released in the CP group. With the increase in H_2O_2 release, the cement surface seemed to be disturbed more because larger defects were evident on the surfaces of the CP and HP groups. Of note, cracks and holes on the disturbed surface may interfere with the mechanical and adhesive properties of the material.[3]

Table 2: *Shear Bond Strength Values (MPa) of Composite Resin to CSC and Distribution of Failure Modes in Groups (n=15)*[a]

Groups	SBS Values (Mean ± SD)	Failure Mode (%) (A/C/M)
Control	6.99 ± 2.66[a]	13.3/66.7/20
SP-DW	6.66 ± 1.61[a]	6.7/73.3/20
SP-HP	6.44 ± 1.94[a]	6.7/66.7/26.6
CP	2.66 ± 1.47[b]	60/0/40
HP	2.41 ± 1.28[b]	66.7/0/33.3

Abbreviations: A, adhesive failure along the cement-resin interface; C, cohesive failure within the materials; M, mixed failure.
[a] *Different superscript letters indicate statistically significant differences between the groups* ($p<0.05$).

Reportedly, the pH of 35% H_2O_2 gel and 35% carbamide peroxide gel is 3.7 and 6.5, respectively,[14] while mixtures of sodium perborate with water or H_2O_2 have a pH of >7.4 when prepared in a 2-g/mL ratio.[15] According to the EDS analysis conducted in the present study, the Ca/Si ratio of the cement surface decreased in the CP and HP groups compared with the control group, while it remained stable in the SP-DW and SP-HP groups. The acidic condition of the bleaching agents in the CP and HP groups may induce the release of Ca ions and lead to an increase in the relative concentration of Si. In line with the present findings, Tsujimoto and others[3] reported that the acidic conditions induced by bleaching agents resulted in deterioration of the MTA surface and caused a marked decrease in the Ca/Si ratio. It is worth mentioning that the pH of bleaching agents increases with time, probably because of the decomposing of acidic H_2O_2 radicals into oxygen and water.[15,16] However, the initial pH levels of the bleaching agents seem to affect the

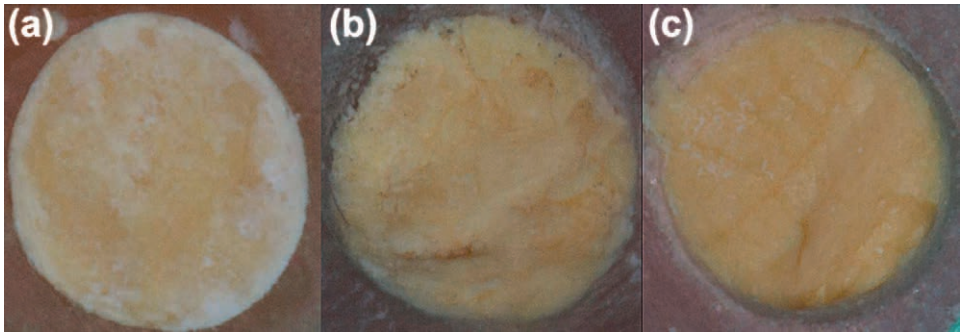

Figure 1. *Representative images of the failure modes. (a): Adhesive failure at CSC and composite resin interface. (b): Cohesive failure within CSC. (c): Mixed failure.*

micromorphology and elemental distribution of the cement surface. Other elements detected by the EDS analysis could be from residue of the bleaching agents or the material itself after exposure to the agents.

The bond strength between restorative and underlying materials is important for optimal quality of the filling as well as the success of restorations. Several studies have evaluated the bond strength between Biodentine and composite resin materials.[17-19] However, the bond strength between Biodentine and composite resin after application of various bleaching agents remains unclear. In the present study, the application of a mixture of sodium perborate with either water or 3% H_2O_2 had no significant effect on the bond strength of composite resin to Biodentine. However, adhesion between the two materials was negatively affected after the placement of either 37% carbamide peroxide or 35% H_2O_2 gel over the cement surface. One might speculate that the bond strength between CSC and composite resin is affected by morphological changes in the surface after application of bleaching agents at high concentrations. The deteriorated surface observed in the CP and HP groups could interfere with micromechanical attachment, thereby resulting in decreased bond strength to composite resin. Furthermore, breakdown of the chemical union could be another reason for the poor bond strength results. Although it is unknown whether chemical adhesion exists between CSC and composite resin, it is possible that resin monomers bind chemically to Ca in CSC.[17] Therefore, the distinctly lower Ca levels in the CP and HP groups could be another explanation for the negative impact on the bond strength.

Bond failures observed in the CP and HP groups were predominantly adhesive, while these were predominantly cohesive in the remaining groups. Interestingly, in a recent study, no adhesive failure was observed at the CSC or composite resin interface.[19] Based on the present findings, the application of bleaching agents at high concentrations may affect the bond strength between CSC and composite resin as well as the failure type. Clinically, this finding should be viewed with caution as the bond could be more acceptable when fracture occurs inside each material rather than in the bonded interface.[20]

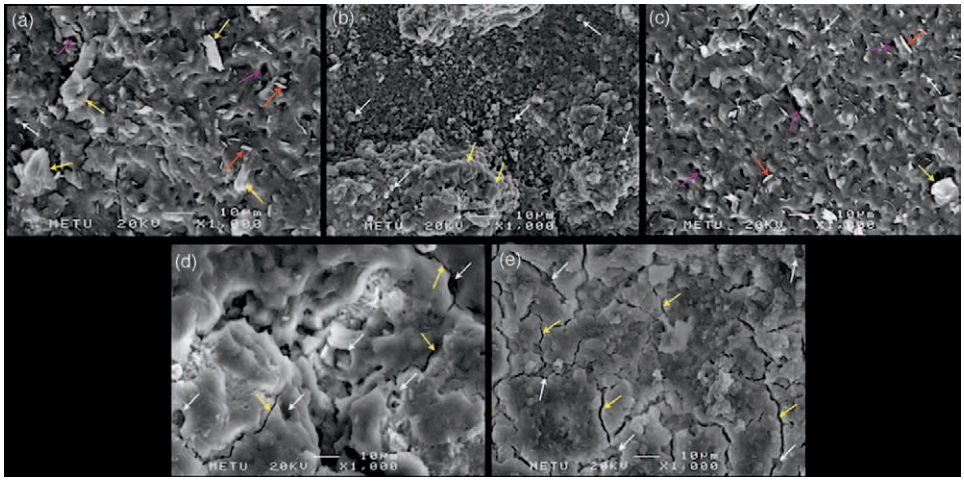

Figure 2. *Photomicrographs obtained by SEM of the representative specimens of the groups (1000x). (a): Platelike (yellow arrows), globular (white arrows), and rodlike (red arrows) structures with air bubbles (purple arrows) on the cement surface in the control group. (b): Globular (white arrows) and cubic (yellow arrows) structures on the cement surface in the SP-DW group. (c): Globular (white arrows), plate-like (yellow arrows), and rod-like (red arrows) structures with air bubbles (purple arrows) on the cement surface in the SP-HP group. (d and e): Crack lines (yellow arrows) and woodpecker holes (white arrows) on the cement surface in the CP and HP groups, respectively.*

CONCLUSIONS

Bleaching agents applied at higher concentrations negatively affected the micromorphology of the CSC surface and the bond strength between CSC and composite resin. Nevertheless, the use of CSC can be recommended as a cervical barrier when intracoronal bleaching is performed with a mixture of sodium perborate with water or 3% H_2O_2.

Conflict of Interest

The authors deny any conflicts of interest related to this study and certify that they have no proprietary, financial, or other personal interest of any nature or kind in any product, service, and/or company that is presented in this article.

(Accepted 21 December 2017)

REFERENCES

1. Attin T, Paque F, Ajam F, & Lennon AM (2003) Review of the current status of tooth whitening with the walking bleach technique *International Endodontic Journal* **36(5)** 313-329.
2. Joiner A (2006) The bleaching of teeth: A review of the literature *Journal of Dentistry* **34(7)** 412-419.
3. Tsujimoto M, Ookubo A, Wada Y, Matsunaga T, Tsujimoto Y, & Hayashi Y (2011) Surface changes of mineral trioxide aggregate after the application of bleaching agents: Electron microscopy and an energy-dispersive X-ray microanalysis *Journal of Endodontics* **37(2)** 231-234.
4. Parirokh M, & Torabinejad M (2010) Mineral trioxide aggregate: a comprehensive literature review—Part III: Clinical applications, drawbacks, and mechanism of action *Journal of Endodontics* **36(3)** 400-413.
5. Grech L, Mallia B, & Camilleri J (2013) Investigation of the physical properties of tricalcium silicate cement-based root-end filling materials *Dental Materials* **29(2)** e20-e28.
6. Cornelio AL, Rodrigues EM, Salles LP, Mestieri LB, Faria G, Guerreiro-Tanomaru JM, & Tanomaru-Filho M (2017) Bioactivity of MTA Plus, Biodentine and experimental calcium silicate-based cements in human osteoblast-like cells *International Endodontic Journal* **50(1)** 39-47.
7. Koubi S, Elmerini H, Koubi G, Tassery H, & Camps J (2012) Quantitative evaluation by glucose diffusion of microleakage in aged calcium silicate-based open-sandwich restorations *International Journal of Dentistry* **2012** 105863.
8. Koubi G, Colon P, Franquin JC, Hartmann A, Richard G, Faure MO, & Lambert G (2013) Clinical evaluation of the performance and safety of a new dentine substitute, Biodentine, in the restoration of posterior teeth—A prospective study *Clinical Oral Investigations* **17(1)** 243-249.
9. Valles M, Mercade M, Duran-Sindreu F, Bourdelande JL, & Roig M (2013) Influence of light and oxygen on the color stability of five calcium silicate-based materials *Journal of Endodontics* **39(4)** 525-528.
10. Bizhang M, Heiden A, Blunck U, Zimmer S, Seemann R, & Roulet JF (2003) Intracoronal bleaching of discolored non-vital teeth *Operative Dentistry* **28(4)** 334-340.
11. Amato M, Scaravilli MS, Farella M, & Riccitiello F (2006) Bleaching teeth treated endodontically: Long-term evaluation of a case series *Journal of Endodontics* **32(4)** 376-378.
12. Abbott P, & Heah SY (2009) Internal bleaching of teeth: An analysis of 255 teeth *Australian Dental Journal* **54(4)** 326-333.
13. Lou EK, Cathro P, Marino V, Damiani F, & Heithersay GS (2016) Evaluation of hydroxyl radical diffusion and acidified thiourea as a scavenger during intracoronal bleaching *Journal of Endodontics* **42(7)** 1126-1130.
14. Price RB, Sedarous M, & Hiltz GS (2000) The pH of tooth-whitening products *Journal of the Canadian Dental Association* **66(8)** 421-426.
15. Rotstein I, & Friedman S (1991) pH variation among materials used for intracoronal bleaching *Journal of Endodontics* **17(8)** 376-379.
16. Lee GP, Lee MY, Lum SO, Poh RS, & Lim KC (2004) Extraradicular diffusion of hydrogen peroxide and pH changes associated with intracoronal bleaching of discoloured teeth using different bleaching agents *International Endodontic Journal* **37(7)** 500-506.
17. Hashem DF, Foxton R, Manoharan A, Watson TF, & Banerjee A (2014) The physical characteristics of resin composite-calcium silicate interface as part of a layered/laminate adhesive restoration *Dental Materials* **30(3)** 343-349.
18. Cantekin K, & Avci S (2014) Evaluation of shear bond strength of two resin-based composites and glass ionomer cement to pure tricalcium silicate-based cement (Biodentine®) *Journal of Applied Oral Science* **22(4)** 302-306.
19. Altunsoy M, Tanriver M, Ok E, & Kucukyilmaz E (2015) Shear bond strength of a self-adhering flowable composite and a flowable base composite to mineral trioxide aggregate, calcium-enriched mixture cement, and Biodentine *Journal of Endodontics* **41(10)** 1691-1695.
20. Tate WH, Friedl KH, & Powers JM (1996) Bond strength of composites to hybrid ionomers *Operative Dentistry* **21(4)** 147-152.

©Operative Dentistry, 2018, **43-6,** 619-630

Influence of Ambient Temperature and Light-curing Moment on Polymerization Shrinkage and Strength of Resin Composite Cements

N Rohr • JA Müller • J Fischer

Clinical Relevance

Polymerization shrinkage at 37°C with light application 5 minutes after mixing ranges from 4.0% to 5.8%. Light application performed as soon as possible after placing a restoration minimizes cement shrinkage.

ABSTRACT

Objective: The purpose of this study was to establish a clinically appropriate light-curing moment for resin composite cements while achieving the highest indirect tensile strength and lowest polymerization shrinkage.

Methods and Materials: Polymerization shrinkage of seven resin composite cements (Multilink Automix, Multilink Speed Cem, RelyX Ultimate, RelyX Unicem 2 Automix, Panavia V5, Panavia SA plus, VITA Adiva F-Cem) was measured at ambient temperatures of 23°C and 37°C. Testing was done for autopolymerized and light-cured specimens after light application at either 1, 5, or 10 minutes after mixing. Indirect tensile strength of all cements was measured after 24 hours of storage at temperatures of 23°C and 37°C, for autopolymerized and light-cured specimens after light application 1, 5, or 10 minutes after mixing. To illustrate filler size and microstructures, SEM images of all cements were captured. Statistical analysis was performed with one-way ANOVA followed by *post hoc* Fisher LSD test (α=0.05).

Results: Final polymerization shrinkage of the resin composite cements ranged from 3.2% to 7.0%. An increase in temperature from 23°C to 37°C as well as the light-curing moment resulted in material dependent effects on the polymerization shrinkage and indirect tensile

*Nadja Rohr, Dr med dent, University Center for Dental Medicine Basel, Division of Dental Materials and Engineering, Department of Reconstructive Dentistry, Basel, Switzerland

Johannes A Müller, Dr med dent, University Center for Dental Medicine, Department of Reconstructive Dentistry, Basel, Switzerland

Jens Fischer, Prof Dr med dent, Dr rer nat, University Center for Dental Medicine, Division of Dental Materials and Engineering, Department of Reconstructive Dentistry, Basel, Switzerland

*Corresponding author: Hebelstr 3, 4051 Basel, Switzerland; e-mail: nadja.rohr@unibas.ch

DOI: 10.2341/17-085-L

strength of the cements. Polymerization shrinkage of the cements did not correlate with the indirect tensile strength of the cement in the respective groups. Highest indirect tensile strengths were observed for the materials containing a homogeneous distribution of fillers with a size of about 1 μm (Multilink Automix, Panavia V5, VITA Adiva F-Cem).

Conclusion: The magnitude of the effect of light-curing moment and temperature increase on polymerization shrinkage and indirect tensile strength of resin composite cements is material dependent and cannot be generalized.

INTRODUCTION

The increased use of esthetic ceramic materials in dentistry requires the application of resin-based luting cement to bond a restoration to the tooth structure. Resin-based composite materials are generally superior to conventional cements in providing higher strength and low margin wear.[1-3] Their polymerization shrinkage may nevertheless lead to microleakage.[4]

The polymerization of dual-cured resin composite cements is catalyzed by a chemically (autopolymerization) and photo-activated (light-curing) initiator. The polymerization reaction starts with the mixing of base and catalyst paste, thus activating the chemical initiator. Hence, the processing time is limited. Photo initiation allows the polymerization reaction to advance at the time a restoration is correctly placed and cement excess is removed. However, areas under an opaque restoration not reached by the light may not polymerize as well as dual-cured areas. Most cement materials reveal a higher degree of conversion by dual-curing compared with autopolymerization.[5-7]

Shrinkage occurs during the crosslinking of polymer chains, thus creating polymerization stress between tooth structure and resin composite cement.[8] In the early stage of polymerization, resin composite cement reveals high viscosity and is therefore able to relax developing stress. After a short time or after light application, the material becomes rigid and is unable to deform, hence, stress starts to increase.[9,10] The magnitude of volumetric shrinkage is determined by the amount and volume of fillers as well as the composition and the degree of conversion of the resin matrix.[10] Filler particle content for resin composite cement is typically around 50 vol%.[11] Shrinkage strain for different resin cements is reported to range from 1.77% to 5.29%.[12] Shrinkage values should be considered approximate as they vary with the extent of the polymerization reaction.[11] The application of light to dual-cured resin composite cements increases their degree of conversion but not necessarily their shrinkage strain.[12] The degree of conversion is, however, material related; some systems are significantly more dependent on light-activation than others.[5,13-17] Due to a slower reaction rate and incorporation of porosity, autopolymerized resin composite cements may develop less shrinkage stress.[18-20] A dual-curing mode, however, improves bond strength,[21] flexural strength, compressive strength, indirect tensile strength, elastic modulus, and hardness.[3,22,23]

An increase in temperature from 23°C to 37°C may also affect the polymerization process. For light-cured resin composites, a more rapid stress build-up—meaning an increased shrinkage-stress rate—was reported when the temperature was increased.[10] Because of the increased temperature, viscosity may also decrease, resulting in additional monomer conversion[24-26] and thus in a higher degree of conversion.[26]

It has been speculated that a delay in light-activation of dual-cured composite resins enhances their properties by allowing the autopolymerization initiators to react to some extent before being entrapped by photo-activated polymeric chains.[27-29] An ideal balance between autopolymerization and time of light-activation is yet to be determined.[29] To our knowledge, there are no studies that report how polymerization shrinkage of resin composite cements is affected by the light-curing moment (time of light application) and temperature increase and how these factors affect the materials' strength.

The purpose of this study was therefore to establish a clinically appropriate light-curing moment while achieving highest indirect tensile strength and lowest polymerization shrinkage. Hypotheses were that 1) an increase in temperature results in higher polymerization shrinkage and higher indirect tensile strength of resin composite cements and that 2) the light-curing moment of resin composite cements does not affect polymerization shrinkage or indirect tensile strength.

METHODS AND MATERIALS

Polymerization shrinkage of four dual-curing adhesive and three self-adhesive resin composite cements (Table 1, 2) was measured. The shrinkage of

Table 1: *Cement Materials Used*

Name	Manufacturer	Type	Monomers	Fillers	Lot.No.
Multilink Automix	Ivoclar Vivadent	Adhesive resin composite cement	Base paste: Bis-GMA, HEMA, 2-dimethylaminoethyl methacrylate Catalyst paste: ethyoxylated bisphenol A dimethacrylate, UDMA, HEMA	40 vol% - Barium glass - Ytterbium trifluoride - Spheroid mixed oxide Particle size: 0.25–3.0 μm	T33131
Multilink Speed CEM	Ivoclar Vivadent	Self-adhesive resin composite cement	Base paste: UDMA, TEGDMA, polyethylene glycol dimethacrylate Catalyst paste: polyethylene glycol dimethacrylate, TEGDMA, Methacrylated phosphoric acid ester, UDMA	40 vol% - Barium glass - Ytterbium trifluoride Particle size: 0.1-7 μm	U49017
RelyX Ultimate	3M ESPE	Adhesive resin composite cement	Base paste: methacrylate monomers containing phosphoric acid groups, methacrylate monomers Catalyst paste: methacrylate monomers	43 vol% - Silanated fillers - Alkaline (basic) fillers Particle size: 13 μm	595287
RelyX Unicem 2 Automix	3M ESPE	Self-adhesive resin composite cement	Base paste: phosphoric acid modified methacrylate monomers, bifunctional methacrylate Catalyst paste: methacrylate monomers	43 vol% - Alkaline (basic) fillers - Silanated fillers Particle size: 12.5 μm	594259
Panavia V5	Kuraray	Adhesive resin composite cement	Paste A: Bis-GMA, TEGDMA, Hydrophobic aromatic dimethacrylate, Hydrophilic aliphatic dimethacrylate Paste B: Bis-GMA, Hydrophobic aromatic dimethacrylate, Hydrophilic aliphatic dimethacrylate	38 vol% - Silanated barium glass filler - Silanated fluoroalminosilicate glass filler - Colloidal silica - Silanated aluminum oxide filler Particle size: 0.01-12 μm	720007
Panavia SA plus	Kuraray	Self-adhesive resin composite cement	Paste A: 10-MDP, Bis-GMA, TEGDMA, Hydrophobic aromatic dimethacrylate, HEMA Paste B: Hydrophobic aromatic dimethacrylate, hydrophobic aliphatic dimethacrylate	40 vol% - Silanated barium glass filler - Silanated colloidal silica Particle size: 0.02-20 μm	5F0046
VITA Adiva F-Cem	VITA Zahnfabrik	Adhesive resin composite Cement	Methacrylates	41 vol% -Inorganic fillers Particle size: 0.05-1 μm	17601812

Abbreviations: 10-MDP: 10-methacryloyloxydecyl dihydrogen phosphate; Bis-GMA: bisphenol A-glycidyl methacrylate; HEMA: 2-hydroxyethyl methacrylate; UDMA: urethane dimethacrylate; TEGDMA: triethyleneglycol dimethacrylate.

autopolymerized specimens was recorded at temperatures of 23°C (23a) and 37°C (37a). A temperature of 23°C was chosen as the room temperature at which most *in vitro* studies are performed and 37°C represents the intraoral temperature. Light-curing was performed for cements at 23°C and 37°C 1 minute after mixing (23L1, 37L1) and at 37°C after 5 minutes (37L5) and after 10 minutes (37L10). Measurements were recorded at 23°C for 12 hours and at 37°C for 2 hours for all cements until their shrinkage process was completed. To evaluate the influence of temperature and curing mode on the strength of the cements, the indirect tensile strength of all cements was measured after air storage at either 23°C or 37°C. The specimens were autopolymerized or light-cured after 1, 5, or 10 minutes. To illustrate filler size and structures, SEM images of all cements were captured.

Table 2: *Group Identifiers for the respective Cements*

MLA	Multilink Automix
MSC	Multilink Speed CEM
RUL	RelyX Ultimate
RUN	RelyX Unicem 2 Automix
PV5	Panavia V5
PSA	Panavia SA plus
VAF	VITA Adiva F-Cem

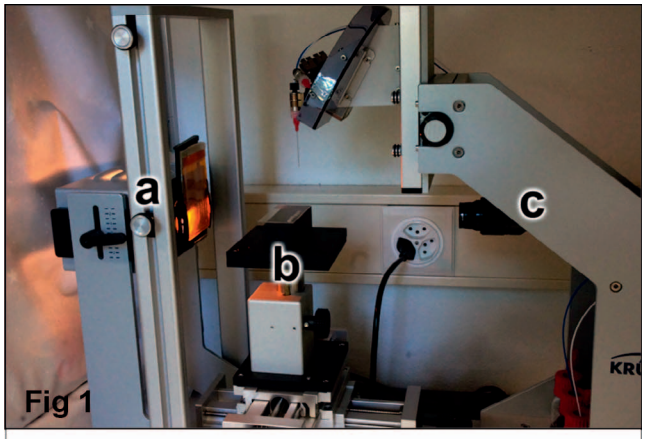

Figure 1. *Polymerization shrinkage was recorded with a drop-shape analyzer. (a) Light source with orange foil to prevent inadvertent light-activation of the cement. (b) Adjustable recording stage in which the cement was placed on a glass slide. (c) Optical system.*

Figure 2. *Cement drop image of a randomly selected specimen before and after shrinkage (PSA 23a specimen 5 [6.22% shrinkage]).*

Polymerization Shrinkage

Polymerization shrinkage data was recorded with a drop shape analyzer (DSA) (DSA305, Krüss, Hamburg, Germany). The intended use of a DSA is to determine the contact angle of a drop of liquid on a solid surface. A drop is automatically placed on the substrate on an adjustable stage and images of the silhouette are captured with the unit's camera, by which the contact angle of the drop can be measured (Advance, 1.2.0.1, Krüss) (Figure 1). To determine the polymerization shrinkage of the cements, the DSA images were obtained within a programmed time frame. The images were then exported and the area of the drops was measured digitally (Leica Application Suite, 4.7.0, Leica Microsystems, Heerbrugg, Switzerland) (Figure 2). Previously, spherical volume calculation of a two-dimensional image determined the cement's volume and consequently its shrinkage.[30] Isotropic shrinkage of the specimens was assumed. To correctly perform a volume calculation from a two-dimensional image, a perfectly semispherical cement specimen has to be produced. Since this was not possible, two-dimensional analysis of the cement area displayed in the image was chosen. To interpret the results, it must be considered that the shrinkage ratio between a semispherical volume ($V=2\pi r^3/3$) and a semicircular area ($A=\pi r^2/2$) was not proportional to the radius. The actual polymerization shrinkage of the volume was slightly higher than it appears in the area measurement. The difference between the shrinkage ratio of volume and area decreases with increasing radius. Therefore, to eliminate bias, similar cement drops with identical volume had to be produced.

Dental resin cement is sticky and viscous and additionally, hardens over time. Hence, the automatic syringe of the DSA could not be used to apply a defined amount of material. Consequently, the weight of the drops was determined during application with a scale (AT261, Mettler, Greifensee, Switzerland). The auto-mix tip was set on the cement syringe and time recording was started as soon as the first drop was discarded on a piece of paper. The second drop with a mean weight of 20.0 ± 2.0 mg was placed on a glass slide. The slide was then placed on the recording stage of the DSA and the focus of the optical system was adjusted. The DSA was covered with a dark box to prevent daylight from entering the stage. An orange foil was previously positioned between the sample area and the DSA's illumination source to prevent inadvertent light-activation of the cement.

For the 12 hour measurement groups (23a, 23L1), DSA recordings started one minute after the first drop left the mixing tip. The DSA was programmed to take an image of the cement drop once every 20 seconds for 10 minutes, then every 10 minutes for 50 minutes and finally every hour for 11 hours. For the 2-hour measurement groups (37a, 37L1, 37L5, 37L10), images were captured once every 20 seconds for 10 minutes, then every 10 minutes. Images were imported into Leica software (Leica Application Suite, 4.7.0, Leica Microsystems, Wetzlar, Germany). The area of each drop was recorded. The cement area of each image was compared with the area on the initial image that was taken 1 minute after the cement first left the syringe. With this data, the percent shrinkage was calculated and graphically displayed.

Measurements of all cements were recorded for autopolymerized specimens at 23°C over 12 hours (23a) and at 37°C over 2 hours (37a) in a tempera-

ture-controlled room (23°C). For measurements at 37°C, a heating device (IPX4, Thermo Technologies, Rohrbach, Germany) with constant temperature control (TSM125 H-Tronic, Hirschau, Germany) was placed on the DSA stage. Light-curing of the cements was performed at 23°C and 37°C. At both temperatures, light-curing was initiated after 1 minute (23L11, 37L1); at 37°C, light-curing was alternatively performed after 5 minutes (37L5) and 10 minutes (37L10). Light-curing was applied with a polymerization lamp (Elipar, 3M ESPE, Seefeld, Germany) having an intensity of 1200 mW/cm^2 for 20 seconds. The intensity of the lamp was checked before each measurement using the device provided by the manufacturer. Time was counted from the first moment the cement left the syringe for the discarded drop. Five specimens were measured in each group for all cements.

Indirect Tensile Strength

Indirect tensile strength of the cements was measured on cylindrical test specimens 3 mm in height and diameter (n=10). The cement was flowed into the respective cavities of a customized Teflon mold and kept in place with a plastic foil and a glass plate on each side. The specimens were either autopolymerized or light-cured (Elipar, 3M ESPE) at the respective times (after 1, 5, or 10 minutes) and immediately stored under temperature control (CTS T-4025, Hechingen, Germany) at 23°C or 37°C, respectively. After 1 hour, the specimens were removed from the molds and stored in a dark box for another 23 hours at the respective temperature. Prior to testing, the diameter and height were determined using a digital caliper (Cal IP 67, Tesa, Renens, Switzerland). The specimens were loaded radially until fracture with a preload of 20 N and a crosshead speed of 1 mm/min (Z020, Zwick/Roell, Ulm, Germany).

The following equation was used to calculate indirect tensile strength:

$$\sigma_t = 2F/\pi dh$$

where σ_t is the indirect tensile strength; F is the fracture load; d, the specimen diameter; and h, the specimen height.

Scanning Electron Microscopy

Discs with a diameter of 15 mm and a thickness of 1 mm were manufactured for all cements using a Teflon mold. The cement was flowed into the mold cavity and kept in place with a polyester foil and a glass plate on each side. Light-curing was performed with overlapping applications of a polymerization lamp (Elipar, 3M ESPE). All specimens were then fixed (UHU plus, UHU, Bühl, Germany) on a slide and simultaneously wet-polished with silicon carbide paper P1200-4000 (Type 401319, Exakt, Norderstedt, Germany). SEM images of gold-sputtered cement structures at 1000× were captured (Philips XL30 FEG ESEM, Philips Electron Optics, Eindhoven, The Netherlands).

Statistical Analysis

Data of all tests were analyzed for normal distribution using the Shapiro-Wilk test and all data were distributed normally. Hence, one-way ANOVA followed by the *post hoc* Fisher LSD test were chosen to test for differences between groups (α=0.05). Correlation between final polymerization shrinkage and the respective indirect tensile strength of each group was investigated.

RESULTS

Polymerization Shrinkage

Polymerization shrinkage of all cements within the different groups is displayed in Figure 3. Means and standard deviations of the final polymerization shrinkage after 12 hours for 23°C and after 2 hours for 37°C for the different groups are listed in Table 3. Final shrinkage ranged from 3.2% to 7.0%.

Indirect Tensile Strength

Indirect tensile strength values are graphically displayed in Figure 4. Values at 0 minute represent autopolymerized specimens. Means and standard deviations of all specimens at 23°C and 37°C are statistically compared in Table 4. Figure 5 plots all groups that were measured for the polymerization shrinkage to the respective indirect tensile strength.

Cement Filler Composition

SEM backscatter images of the cement surfaces are displayed in Figure 6 at a magnification of 1000×. A regular distribution of small filler particles (around 1 μm in diameter) was found for MLA and VAF. (See Table 2 for full names of these and other cements used.) Slightly larger particles (up to 5 μm in diameter) were detected for PV5. RUN and RUL revealed similar filler patterns: a mixture between small- and medium-sized particles up to 10 μm. PSA and MSC contained a mixture between small, medium, and large filler particles. For MSC, particle clusters up to 20 μm were detected. Particle sizes

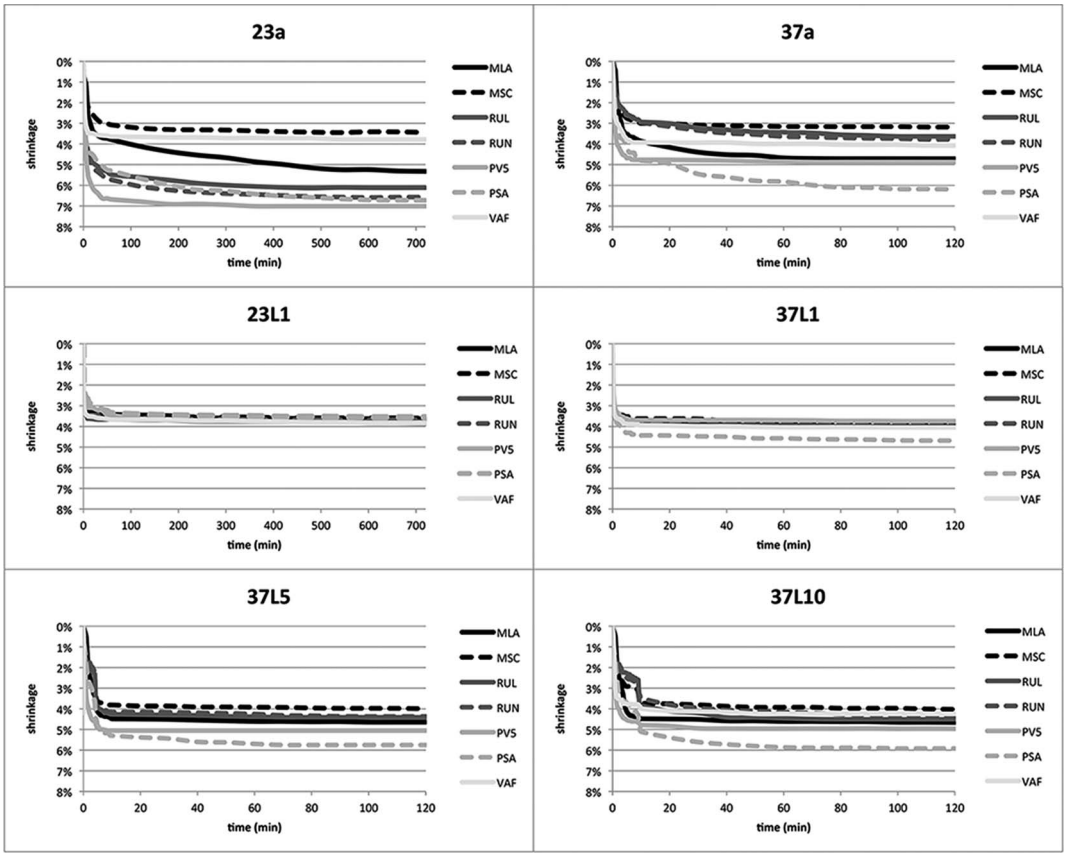

Figure 3. *Polymerization shrinkage of all cements within the different groups.*

reflected those provided by the manufacturer except for MSC, in which the filler sizes were twice the size described and PV5 that revealed rather smaller filler sizes.

DISCUSSION

The purpose of this study was to establish a clinically appropriate time of light-curing while achieving best material properties and lowest polymerization shrinkage. The first hypothesis, that an increase in temperature results in higher polymerization shrinkage and higher indirect tensile strength of resin composite cements was rejected because the increase of temperature resulted in different effects for each cement. The second hypothesis that the light-curing moment of resin composite cements does not affect polymerization shrinkage or indirect tensile strength was also rejected. Early light-curing after 1 minute was beneficial to decrease polymerization shrinkage for most cements. The effect of the light-curing moment on indirect tensile strength was also material related.

Table 3: *Means and Standard Deviations of Final Polymerization Shrinkage After 12 h for 23°C and After 2 h for 37°C of the Different Groups*[a]

	23a	37a	23L1	37L1	37L5	37L10
MLA	5.3% ± 0.1%^{A,a*}	4.7% ± 0.1%^{A,b}	3.6% ± 0.3%^{A,B,C,c}	4.0% ± 0.1%^{A,B,d}	4.6% ± 0.3%^{A,b}	4.7% ± 0.3%^{A,b}
MSC	3.5% ± 0.2%^{B,a,b}	3.2% ± 0.1%^{B,b}	3.6% ± 0.2%^{A,C,a,c}	3.8% ± 0.2%^{B,C,c,d}	4.0% ± 0.1%^{B,d}	4.0% ± 0.2%^{B,d}
RUL	6.1% ± 0.5%^{C,a}	3.6% ± 0.1%^{C,b}	3.8% ± 0.1%^{A,B,C,b}	4.0% ± 0.1%^{A,B,C,b}	4.4% ± 0.2%^{A,C,c}	4.5% ± 0.3%^{C,c}
RUN	6.6% ± 0.5%^{C,D,a}	3.8% ± 0.2%^{C,D,b}	3.7% ± 0.1%^{A,B,C,b}	3.9% ± 0.1%^{A,B,C,b}	4.4% ± 0.2%^{A,C,c}	4.4% ± 0.3%^{B,C,c}
PV5	7.0% ± 0.4%^{D,E,a}	4.9% ± 0.2%^{A,b}	3.5% ± 0.3%^{C,c}	3.7% ± 0.2%^{C,c}	5.1% ± 0.2%^{D,b}	5.0% ± 0.4%^{A,b}
PSA	6.7% ± 0.7%^{C,E,a}	6.2% ± 0.3%^{E,b}	3.9% ± 0.1%^{B,c}	4.7% ± 0.2%^{D,d}	5.8% ± 0.2%^{E,e}	5.9% ± 0.1%^{D,e}
VAF	3.8% ± 01%^{B,a}	4.1% ± 0.2%^{D,b}	3.8% ± 0.2%$^{A,B.a}$	4.1% ± 0.1%^{A,b}	4.2% ± 0.2%^{B,C,b}	4.2% ± 0.3%^{B,C,b}

[a] *Superscript letters indicate statistical similar groups (vertical comparison: uppercase letters; horizontal comparison: lowercase letters).*

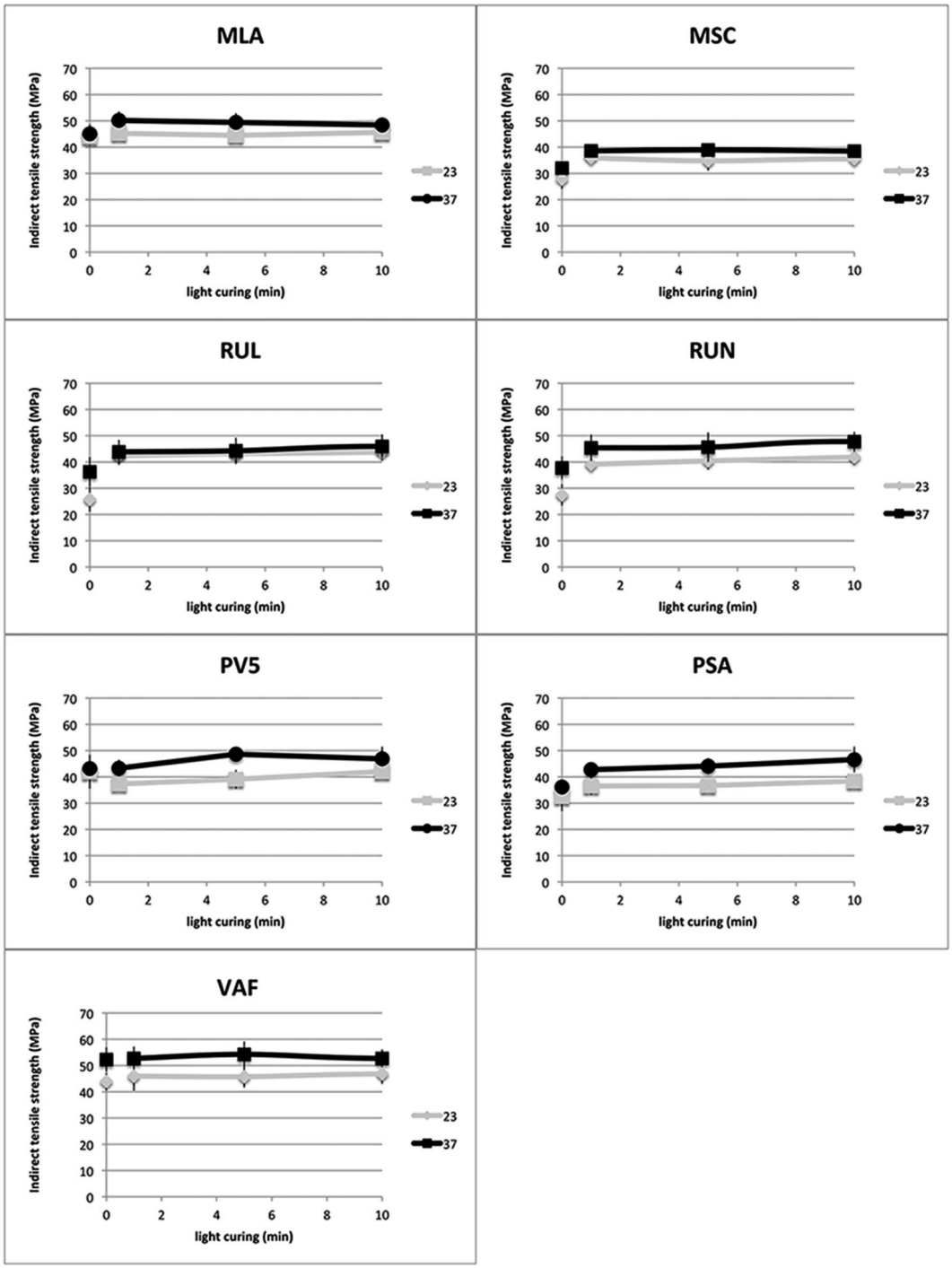

Figure 4. *Indirect tensile strength of all cements at 23°C and 37°C after autopolymerization (0 minute) or light-curing after 1, 5, or 10 minutes.*

Test Design

Numerous methods have been proposed to measure polymerization shrinkage kinetics; each has its disadvantages.[9,12,29,31] Results for the same material may differ between methods due to various testing parameters. Shrinkage strain for RUN (4.10 ± 0.03%) and MLA (4.65 ± 0.06%) at 23°C dual-cured have been reported in the literature but should not be compared with the area shrinkage values found in this study for these cements due to varying test set-ups.[12] The volumetric shrinkage of composites has been shown to be proportional to its degree of

Table 4: *Mean and Standard Deviation of Indirect Tensile Strength of All Cements at 23°C and 37°C of Autopolymerized and Light-Cured Specimens*[a]

(MPa)	23a	23L1	23L5	23L10	37a	37L1	37L5	37L10
MLA	44.4 ± 1.5^{A,a}	45.2 ± 2.6^{A,B,a}	44.5 ± 2.5^{A,a*}	45.6 ± 2.4^{A,B,a,b}	45.1 ± 3.6^{A,a}	50.2 ± 3.4^{A,c}	49.4 ± 3.5^{A,c}	48.4 ± 2.7^{A,b,c}
MSC	27.8 ± 3.8^{B,a}	35.2 ± 1.9^{C,b,c}	34.8 ± 3.7^{B,b,c}	35.5 ± 1.8^{C,b,d}	32.0 ± 4.6^{B,c}	38.6 ± 3.1^{B,d,e}	38.9 ± 2.9^{B,e}	38.5 ± 2.2^{B,d,e}
RUL	25.7 ± 4.7^{B,a}	42.4 ± 3.4^{B,D,b}	43.1 ± 3.1^{A,C,b}	43.8 ± 3.2^{B,D,b}	36.3 ± 5.6^{B,C,c}	43.9 ± 4.6^{C,b}	44.3 ± 5.0^{C,b}	46.0 ± 4.5^{A,b}
RUN	27.4 ± 4.1^{B,a}	39.1 ± 2.3^{D,E,b}	40.4 ± 3.3^{C,D,b}	41.9 ± 2.8^{D,b,c}	37.7 ± 4.4^{C,b}	45.4 ± 5.0^{C,c,d}	45.6 ± 5.6^{A,C,c,d}	47.8 ± 3.8^{A,d}
PV5	41.9 ± 6.3^{A,a,b}	37.3 ± 2.3^{C,E,c}	39.1 ± 3.6^{D,E,a,c}	42.0 ± 2.6^{D,a,b}	43.2 ± 5.3^{A,a,b,d}	43.3 ± 3.3^{C,b,d}	48.6 ± 2.7^{A,e}	46.9 ± 4.6^{A,d,e}
PSA	32.5 ± 5.6^{C,a}	36.5 ± 3.4^{C,E,b,c}	36.7 ± 2.7^{B,E,b,d}	38.2 ± 2.1^{C,b,d}	36.1 ± 2.7^{B,C,a,c,d}	42.8 ± 2.8^{C,e}	44.1 ± 3.6^{C,e,f}	46.4 ± 4.4^{A,f}
VAF	43.9 ± 3.2^{A,a}	46.0 ± 5.6^{A,a}	45.7 ± 4.1^{A,a}	46.8 ± 3.8^{B,a}	52.3 ± 4.6^{D,b}	52.7 ± 4.5^{A,b}	54.2 ± 5.0^{D,b}	52.7 ± 3.4^{C,b}

[a] *Superscript letters indicate statistical similar groups (vertical comparison: uppercase letters; horizontal comparison: lowercase letters).*

conversion.[32] The area shrinkage measurement in this study is easy to perform and allows monitoring of the shrinkage over a long time period. To interpret the results, it must be considered that the shrinkage ratio between a semispherical volume and a semicircular area is not proportional to the radius, therefore the actual polymerization shrinkage of the volume is slightly higher than it appears in the area measurement. Also, the actual polymerization shrinkage in a clinical situation may differ since the cement layer is thinner and not exposed to oxygen in most areas. The presence of oxygen at the cement surface inhibits the polymerization process.[33] Also, clinically, the cement is confined between a restoration and the tooth surface and the configuration-factor was not considered in the present study. Testing these luting materials away from the tooth structure cannot lead to solid conclusions, as the interaction between the different adhesive systems and luting cements or between the moist dentin and cements might affect their properties, hydrolytic stability, or strength.

When measuring dual-curing materials, the time of the first contact between the base and catalyst, the exact light-curing moment, as well as the starting time of the measurement must be standardized to achieve reproducible results. Since area shrinkage measurements cannot completely predict resin composite cement behavior regarding stress development,[10] further investigations are to be performed.

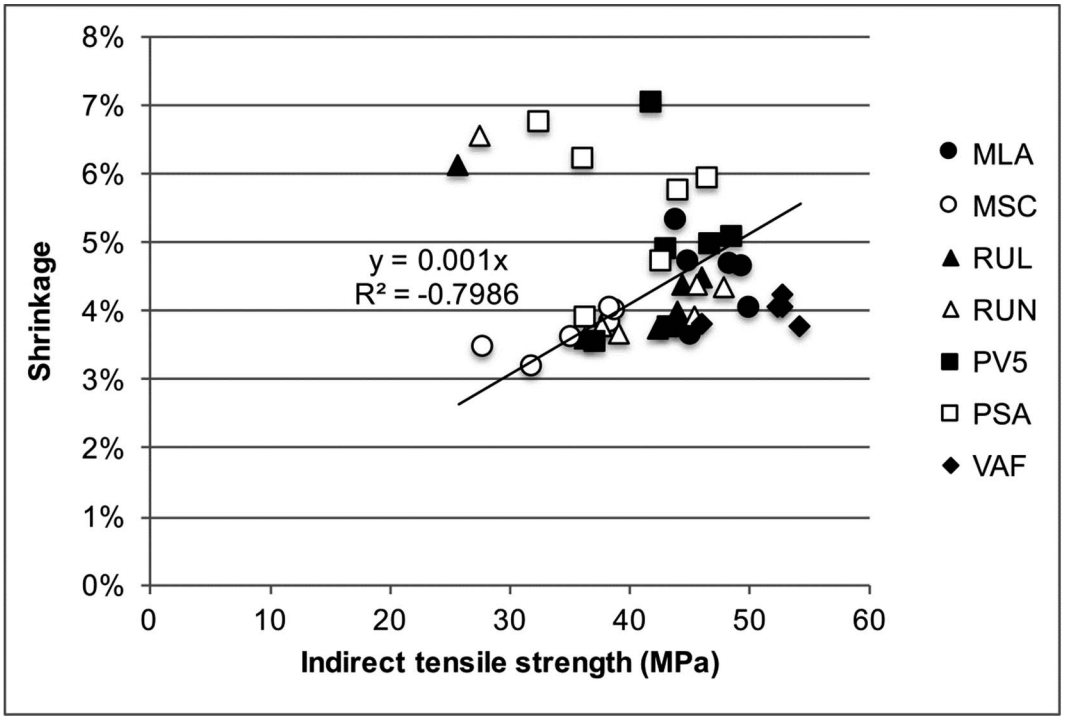

Figure 5. *Correlation between polymerization shrinkage and indirect tensile strength of the respective groups of all cements.*

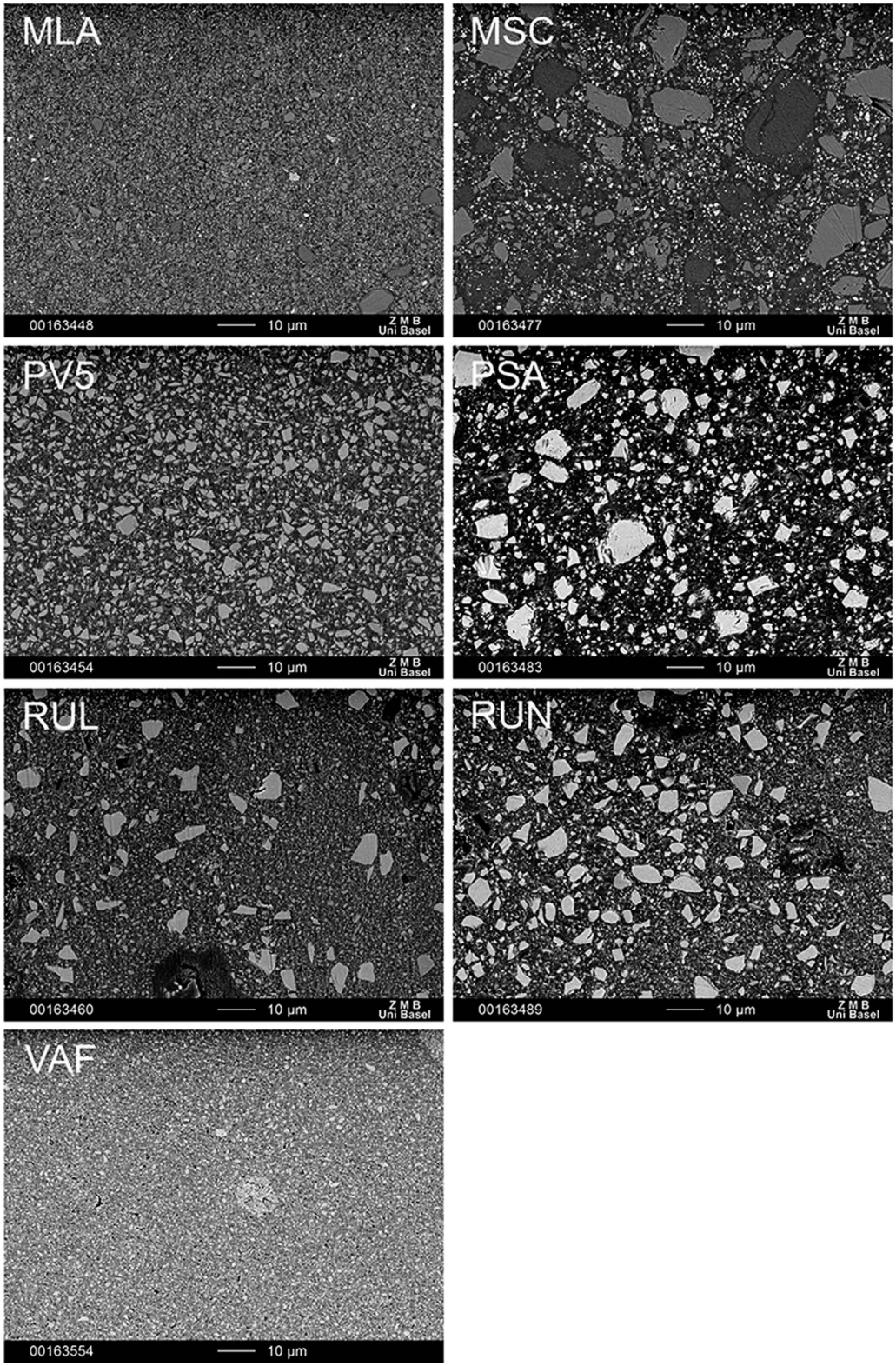

Figure 6. *SEM backscatter images of cement surfaces (1000×).*

Measuring the indirect tensile strength can be considered a standard method of screening material strengths.[34,35] The test provides reliable information on the mechanical strength of resin composites with the advantage of easy handling.[35-37]

Polymerization Shrinkage and Indirect Tensile Strength

Light-curing temperature effects on polymerization shrinkage and indirect tensile strength are material related. No correlation was observed between polymerization shrinkage and indirect tensile strength of the respective groups ($y=0.001x$, $R^2=-0.7986$; Figure 5). Several factors such as filler size and material, degree of conversion, initiator system, and cement monomer effect polymerization shrinkage and strength.[10] Some cements (MSC, RUL, RUN) revealed a strong dependence of the initiator system on light-curing, indicated by the significantly lower polymerization shrinkage as well as lower indirect tensile strength of autopolymerized specimens at 37°C than that of light-cured specimens. Increased temperature decreased the polymerization shrinkage of autopolymerized specimens MLA, RUL, RUN, and PV5 hastened activation of the initiator and, therefore, also ended polymerization sooner (Figure 3). In the literature, increased temperature was associated with a higher polymerization stress rate and a higher degree of conversion for light-cured resin composites[21,38] because of increased free radical and monomer mobility.[39,40] A decrease in viscosity of the cement due to the higher temperature also results in a higher collision frequency of the unreacted active groups.[41]

For light-cured specimens at 1 minute, an increase in temperature from 23°C to 37°C also increased the polymerization shrinkage of all cements. This was probably due to the polymerization process of the specimens being in a more advanced state when the light was applied at 37°C than it was at 23°C because of the enhanced energy supply. The application of light resulted in a freezing of the system: the cement became rigid and was unable to shrink further.

Indirect tensile strength of the cements was lowest for all cements when the specimens were stored at 23°C and no light was applied. The indirect tensile strength was enhanced when either the temperature was increased or light-curing was performed. The degree of the effect was material related.

The cement providing the highest indirect tensile strength (54.3±5.0 MPa) and lowest polymerization shrinkage (4.2%±0.2%) at 37°C with light-curing after 5 minutes was VAF. In addition, MSC demonstrated a low polymerization shrinkage of 4.0 ± 0.1%, but this cement revealed the lowest indirect tensile strength of all cements (38.9±2.9 MPa). Regarding the filler size, the highest indirect tensile strengths were observed for the materials containing a homogeneous distribution of small fillers of about 1 μm (MLA, PV5, VAF).

Clinical Implications

For clinical application, the following procedures are recommended to achieve best material properties: For MLA, MSC, RUL, and RUN, light application should be performed as soon as possible within the first 5 minutes after placing the restoration. For these materials, indirect tensile strength at 37°C was not significantly influenced by the time of light application but polymerization shrinkage was smaller when the light was applied earlier. Polymerization shrinkage for these cements ranged around 4%. It has been speculated that a delay in light-activation of dual-cured resin cements would enhance their mechanical properties,[42] although no effect was observed on the bond strength of resin cements to the substrate when the light-curing was delayed for 5 minutes.[43] In the present study, a delayed light-curing of 5 minutes for PV5 and 10 minutes for PSA was beneficial and resulted in an increase in their indirect tensile strength. However, it has been found that prolonged self-curing of the cements of 10 minutes may compromise the overall degree of conversion[28] and increase water sorption.[44] These findings must be interpreted with care and should not be generalized because the present study revealed that resin composite cements differ greatly in their curing behavior. PSA revealed slow polymerization reactions according to Figure 3, especially for autopolymerization. This might have been caused by the content of 10-methacryloyloxydecyl dihydrogen phopshate (10-MDP). Although 10-MDP enhances bond strength, it also inhibits the polymerization reaction.[45] 10-MDP is an acidic monomer that interferes with the amine initiator and therefore negatively affects the cement degree of conversion[46] in both autopolymerization and dual-curing mode.[47]

If polymerization shrinkage must be decreased for PV5 or PSA, an early light application can be performed, but it might result in insufficient polymerization. PV5 and PSA displayed higher polymerization shrinkage of 4% to 6%. For VAF, light application does not increase the strength or polymerization shrinkage (4%) significantly and may be

omitted. For the other cements, light application is essential to increase strength: even when performed 10 minutes after mixing, it still increased the material's strength between 4 and 11 MPa. The application of a high-strength cement such as MLA, PV5, or VAF is recommended for cementing silicate ceramics to improve the stability of the restorations.[48]

CONCLUSIONS

The magnitude of the effect of light-curing and temperature increase on polymerization shrinkage and indirect tensile strength of resin composite cements is material dependent and cannot be generalized.

The tested resin composite cements provided polymerization shrinkages of 4% to 6% at 37°C with light-curing after 5 minutes. To keep shrinkage at a minimum, light application can be performed as soon as possible within the first 5 minutes after restoration placement.

Acknowledgements

The authors are grateful to VITA Zahnfabrik, Bad Säckingen, for providing the cement materials.

Conflict of Interest

The authors of this manuscript certify that they have no proprietary, financial or other personal interest of any nature or kind in any product, service and/or company that is presented in this article, except for the following: Jens Fischer is Head of the Division of Dental Materials and Engineering at University of Basel. Dr Fischer is also Head of Research & Development at VITA Zahnfabrik.

(Accepted 8 August 2017)

REFERENCES

1. Ban S, Hasegawa J, & Anusavice KJ (1992) Effect of loading conditions on bi-axial flexure strength of dental cements *Dental Materials* **8(2)** 100-104.
2. Peutzfeldt A (1995) Dual-cure resin cements: In vitro wear and effect of quantity of remaining double bonds, filler volume, and light curing *Acta Odontologica Scandinavica* **53(1)** 29-34.
3. Ilie N, & Simon A (2012) Effect of curing mode on the micro-mechanical properties of dual-cured self-adhesive resin cements *Clinical Oral Investigations* **16(2)** 505-512.
4. Braga RR, Ferracane JL, & Condon JR (2002) Polymerization contraction stress in dual-cure cements and its effect on interfacial integrity of bonded inlays *Journal of Dentistry* **30(7-8)** 333-340.
5. Caughman WF, Chan DC, & Rueggeberg FA (2001) Curing potential of dual-polymerizable resin cements in simulated clinical situations *Journal of Prosthetic Dentistry* **85(5)** 479-484.
6. Braga RR, Condon JR, & Ferracane JL (2002) In vitro wear simulation measurements of composite versus resin-modified glass ionomer luting cements for all-ceramic restorations *Journal of Esthetic and Restorative Dentistry* **14(6)** 368-376.
7. Fonseca RG, Santos JG, & Adabo GL (2005) Influence of activation modes on diametral tensile strength of dual-curing resin cements *Brazilian Oral Research* **19(4)** 267-271.
8. Hashimoto M, de Gee AJ, & Feilzer AJ (2008) Polymerization contraction stress in dentin adhesives bonded to dentin and enamel *Dental Materials* **24(10)** 1304-1310.
9. Watts DC, & Alnazzawi A (2014) Temperature-dependent polymerization shrinkage stress kinetics of resin-composites *Dental Materials* **30(6)** 654-660.
10. Braga RR, Ballester RY, & Ferracane JL (2005) Factors involved in the development of polymerization shrinkage stress in resin-composites: A systematic review *Dental Materials* **21(10)** 962-970.
11. Labella R, Lambrechts P, Van Meerbeek B, & Vanherle G (1999) Polymerization shrinkage and elasticity of flowable composites and filled adhesives *Dental Materials* **15(2)** 128-137.
12. Spinell T, Schedle A, & Watts DC (2009) Polymerization shrinkage kinetics of dimethacrylate resin-cements *Dental Materials* **25(8)** 1058-1066.
13. Braga RR, Ballester RY, & Daronch M (2000) Influence of time and adhesive system on the extrusion shear strength between feldspathic porcelain and bovine dentin *Dental Materials* **16(4)** 303-310.
14. Braga RR, Cesar PF, & Gonzaga CC (2002) Mechanical properties of resin cements with different activation modes *Journal of Oral Rehabilitation* **29(3)** 257-262.
15. Frassetto A, Navarra CO, Marchesi G, Turco G, Di Lenarda R, Breschi L, Ferracane JL, & Cadenaro M (2012) Kinetics of polymerization and contraction stress development in self-adhesive resin cements *Dental Materials* **28(9)** 1032-1039.
16. Oliveira M, Cesar PF, Giannini M, Rueggeberg FA, Rodrigues J, & Arrais CA (2012) Effect of temperature on the degree of conversion and working time of dual-cured resin cements exposed to different curing conditions *Operative Dentistry* **37(4)** 370-379.
17. Yan YL, Kim YK, Kim KH, & Kwon TY (2010) Changes in degree of conversion and microhardness of dental resin cements *Operative Dentistry* **35(2)** 203-210.
18. Feilzer AJ, De Gee AJ, & Davidson CL (1990) Quantitative determination of stress reduction by flow in composite restorations *Dental Materials* **6(3)** 167-171.
19. Feng L, & Suh BI (2006) The effect of curing modes on polymerization contraction stress of a dual cured composite *Journal of Biomedical Materials Research Part B: Applied Biomaterials* **76(1)** 196-202.
20. Alster D, Feilzer AJ, De Gee AJ, Mol A, & Davidson CL (1992) The dependence of shrinkage stress reduction on porosity concentration in thin resin layers *Journal of Dental Research* **71(9)** 1619-1622.

21. Lührs AK, De Munck J, Geurtsen W, & Van Meerbeek B (2014) Composite cements benefit from light-curing *Dental Materials* **30(3)** 292-301.
22. Hofmann N, Papsthart G, Hugo B, & Klaiber B (2001) Comparison of photo-activation versus chemical or dual-curing of resin-based luting cements regarding flexural strength, modulus and surface hardness *Journal of Oral Rehabilitation* **28(11)** 1022-1028.
23. Kim AR, Jeon YC, Jeong CM, Yun MJ, Choi JW, Kwon YH, & Huh JB (2016) Effect of activation modes on the compressive strength, diametral tensile strength and microhardness of dual-cured self-adhesive resin cements *Dental Materials Journal* **35(2)** 298-308.
24. Lovell LG, Newman SM, & Bowman CN (1999) The effects of light intensity, temperature, and comonomer composition on the polymerization behavior of dimethacrylate dental resins *Journal of Dental Research* **78(8)** 1469-1476.
25. Lucey S, Lynch CD, Ray NJ, Burke FM, & Hannigan A (2010) Effect of pre-heating on the viscosity and microhardness of a resin composite *Journal of Oral Rehabilitation* **37(4)** 278-282.
26. Calheiros FC, Daronch M, Rueggeberg FA, & Braga RR (2014) Effect of temperature on composite polymerization stress and degree of conversion *Dental Materials* **30(6)** 613-618.
27. Moraes RR, Faria-e-Silva AL, Ogliari FA, Correr-Sobrinho L, Demarco FF, & Piva E (2009) Impact of immediate and delayed light-activation on self-polymerization of dual-cured dental resin luting agents *Acta Biomaterialia* **5(6)** 2095-2100.
28. Truffier-Boutry D, Demoustier-Champagne S, Devaux J, Biebuyck JJ, Mestdagh M, Larbanois P, & Leloup G (2006) A physico-chemical explanation of the post-polymerization shrinkage in dental resins *Dental Materials* **22(5)** 405-412.
29. De Souza G, Braga RR, Cesar PF, & Lopes GC (2015) Correlation between clinical performance and degree of conversion of resin cements: A literature review *Journal of Applied Oral Science* **23(4)** 358-368.
30. Tiba A, Charlton DG, Vandewalle KS, & Ragain JC Jr (2005) Comparison of two video-imaging instruments for measuring volumetric shrinkage of dental resin composites *Journal of Dentistry* **33(9)** 757-763.
31. Kaisarly D, & Gezawi ME (2016) Polymerization shrinkage assessment of dental resin composites: A literature review *Odontology* **104(3)** 257-270.
32. Braga RR, & Ferracane JL (2002) Contraction stress related to degree of conversion and reaction kinetics *Journal of Dental Research* **81(2)** 114-118.
33. Shawkat ES, Shortall AC, Addison O, & Palin WM (2009) Oxygen inhibition and incremental layer bond strengths of resin composites *Dental Materials* **25(11)** 1338-1346.
34. Cassina G, Fischer J, & Rohr N (2016) Correlation between flexural and indirect tensile strength of resin composite cements *Head & Face Medicine* **12(1)** 29.
35. Blumer L, Schmidli F, Weiger R, & Fischer J (2015) A systematic approach to standardize artificial aging of resin composite cements *Dental Materials* **31(7)** 855-863.
36. Della B, Benetti P, Borba M, & Cecchetti D (2008) Flexural and diametral tensile strength of composite resins *Brazilian Oral Research* **22(1)** 84-89.
37. Penn RW, Craig RG, & Tesk JA (1987) Diametral tensile strength and dental composites *Dental Materials* **3(1)** 46-48.
38. Trujillo M, Newman SM, & Stansbury JW (2004) Use of near-IR to monitor the influence of external heating on dental composite photopolymerization *Dental Materials* **20(8)** 766-777.
39. Acquaviva PA, Cerutti F, Adami G, Gagliani M, Ferrari M, Gherlone E, & Cerutti A (2009) Degree of conversion of three composite materials employed in the adhesive cementation of indirect restorations: A micro-Raman analysis *Journal of Dentistry* **37(8)** 610-615.
40. Daronch M, Rueggeberg FA, De Goes MF, & Giudici R (2006) Polymerization kinetics of pre-heated composite *Journal of Dental Research* **85(1)** 38-43.
41. Di Francescantonio M, Aguiar TR, Arrais CA, Cavalcanti AN, Davanzo CU, & Giannini M (2013) Influence of viscosity and curing mode on degree of conversion of dual-cured resin cements *European Journal of Dentistry* **7(1)** 81-85.
42. Pegoraro TA, da Silva NR, & Carvalho RM (2007) Cements for use in esthetic dentistry *Dental Clinics of North America* **51(2)** 453-471.
43. Faria-e-Silva AL, Fabião MM, Arias VG, & Martins LR (2010) Activation mode effects on the shear bond strength of dual-cured resin cements *Operative Dentistry* **35(5)** 515-521.
44. Svizero Nda R, Silva MS, Alonso RC, Rodrigues FP, Hipólito VD, Carvalho RM, & D'Alpino PH (2013) Effects of curing protocols on fluid kinetics and hardness of resin cements *Dental Materials Journal* **32(1)** 32-41.
45. Nakamura T, Wakabayashi K, Kinuta S, Nishida H, Miyamae M, & Yatani H (2010) Mechanical properties of new self-adhesive resin-based cement *Journal of Prosthodontic Research* **54(2)** 59-64.
46. Vrochari AD, Eliades G, Hellwig E, & Wrbas KT (2009) Curing efficiency of four self-etching, self-adhesive resin cements *Dental Materials* **25(9)** 1104-1108.
47. Uhl A, Michaelis C, Mills RW, & Jandt KD (2004) The influence of storage and indenter load on the Knoop hardness of dental composites polymerized with LED and halogen technologies *Dental Materials* **20(1)** 21-28.
48. Rohr N, Coldea A, Zitzmann NU, & Fischer J (2015) Loading capacity of zirconia implant supported hybrid ceramic crowns *Dental Materials* **31(12)** e279-e288.

©Operative Dentistry, 2018, **43-6,** 631-641

Incremental and Bulk-fill Techniques With Bulk-fill Resin Composite in Different Cavity Configurations

S-H Han • S-H Park

Clinical Relevance

In high C-factor cavities, the incremental technique for composite restoration showed a higher bond strength on the cavity floor than did the bulk-fill technique. However, in low C-factor cavities, there was no statistical difference in the bond strength between the two techniques.

SUMMARY

Purpose: To compare the microtensile bond strengths of incremental and bulk-fill techniques under different C-factor and compliance conditions.

Methods and Materials: Extracted human third molars were divided into three experimental groups. For group I, Class I cavities were prepared. For group II, MOD cavities of the same size were prepared. For group III, the cavities were prepared the same way as group II only with high compliance cavity walls. The cavity wall compliance of the specimens was evaluated. Each of these groups was divided into four subgroups. The teeth were restored using two different materials: TB (Tetric N-Ceram Bulk Fill; Ivoclar Vivadent, Hanau, Germany) and VB (Venus Bulk Fill; Heraeus Kulzer, Armonk, NY, USA), and two methods, either an incremental or bulk-fill technique. Then, the microtensile bond strengths (μ-TBSs) were measured and compared. The polymerization stresses of the composites were calculated using a custom-made device. The results were statistically analyzed using the Kruskal-Wallis test and Weibull analysis.

Results: In group I, the μ-TBS obtained using the incremental technique was significantly higher than that obtained by the bulk-fill technique ($p<0.05$). In contrast, no difference of the μ-TBS value was observed between the two techniques in groups II and III. The μ-TBS value of group I was significantly lower than those of groups II and III ($p<0.05$). No statistical difference in the μ-TBS was observed when the cavities were filled with either TB or VB ($p>0.05$).

Seung-Hoon Han, St Vincent Hospital, Catholic University of Korea, Dept of Conservative Dentistry, #93 Jungbu-daero, Paldal-gu, Suwon, 16247, Republic of Korea

*Sung-Ho Park, Yonsei University College of Dentistry, Department of Conservative Dentistry and Oral Science Research Center, Seoul, Republic of Korea

*Corresponding author: 50-1 Yonsei-ro, Seodaemun-gu, Seodaemun-gu, Seoul, 03722, Republic of Korea; e-mail: sunghopark@yuhs.ac

DOI: 10.2341/17-279-LR

Conclusions: The incremental technique showed higher bond strength than did the bulk-fill technique in high C-factor cavities. However, no difference was found between the two techniques in the low C-factor cavities. The bond strength in the high C-factor cavities was significantly lower than that of the low C-factor cavities.

INTRODUCTION

The properties of resin composite have improved significantly during the past decade. Nonetheless, polymerization shrinkage of composite resin is still a major cause of restoration failure. To optimally restore a large cavity with composite, incremental techniques have been recommended in order to reduce microleakage and polymerization stress.[1-4] However, some studies have reported that there was no difference when the results of incremental and bulk-fill techniques were compared.[5-9]

Many studies have compared the results of incremental and bulk-fill techniques with respect to bond strength, polymerization stress, cuspal deflection, gap width, and microleakage. Research on bond strength to the cavity floor can be divided into two groups depending on whether the depth of the specimen cavity is more or less than 3 mm. In general, when the microtensile bond strength to the cavity floor was compared using specimens with less than a 3-mm-deep cavity, no differences in the results were obtained, irrespective of the technique used. Loguercio and others compared the incremental and bulk-fill techniques in high and low C-factor cavities with depths of 2 mm.[5] The microtensile bond strength and gap width results obtained by the two techniques were similar in both the high and low C-factor cavities. Van Ende and others investigated the two techniques by comparing microtensile bond strength in 2.5 mm-deep Class I cavities.[10] The results demonstrated that in four out of five groups of composites, the microtensile strength was not significantly different when using incremental vs bulk-fill techniques.

In contrast to the results obtained using specimens with a shallow cavity, the results obtained in studies comparing incremental and bulk-fill techniques using specimens with a cavity depth of more than 3 mm generally differed from those obtained with a 2-mm depth. Nikolaenko and others investigated the effect of the layering technique on the microtensile bond strength in a 4-mm-deep cavity.[2] They found that the bulk-fill technique led to significantly lower adhesion at the cavity floor. According to Reis and others, bulk-fill groups presented the lowest microtensile bond strength with a 5-mm deep cavity.[3] Likewise, Chikawa and others demonstrated that the incremental filling technique was more effective for adhesion to a 5-mm-deep cavity floor than the bulk-fill technique.[4] He and others investigated the effects of cavity size on the microtensile bond strength in Class I cavities using incremental/bulk-fill techniques.[1] They reported that there was no difference in microtensile bond strength in small cavities (3-mm deep). However, there was a significant difference between the two techniques in large cavities (5-mm deep).

The incremental and bulk-fill techniques can also yield different results depending on the cavity configuration of the specimens. No differences in polymerization stress or marginal leakage were observed between the incremental and bulk-filling techniques when they were performed in MO or MOD cavities.[6-9,11] However, studies conducted on the bond strength of Class I cavities demonstrated a difference between the two techniques wherein a higher bond strength was obtained using the incremental technique.[1,2,4,12] We conclude from a brief review of the literature that the effectiveness of the two techniques may differ depending on the cavity size and configuration. Therefore, it was determined that cavities of the same size and shape but with different configurations should be compared to identify the effectiveness of the two techniques.

The C-factor can be used as a criterion to classify cavity configuration. However, the C-factor alone may not represent all the characteristics of the cavity configuration, for example, the cavity wall compliance. Even though cavities have the same C-factor, they can have a different shape and compliance, which is the inverse of stiffness and it can demonstrate how flexible the cavity wall is. A high compliance represents that the deflection of the cavity wall is greater at a given force. It has been reported that the magnitude of the stress developed at the interface is related to the compliance of the surrounding structures.[13] However, polymerization stresses are not uniformly distributed along the cavity walls.[14] Bond strength may also vary in relation to the C-factor and compliance of the cavity,[15] which is the main concern of our study.

Bulk-fill composites, which can be adequately light-cured on the deep cavity floor, can be used to compare the two techniques.[16] A recent development in composite resins is bulk-fill technology, which allows placement of resin composite in a single

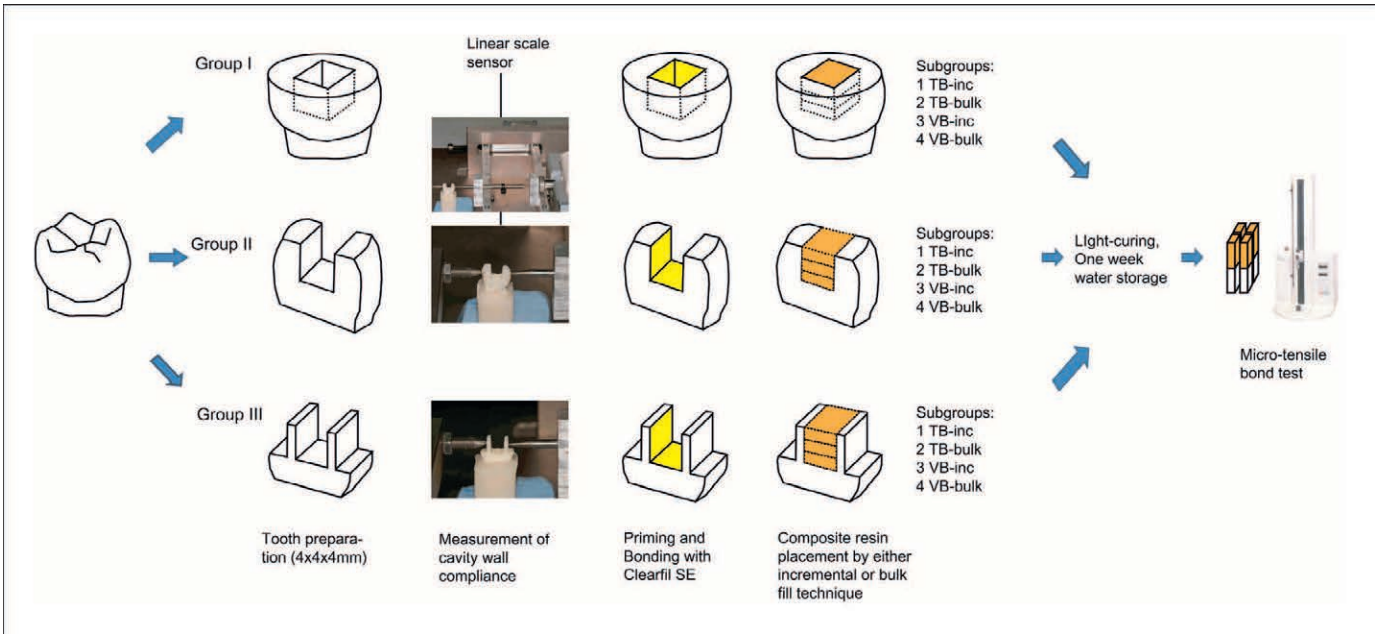

Figure 1. *Experimental procedure employed in this study.*

increment up to 4-5 mm in depth without compromising polymerization efficiency.[17-19] With micro- or nano-hybrid composites, there are concerns that the composite may not be completely light cured over the entire depth of large restorations. Incomplete curing of the composite precludes a valid comparison of the two techniques. Bulk-fill composites can be divided into two categories: flowable types and packable types. In several studies, the two types were shown to have different physical properties, including polymerization stress.[17,20] A final point of interest is whether the bond strength to the cavity floor would be the same with two different types of bulk-fill composites.

The present study was performed to understand how the following factors affect the microtensile bond strength to the cavity floor: incremental vs bulk-fill technique, high C-factor cavity vs low C-factor cavity with different compliances of the cavity walls, and the two different bulk-fill composites. The null hypotheses in this study were

1. There was no difference in bond strength between incrementally cured and bulk-cured composites.
2. There was no difference in bond strength between high C-factor and low C-factor cavities.
3. There was no difference in bond strength between cavities with a low compliance and those with a high compliance.
4. There was no difference in bond strength between two composites of different polymerization stresses.

METHODS AND MATERIALS

Specimen Preparation

The set-up employed in this study is schematically illustrated in Figure 1. Noncarious human third molars were stored in a 0.5% chloramine solution at 4°C. The protocol for use of the teeth was approved by the institutional review board under approval No. VC15EISI0163. The teeth were used in the experiment within 2 months after extraction. Eighty-four teeth were chosen with a buccolingual dimension of 10.5 (±0.5) mm. The teeth were randomly divided into three experimental groups (I, II, and III) with 28 teeth per group. For group I, standard Class I cavities (length, width, and depth: 4×4×4 mm) were prepared with a flat-end, straight diamond bur (6837-016, Komet Brasseler, Lemgo, Germany). For group II, the teeth were reduced on both the mesial and distal sides until the width of the specimen was 4 mm. Then, MOD cavities having the same dimensions were prepared. For group III, the same reductions and preparations employed for group II were performed. Then, the buccal and lingual cusps were reduced with the same-size bur (Brasseler) until the cuspal walls had a 1-mm-thick layer of parallel dentin (group III, Figure 1). The cavity

dimensions of group III were the same as those of group II. However, reduced buccal and lingual cusps represent different compliances of the cavity walls. The resulting C-factors were C = 5 for group I and C = 1 for groups II and III.

Measuring Cavity Wall Compliance

The specimen was positioned in a custom-made device (R&B Inc, Daejon, Korea) to measure the compliance using screws, pins, and a linear scale sensor (inset photographs in Figure 1). The system was designed to detect the amount of cavity wall deflection while an external force was applied. Two measuring pins were kept in contact with the center of the buccal and lingual surfaces of the cusps. An individual specimen stabilizer made of self-curing acrylic resin was used to minimize the mobility of the specimen. When a force of 20 N (2.04 kgf) was applied, the inward cavity wall deflection (μm) was detected by a linear scale sensor (Lie 5, Numeric Jena Gmbh, Jena, Germany). The amount of deflection for each specimen was recorded after the 20 N force was held for 3 minutes. Cavity wall compliances were calculated for all specimens in groups II and III by dividing the deflection amount by the applied force (μm/N). The parameter for compliance of the cavity wall was based on the research presented by Lee and others.[21] The compliance of each specimen was recorded and the relationship between compliance and microtensile bond strength was evaluated.

Restorative Procedures and Subgroups

After measuring the compliance of all specimens, a two-step, self-etch bonding system (Clearfil SE Bond, Kuraray Noritake Dental, Tokyo, Japan) was applied to all the specimens and then the samples were light-cured for 10 seconds (1200 mW/cm^2, Elipar S10, 3M ESPE, St Paul, MN, USA). Next, each group was divided into four subgroups with seven teeth each. For groups II and III, a matrix band was applied before placing the composite. These cavities were filled with either three equal horizontal composite layers or a single placement. For subgroup 1, TB-inc, the specimen was restored with Tetric N-Ceram Bulk Fill (Ivoclar Vivadent, Schaan, Liechtenstein) by an incremental technique, which consisted of three equal increments of horizontal layering. After the first layer of composite (having a thickness of about 1.3 mm) was placed, light curing was carried out for 10 seconds. Then the second layer was placed, followed by 10 seconds of light curing. After the placement of the third layer, light curing was performed for 20 seconds. For subgroup 2, TB-bulk, the specimen was restored with Tetric N-Ceram Bulk Fill composite by the bulk-fill technique. Single placement of the composite resin was followed by light curing for 40 seconds. For subgroup 3, VB-inc, the specimen was restored with Venus Bulk Fill (Heraeus Kulzer, Dormagen, Germany) by applying the same incremental technique used for subgroup 1. For subgroup 4, VB-bulk, the specimen was restored with Venus Bulk Fill by using the same bulk fill technique as that used for subgroup 2. The specimens were stored for 7 days in room temperature water before microtensile bond testing (μ-TBS).

Micro-tensile Bond Test

The specimens were sectioned vertically into 1-mm-thick slices with a low-speed diamond saw (Metsaw, R&B) and then sectioned again at a right angle. Resin-dentin sticks were obtained at the cavity floor interface. The cross-sectional area was calculated exactly for each specimen by measuring the width and length using a digital caliper (Digimatic caliper, Mitutoyo, Japan). Twenty-eight specimens (four beams per tooth × seven teeth) were made for each subgroup. The specimen was attached to a universal testing machine (EZ test, Shimadzu, Kyoto, Japan) with cyanoacrylate adhesive (Zapit, DVA, Anaheim, CA, USA). It was then stressed in the testing device at a crosshead speed of 1 mm/min until failure. The value for μ-TBS (MPa) was obtained by dividing the measured force (N) by the individual bonded area (mm^2). If the specimen failed while being sectioned or attached to the tester, it was recorded as a pretesting failure (PTF), which was given a value of 0 MPa for the statistical analysis.

The mode of failure was determined using a light stereo microscope (S8APO, Leica, Wetzlar, Germany) at 50× magnification. The failure mode was classified into four types according to the characteristics of the fractured dentin side: cohesive failure in resin composite, cohesive failure in dentin, mixed failure, and adhesive failure between the adhesive and dentin. The failure mode was classified as mixed failure when a large region from the surface (>10%) was included as cohesive failure in both dentin and resin.[12] The percentages among each category were then calculated.

Measurement of Polymerization Shrinkage Stress

The polymerization shrinkage stress of the resin composite was measured using a custom-made device and software (R&B).[22] The instrument was driven by a motor and was designed to move a metal

Table 1: *Composition of Resin Composites Used in This Study*

Code	Product	Manufacturer	Base Resin	Filler (Wt/Vol%)
TB	Tetric N-Ceram Bulk Fill	Ivoclar Vivadent, Schaan, Liechtenstein	Bis-GMA, UDMA dimethacrylate co-monomers	78/55% (including prepolymer)
VB	Venus Bulk Fill	Heraeus Kulzer, Dormagen, Germany	UDMA, EBPADMA	65/38%

Abbreviations: Bis-GMA, bisphenol A glycidyl dimethacrylate; UDMA, urethane dimethacrylate; EBPADMA, ethoxylated bisphenol A dimethacrylate. The base resin composition and filler % were supplied by the manufacturers.

bar up and down. The polymerization shrinkage force applied to the acrylic tension rod was measured by a load cell (100 kgf) connected to the bar. The light required for polymerization of the resin composite sample was projected from beneath the transparent disc. The entire process was controlled by software made by R&B.

Prior to the measurements, the setup was switched to the compliance-allowed mode in which the acrylic rod could be moved freely during resin polymerization. The compliance of the system was 0.5 μm/N when the acrylic rod was used. Before connecting the acrylic rod, its surface was roughened with sandpaper (180 grit), treated with adhesive resin (bonding agent, Clearfil SE bond, Kuraray Noritake Dental, Okayama, Japan), and then light-cured for 10 seconds. Next, 0.035 g (12.6 mm^2) of resin composite was placed onto an acrylic disc, and the upper acrylic rod was positioned to ensure that the thickness of the specimen was 1 mm and its diameter was 4 mm. The stress measurement between the tension rod and the resin composite was set to zero before light curing. Then, the resin composite was cured using a light-curing unit (Bluephase, Ivoclar Vivadent; 800 mW/cm^2) for 20 seconds through the transparent disc. While the shrinkage stress was developing, displacement of the acrylic rod was allowed to move as the composite shrank. Along with the load-cell signal, the displacement was continuously recorded by the computer every 0.1 second for a period of 180 seconds. This measurement was repeated five times for each material and then the average value was calculated.

Statistical Analysis

Statistical analysis was performed using SPSS 18 for Windows (SPSS Inc, Chicago, IL, USA). The μ-TBS data were statistically analyzed using a Kruskal-Wallis test followed by the Mann-Whitney U-test to compare the groups at the 0.05 level of significance. Pairwise comparisons were carried out using Bonferroni's correction. Regression analysis was employed to identify whether there was any correlation between the μ-TBS and compliance of the cavity wall.

μ-TBS data were also analyzed by the Weibull analysis using a software package (R3.1.1, R Foundation for Statistical Computing, Vienna, Austria). The PTFs were excluded from the Weibull analysis because they cannot operate with zero values. The slope (β) of the distribution curve was calculated. Pivotal confidence bounds were also defined using Monte Carlo simulations.[23] B10 was calculated at the 10% probability of failure (unreliability) level, and the characteristic strength (scale parameter) at a probability of failure of 0.632 was also measured. The different groups were compared at the 10% unreliability level (B10) and at the characteristic strength.

RESULTS

Microtensile Bond Strength and the Fracture Mode Analysis

Table 2 shows the results of the microtensile bond strength at the cavity floor of each of the three groups using different composite filling methods. The results show significant differences between the incremental and bulk-fill techniques in group I (p=0.024 for subgroups 1 and 2; p=0.019 for subgroups 3 and 4). When each subgroup of group I was compared with that of groups II or III, a statistical difference was also found (p<0.05). No statistical difference was found when the cavity was filled with either TB or VB (subgroup 1 was compared with subgroup 3, and subgroup 2 was compared with subgroup 4 in each of groups I, II, and III; p>0.05). Figure 2 shows the results of the fracture mode analysis after bond testing, revealing that group I demonstrated a relatively high percentage of adhesive failures. In groups II and III, the proportions of adhesive failures and mixed failures were similar.

Compliance of Cavity Wall Results

The average measurement of cavity wall compliance in group II was 5.1 μm/N with a standard deviation of 0.62. The average measurement in group III was 8.7 μm/N with a standard deviation of 0.77.

Table 2: *Microtensile Bond Strengths (MPa)*[a]

Composite-filling Method	Group I	Group II	Group III
1. TB-inc	12.72 (10.75)[a] *†	21.08 (9.31)[b]	20.81 (9.04)[b]
2. TB-bulk	6.35 (8.43)[a]*	18.93 (9.82)[b]	19.03 (9.21)[b]
3. VB-inc	11.81 (10.75)[a] *	19.86 (9.76)[b]	21.17 (8.29)[b]
4. VB-bulk	5.36 (7.93)[a]*	19.25 (9.30)[b]	18.50 (9.57)[b]

**Indicates a statistically significant difference between the incremental and bulk fill techniques in group I (Kruskal-Wallis test followed by Mann-Whitney U test; $p<0.05$).*
[a] An identical lower superscript represents no statistically significant difference among the groups (compared in each row, Kruskal-Wallis test followed by Mann-Whitney U-test; $p>0.05$).
†Values in parentheses represent standard deviations.

Relationship Between M-TBS and Compliance of the Cavity Wall

The compliance of each specimen is plotted against the μ-TBS values of the specimens in Figure 3. The results show that in low C-factor cavities, there was no correlation between μ-TBS and compliance of the cavity wall.

Polymerization Stress of Composite Resins

The average polymerization stress for TB was 1.88 MPa with a standard deviation of 0.14; for VB, it was 2.76 MPa, with a standard deviation of 0.38.

Results of Weibull Analysis

Table 3 shows the PTF (%) and results of the Weibull analysis. PTF (%) is the number of failed specimens in each subgroup divided by the total number of specimens, in percent. The modulus parameter, β, was determined by linear regression of a plot of the ln of the inverse of survival probability (ln[1/survival probability]) against μ-TBS. The scale parameter, η, also called characteristic strength, represents the bond strength at which 63.2% of the specimens failed. B10 indicates the bond strength at a 10% probability of failure. Figure 4 is a representative graph illustrating the Weibull analysis of groups I-1, I-2, II-1, and II-2.

DISCUSSION

The incremental filling technique showed a higher μ-TBS than did the bulk-fill technique in the high C-factor cavities (group I). There was no statistical difference between the two techniques in the low C-factor cavities (groups II and III). Thus, the first hypothesis was partially rejected (Table 1). Because the proportion of the unbounded surface was small in the group I cavities, the polymerization stress could not be relieved under the restricted conditions.[24] With the incremental technique, each increment with a reduced volume of resin could provide

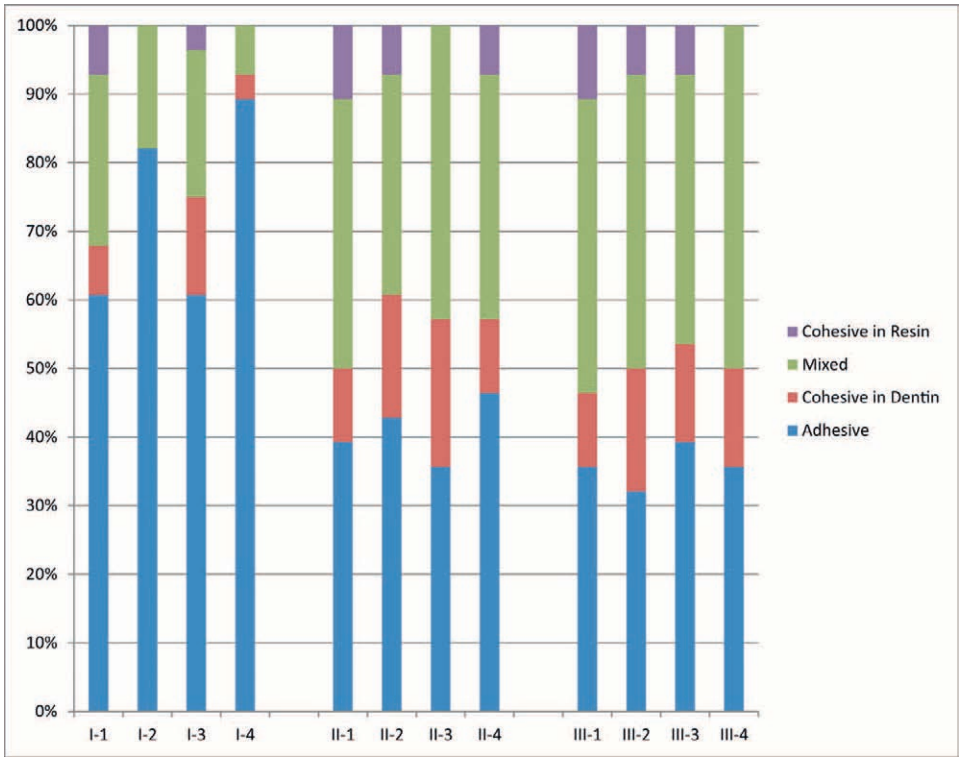

Figure 2. *Analysis of the fracture mode: cohesive in resin, cohesive failure in resin composite; cohesive in dentin, cohesive failure in dentin; mixed, cohesive failure in both dentin and resin; adhesive, adhesive failure between adhesive and dentin. All specimens showing pretesting failure are identified as adhesive failure between adhesive and dentin.*

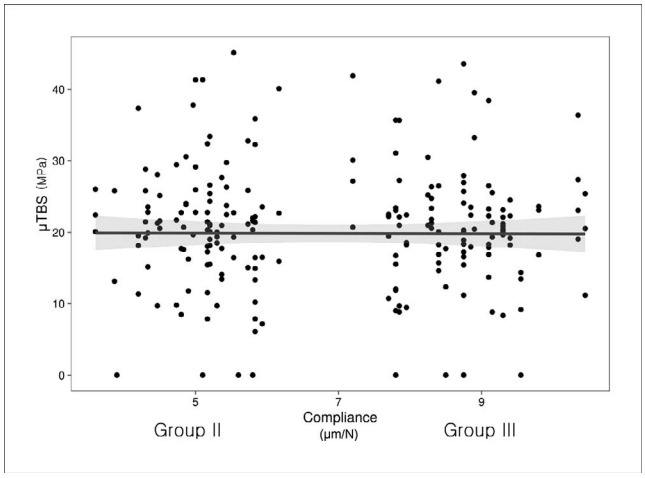

Figure 3. *Compliance of cavity wall vs μ-TBS for groups II and III. Solid line is the regression line resulting from linear regression analysis. Shaded area shows the 95% confidence level.*

an additional free surface for the composite to relieve the polymerization stress. Ferracane and others indicated that maximizing the free surface is likely to enhance stress relief by allowing increased flow of material.[25] However, in groups II and III, the incremental technique was not proven to be as effective as in group I. This may be because the MOD cavity already had enough free surfaces for the composite to relieve the stress. Nayif and others speculated that the polymer network formation was partly interrupted during polymerization under restricted conditions.[26] Rearrangement of the polymer network may be differently related to the bond strength in high and low C-factor cavities.

While the cavity configuration is undoubtedly one of the most important reasons for the difference, light attenuation may be another cause for the differences obtained between the two techniques for group I. Light curing of a bulk-fill composite can be affected by several variables associated with the light source, including distance, radiant exposure (known as energy density), radiant emittance (as power density), curing time, and the interval of light curing. Light attenuation may vary with the layer thickness or layering method.[2,3,9,27] It was previously demonstrated that the first increment of the composite on the bonding layer may play the most important role with regard to bond strength.[4] Van Ende and others asserted that less light was attenuated at the cavity bottom when a thin increment was cured first. As a result, this layer may polymerize adequately.[12] When the first layer was thinner than the following layer, a higher bond strength was observed.[1,4] In the bulk-fill technique, if a composite layer is relatively thick, there may not be enough double bonds for the composite to link to the adhesive layer.[28,29] A lower bond strength was also observed with shorter light-curing times.[10,30] According to several studies, low radiant emittance generates a small number of free radicals, resulting in longer polymeric chains with a low cross-linking density.[31,32] Thus, there may be both quantitative and qualitative differences of bond structure.

Differences of the μ-TBS were observed between group I and group II or group III. Hence, the second hypothesis was rejected. The bond strength of low C-factor cavities was higher than that of high C-factor

Table 3: *PTF (%) and Weibull Analysis Results of μ-TBS*[f]

	Subgroup	PTF (%)[a]	β[b]	η[c]	B10[d]	Characteristic Strength[e]
Group I	TB-inc	9 (32.1%)	2.87	20.99	9.6 [5.7-13.4][b,c]	21.0 [17.6-25.1][a,b]
	TB-bulk	14 (50%)	2.43	13.77	5.4 [2.6-8.5][c]	13.8 [10.8-17.8][b]
	VB-inc	10 (35.7%)	2.88	20.52	9.4 [5.5-13.2][b,c]	20.5 [17.2-24.7][a,b]
	VB-bulk	16 (57.1%)	2.28	13.68	5.1 [2.1-8.4][c]	13.7 [10.3-18.4][b]
Group II	TB-inc	2 (7.1%)	3.18	25.39	12.5 [8.6-16.3][a]	25.4 [22.3-29.1][a]
	TB-bulk	3 (10.7%)	3.02	23.74	11.3 [7.5-15.0][a,b]	23.7 [20.6-27.5][a]
	VB-inc	2 (7.1%)	3.14	23.75	11.6 [7.9-15.2][a]	23.8 [20.8-27.2][a]
	VB-bulk	2 (7.1%)	3.08	23.07	11.1 [7.5-14.6][a,b]	23.1 [20.1-26.6][a]
Group III	TB-inc	2 (7.1%)	3.66	24.74	13.4 [9.6-16.9][a]	24.7 [22.0-27.8][a]
	TB-bulk	2 (7.1%)	3.36	22.64	11.6 [8.1-14.9][a]	22.6 [20.0-25.7][a]
	VB-inc	1 (3.6%)	3.41	24.39	12.6 [8.9-16.1][a]	24.4 [21.6-27.6][a]
	VB-bulk	3 (10.7%)	3.29	23.0	11.6 [8.0-15.1][a]	23.0 [20.2-26.3][a]

[a] *PTF indicates pretesting failures, the number of failed specimens (as a percentage).*
[b] *Modulus, shape, or slope of the Weibull analysis.*
[c] *Eta or scale of the Weibull analysis.*
[d] Estimation and 95% confidence interval at a 10% probability of failure.
[e] Characteristic strength and 95% confidence interval at B63.2 (63.2% unreliability).
[f] An identical superscript represents no significant difference among the groups within each column.

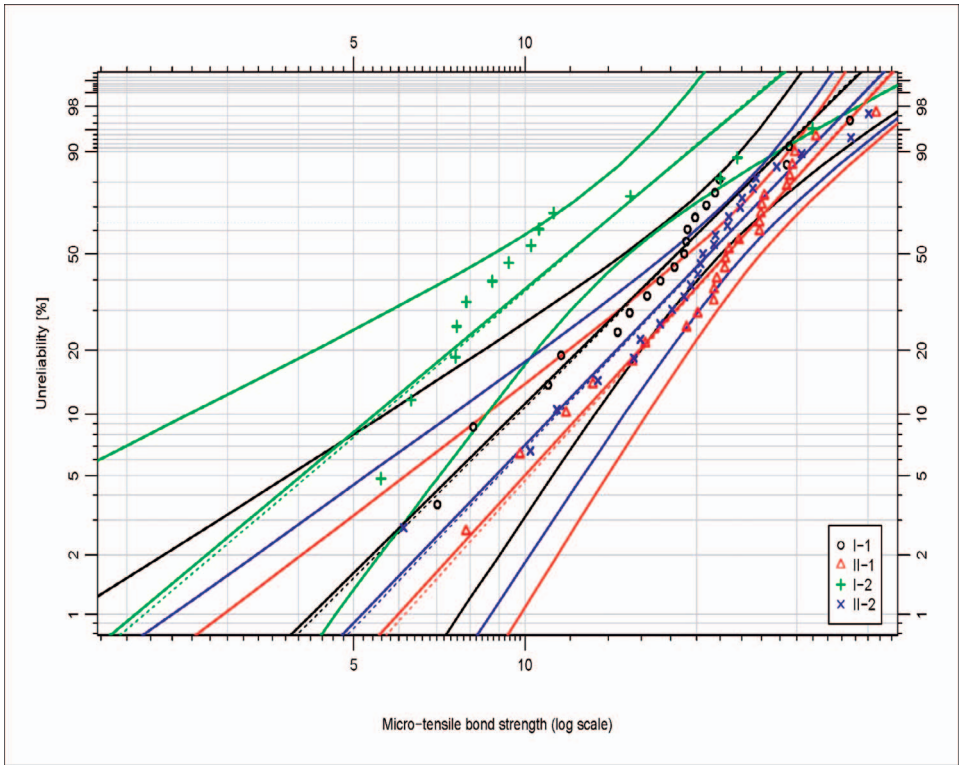

Figure 4. *Weibull plot of μ-TBS values for groups I-1, I-2, II-1, and II-2. Solid/dotted lines represent the Weibull line and the pure solid lines represent the 95% confidence bounds, as calculated from Monte Carlo simulations.*

cavities (Table 2). Polymerization stress can vary depending on cavity configuration.[33,34] The low bond strength in group I may be due to the high polymerization stress in high C-factor cavities.[15] Feilzer and others demonstrated with their *in vitro* model that restorations involving cavities with a C-factor of less than one are more likely to survive polymerization shrinkage stress.[33] Watts and others reported that polymerization stress can be greatly affected by the volume of composite.[35] The effect of the C-factor should be investigated with specimens of the same volume. In addition to the cavity configuration, the volume was also identical to ensure valid comparison in this experiment.

We also investigated the effect of cavity wall compliance in this experiment. The magnitude of the stress developed at the restoration's interface is related to the compliance of the surrounding structures.[13] The bond strength of two groups (II and III) showed no difference and as a result, the third hypothesis was accepted. Thus, there is little influence of the compliance on μ-TBS in low-C-factor cavities. A possible explanation could be that low C-factor cavities provide enough free surfaces such that the flexible walls of group III may not have any influence. For Class I cavities, however, it was not possible to measure the compliance of the wall using the device employed in this experiment. Rodrigues and others calculated the compliance for tooth preparation in Class I cavities using the finite element method.[36] They demonstrated different cavity compliances depending on the shape and dimension of Class I cavities. Whether the compliance of high C-factor cavity walls can affect the bond strength remains to be seen. Further studies should be conducted in high C-factor cavities to determine the relationship between bond strength and compliance.

Because different results were found in previous research involving large and small cavities, large cavities were chosen in this experiment to compare the two techniques.[1] A large cavity is an unfavorable condition for bonding composite to tooth material. It was previously asserted that use of the incremental technique can be effective in large cavities.[1] In contrast, research with small cavities has shown no difference between the two techniques.[5] Other studies have verified that the volume of the shrinking composite influenced the polymerization stress value.[13,37] In small cavities, the reduction of polymerization stress obtained by incremental filling may not be sufficient to allow a significant difference to be observed between the two techniques.[38]

There was no difference in μ-TBS between subgroups 1 and 3 or between 2 and 4 in each group, which allowed the last hypothesis to be accepted. TB

showed lower polymerization stress than did VB. However, no statistical difference was found between the μ-TBS values of TB and VB. In studies concerning the degree of conversion, TB showed a significantly lower degree of conversion than did VB.[20,39] The degree of conversion of TB was 54.5% and that of VB was 71.9%, as determined by Fourier transform infrared spectrometry.[39] For TB and VB, a recent study investigated the bottom/top surface hardness ratios. According to this study, the TB and VB ratios were 0.82 and 0.91, respectively, which indicated higher polymerization of the VB composite on the floor side.[40] A lower degree of composite conversion was reported to be associated with a lower bond strength.[41,42] VB is also known to have a significantly lower elastic modulus than TB, which may help to relieve the stress.[17,20] In other studies, TB and VB demonstrated different physical properties.[17,20] Not only the polymerization stress of the material but also other factors, such as the degree of conversion and elastic modulus, might have affected the bond strength to the floor.

Research has demonstrated that μ-TBS to dentin exhibits wide variability, which can mean that the bond strength of a composite to tooth material may vary in magnitude along the interface.[43-46] Several studies excluded specimens that failed during the procedure, which Nikolaenko and others had claimed to be inadequate.[2] Failed specimens may have two explanations: procedural error or too weak bonding. Therefore, the validity of including failed specimens for statistical analysis has been questioned. As an answer to this question, reporting the number of PTFs has been suggested,[47] as they can be an indicator of a specimen's ability to estimate bonding quality. The PTF was highest in groups I-2 and I-4, which could indicate that more of the cavity floor was detached or bonded weakly. In this experiment, four beams per tooth were obtained for a μ-TBS test at the identical position of each tooth. The cavity bottom dentin in all the specimens was midcoronal and at the central pit position to make sure that the effects of regional variability would be minimal.

Another approach to compensate for the shortcomings of the μ-TBS would be the Weibull analysis. The main difference is that the distribution of the failures is not determined from actual measurements, but is estimated from the data. Each Weibull analysis is characterized by two parameters: β (modulus) and η (scale) parameters. If the modulus is higher, it can mean that the bonding procedure is more reliable. Inokoshi and others have proposed that if the scale is higher, the bonding effectiveness will actually be better.[48] The modulus and scale parameters were found to be higher in incremental filling groups than in bulk-fill groups (Table 3). This difference was more evident in group I than in groups II or III.

CONCLUSIONS

In high C-factor cavities, the incremental technique showed higher bond strength than did the bulk-fill technique on the cavity floor. In the low C-factor cavities, there was no difference in bond strength between the two techniques. The bond strength in the high C-factor cavities was significantly lower than that in the low C-factor cavities. In the latter, the bond strength was not dependent on the compliance of the cavity walls. Two composite resins of different polymerization stresses did not show a significant difference in bond strength.

Acknowledgements

We would like to thank Prof Jan De Munck and his colleagues at the Catholic University of Leuven, Belgium, for their contribution to our Weibull analysis as well as for the support of the R-code and their helpful advice.

Regulatory Statement

This study was conducted in accordance with all the provisions of the local human subjects oversight committee guidelines and policies of St Vincent Hospital, Catholic University of Korea. The approval code for this study is VC15EISI0163.

Conflict of Interest

The authors of this manuscript certify that they have no proprietary, financial, or other personal interest of any nature or kind in any product, service and/or company presented in this article.

(Accepted 8 December 2017)

REFERENCES

1. He Z, Shimada Y, & Tagami J (2007) The effects of cavity size and incremental technique on micro-tensile bond strength of resin composite in Class I cavities *Dental Materials* **23(5)** 533-538.
2. Nikolaenko SA, Lohbauer U, Roggendorf M, Petschelt A, Dasch W, & Frankenberger R (2004) Influence of c-factor and layering technique on microtensile bond strength to dentin *Dental Materials* **20(6)** 579-585.
3. Figueiredo Reis A, Giannini M, Ambrosano GM, & Chan DC (2003) The effects of filling techniques and a low-viscosity composite liner on bond strength to class II cavities *Journal of Dentistry* **31(1)** 59-66.
4. Chikawa H, Inai N, Cho E, Kishikawa R, Otsuki M, Foxton RM, & Tagami J (2006) Effect of incremental

filling technique on adhesion of light-cured resin composite to cavity floor *Dental Materials J* **25(3)** 503-508.

5. Loguercio AD, Reis A, & Ballester RY (2004) Polymerization shrinkage: effects of constraint and filling technique in composite restorations *Dental Materials* **20(3)** 236-243.
6. Versluis A, Douglas WH, Cross M, & Sakaguchi RL (1996) Does an incremental filling technique reduce polymerization shrinkage stresses? *Journal of Dental Research* **75(3)** 871-878.
7. Heintze SD, Monreal D, & Peschke A (2015) Marginal quality of Class II composite restorations placed in bulk compared to an incremental technique: evaluation with SEM and stereomicroscope *Journal of Adhesive Dentistry* **17(2)** 147-154.
8. Wilson J (1993) Effects of design features and restorative techniques on marginal leakage of MO composites: an in vitro study *Operative Dentistry* **18(4)** 155-159.
9. Tjan AH, Bergh BH, & Lidner C (1992) Effect of various incremental techniques on the marginal adaptation of class II composite resin restorations *Journal of Prosthetic Dentistry* **67(1)** 62-66.
10. Van Ende A, Mine A, De Munck J, Poitevin A, & Van Meerbeek B (2012) Bonding of low-shrinking composites in high C-factor cavities *Journal of Dentistry* **40(4)** 295-303.
11. Kuijs RH, Fennis WM, Kreulen CM, Barink M, & Verdonschot N (2003) Does layering minimize shrinkage stresses in composite restorations? *Journal of Dental Research* **82(12)** 967-971.
12. Van Ende A, De Munck J, Van Landuyt KL, Poitevin A, Peumans M, & Van Meerbeek B (2013) Bulk-filling of high C-factor posterior cavities: effect on adhesion to cavity-bottom dentin *Dental Materials* **29(3)** 269-277.
13. Braga RR, & Ferracane JL (2004) Alternatives in polymerization contraction stress management *Journal of Applied Oral Science* **12(special issue)** 1-11.
14. Kinomoto Y, & Torii M (1998) Photoelastic analysis of polymerization contraction stresses in resin composite restorations *Journal of Dentistry* **26(2)** 165-171.
15. Yoshikawa T, Sano H, Burrow MF, Tagami J, & Pashley DH (1999) Effects of dentin depth and cavity configuration on bond strength *Journal of Dental Research* **78(4)** 898-905.
16. Zorzin J, Maier E, Harre S, Fey T, Belli R, Lohbauer U, Petschelt A, & Taschner M (2015) Bulk-fill resin composites: polymerization properties and extended light curing *Dental Materials* **31(3)** 293-301.
17. El-Damanhoury H, & Platt J (2014) Polymerization shrinkage stress kinetics and related properties of bulk-fill resin composites *Operative Dentistry* **39(4)** 374-382.
18. Ilie N, Kessler A, & Durner J (2013) Influence of various irradiation processes on the mechanical properties and polymerisation kinetics of bulk-fill resin based composites *Journal of Dentistry* **41(8)** 695-702.
19. Kim EH, Jung KH, Son SA, Hur B, Kwon YH, & Park JK (2015) Effect of resin thickness on the microhardness and optical properties of bulk-fill resin composites *Restorative Dentistry & Endodontics* **40(2)** 128-135.
20. Leprince JG, Palin WM, Vanacker J, Sabbagh J, Devaux J, & Leloup G (2014) Physico-mechanical characteristics of commercially available bulk-fill composites *Journal of Dentistry* **42(8)** 993-1000.
21. Lee SH, Chang J, Ferracane J, & Lee IB (2007) Influence of instrument compliance and specimen thickness on the polymerization shrinkage stress measurement of light-cured composites *Dental Materials* **23(9)** 1093-1100.
22. Han SH, Sadr A, Tagami J, & Park SH (2016) Internal adaptation of resin composites at two configurations: influence of polymerization shrinkage and stress *Dental Materials* **32(9)** 1085-1094.
23. Symynck J, & De Bal F (2011) Monte Carlo pivotal confidence bounds for Weibull analysis, with implementations in R *New Technologies and Products in Machine Manufacturing Technologies* 43-50.
24. Feilzer AJ, De Gee AJ, & Davidson CL (1990) Quantitative determination of stress reduction by flow in composite restorations *Dental Materials* **6(3)** 167-171.
25. Ferracane JL (2008) Buonocore Lecture. Placing dental composites—a stressful experience *Operative Dentistry* **33(3)** 247-257.
26. Nayif MM, Nakajima M, Aksornmuang J, Ikeda M, & Tagami J (2008) Effect of adhesion to cavity walls on the mechanical properties of resin composites *Dental Materials* **24(1)** 83-89.
27. Soares CJ, Bicalho AA, Tantbirojn D, & Versluis A (2013) Polymerization shrinkage stresses in a premolar restored with different composite resins and different incremental techniques *Journal of Adhesive Dentistry* **15(4)** 341-350.
28. Peutzfeldt A, & Asmussen E (2000) The effect of postcuring on quantity of remaining double bonds, mechanical properties, and in vitro wear of two resin composites *Journal of Dentistry* **28(6)** 447-452.
29. Peutzfeldt A, & Asmussen E (2005) Resin composite properties and energy density of light cure *Journal of Dental Research* **84(7)** 659-662.
30. Xu X, Sandras DA, & Burgess JO (2006) Shear bond strength with increasing light-guide distance from dentin *Journal of Esthetic and Restorative Dentistry* **18(1)** 19-27; discussion 28.
31. Asmussen E, & Peutzfeldt A (2001) Influence of pulse-delay curing on softening of polymer structures *Journal of Dental Research* **80(6)** 1570-1573.
32. Asmussen E, & Peutzfeldt A (2003) Two-step curing: influence on conversion and softening of a dental polymer *Dental Materials* **19(6)** 466-470.
33. Feilzer AJ, De Gee AJ, & Davidson CL (1987) Setting stress in composite resin in relation to configuration of the restoration *Journal of Dental Research* **66(11)** 1636-1639.
34. Witzel MF, Ballester RY, Meira JB, Lima RG, & Braga RR (2007) Composite shrinkage stress as a function of specimen dimensions and compliance of the testing system *Dental Materials* **23(2)** 204-210.
35. Watts DC, & Satterthwaite JD (2008) Axial shrinkage-stress depends upon both C-factor and composite mass *Dental Materials* **24(1)** 1-8.

36. Rodrigues FP, Lima RG, Muench A, Watts DC, & Ballester RY (2014) A method for calculating the compliance of bonded-interfaces under shrinkage: validation for Class I cavities *Dental Materials* **30(8)** 936-944.

37. Miguel A, & de la Macorra JC (2001) A predictive formula of the contraction stress in restorative and luting materials attending to free and adhered surfaces, volume and deformation *Dental Materials* **17(3)** 241-246.

38. Braga RR, Ballester RY, & Ferracane JL (2005) Factors involved in the development of polymerization shrinkage stress in resin-composites: a systematic review *Dental Materials* **21(10)** 962-970.

39. Al-Ahdal K, Ilie N, Silikas N, & Watts DC (2015) Polymerization kinetics and impact of post polymerization on the degree of conversion of bulk-fill resin-composite at clinically relevant depth *Dental Materials* **31(10)** 1207-1213.

40. Jung JH, & Park SH (2017) Comparison of polymerization shrinkage, physical properties, and marginal adaptation of flowable and restorative bulk fill resin-based composites *Operative Dentistry* **42(4)** 375-386.

41. Cekic-Nagas I, Ergun G, Vallittu PK, & Lassila LV (2008) Influence of polymerization mode on degree of conversion and micropush-out bond strength of resin core systems using different adhesive systems *Dental Materials Journal* **27(3)** 376-385.

42. Price RB, Doyle G, & Murphy D (2000) Effects of composite thickness on the shear bond strength to dentin *Journal of the Canadian Dental Association* **66(1)** 35-39.

43. Shono Y, Ogawa T, Terashita M, Carvalho RM, Pashley EL, & Pashley DH (1999) Regional measurement of resin-dentin bonding as an array *Journal of Dental Research* **78(2)** 699-705.

44. Tanumiharja M, Burrow MF, & Tyas MJ (2000) Microtensile bond strengths of seven dentin adhesive systems *Dental Materials* **16(3)** 180-187.

45. Phrukkanon S, Burrow MF, & Tyas MJ (1998) Effect of cross-sectional surface area on bond strengths between resin and dentin *Dental Materials* **14(2)** 120-128.

46. Phrukkanon S, Burrow MF, & Tyas MJ (1998) The influence of cross-sectional shape and surface area on the microtensile bond test *Dental Materials* **14(3)** 212-221.

47. Okuda M, Pereira PN, Nakajima M, Tagami J, & Pashley DH (2002) Long-term durability of resin dentin interface: nanoleakage vs. microtensile bond strength *Operative Dentistry* **27(3)** 289-296.

48. Inokoshi M, Kameyama A, De Munck J, Minakuchi S, & Van Meerbeek B (2013) Durable bonding to mechanically and/or chemically pre-treated dental zirconia *Journal of Dentistry* **41(2)** 170-179.

©Operative Dentistry, 2018, **43-6,** 642-655

Color and Translucency of Resin-based Composites: Comparison of A-shade Specimens Within Various Product Lines

D Kim • S-H Park

Clinical Relevance

Color and translucency of resin-based composites (RBCs) vary among the different shades within each product line. These differences do not always follow the order of the shade numbers. Clinicians should be aware of the optical characteristics of individual RBC products to achieve predictable results.

SUMMARY

Objectives: The purpose of this study was to examine and compare the color and translucency of currently available resin-based composites (RBCs) with respect to the shade numbers within each product line.

Methods and Materials: Four A-shades (A1, A2, A3, and A3.5) of nine RBC products (Beautifil II, Ceram-X One, Estelite Sigma Quick, Esthet-X HD, Filtek Z250, Filtek Z350 XT, Gradia Direct, Herculite Precis, and Tetric N-Ceram) were investigated. Ten disk-shaped specimens of two different thicknesses (1 and 2 mm) were prepared for each shade of the RBCs. The maximum blue light irradiance (I_{max}) through the specimen was recorded using a digital optometer. The color measurements were made according to the CIELAB color scale (quantifying L*, a*, and b*) using a colorimeter, and the translucency parameter (TP) was calculated. The L*, a*, b*, TP, and I_{max} values were compared among the different shades and thicknesses of each product using one-way analysis of variance followed by Tukey's *post hoc* test.

Results: There were significant differences in the color and translucency among the shades and thicknesses within each product line ($p<0.001$). The L*, I_{max}, and TP of the 1-mm specimens were higher than those of the 2-mm specimens. The specimens showed equal or lower L* and I_{max} for higher shade numbers. The a* values differed only slightly among the shades, whereas the b* values were distributed over a relatively wide range. The TP values were independent of the order of shade numbers.

Dohyun Kim, DDS, PhD, clinical assistant professor, Department of Conservative Dentistry and Oral Science Research Center, Yonsei University College of Dentistry, Seoul, Republic of Korea

*Sung-Ho Park, DDS, PhD, professor, Department of Conservative Dentistry and Oral Science Research Center, Yonsei University College of Dentistry, Seoul, Republic of Korea

*Corresponding author: 50-1 Yonsei-ro, Seodaemun-gu, Seoul 03722, Republic of Korea; e-mail: sunghopark@yuhs.ac

DOI: 10.2341/17-228-L

Conclusions: Within the limitations of this study, the RBCs became darker and yellowish as the shade number increased. The blue light irradiance decreased in increasing order of the shade numbers. Changes in the translucency demonstrated different trends among the shades, depending on the product line.

INTRODUCTION

Resin-based composites (RBCs) have been widely used as direct esthetic restorative materials in dental clinics. There are various kinds of RBC products supplied by different manufacturers, and each of them has its own color and optical characteristics. To satisfy increasing esthetic demands, it is a challenge for clinicians to select an appropriate product and technique that can best reproduce the color and overall appearance of the patient's teeth.

The color of an RBC is generally described as a "shade" based on the Munsell color system, which consists of three primary color attributes: hue, lightness, and chroma.[1] Currently, most of the manufacturers follow the VITA classical shade system (VITA Zahnfabrik, Säckingen, Germany) (Figure 1), where each RBC is labeled as a match to one of 16 shade tabs.[2] The shades are classified by the hue (represented by letters, eg, A, B, C, and D) and by the lightness (represented by numbers, eg, 1, 2, 3, and 4).

In addition to the primary color attributes, there are other subtle optical properties to be considered, such as translucency, opacity, opalescence, iridescence, surface gloss, and fluorescence.[3] Among these, translucency is regarded as one of the most important factors influencing the esthetics of restorations.[4] Translucency is the ability of a layer of a colored substance to allow an underlying background to show through.[5] RBCs are optically translucent materials because of their structure, which is composed of a highly transparent matrix and small filler particles. Incident light undergoes reflection, absorption, scattering, and transmission within the RBC material, and the translucency is expressed as a consequence of the interactions of these phenomena.[6]

Several authors have shown that the color and translucency of RBCs depend on the manufacturer and the shade classification.[7-12] Schmeling and others[13] reported that RBCs with a high lightness were more translucent than medium- and low-lightness materials within the same product line (4 Seasons, Ivoclar Vivadent, Schaan, Liechtenstein). In a recent study, the A3 shade showed the highest translucency among the A1, A2, A3, and A3.5 shades in another RBC product (Filtek Supreme XTE, 3M ESPE, St Paul, MN, USA).[14] These results suggest that the translucency of RBCs can differ, depending on the lightness, represented by the shade number, even within the same product line. Although each of these studies investigated only a single RBC product, their findings should be considered carefully by clinicians providing esthetic restorations. Yu and Lee[15] evaluated the relationship between the color parameters and the translucency of various shades of RBCs and reported that the lightness and translucency showed a weak positive correlation (r=0.117, p<0.05). However, they calculated only the overall correlations between various brands and shades of RBCs thoroughly; therefore, the color and translucency of each shade and product need to be reported and compared individually. In this regard, there is a need for studies that cover a wide range of currently available RBC products, evaluating the

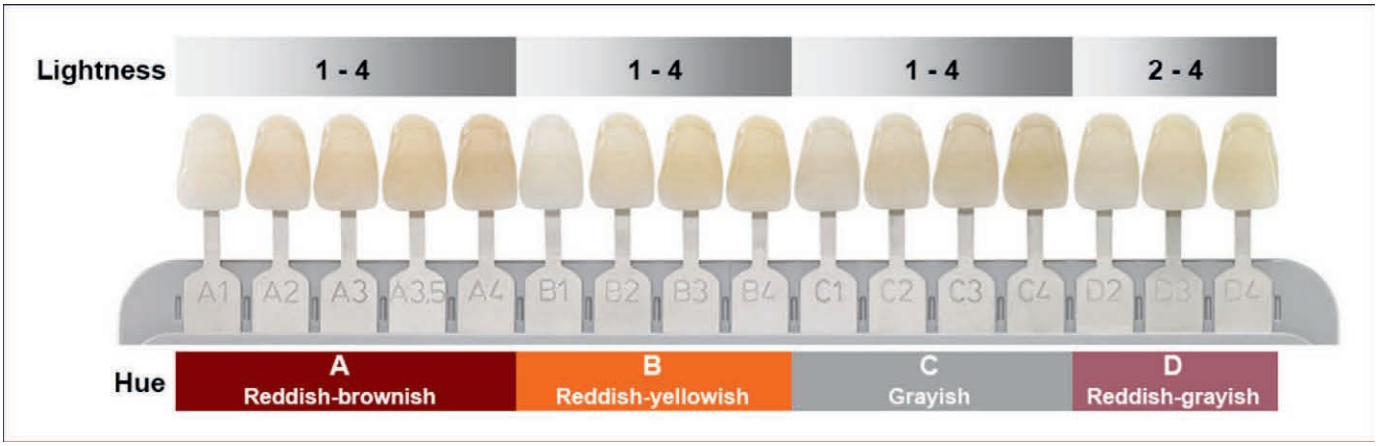

Figure 1. *VITA Classical shade system (VITA Zahnfabrik, Säckingen, Germany) (from manufacturer's instructions).*

Table 1: *Resin-Based Composites Used in the Study*

Code	Manufacturer	Product Name	Shades/Lot Numbers			
	A1	A2	A3	A3.5		
BF	Shofu Inc (Kyoto, Japan)	Beautifil II	121476	011596	051520	051590
CX	Dentsply (Konstanz, Germany)	Ceram-X One	1501000396	1503000560	1503000817	1501000306
ES	Tokuyama Dental (Tokyo, Japan)	Estelite Sigma Quick	129E85	138EY4	158EY4	123E45
EX	Dentsply (Milford, DE, USA)	Esthet-X HD	131002	1310023	131029	1412101
F2	3M ESPE (St Paul, MN, USA)	Filtek Z250	N683493	N651172	N699362	N676563
F3	3M ESPE	Filtek Z350 XT	N676527	N617414	N676525	N670694
GD	GC Corporation (Tokyo, Japan)	Gradia Direct	1409043	1409021	1406262	1509101
HC	Kerr (Orange, CA, USA)	Herculite Precis	4944388	5552574	5552583	5518416
TC	Ivoclar Vivadent (Schaan, Liechtenstein)	Tetric N-Ceram	U28046	U29443	U26780	U13046

color and translucency of RBCs with respect to the shade numbers.

Color and translucency affect the esthetics of a restoration as well as the polymerization of the RBC itself, as light needs to penetrate to a sufficient depth in the material in order to activate the photoinitiators. Adequate polymerization of RBCs depends on the available light energy; the materials cannot be completely polymerized with insufficient light energy.[16] While the esthetics depends on the overall translucency of RBC material, the effect of translucency on the polymerization may be different to that considering the esthetics, as most photoinitiators absorb light over a certain range of wavelengths. For example, camphorquinone, the most widely used photoinitiator, absorbs light at wavelengths between 460 and 480 nm;[17] thus, a transmittance confined to the blue light range would be a decisive factor for the polymerization of RBCs containing camphorquinone as a photoinitiator. Although some studies have reported that the light transmittance at blue wavelengths differed among the different shades and types of RBCs,[18-20] further systematic studies of the blue light transmittance of current RBC products are required.

Therefore, the purpose of this study was to examine and compare the color and translucency of RBCs with respect to the shade numbers within the same product line. We also aimed to evaluate the blue light transmittance of each RBC separately. We expect that these findings can provide clinically helpful information for using such RBCs in esthetic restorative treatments.

METHODS AND MATERIALS

RBC Materials

Four A-shade materials with different shade numbers (A1, A2, A3, and A3.5) of nine RBC products (Beautifil II [BF], Ceram-X One [CX], Estelite Sigma Quick [ES], Esthet-X HD [EX], Filtek Z250 [F2], Filtek Z350 XT [F3], Gradia Direct [GD], Herculite Precis [HC], and Tetric N-Ceram [TC]) were selected for the present study (as detailed in Table 1). The characteristics and compositions of the RBCs are summarized in Table 2.

Specimen Preparation

Ten disk-shaped specimens with two different thicknesses (1 and 2 mm) were prepared for each shade of the nine RBC products, according to the International Organization for Standardization (ISO) 4049[21] with a slight modification (Figure 2). A custom-made stainless-steel mold (6 mm in diameter) was placed on a transparent film on a glass slide. RBC material was packed into the mold and covered with a transparent film and a flat stainless-steel cylinder. Then the mold was pressed to displace excess material and to produce a disk of uniform thickness. The glass slide and the cylinder were removed, and the RBC was light cured for 40 seconds using a light curing unit (Bluephase, Ivoclar Vivadent) placed directly on the surface of the material. After polymerization, the specimen was removed, and a digital caliper (500-181, Mitutoyo, Tokyo, Japan) was used to measure the thicknesses with a precision of 0.05 mm. The surface was examined by visual inspection, and the specimen

Table 2: *Compositions and Characteristics of the Resin-Based Composite Materials (From Manufacturer's Instructions)*

Code	Type	Composition		Filler Size (μm)	Filler Content (wt%/vol%)
		Matrix	Filler		
BF	Nanohybrid	Bis-GMA TEGDMA	Surface prereacted glass ionomer Multifunctional glass filler Nanofiller	0.01-4.0/mean 0.8 0.01-0.02	83.3/68.6
CX	Nanohybrid	Dimethacrylate based	Methacrylate modified polysiloxane Barium-aluminum-borosilicate glass Silica nanofiller	[a]	[a]
ES	Suprananofill	Bis-GMA TEGDMA	Silica/zirconia filler Composite filler Spherical submicron filler	0.1-0.3/mean 0.2	82/71
EX	Nanohybrid	Bis-GMA Bis-EMA TEGDMA	Barium fluoroborosilicate glass Silica nanofiller	<1.0 0.04	77/60
F2	Microhybrid	Bis-GMA UDMA Bis-EMA	Silica/zirconia filler	0.01-3.5	78/60
F3	Nanofill	Bis-GMA UDMA TEGDMA PEGDMA Bis-EMA	Nonaggregated silica/zirconia filler Aggregated silica/zirconia cluster	Silica 0.02/zirconia 0.004-0.011 0.6-20	78.5/63.3
GD	Microhybrid	UDMA	Microhybrid filler (no barium glass)	Mean 0.85	73/64
HC	Nanohybrid	Bis-GMA TEGDMA	Prepolymerized filler Silica nanofiller Hybrid filler (barium glass)	30-50 0.02-0.05 Mean 0.4	78/59
TC	Nanohybrid	Bis-GMA UDMA	Barium glass Ytterbium trifluoride Mixed oxide and copolymers	0.04-3.0	80-81/55-57

Abbreviations: wt%, weight percentage; vol%, volume percentage; Bis-GMA, bisphenol-A-glycidyl dimethacrylate; TEGDMA, triethylene glycol dimethacrylate; Bis-EMA, ethoxylated bisphenol-A-dimethacrylate; UDMA, urethane dimethacrylate.
[a] No information is available about the filler size and content of Ceram-X One.

was rejected if there were any defects or irregularities. Each specimen was stored in distilled water for 24 hours.

Measurement of Blue Light Irradiance

During specimen preparation, prior to light curing, the mold was placed at the entry of an integrating sphere (UMBB-150, Gigahertz-Optik, Turkenfeld, Germany) to measure the blue light irradiance. The mold was custom designed and made for mounting on this integrating sphere. During the curing time, a digital optometer device (P-9710, Gigahertz-Optik) was connected to the integrating sphere and used to measure the transmitted irradiance through the bottom of the specimen in real time (Figure 2). The maximum irradiance during the curing time (I_{max}; mW/cm^2) was recorded for each specimen. The light intensity of the curing unit, the irradiance measured without any specimen, was 1405 mW/cm^2.

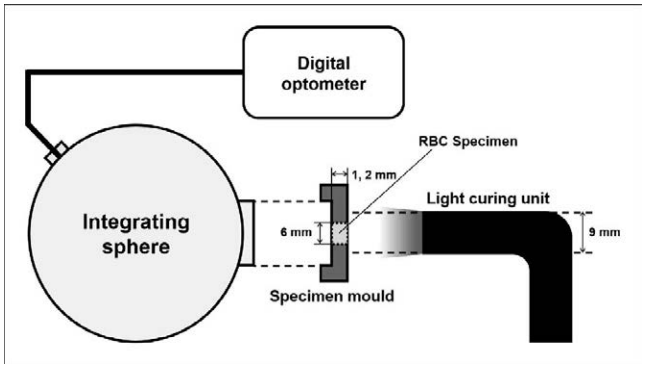

Figure 2. *Schematic diagram of the apparatus for the specimen preparation and the blue light irradiance measurement.*

Measurement of Color and Translucency

The color measurements were made according to the Commission Internationale de l'Eclairage CIELAB color scale[22] using a colorimeter (CR-321, Minolta, Osaka, Japan). L* indicates lightness (0 to 100), and a* and b* indicate levels of red (+a*), green (−a*), yellow (+b*), and blue (−b*) (−60 to 60). The L*, a*, and b* values of each specimen were recorded

relative to the standard illuminant D65 against black (L*=1.38, a*=0.00, b*=0.06) and white (L*=94.44, a*=0.26, b*=1.69) reflectance standards (Spectralon, Labsphere, North Sutton, NH, USA). The aperture diameter of the colorimeter was 3 mm, and each specimen was measured in triplicate. The color difference between the specimens (ΔE) was determined using the formula

$$\Delta E = \left[(L_x^* - L_y^*)^2 + (a_x^* - a_y^*)^2 + (b_x^* - b_y^*)^2\right]^{1/2}$$

where the L*, a*, and b* values were measured against the white standard. The subscripts "x" and "y" refer to the shades (eg, A1, A2, A3, and A3.5). A value of $\Delta E \geq 3.3$ was used as the threshold for a clinically perceivable color difference.[23]

The translucency parameter (TP) of each specimen was obtained by calculating the color difference of the specimen against the black and white standards according to the formula[5]

$$TP = \left[(L_B^* - L_W^*)^2 + (a_B^* - a_W^*)^2 + (b_B^* - b_W^*)^2\right]^{1/2}$$

where L^*_B, a^*_B, and b^*_B were measured against the black background and L^*_W, a^*_W, and b^*_W were measured against the white background. The difference in TP (ΔTP) was calculated by

$$\Delta TP = |TP_x - TP_y|$$

where the subscripts "x" and "y" refer to the shades (eg, A1, A2, A3, and A3.5). A value of $\Delta TP \geq 2.0$ was used as the threshold for a clinically perceivable translucency difference.[24]

Statistical Analysis

The color parameters measured against the white background (L*, a*, and b*), TP, and I_{max} were compared among the different shades and thicknesses within each RBC product line using one-way analysis of variance followed by Tukey's *post hoc* test. All statistical analyses were performed under a 95% confidence level using the SPSS 23 (IBM Corp, Somers, NY, USA) software program.

RESULTS

The mean and standard deviation of the L*, a*, b*, TP, and I_{max} values of each shade of the RBCs are presented in Table 3 and Figure 3. All variables showed significant differences among the different shades and sample thicknesses within each product line ($p<0.05$). The ΔE and ΔTP values between the shades are presented in Table 4, and clinically perceivable differences are indicated in Figure 3; it can be seen that these parameters also differed depending on the product line. The colors of all four shades of each RBC product are indicated in the three-dimensional CIELAB color space in Figure 4.

Color

For all RBC products, the 1-mm specimens showed higher L* values than the 2-mm specimens. Most specimens showed equal or lower L* values for higher shade numbers. Only in the case of the 2-mm specimen of EX was a higher L* value observed for the A3 shade compared to the A2 shade. Significant decreases in L* were observed for the CX and GD samples as a function of increasing shade number. In the ES and HC product lines, there was no significant difference in L* values between the A3 and A3.5 shades. For the EX, F2, and TC samples, the A2 and A3 shades showed no difference in L*, while in the BF, F3, and HC product lines, the L* values of A1 and A2 shades showed no significant difference (Table 3; Figure 3).

The a* values varied only slightly among the shades and thicknesses, whereas the b* values were distributed over a relatively wide range with respect to the shade numbers and RBC products. The a* values increased with increasing shade number for the BF, CX, F2, F3, and HC samples. In the ES product line, the A3 shade showed the highest a* value among the four shades, while the EX samples showed almost equal a* values for all shades. The GD and TC samples showed no correlation between the a* values and the shade numbers. All of the RBCs demonstrated an increase in b* with increasing shade number (Table 3; Figure 3).

Regardless of the significant differences in the L*, a*, and b* values, there were some shades whose color differences were not clinically perceivable ($\Delta E<3.3$) within every product line except EX, which showed distinct color differences ($\Delta E\geq3.3$) among all shades (Table 4; Figure 3). For the 1-mm specimens, between the A1 and A2 shades, F2 showed relatively distinct color differences ($\Delta E=7.6$) compared to the other products, and the BF and HC samples showed color differences that were clinically unperceivable ($\Delta E<3.3$). Between the A2 and A3 shades, the color differences were only slightly different among the products, where the CX, F2, and TC samples showed ΔE values less than 3.3. Between the A3 and A3.5 shades, the EX showed a maximum ΔE of 9.3, and four out of the

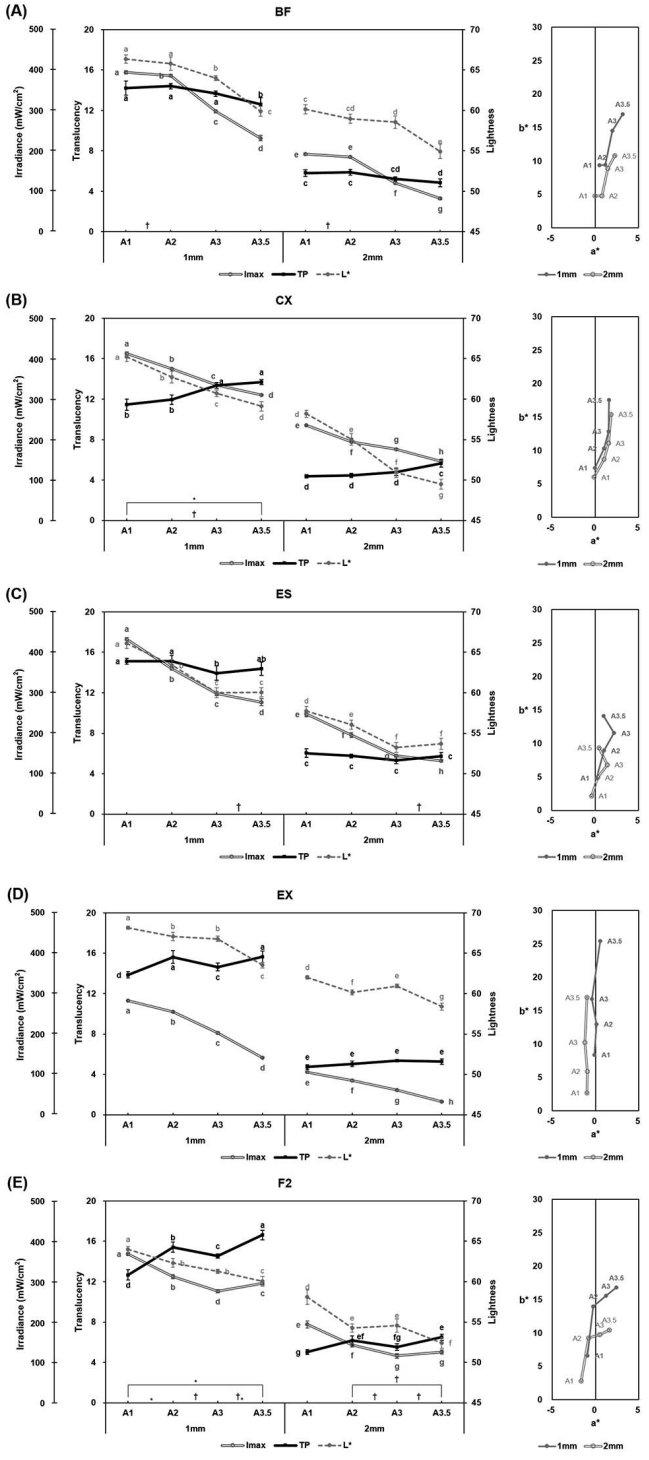

Figure 3. *Mean L*, a*, b*, TP, and I_{max} values of each shade of the RBC products. (A): Beautifil II (BF). (B): Ceram-X One (CX). (C): Estelite Sigma Quick (ES). (D): Esthet-X HD (EX). (E): Filtek Z250 (F2). (F): Filtek Z350 XT (F3). (G): Gradia Direct (GD). (H): Herculite Precis (HC). (I): Tetric N-Ceram (TC). Different letters denote significant differences among the specimens within each RBC product line (*$p<0.05$*). † Color difference that is clinically unperceivable (*$\Delta E<3.3$*). * Translucency difference that is clinically perceivable (*$\Delta TP\geq 2.0$*).*

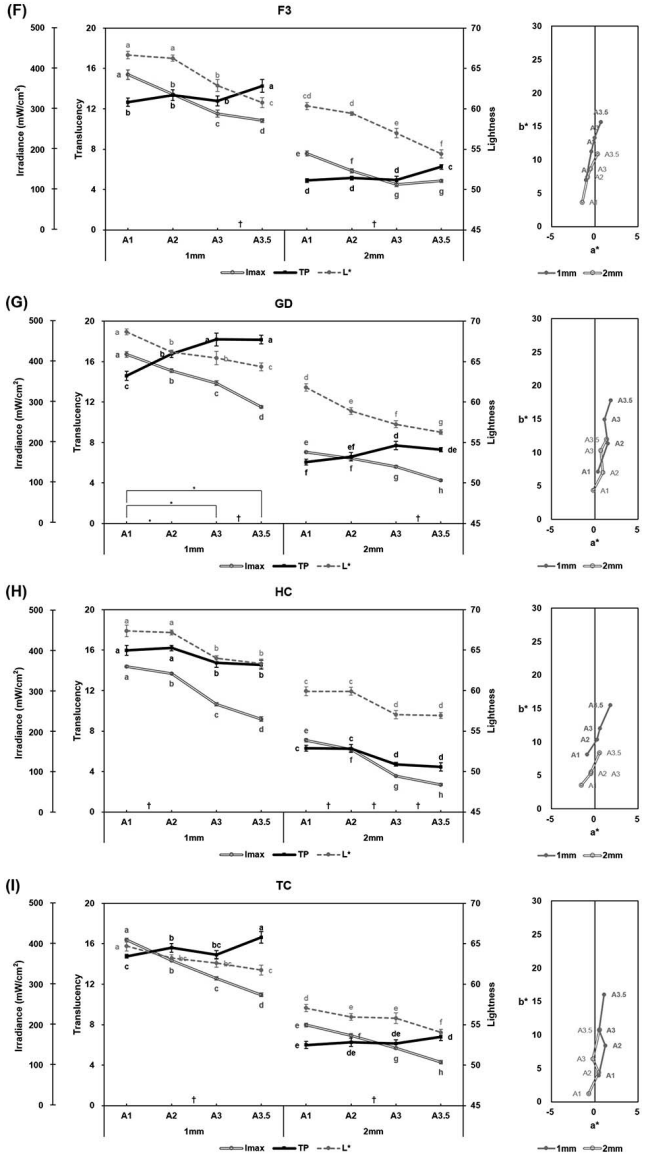

Figure 3. *Continued.*

nine products (ES, F2, F3, and GD) showed clinically unperceivable color differences ($\Delta E<3.3$). Between the A1 and A3, A1 and A3.5, and A2 and A3.5 shades, all specimens showed color differences that were clinically perceivable ($\Delta E\geq 3.3$); the greatest color difference was observed between the A1 and A3.5 shades of the EX product ($\Delta E=17.68$). For the 2-mm specimens, the BF, ES, EX, GD, and TC samples demonstrated similar color difference patterns among the shades compared to those of the 1-mm specimens. CX showed ΔE values of more than 3.3 among all shades. In the F2 product, there was no distinct color difference even between the A2 and A3.5 shades ($\Delta E=3.27$). The HC product showed clinically unperceivable color differences

Table 3: *L*, a*, b*, TP, and I_{max} Values of Each Shade of the Resin-Based Composites*[a]

Code	Thickness	Shade	L*			a*			b*			TP			I_{max}		
			Mean	SD		Mean	SD		Mean	SD		Mean	SD		Mean	SD	
BF	1 mm	A1	66.35	0.49	A	0.48	0.07	G	9.38	0.21	D	14.22	0.69	A	394.20	4.17	A
		A2	65.79	0.82	A	1.18	0.08	E	9.45	0.34	D	14.41	0.27	A	385.99	3.19	B
		A3	64.00	0.30	B	1.96	0.03	C	14.53	0.12	B	13.66	0.27	A	297.37	3.68	C
		A3.5	59.90	0.61	C	3.17	0.11	A	17.01	0.47	A	12.61	0.66	B	231.65	6.82	D
	2 mm	A1	60.14	0.58	C	−0.03	0.14	H	4.81	0.14	E	5.81	0.32	C	191.74	2.88	E
		A2	58.99	0.56	CD	0.77	0.08	F	4.81	0.25	E	5.88	0.29	C	184.98	2.55	E
		A3	58.57	0.78	D	1.44	0.12	D	8.85	0.34	D	5.23	0.20	CD	120.53	3.05	F
		A3.5	54.93	0.91	E	2.25	0.15	B	10.79	0.68	C	4.85	0.39	D	82.10	2.30	G
CX	1 mm	A1	65.23	0.55	A	−0.03	0.02	D	7.40	0.08	G	11.45	0.55	B	412.63	3.75	A
		A2	62.70	0.72	B	1.03	0.03	C	10.31	0.20	E	11.94	0.47	B	374.88	2.25	B
		A3	60.73	0.41	C	1.54	0.03	B	12.88	0.11	C	13.34	0.29	A	335.03	2.27	C
		A3.5	59.11	0.59	D	1.62	0.04	B	17.54	0.25	A	13.68	0.25	A	310.20	2.29	D
	2 mm	A1	58.19	0.44	D	−0.11	0.11	D	6.00	0.26	H	4.37	0.17	D	235.32	1.43	E
		A2	55.02	0.72	E	1.04	0.12	C	8.71	0.25	F	4.47	0.21	D	194.11	1.18	F
		A3	50.93	0.61	F	1.55	0.02	B	11.09	0.16	D	4.78	0.31	D	175.77	2.21	G
		A3.5	49.51	0.63	G	1.84	0.09	A	15.40	0.36	B	5.65	0.38	C	146.18	1.76	H
ES	1 mm	A1	66.08	0.60	A	0.19	0.14	E	4.82	0.23	E	15.12	0.29	A	432.76	3.77	A
		A2	63.42	0.66	B	1.00	0.08	C	8.94	0.14	C	15.13	0.58	A	359.41	4.12	B
		A3	60.01	0.63	C	2.19	0.09	A	11.54	0.27	B	13.94	0.73	B	297.70	5.15	C
		A3.5	60.06	0.57	C	0.97	0.11	C	14.13	0.47	A	14.36	0.66	AB	276.73	8.61	D
	2 mm	A1	57.72	0.59	D	−0.42	0.08	F	2.15	0.34	F	6.03	0.42	C	247.28	6.69	E
		A2	56.08	0.56	E	0.32	0.11	DE	4.92	0.43	E	5.76	0.19	C	195.87	6.16	F
		A3	53.26	0.62	F	1.40	0.12	B	6.80	0.31	D	5.32	0.34	C	144.07	2.47	G
		A3.5	53.67	0.70	F	0.47	0.10	D	9.36	0.45	C	5.73	0.37	C	131.79	2.94	H
EX	1 mm	A1	68.16	0.17	A	−0.14	0.05	C	8.40	0.14	E	13.86	0.32	D	282.74	2.26	A
		A2	67.07	0.51	B	0.12	0.06	B	12.96	0.45	C	15.62	0.64	A	255.37	1.90	B
		A3	66.79	0.35	B	−0.39	0.09	D	16.75	0.34	B	14.64	0.39	C	202.92	3.10	C
		A3.5	63.52	0.32	C	0.53	0.08	A	25.45	0.83	A	15.65	0.59	A	141.32	1.42	D
	2 mm	A1	62.01	0.22	D	−0.97	0.10	E	2.69	0.19	G	4.74	0.23	E	105.25	2.52	E
		A2	60.15	0.32	F	−0.93	0.10	E	5.91	0.22	F	5.05	0.26	E	84.81	1.96	F
		A3	60.95	0.22	E	−1.24	0.04	F	10.25	0.05	D	5.34	0.10	E	60.90	1.59	G
		A3.5	58.40	0.43	G	−0.97	0.15	E	16.97	0.68	B	5.26	0.27	E	32.23	1.35	H
F2	1 mm	A1	63.97	0.36	A	−0.93	0.38	F	6.59	0.17	F	12.68	0.52	D	368.65	4.47	A
		A2	62.32	0.54	B	−0.25	0.11	E	13.98	1.12	C	15.41	0.51	B	312.23	4.98	B
		A3	61.28	0.27	B	1.20	0.08	C	15.55	0.11	B	14.54	0.21	C	276.27	4.19	D
		A3.5	60.07	0.62	C	2.42	0.09	A	16.79	0.27	A	16.62	0.47	A	296.26	4.23	C
	2 mm	A1	58.08	0.89	D	−1.67	0.08	G	2.83	0.17	G	5.02	0.24	G	193.89	8.22	E
		A2	54.27	0.51	E	−0.80	0.10	F	9.24	0.24	E	6.17	0.46	EF	143.15	4.66	F
		A3	54.55	0.81	E	0.48	0.13	D	9.73	0.39	DE	5.52	0.34	FG	116.11	5.49	G
		A3.5	52.41	0.68	F	1.60	0.14	B	10.46	0.55	D	6.49	0.31	E	125.83	5.09	G
F3	1 mm	A1	66.66	0.46	A	−1.03	0.06	F	6.99	0.26	E	12.64	0.41	B	384.86	11.61	A
		A2	66.28	0.40	A	−0.40	0.04	D	11.23	0.28	C	13.34	0.53	B	336.16	3.31	B
		A3	62.90	0.74	B	−0.02	0.06	C	13.30	0.33	B	12.78	0.50	B	288.12	8.87	C
		A3.5	60.76	0.62	C	0.69	0.05	A	15.68	0.23	A	14.26	0.64	A	271.23	4.69	D
	2 mm	A1	60.34	0.41	CD	−1.46	0.09	G	3.65	0.12	F	4.90	0.17	D	189.09	6.38	E
		A2	59.42	0.23	D	−0.83	0.06	E	7.44	0.18	E	5.14	0.20	D	146.14	5.34	F
		A3	57.00	0.58	E	−0.49	0.31	D	8.64	0.88	D	4.95	0.37	D	112.81	5.97	G
		A3.5	54.41	0.51	F	0.30	0.06	B	10.85	0.08	C	6.25	0.22	C	121.26	3.89	G

Table 3: *L*, a*, b*, TP, and I_{max} Values of Each Shade of the Resin-Based Composites[a] (cont.)*

Code	Thickness	Shade	L*			a*			b*			TP			I_{max}		
			Mean	SD		Mean	SD		Mean	SD		Mean	SD		Mean	SD	
GD	1 mm	A1	68.68	0.34	A	0.36	0.11	E	7.14	0.31	F	14.59	0.44	C	417.72	6.90	A
		A2	66.18	0.23	B	1.49	0.08	B	11.36	0.20	D	16.77	0.37	B	377.58	4.61	B
		A3	65.43	0.81	B	1.10	0.13	C	14.95	0.24	B	18.19	0.64	A	346.75	5.56	C
		A3.5	64.36	0.49	C	1.82	0.08	A	17.82	0.22	A	18.18	0.44	A	288.12	2.72	D
	2 mm	A1	61.81	0.48	D	−0.17	0.12	F	4.34	0.23	G	6.07	0.30	F	176.24	2.60	E
		A2	58.89	0.43	E	0.94	0.10	C	7.00	0.33	F	6.60	0.39	EF	161.12	1.47	F
		A3	57.27	0.45	F	0.70	0.06	D	10.29	0.25	E	7.70	0.40	D	140.48	3.26	G
		A3.5	56.30	0.27	G	1.34	0.13	B	11.95	0.28	C	7.30	0.22	DE	106.86	1.98	H
HC	1 mm	A1	67.37	0.71	A	−0.86	0.10	E	8.13	0.38	D	15.98	0.50	A	359.41	3.53	A
		A2	67.18	0.31	A	0.24	0.07	C	10.39	0.18	C	16.22	0.26	A	342.48	1.67	B
		A3	63.97	0.35	B	0.59	0.11	B	12.07	0.29	B	14.74	0.44	B	266.05	3.77	C
		A3.5	63.35	0.52	B	1.80	0.08	A	15.53	0.46	A	14.56	0.42	B	229.70	5.69	D
	2 mm	A1	59.91	0.54	C	−1.55	0.08	F	3.54	0.35	F	6.29	0.30	C	177.31	4.24	E
		A2	59.91	0.48	C	−0.44	0.14	D	5.30	0.25	E	6.28	0.40	C	154.25	4.84	F
		A3	57.03	0.53	D	−0.40	0.34	D	5.54	1.17	E	4.71	0.18	D	89.12	1.33	G
		A3.5	56.92	0.37	D	0.55	0.11	B	8.39	0.26	D	4.45	0.41	D	67.68	2.79	H
TC	1 mm	A1	64.69	0.59	A	0.47	0.17	B	3.94	0.25	E	14.77	0.19	C	409.27	4.88	A
		A2	63.23	0.41	BC	1.23	0.09	A	8.43	0.17	C	15.59	0.44	B	358.76	3.20	B
		A3	62.60	0.49	BC	0.51	0.14	B	10.71	0.20	B	14.92	0.39	BC	314.84	4.13	C
		A3.5	61.74	0.63	C	1.09	0.13	A	16.04	0.54	A	16.63	0.57	A	273.74	4.57	D
	2 mm	A1	57.05	0.43	D	−0.70	0.05	D	1.23	0.31	F	5.99	0.35	E	199.25	4.38	E
		A2	55.96	0.42	E	0.46	0.14	B	4.35	0.20	E	6.26	0.42	DE	172.45	5.25	F
		A3	55.80	0.65	E	−0.22	0.10	C	6.43	0.32	D	6.12	0.37	DE	141.74	2.88	G
		A3.5	54.08	0.34	F	0.54	0.07	B	10.74	0.52	B	6.80	0.36	D	107.55	3.97	H

[a] *Different letters denote significant differences among the specimens within each resin-based composite product* ($p<0.05$).

between the A1 and A2, A2 and A3, and A3 and A3.5 shades ($\Delta E<3.3$). The greatest color difference was observed between the A1 and A3.5 shades of the EX product ($\Delta E=14.73$).

Translucency

The translucency properties varied depending on the RBC product line. The TP values of BF and ES samples were similar for all four shades. In addition, the HC line showed TP values confined within a narrow range, even though there were significant differences between A1/A2 and A3/A3.5. On the contrary, CX, F3, GD, and TC samples showed equal or higher TP values for higher shade numbers. For the EX and F2 samples, the TP values increased according to A1 < A3 < A2 < A3.5, ie, no correlation. The correlations between the translucency and the shade were the same for both the 1-mm and the 2-mm specimens, where the 1-mm specimens showed higher TP values than the 2-mm specimens for every RBC product line (Table 3; Figure 3).

Unlike the TP value, I_{max} decreased when the shade number increased for all nine RBC products except the 1-mm F2 specimen, which showed a higher I_{max} value for the A3.5 shade compared to the A3 shade (Table 3; Figure 3).

The ΔTP values of the different shades also differed with respect to the product line. For the 1-mm specimens, the BF, ES, EX, F3, HC, and TC samples showed a maximum ΔTP less than 2.0, which is regarded as clinically unperceivable. The CX samples showed a maximum ΔTP of 2.3 between the A1 and A3.5 shades. The F2 and GD product lines showed relatively clear differences in TP among the shades, where the maximum ΔTP was more than 3.5. For the 2-mm specimens, none of the RBC products showed a perceivable ΔTP among the shades (Table 4; Figure 3).

DISCUSSION

In the present study, the color and translucency of four different shades (A1, A2, A3, and A3.5) of nine RBC products were compared within each product

Table 4: *ΔE and ΔTP Among the Four Shades of Each Resin-Based Composite*[a]

Code	Thickness	1 mm				2 mm			
	Shade	A1	A2	A3	A3.5	A1	A2	A3	A3.5
BF	A1		0.90[b]	5.85	10.34		1.40[b]	4.58	8.25
	A2	*0.19*		5.45	9.79	*0.07*		4.11	7.37
	A3	*0.55*	*0.75*		4.94	*0.59*	*0.65*		4.20
	A3.5	*1.61*	*1.80*	*1.06*		*0.97*	*1.03*	*0.38*	
CX	A1		4.00	7.26	11.96		4.32	9.02	12.94
	A2	*0.49*		3.27[b]	8.10	*0.10*		4.76	8.70
	A3	*1.89*	*1.40*		4.94	*0.42*	*0.31*		4.55
	A3.5	*2.23*[c]	*1.74*	*0.35*		*1.29*	*1.18*	*0.87*	
ES	A1		4.98	9.28	11.11		3.31	6.70	8.32
	A2	*0.02*		4.45	6.18	*0.27*		3.55	5.05
	A3	*1.17*	*1.19*		2.86[b]	*0.71*	*0.44*		2.75[b]
	A3.5	*0.75*	*0.77*	*0.42*		*0.30*	*0.03*	*0.41*	
EX	A1		4.70	8.46	17.68		3.71	7.63	14.73
	A2	*1.76*		3.83	12.98	*0.31*		4.42	11.20
	A3	*0.78*	*0.98*		9.34	*0.61*	*0.29*		7.20
	A3.5	*1.78*	*0.02*	*1.01*		*0.53*	*0.21*	*0.08*	
F2	A1		7.61	9.59	11.42		7.51	8.04	10.06
	A2	*2.74*[c]		2.37[b]	4.48	*1.15*		1.39[b]	3.27[b]
	A3	*1.87*	*0.87*		2.12[b]	*0.50*	*0.65*		2.53[b]
	A3.5	*3.95*[c]	*1.21*	*2.08*[c]		*1.48*	*0.32*	*0.97*	
F3	A1		4.31	7.42	10.64		3.95	6.08	9.49
	A2	*0.70*		3.98	7.17	*0.24*		2.72[b]	6.17
	A3	*0.14*	*0.56*		3.27[b]	*0.06*	*0.18*		3.49
	A3.5	*1.62*	*0.92*	*1.48*		*1.36*	*1.12*	*1.30*	
GD	A1		5.03	8.49	11.61		4.11	7.54	9.52
	A2	*2.18*[c]		3.69	6.72	*0.54*		3.68	5.60
	A3	*3.60*[c]	*1.42*		3.15[b]	*1.63*	*1.10*		2.02[b]
	A3.5	*3.59*[c]	*1.41*	*0.01*		*1.23*	*0.70*	*0.40*	
HC	A1		2.52[b]	5.40	8.83		2.09[b]	3.69	6.08
	A2	*0.23*		3.64	6.60	*0.02*		2.89[b]	4.41
	A3	*1.25*	*1.48*		3.71	*1.58*	*1.57*		3.01[b]
	A3.5	*1.42*	*1.66*	*0.18*		*1.85*	*1.83*	*0.26*	
TC	A1		4.78	7.08	12.47		3.51	5.37	10.04
	A2	*0.83*		2.47[b]	7.75	*0.27*		2.20[b]	6.66
	A3	*0.15*	*0.68*		5.43	*0.13*	*0.14*		4.70
	A3.5	*1.86*	*1.04*	*1.71*		*0.81*	*0.54*	*0.68*	

[a] *Values in roman text indicate ΔE between the shades. Values in italic text indicate ΔTP between the shades.*
[b] *Color difference that is clinically unperceivable (ΔE<3.3).*
[c] *Translucency difference that is clinically perceivable (ΔTP≥2.0).*

line. The A shade was selected according to Paravina and others,[25] who reported that most human teeth match the A shade of the VITA classical shade system. Although there have been a number of studies that evaluated the color and translucency of RBCs,[7-14] only few studies analyzed different shades of various RBC products in numerical order. In this regard, the results of this study are expected to provide relevant information for the clinical use of contemporary RBC products.

There were significant differences in L*, a*, and b* values among the different shades of each RBC product line (Table 3; Figure 3). The L* values of the specimens tended to decrease as the shade number increased, which is consistent with the shade number indicating the lightness of the material. In

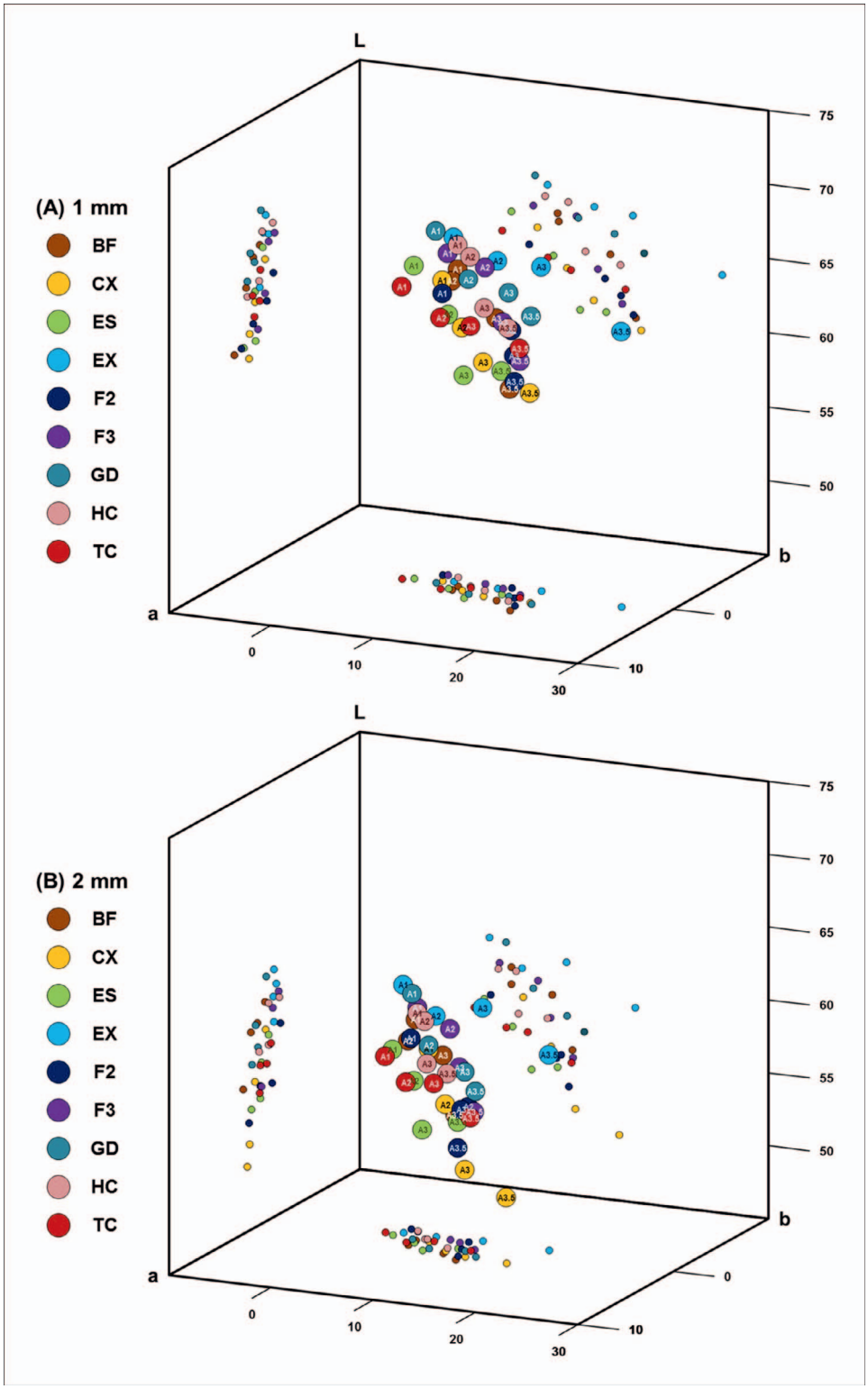

Figure 4. *The color distribution of each shade of the RBC products in the CIELAB color space. (A): 1-mm specimens. (B): 2-mm specimens.*

the CIELAB color space, as the a* and b* values increase, the chroma of the color increases. In this study, the RBCs showed various patterns of color distribution with respect to the shade and product line. This implies that the shade number includes information about the hue and chroma in addition to the lightness, consistent with the VITA classical shade system.[26] Overall, the a* values did not vary

much among the shades, whereas the b* values covered a relatively wide range and gradually increased with increasing shade number. From these results, it is concluded that the RBC becomes darker and yellowish when the shade number increases.

When the thickness of the specimen increased from 1 mm to 2 mm, the L* and b* values decreased significantly, whereas the a* values were either unchanged or slightly increased for all products (Table 3; Figure 3). In other words, the RBCs became darker and bluish when they were thicker. Therefore, for the restoration of a deep cavity, layering the RBC using a slightly lighter-colored material could be a way of avoiding it from looking dark. When the restoration is thought to be slightly lighter than the adjacent tooth structure in the final layering step near the surface layer, we can use a higher shade number to reduce the lightness and increase the yellowish hue.

The TP and I_{max} values were measured separately for evaluating the translucency considering two different aspects: esthetics and polymerization. Both TP and I_{max} differed significantly among the shade numbers within each RBC product investigated in this study (Table 3; Figure 3). The I_{max} decreased with increasing shade number for all RBC product lines, whereas the TP did not always follow the order of the shade number. This implies that a specimen with a higher shade number may need a longer light curing time for complete polymerization; however, it may not be directly related to the overall translucency of the specimen. The blue light irradiance is thought to be influenced mainly by the L* and b* values of the specimen, which make it consistently darker and yellowish when the shade number increases.

The BF, ES, and HC product lines showed almost no differences in TP values among the shades despite distinguishable color differences. Hence, restorations using these products would have similar translucency regardless of the shade within the same product line. Although the constant translucency may be convenient and predictable for clinicians, we should consider the additional use of either translucent or opaque composites to reproduce a varied translucency in a natural tooth. In CX, F3, GD, and TC samples, the TP values increased with increasing shade number. For these products, light restorations would appear to be more opaque than dark restorations. When we use the A1 or A2 shades of these RBCs, especially in anterior regions, we need to accompany it with a translucent shade to obtain proper translucency of the restoration. The EX and F2 samples showed no correlation between the TP and shade number (A1<A3<A2<A3.5); hence, these products should be used with caution.

Several authors have investigated the effect of the matrix and fillers on the color and translucency of RBCs, such as the composition and distribution of the matrix and fillers,[27-30] size and shape of filler particles,[19,31] and refractive indices (RIs).[32,33] The amount of Bis-GMA in the matrix had a significant effect on the translucency of RBCs,[27] and the translucency of Bis-GMA–based RBCs were much higher than TEGDMA/UDMA-based RBCs.[28] The translucency was shown to decrease as the amount of filler increased.[29] The lightness was highly correlated with the amount of filler, whereas the hue and chroma were only moderately affected.[30] The translucency decreased with a greater mismatch between the RIs of the matrix and filler, as light is scattered at the matrix-filler interfaces when it passes through the RBCs.[32] Ota and others[33] reported that the L* and a* values increased and TP decreased with increasing RI mismatch. The development of filler technology makes it possible to produce higher-translucency RBC materials; nano-sized (smaller than 100 nm) filler particles do not scatter light, as they are below the wavelength range of visible light (380 to 780 nm).[34] In addition to the effect of the matrix and fillers, the color and translucency of RBCs also depend on additives such as dyes and other chemicals.[35] Small amounts of inorganic oxides are often added to change the color and opacity of RBCs.[36] The coloring material or pigments absorb various wavelengths of visible light, allowing other wavelengths to scatter out of the object.[6] When many internal particles are present in the RBCs, the light is likely to be scattered and the translucency decreased.[15] White or high-lightness gray pigments can be used to increase the lightness while reducing the translucency.[37]

The exact reason for the different translucency behavior among the products is uncertain; as the RBCs were compared within the same product line, all compositions were probably very similar. The optical properties of RBCs may depend on the specific manufacturing process, which is confidential information. Nevertheless, it is worth noting that the RBC products with similar characteristics showed comparable translucency trends. The BF and HC products include unique large fillers, prereacted glass ionomer and prepolymerized fillers, respectively. The ES materials have relatively uniform filler shapes and sizes and spherical fillers

with a size of 0.1 to 0.3 μm. The CX, EX, F2, F3, GD, and TC products contain small hybrid filler particles.

In this study, we used $\Delta E \geq 3.3$ as a threshold for clinically visible color changes.[23] We observed that some specimens demonstrated ΔE values less than 3.3, even though they demonstrated significant differences in either L*, a*, or b*. In particular, between the A1 and A2 shades of BF and HC, between the A2 and A3 shades of F2 and TC, and between the A3 and A3.5 shades of ES, F2, and GD, there were no perceivable differences in TP regardless of thickness; these shades could be used without differentiation in clinics. A perception threshold for ΔTP has only recently been suggested; Lee[24] proposed a ΔTP value of 2.0 as the perception threshold of translucency, and this was applied in the present study. However, this was calculated based only on the threshold of the contrast ratio.[38] Further investigations should be carried out regarding the clinically perceivable difference of translucency.

Although color and translucency of natural teeth should be the reference for restorative materials, little information is available regarding the optical properties of human teeth. The enamel and dentin layers have natural variations among individuals, tooth types, and sites on particular teeth. Hasegawa and others[39] evaluated the color and translucency of human central incisors and found that the a* and b* values of natural teeth tended to increase from incisal to cervical, whereas the lightness and translucency decreased. Yu and others[40] reported that the mean TPs of 1-mm human enamel and dentin were 18.7 and 16.4, respectively, using a spectrophotometer. They also mentioned that enamel showed lower a* and b* values than dentin, which means dentin is more reddish and yellowish in color. Pop-Ciutrila and others[41] evaluated the color and translucency of 2-mm specimens of human dentin. The mean TP of dentin specimens from anterior teeth was 6.85 as measured using a spectrophotometer. In our study, the TP of 1-mm specimens of RBC ranged from 11.45 (A1 shade of CX) to 18.19 (A3 shade of GD) and that of 2-mm specimens ranged from 4.37 (A1 shade of CX) to 7.70 (A3 shade of GD). Even though the data from different studies are not directly comparable due to differences in measuring instruments and methods, we can assume that the translucency of currently used RBCs is appropriate for replacing natural tooth structures. A recent case report showed that highly acceptable esthetic results could be obtained clinically by combining two body shades, without the use of opaque or translucent RBCs.[42]

The color and translucency of teeth changes during aging.[43] Over time, the enamel gets thinner due to abrasion, and the dentin becomes thicker by lifelong deposition and shrinkage of pulp. This makes the overall color tone of a tooth yellowish. Meanwhile, dentin sclerosis proceeds inside the dentinal tubules, which makes dentin become more homogeneous.[44] In this respect, for the restorative treatment of relatively old patients, it seems to be reasonable to use a single shade of an RBC product whose translucency increases with higher shade numbers. However, from a different viewpoint, the opposite also could be reasonable. For example, when restoring a large anterior class IV cavity, clinicians may use the layering technique (a dark opaque shade for the inner dentin layer and a light transparent shade for the outer enamel layer). In this situation, it could be more favorable if the translucency is inversely proportional to the shade number.

Yu and Lee[45] reported that the stability of the optical properties of RBCs varied depending on their type, brand, and shade. Considering the long-term clinical aspects that the restoration is exposed directly to the oral environment and the material undergoes aging, the long-term stability of the color and translucency of RBCs is another important aspect to be considered. Further research related to the stability of RBC products should be undertaken.

The optical properties of RBCs are the result of complicated interactions of various factors, and detailed knowledge is still lacking. For predictable clinical applications, further detailed investigations should be performed considering the color and optical properties of the RBCs as well as their stability considering the light source, surface morphology, background color, and storage medium and period. When clinicians perform restorative treatments with high esthetic demands, such as anterior class III or IV lesions, they should be aware of the color and translucency characteristics of the individual RBC product in order to successfully reproduce the appearance of natural teeth. The combination of layers with different shade and translucency values could be considered for this purpose, which would provide more possibilities if several types of RBC products were prepared in the clinic.

CONCLUSIONS

Within the limitations of this study, we observed significant differences in the color and translucency among the different shade numbers within each RBC product line. Overall, the RBCs became darker

and yellowish as the shade number increased. The variations in the translucency were not correlated with the order of the shade numbers. On the contrary, the blue light transmittance consistently decreased with increasing shade numbers for all RBC types.

Acknowledgments

This research was supported by a grant of the Korea Health Technology R&D Project through the Korea Health Industry Development Institute (KHIDI), funded by the Ministry of Health & Welfare, Republic of Korea (grant number: HI17C1719).
The authors thank 3M Korea, Dentsply Sirona Korea, Ivoclar Vivadent Korea, Midong, and Shinhung for providing the materials for this research.

Conflict of Interest

The authors of this article certify that they have no proprietary, financial, or other personal interest of any nature or kind in any product, service, and/or company that is presented in this article.

(Accepted 14 October 2017)

REFERENCES

1. Munsell AH (1905) *A Color Notation* GH Ellis Company.
2. Browning WD, Contreras-Bulnes R, Brackett MG, & Brackett WW (2009) Color differences: Polymerized composite and corresponding Vitapan Classical shade tab *Journal of Dentistry* **37(Supplement 1)** e34-e39.
3. Terry DA, Geller W, Tric O, Anderson MJ, Tourville M, & Kobashigawa A (2002) Anatomical form defines color: Function, form, and aesthetics *Practical Procedures and Aesthetic Dentistry* **14(1)** 59-67; quiz 68.
4. Winter R (1993) Visualizing the natural dentition *Journal of Esthetic Dentistry* **5(3)** 102-117.
5. Johnston WM, Ma T, & Kienle BH (1995) Translucency parameter of colorants for maxillofacial prostheses *International Journal of Prosthodontics* **8(1)** 79-86.
6. Lee YK (2007) Influence of scattering/absorption characteristics on the color of resin composites *Dental Materials* **23(1)** 124-131.
7. Ryan EA, Tam LE, & McComb D (2010) Comparative translucency of esthetic composite resin restorative materials *Journal of the Canadian Dental Association* **76** a84.
8. Kim DH, & Park SH (2013) Evaluation of resin composite translucency by two different methods *Operative Dentistry* **38(3)** E1-E15.
9. Yu B, & Lee YK (2008) Translucency of varied brand and shade of resin composites *American Journal of Dentistry* **21(4)** 229-232.
10. Kim SJ, Son HH, Cho BH, Lee IB, & Um CM (2009) Translucency and masking ability of various opaque-shade composite resins *Journal of Dentistry* **37(2)** 102-107.
11. Mikhail SS, Schricker SR, Azer SS, Brantley WA, & Johnston WM (2013) Optical characteristics of contemporary dental composite resin materials *Journal of Dentistry* **41(9)** 771-778.
12. Perez MM, Ghinea R, Ugarte-Alvan LI, Pulgar R, & Paravina RD (2010) Color and translucency in siloranebased resin composite compared to universal and nanofilled composites *Journal of Dentistry* **38(Supplement 2)** e110-e116.
13. Schmeling M, DE Andrada MA, Maia HP, & DE Araujo EM (2012) Translucency of value resin composites used to replace enamel in stratified composite restoration techniques *Journal of Esthetic and Restorative Dentistry* **24(1)** 53-58.
14. Pecho OE, Ghinea R, do Amaral EA, Cardona JC, Della Bona A, & Perez MM (2016) Relevant optical properties for direct restorative materials *Dental Materials* **32(5)** e105-e112.
15. Yu B, & Lee YK (2008) Influence of color parameters of resin composites on their translucency *Dental Materials* **24(9)** 1236-1242.
16. Calheiros FC, Daronch M, Rueggeberg FA, & Braga RR (2008) Influence of irradiant energy on degree of conversion, polymerization rate and shrinkage stress in an experimental resin composite system *Dental Materials* **24(9)** 1164-1168.
17. Stansbury JW (2000) Curing dental resins and composites by photopolymerization *Journal of Esthetic Dentistry* **12(6)** 300-308.
18. Bucuta S, & Ilie N (2014) Light transmittance and micromechanical properties of bulk fill vs. conventional resin based composites *Clinical Oral Investigations* **18(8)** 1991-2000.
19. dos Santos GB, Alto RV, Filho HR, da Silva EM, & Fellows CE (2008) Light transmission on dental resin composites *Dental Materials* **24(5)** 571-576.
20. Masotti AS, Onofrio AB, Conceicao EN, & Spohr AM (2007) UV-vis spectrophotometric direct transmittance analysis of composite resins *Dental Materials* **23(6)** 724-730.
21. International Organization for Standardization (2009) ISO 4049 Dentistry—Polymer-based restorative materials Geneva: International Organization for Standardization.
22. Commission Internationale de l'Eclairage (2004) *Colorimetry: Technical Report* Central Bureau of the CIE, Vienna.
23. Ruyter IE, Nilner K, & Moller B (1987) Color stability of dental composite resin materials for crown and bridge veneers *Dental Materials* **3(5)** 246-251.
24. Lee YK (2016) Criteria for clinical translucency evaluation of direct esthetic restorative materials *Restorative Dentistry and Endodontics* **41(3)** 159-166.
25. Paravina RD, Majkic G, Imai FH, & Powers JM (2007) Optimization of tooth color and shade guide design *Journal of Prosthodontics* **16(4)** 269-276.
26. Paravina RD, Powers JM, & Fay RM (2002) Color comparison of two shade guides *International Journal of Prosthodontics* **15(1)** 73-78.

27. Azzopardi N, Moharamzadeh K, Wood DJ, Martin N, & van Noort R (2009) Effect of resin matrix composition on the translucency of experimental dental composite resins *Dental Materials* **25(12)** 1564-1568.

28. Manojlovic D, Dramicanin MD, Lezaja M, Pongprueksa P, Van Meerbeek B, & Miletic V (2016) Effect of resin and photoinitiator on color, translucency and color stability of conventional and low-shrinkage model composites *Dental Materials* **32(2)** 183-191.

29. Lee YK (2008) Influence of filler on the difference between the transmitted and reflected colors of experimental resin composites *Dental Materials* **24(9)** 1243-1247.

30. Lim YK, Lee YK, Lim BS, Rhee SH, & Yang HC (2008) Influence of filler distribution on the color parameters of experimental resin composites *Dental Materials* **24(1)** 67-73.

31. Arikawa H, Kanie T, Fujii K, Takahashi H, & Ban S (2007) Effect of filler properties in composite resins on light transmittance characteristics and color *Dental Materials Journal* **26(1)** 38-44.

32. Shortall AC, Palin WM, & Burtscher P (2008) Refractive index mismatch and monomer reactivity influence composite curing depth *Journal of Dental Research* **87(1)** 84-88.

33. Ota M, Ando S, Endo H, Ogura Y, Miyazaki M, & Hosoya Y (2012) Influence of refractive index on optical parameters of experimental resin composites *Acta Odontologica Scandinavica* **70(5)** 362-367.

34. Mitra SB, Wu D, & Holmes BN (2003) An application of nanotechnology in advanced dental materials *Journal of the American Dental Association* **134(10)** 1382-1390.

35. Johnston WM, & Reisbick MH (1997) Color and translucency changes during and after curing of esthetic restorative materials *Dental Materials* **13(2)** 89-97.

36. Klapdohr S, & Moszner N (2005) New inorganic components for dental filling composites *Monatshefte für Chemie* **136(1)** 21-45.

37. Miller L (1987) Organizing color in dentistry *Journal of the American Dental Association* **Special No** 26E-40E.

38. Liu MC, Aquilino SA, Lund PS, Vargas MA, Diaz-Arnold AM, Gratton DG, & Qian F (2010) Human perception of dental porcelain translucency correlated to spectrophotometric measurements *Journal of Prosthodontics* **19(3)** 187-193.

39. Hasegawa A, Ikeda I, & Kawaguchi S (2000) Color and translucency of in vivo natural central incisors *Journal of Prosthetic Dentistry* **83(4)** 418-423.

40. Yu B, Ahn JS, & Lee YK (2009) Measurement of translucency of tooth enamel and dentin *Acta Odontologica Scandinavica* **67(1)** 57-64.

41. Pop-Ciutrila IS, Ghinea R, Colosi HA, & Dudea D (2016) Dentin translucency and color evaluation in human incisors, canines, and molars *Journal of Prosthetic Dentistry* **115(4)** 475-481.

42. Romero MF, Haddock FJ, Freites AG, Brackett WW, & Brackett MG (2016) Restorative technique selection in class IV direct composite restorations: A simplified method *Operative Dentistry* **41(3)** 243-248.

43. Goodkind RJ, & Schwabacher WB (1987) Use of a fiber-optic colorimeter for in vivo color measurements of 2830 anterior teeth *Journal of Prosthetic Dentistry* **58(5)** 535-542.

44. Vasiliadis L, Darling AI, & Levers BG (1983) The histology of sclerotic human root dentine *Archives of Oral Biology* **28(8)** 693-700.

45. Yu B, & Lee YK (2013) Comparison of stabilities in translucency, fluorescence and opalescence of direct and indirect composite resins *European Journal of Esthetic Dentistry* **8(2)** 214-225.

©Operative Dentistry, 2018, **43-6,** 656-664

Influence of Shrinkage and Viscosity of Flowable Composite Liners on Cervical Microleakage of Class II Restorations: A Micro-CT Analysis

J Nie • AU Yap • XY Wang

Clinical Relevance

Interfacial integrity of Class II restorations is improved by the use of flowable composite liners, particularly those with low filler content. Giomer restorations had significantly less microleakage than those restored with nano-filled composites.

SUMMARY

This study determined the influence of shrinkage and viscosity of flowable composite liners on the cervical microleakage of Class II restorations using micro-CT. Seven composites of varying viscosities were selected and included five giomers (Shofu Beautifil II [BF], Flow Plus F00 and F03 [F00 and F03], Flow F02 and F10 [F02 and F10]) and 2 nano-filled composites (3M-ESPE Filtek Z350 [Z350] and Filtek Z350 Flowable [Z350F]). Polymerization shrinkage (n=7) was assessed with the Acuvol volumetric shrinkage analyzer while complex viscosity was determined with the advanced rheometric expansion system at 25°C. Standardized Class II restorations incorporating 1-mm horizontal layers of different flowable liners and 3-mm oblique layers of BF or Z350 were subjected to a silver nitrate test for 24 hours and examined using micro-CT. Microleakage was determined at 0.1-mm intervals from the buccal to lingual surfaces providing 30 sites per specimen and scored accordingly. Statistical analysis was performed with the one-way ANOVA, Kruskal-Wallis test, and Spearman's rho correlation at a significance level of $p<0.05$. Mean volumetric shrinkage ranged from 5.33±0.17% to 2.35±0.02% for F02 to Z350, respectively. The flowable materials had significantly higher shrinkage than did their sculptable counterparts (BF and Z350). Complex viscosities

Jie Nie, BDS, MD, Cariology and Endodontology, Peking University School and Hospital of Stomatology, Beijing, 100081 China

Adrian Ujin Yap, BDS, MSc, PhD, Grad Dip Psychotherapy, Department of Dentistry, Ng Teng Fong General Hospital, National University Health System, Faculty of Dentistry, National University of Singapore, Singapore 609606

*Xiao-Yan Wang, BDS, MD, PhD, Department of Cariology and Endodontology, Peking University School and Hospital of Stomatology, Beijing, China

*Corresponding author: 22 Zhongguancun Avenue South, Haidian District, Beijing, 100081 China; e-mail: wangxiaoyan@pkuss.bjmu.edu.cn

DOI: 10.2341/17-091-L

ranged from 9.65 to 4.20 (Z350 and F10, respectively) at a frequency of 10 rad/s and from 8.16 to 3.28 (Z350 and F03, respectively) for 100 rad/s. Giomer restorations had significantly less leakage than did those restored with nano-filled composites. No microleakage was observed with restorations lined with F02 or F10. The use of flowable liners reduced cervical microleakage of Class II restorations. Interfacial integrity of Class II restorations was significantly correlated with liner viscosity, filler volume, and shrinkage.

INTRODUCTION

Flowable composites were introduced in the mid-1990s.[1] They were developed to simplify placement procedures, enhance adaption to the internal surfaces of cavity preparations, improve cavity seal, and expand the clinical applications of resin-based composites. To decrease viscosity and increase flowability, filler loading of flowable composites was substantially reduced. Filler volume of flowable composites ranged from 37% to 53% compared with 50% to 70% of sculptable composite. While this allows flowable materials to be dispensed through fine-gauge needles, the higher resin content results in reduced strength, wear resistance, rigidity, and increased polymerization shrinkage.[2] Polymerization shrinkage stress at the tooth-restoration interface can lead to enamel fractures, interfacial debonding, and microleakage.[3,4] Microleakage may well cause marginal staining, postoperative sensitivity, secondary caries, pulpal pathology, and restoration failure.[5]

Flowable composite liners have been advocated as the first increment at the cervical or gingival floor of Class II restorations. They adapt well to microstructural irregularities of cavity preparations preceding sculptable composite placement. Several studies have reported a trend toward decreased microleakage in teeth restored with this technique.[6-8] In addition, a thinner layer of flowable composite liner appears to provide better marginal seal and adaptation and fewer voids.[9-11] Nevertheless, microleakage data from other authors do not support the use of flowable composite liners.[12]

This incongruity can be attributed somewhat to the fact that flowable composites are not a homogeneous group of materials. They vary significantly in terms of formulation, handling, and viscosity due to differences in resin and filler compositions. When resin content increases, flowability and shrinkage stress is higher, while elastic modulus is reduced.[13] The reduced material rigidity together with enhanced cavity adaption may mitigate the greater shrinkage stress accompanying the lower filler-volume fractions of flowable composites.

While studies have investigated the influence of polymerization shrinkage on microleakage of dental composites,[14-16] little is known about the impact of flowable composite viscosity on cervical microleakage. Nor has the efficacy of flowable giomers as liners been established. Giomers, offered in a wide range of viscosities, are based on prereacted glass ionomer (PRG) technology in which acid-reactive fluorosilicate glass is reacted with polyacids in the presence of water, freeze-dried, milled, silanized, ground, and used as fillers. The objectives of this study were to determine the influence of shrinkage and viscosity of flowable composite liners on the cervical microleakage of Class II restorations using micro-CT. The relationships between polymerization shrinkage, viscosity, and microleakage were also established. The null hypotheses were as follows: 1) polymerization shrinkage and viscosity of flowable composite liners do not affect the cervical microleakage of Class II restorations and 2) there are no correlations between shrinkage, viscosity, and microleakage.

METHODS AND MATERIALS

Seven composite materials of varying viscosities were selected for this study including one sculptable giomer (Beautifil II [BF]) and four flowable giomers (Beautifil Flow Plus F00 [F00], Beautifil Flow Plus F03 [F03], Beautifil Flow F02 [F02], and Beautifil Flow F10 [F10]) in addition to a sculptable composite (Filtek Z350 [Z350]) and a flowable nano-filled composite (Filtek Z350 Flowable [Z350F]). The composite materials were used in conjunction with their corresponding conditioning/adhesive systems. The technical profiles of the materials evaluated are listed in Table 1. Information pertaining to material composition and filler volume were supplied by the manufacturers.

Volumetric Polymerization Shrinkage

The volumetic shrinkage of the composites was determined with the Acuvol volumetric shrinkage analyzer (X-81100P, Bisco, Schaumburg, IL, USA) at 25°C using the single-view mode. Seven specimens of each composite (n=7) were fabricated and tested. Flowable materials were syringed onto the Teflon pedestal and shaped into a hemisphere; sculptable materials were rolled into a ball and placed on the pedestal. The specimens were allowed to stand for 5

Table 1: *Technical Profiles of the Various Materials Evaluated*

Materials	Batch Number	Composition	Filler Volume (%)
Beautifil Flow Plus F00 (F00)	091013	Bis-GMA[a] TEGDMA Aluminofluoro-borosilicate glass Al_2O_3, DL-camphorquinone	47.0
Beautifil Flow F02 (F02)	041156	Bis-GMA TEGDMA Aluminofluoro-borosilicate glass Al_2O_3, DL-camphorquinone	34.6
Beautifil Flow Plus F03 (F03)	041004	Bis-GMA TEGDMA Aluminofluoro-borosilicate glass Al_2O_3, DL-camphorquinone	46.3
Beautifil Flow F10 (F10)	041125	Bis-GMA TEGDMA Aluminofluoro-borosilicate glass Al_2O_3, DL-camphorquinone	33.3
Beautifil II (BF)	061139	Bis-GMA TEGDMA Aluminofluoro-borosilicate glass Al_2O_3, DL-camphorquinone	68.6
Filtek Z350 Flowable (Z350F)	N313982	Bis-GMA TEGDMA Bis-EMA Zirconia/silica filler	55.0
Filtek Z350 (Z350)	N142553	Bis-GMA TEGDMA Bis-EMA UDMA Zirconia/silica filler	59.5

[a] Bis-GMA, bisphenylglycidyl dimethacrylate; TEGDMA, triethylenglycol dimethacrylate; Bis-EMA, bisphenol A ethoxylated dimethacrylate; UDMA, urethanedimethacrylate.

minutes before the initial precure volume (V1) was recorded. The specimens were then cured for 20 seconds using a LED curing light with an intensity of 500 mW/cm^2 (Bluphase, Ivoclar Vivadent, Shaan, Liechtenstein). The light cure tip was positioned 1 mm above the top of the specimens. Postcure volume (V2) was recorded 2 minutes after removal of the light source. The volumetric polymerization shrinkage of the materials was calculated according to the equation: polymerization shrinkage = (V1–V2)/V1×100%. Shrinkage data was subjected to normality testing with the Kolmogorov-Smirnov test. As data was normally distributed, it was consequently analyzed using the one-way ANOVA/LSD post hoc test at a significance level of α=0.05. Correlation between filler volume and shrinkage was analyzed using Pearson's correlation test (2-tailed, α=0.05).

Viscosity

Viscosity measurements were performed using an Advanced Rheometric Expansion System (ARES, TA Instruments, New Castle, DE, USA) at a temperature of 25°C. The parallel plates viscometer module with a diameter of 25 mm was utilized to determine the viscosity of the composites. The gap between the plates was set at 1 mm. Strain sweep tests were performed to check the range of uniform output signals to ensure that all measurements were carried out within the linear limit of each material's deformation. A time sweep test was then conducted to destroy the internal structure of the specimens and to reveal any potential thixotropic behavior. A frequency sweep test was subsequently performed from 0.01 to 100 rad/s to determine the variation of the complex viscosity (η^*) as a function of frequency.[17]

Microleakage

Twenty-one caries-free human premolars freshly extracted for orthodontic reasons were randomly divided into seven groups. Standardized Class II cavities (3 mm buccolingually, 4 mm occlusogingivally, and 2 mm deep [width of the gingival floor]) were prepared in each tooth using cylindrical

Table 2: *Restorative Protocol for the Class II Restorations*[a]

Group	Bonding system	Material Used in Each Layer	
		Horizontal Layer (1 mm)	Oblique Layer (3 mm)
F00-BF	FL-Bond II	F00	BF
F02-BF	FL-Bond II	F02	BF
F03-BF	FL-Bond II	F03	BF
F10-BF	FL-Bond II	F10	BF
BF-BF	FL-Bond II	BF	BF
Z350F-Z350	Adper Easy One	Z350F	Z350
Z350-Z350	Adper Easy One	Z350	Z350

[a] Abbreviations are given in Table 1.

diamond burs (Dia-burs, Mani, Tochigi, Japan) with water spray. The cervical cavity margins of the preparations were all in enamel. The teeth were then fixed in resin blocks (denture base resin type II, Shanhai Medical Instruments, Shanghai, China). A typodont model was established to simulate the interproximal relationship between two adjacent premolars. Sectional matrices (Palodent System, Dentsply, Milford, DE, USA) were placed, secured with wooden wedges (Hawe-Sycamore interdental wedges, Kerr, Bioggio, Switzerland), and checked with a hand instrument (Silver probe, Hu-Friedy, Chicago, IL, USA) to ensure that no detectable space existed between the matrices and cavity margins.

The Class II preparations were restored with different material combinations as shown in Table 2. Approximately 1-mm thick horizontal layers of composites were placed at the cervical margins and light cured for 20 seconds from the occlusal. Two oblique layers were subsequently applied in less than 2-mm increments and cured for 20 seconds each. After removal of the matrices, the restorations were cured for an additional 20 seconds from the buccal and lingual surfaces. The restored teeth were then polished (Super-snap polishing system, Shofu, Kyoto, Japan) and checked under a stereomicroscope (Zoom-630E, Shanghai Changfang Optical Instrument, Shanghai, China) at 40× magnification to prevent any detectable overhangs or microgaps along the margins. The teeth were then stored in distilled water at 25°C for 24 hours prior to microleakage testing.

The restored teeth were coated with two layers of nail varnish 1 mm short of the restoration margins and allowed to dry for 10 minutes. The primed teeth were then immersed in 50% $AgNO_3$ solution ($AgNO_3$, Sinopharm, Beijing, China) for 24 hours, washed under running water, stored in developer (RPX-OMAT, Kodak China, Shanghai, China) for 3 hours, and ultrasonically cleaned for 1 minute to eliminate silver particles from the tooth surfaces. A micro-CT system (Micro-CT, Institute of High Energy Physics, Chinese Academy of Science, Beijing, China) with an X-ray source of 70 kV/90 mA was used to scan the specimens. Each specimen was rotated 360° with a rotation step of 0.4°, and 900 projections were taken for each sample. The projections were reconstructed and converted to 2D bitmap format images. Resolution of the image was 1024*1024, with a pixel size of 11.5 μm. Cervical microleakage was scored according to the depth of dye penetration at the tooth-restoration interfaces using Mimics 10.01 software (Mimics, Materialise, Leuven, Belgium). Microleakage was recorded at 0.1-mm intervals from the buccal to lingual surfaces providing 30 sites per specimen and a total of 90 sites per group. Scoring for microleakage (Figure 1) was as follows: 0 = no dye penetration, 1 = dye penetration 0.0–0.5 mm, 2 = dye penetration 0.5–1.0 mm, 3 = dye penetration 1.0–1.5 mm, and 4 = dye penetration extending beyond 1.5 mm to the cavity wall. Microleakage data for the various material combinations were computed and analyzed using the Kruskal-Wallis test at significance level $p<0.05$. Correlations between microleakge, viscosity, shrinkage, and filler volume were performed with Spearman's rho correlation at significance level $\alpha=0.05$. Statistical analysis was carried out using SPSS version 20.0 (IBM, SPSS, Chicago, IL, USA).

RESULTS

Mean volumetric shrinkage for the flowable and sculptable composites is shown in Table 3. The flowable materials shrank more than their sculptable counterparts BF and Z350. F02 and F10 had significantly higher shrinkage than did F00, F03, or Z350F. Correlation coefficient between filler volume and volumetric shrinkage was −0.86 for all composites and −0.98 for the giomer materials. Complex

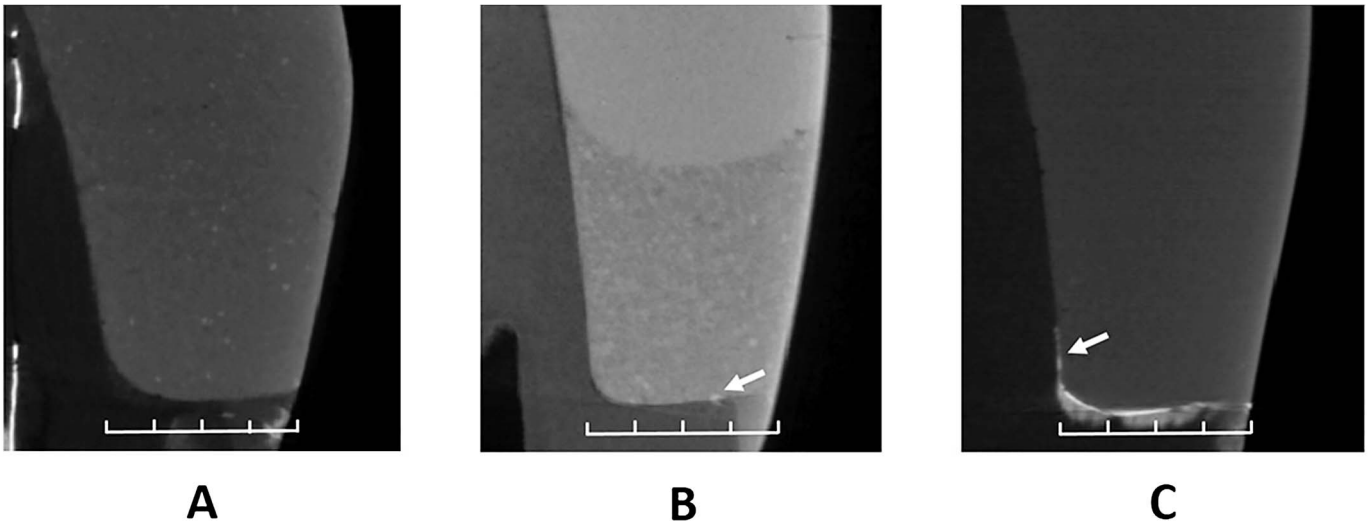

Figure 1. *Representative images depicting cervical microleakage scoring according to depth of dye penetration at the tooth-restoration interfaces using micro-CT. (A-C): Microleakage scores of 0, 2, and 4 according to the depth of silver penetration.*

viscosity is an objective rheologic index of flowability of materials. A lower complex viscosity stipulates easier flow. The flowability of all composites improved with increasing frequency (Figure 2). Table 4 indicates the complex viscosities, after natural logarithmic transformation, at frequencies $\omega = 100$ rad/s and 10 rad/s that represent the viscosities of the composites during and after extrusion through the syringe needle. At both 10 rad/s and 100 rad/s, the sculptable materials BF and Z350 had the highest complex viscosities. For the flowable composites, three-clustering of complex viscosities was observed as follows: Z350F and F02 > F00 > F03 and F10.

Distribution and mean rank of cervical microleakage scores are reflected in Table 5. The use of flowable and sculptable giomer materials resulted in less microleakage than that of their nano-filled counterparts. No microleakage was observed for restorations restored with F02 or F10 flowable giomer liners. For both composite types, the use of flowable liners resulted in significantly less microleakage. Table 6 displays the correlations between viscosity and microleakage as well as shrinkage and microleakage. Significant correlations were observed between shrinkage and microleakage ($r=-0.78$), also between filler volume and microleakage ($r=0.88$). Significant correlations were also noted between viscosity and microleakage at frequencies of 10 rad/s ($r=0.81$) and 100 rad/s ($r=0.76$). Although viscosity was negatively related to shrinkage ($r=-0.61$ and -0.54), the correlations were not significant.

DISCUSSION

The effect of flowable composite liner shrinkage and viscosity on the cervical microleakage of Class II restorations was evaluated using micro-CT. The null hypotheses were rejected as microleakage was significantly influenced by and correlated with polymerization shrinkage and viscosity of the flowable composite liners. Complex viscosities of the flowable composites were significantly lower than were their sculptable counterparts BF and Z350. The flowable materials evaluated were non-Newtonian in nature, exhibiting decreased viscosity with increased shear (frequency) rate. This "shear-thinning" behavior allows the flowable composites to be injected easily through fine gauge needles.[18] Complex viscosities of the flowable materials, which were shear-rate dependent, varied markedly as with other commercially available flowable composites.[19] Dental composites consist primarily of an organic resin matrix and inorganic glass fillers. When shear stresses are applied, the arrangement of the resin monomer molecules and glass fillers are altered. Moreover,

Table 3: *Mean Volumetric Shrinkage of the Various Materials*

	F00	F02	F03	F10	BF	Z350F	Z350
Shrinkage (%)	4.63 (0.23)[a]	5.33 (0.17)[b]	4.72 (0.24)[a]	5.20 (0.21)[b]	2.55 (0.09)[c]	4.81 (0.04)[a]	2.35 (0.02)[c]

[a-c] Letters indicate statistically significant differences. Results of one-way ANOVA and LSD post hoc test ($p<0.05$).

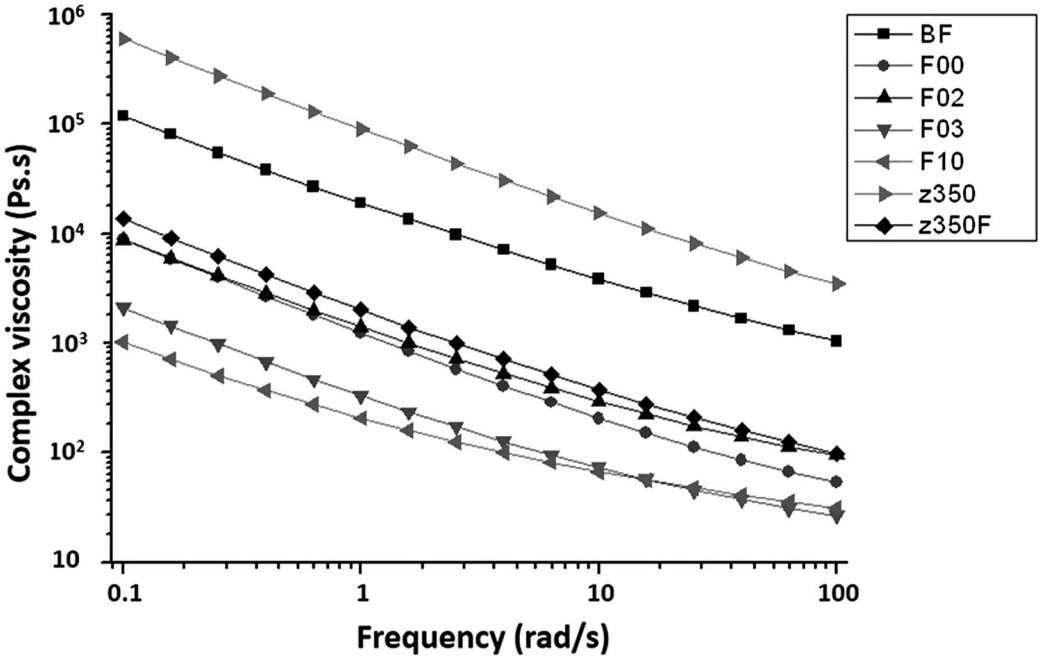

Figure 2. *Complex viscosities of the materials at different frequencies.*

interactions between the resin matrix and fillers are also weakened, leading to decreased viscosity with increasing shear frequency (Figure 1). The variance in complex viscosities between flowable materials is an intricate phenomenon that can be attributed to disparities in resin composition as well as filler size, content, surface morphology, and treatment method.[20]

Although volumetric polymerization shrinkage can be assessed by a variety of methods, the optical video imaging technique was selected because of its relative simplicity and comparable dilatometry results.[21] Polymerization shrinkage is affected by the resin matrix composition, filler type, and content.[22] The PRG fillers in the giomer composites can release and recharge fluoride, depending on environmental fluoride concentrations, without compromising strength and stability.[23] The giomer materials evaluated contained the same resins and fillers but in varying quantities (Table 1). When filler content decreased from 68.6% to 33.3%, volumetric shrinkage increased from 2.55% to 5.20% accordingly. The association between filler volume and shrinkage for the giomer composites was significant and very strong (r=−0.98). When data for all composites were considered, filler volume was found to be the dominant factor affecting volumetric shrinkage. Our data corroborated those of other authors evaluating the polymerization shrinkage of commercial and experimental composites based on zirconia, silica, and other types of fillers.[24,25]

In addition to filler content, the relative proportion of Bis-GMA, TEGDMA, and other monomers were reported to affect volumetric shrinkage.[26] The resin matrix of most dental composites is a blend of BisGMA and TEGDMA. TEGDMA, which has lower molecular weight and viscosity than Bis-GMA, serves as a diluent and facilitates the incorporation of inorganic fillers. TEGDMA's low molecular weight, however, offers a large number of double bonds and provides a high degree of cross-linking leading to greater shrinkage.[18] The aforementioned may explain in part the slightly higher shrinkage of BF (2.55%) compared with that of Z350 (2.35%) despite BF's higher filler content (Table 1). The flowable "Plus" giomers (ie, F00 and F03) also contain more TEGDMA than do their predecessors F02 and F10,[27] which may have negated some of the

Table 4: *Complex Viscosity of the Materials at Frequencies of 10 rad/s and 100 rad/s*

	F00	F02	F03	F10	BF	Z350F	Z350
Complex viscosity frequency (10 rad/s)	5.33	5.68	4.29	4.20	8.88	5.93	9.65
Complex viscosity frequency (100 rad/s)	3.98	4.56	3.28	3.44	7.40	4.58	8.16

Table 5: *Distribution and Mean Ranks of the Cervical Microleakage Scores for the Various Materials*

	Score					n	Mean Ranks
	0 0	0<a≤0.5 1	0.5<a≤1 2	1<a≤1.5 3	1.5<a≤2 4		
F00	73	17	–	–	–	90	265.8[a,b]
F02	90	–	–	–	–	90	218.5[a]
F03	76	14	–	–	–	90	257.5[a,b]
F10	90	–	–	–	–	90	218.5[a]
BF	65	15	2	5	3	90	298.5[b]
Z350F	41	12	17	4	16	90	391.7[c]
Z350	1	7	5	50	27	90	558.0[d]

[a-c] Letters indicate statistically significant differences. Results of Kruskal-Wallis test ($p<0.05$).

positive effects on polymerization shrinkage offered by the higher filler content of F00 and F03.

Micro-CT has been used to study dental composite shrinkage, gap formation, and microleakge.[28] This nondestructive technique requires a radiopaque dye such as silver nitrate for studying the interfacial integrity of composite restorations. Cross-sectional analysis was performed as 3D reconstruction software was not available for the micro-CT used. A 1-mm layer of flowable composite liner was used before placing the sculptable materials, as this has been shown to result in the least microleakage.[29] No microleakage was observed when F02 and F10 were used as flowable liners. Both these materials had the lowest filler volume and highest resin content.

Although higher resin content is associated with greater shrinkage stress,[22] a strong and negative association was observed between shrinkage and microleakage ($r=-0.78$). The greater shrinkage stress accompanying the higher resin content of flowable liners might be mitigated by their lower elastic modulus and viscosity.[30,31] Shrinkage stress of the sculptable composites is absorbed by the relatively elastic initial layer of liner, thereby preserving the cervical interfacial integrity of the Class II restorations.[31,32] Microleakage was significantly and strongly correlated with viscosity due to poorer cavity adaptations. Findings corroborated the results of previous studies on nongiomer materials.[6-8] The giomer restorations had significantly less microleakage than those restored with nano-filled composites. This, along with their fluoride release/recharge and antibacterial properties, accounts partly for their long-term, favorable performance.[33]

The current study had several limitations. First, the cervical cavity margins of the Class II preparations were located in enamel and not dentin. Bonding to enamel results in less microleakage and merely embodies a best-case scenario.[34] The ability of flowable composite liners to reduce microleakage at dentin margins is still contentious[35,36] and warrants additional investigation. Moreover, the aging and thermal cycling of restorations is known to adversely affect enamel microleakage.[34,37] These events are beyond the scope of the current study and should be considered for future work. Adhesive strategies and systems may possibly influence microleakage and bond strengths.[37-39] The aforementioned, together with clinical data from longevity studies, are merited to substantiate the clinical utility of flowable composite liners in Class II restorations.

CONCLUSIONS

The influence of polymerization shrinkage and viscosity of flowable composite liners on the cervical microleakage of Class II restorations was evaluated using micro-CT. Within the limitations of this in-vitro study, the following conclusions can be made:

1. Flowable composite liners should be used to reduce cervical microleakge of Class II restorations.

Table 6: *Correlations Between Shrinkage, Microleakage, Resin Content, and Viscosity*

	Viscosity				Microleakage	
	Shrinkage		Microleakage		Filler Volume	Shrinkage
	10 rad/s	100 rad/s	10 rad/s	100 rad/s		
r	−0.61	−0.54	0.81*	0.76*	0.88*	−0.78*

* indicates significant correlation. Results of Spearman's rho correlation ($p<0.05$, 2-tailed).

2. Cervical microleakage is associated with the polymerization shrinkage and viscosity of the flowable composite liners employed.
3. When selecting composite liners, those with lower filler volume are encouraged despite their higher shrinkage.
4. Giomer restorations had significantly less cervical microleakage than those restored with nano-filled composites.

Regulatory Statement

This in vitro study was conducted in accordance with all the provisions of the local human subjects oversight committee guidelines and policies of the Department of Cariology and Endodontology at Peking University School and Hospital of Stomatology.

Conflict of Interest

The authors of this manuscript certify that they have no proprietary, financial, or other personal interest of any nature or kind in any product, service, and/or company that is presented in this article.

(Accepted 4 July 2017)

REFERENCES

1. Bayne SC, Thompson JY, Swift EJ, Stamatiades P, & Wilkerson M (1998) A characterization of first-generation flowable composites *Journal of the American Dental Association* **129(5)** 567-577.
2. Baroudi K, & Rodrigues JC (2015) Flowable resin composites: A systematic review and clinical considerations *Journal of Clinical Diagnostic Research* **9(6)** E18-E24.
3. Davidson CL, & Feilzer AJ (1997) Polymerization shrinkage and polymerization shrinkage stress in polymer-based restoratives *Journal of Dentistry* **25(6)** 435-440.
4. Kim RJ, Kim YJ, Choi NS, & Lee IB (2015) Polymerization shrinkage, modulus, and shrinkage stress related to tooth-restoration interfacial debonding in bulk-fill composites *Journal of Dentistry* **43(4)** 430-439.
5. Alani AH, & Toh CG (1997) Detection of microleakage around dental restorations: a review *Operative Dentistry* **22(4)** 173-185.
6. Lokhande NA, Padmai AS, Rathore VP, Shingane S, Jayashankar DN, & Sharma U (2014) Effectiveness of flowable resin composite in reducing microleakage—An in vitro study *Journal of International Oral Health* **6(3)** 111-114.
7. Arora R, Kapur R, Sibal N, & Juneja S (2012) Evaluation of microleakage in class II cavities using packable composite restorations with and without use of liners *International Journal of Clinical Pediatric Dentistry* **5(3)** 178-184.
8. M R, Sajjan GS, B NK, & Mittal N (2010) Effect of different placement techniques on marginal microleakage of deep class II cavities restored with two composite resin formulations *Journal of Conservative Dentistry* **13(1)** 9-15.
9. Hernandes NM, Catelan A, Soares GP, Ambrosano GM, Lima DA, Marchi GM, Martins LR, & Aguiar FH (2014) Influence of flowable composite and restorative technique on microleakage of class II restorations *Journal of Investigative Clinical Dentistry* **5(4)** 283-288.
10. Majety KK, & Pujar M (2011) In vitro evaluation of microleakage of class II packable composite resin restorations using flowable composite and resin modified glass ionomers as intermediate layers *Journal of Conservative Dentistry* **14(4)** 414-417.
11. Fabianelli A, Sgarra A, Goracci C, Cantoro A, Pollington S, & Ferrari M (2010) Microleakage in class II restorations: Open vs closed centripetal build-up technique *Operative Dentistry* **35(3)** 308-313.
12. Tredwin CJ, Stokes A, & Moles DR (2005) Influence of flowable liner and margin location on microleakage of conventional and packable class II resin composites *Operative Dentistry* **30(1)** 32-38.
13. Masouras K, Silikas N, & Watts DC (2008) Correlation of filler content and elastic properties of resin-composites *Dental Materials* **24(7)** 932-939.
14. Karaman E, & Ozgunaltay G (2014) Polymerization shrinkage of different types of composite resins and microleakage with and without liner in class II cavities *Operative Dentistry* **39(3)** 325-331.
15. Gao BT, Lin H, Han JM, & Zheng G (2011) Polymerization characteristics, flexural modulus and microleakage evaluation of silorane-based and methacrylate-based composites *American Journal of Dentistry* **24(2**) 97-102.
16. Calheiros FC, Sadek FT, Braga RR, & Cardoso PE (2004) Polymerization contraction stress of low-shrinkage composites and its correlation with microleakage in class V restorations *Journal of Dentistry* **32(5)** 407-412.
17. Beun S, Bailly C, Devaux J, & Leloup G (2008) Rheological properties of flowable resin composites and pit and fissure sealants *Dental Materials* **24(4)** 548-555.
18. Lee JH, Um CM, & Lee IB (2006) Rheological properties of resin composites according to variations in monomer and filler composition *Dental Materials* **22(6)** 515-526.
19. Lee IB, Min SH, Kim SY, & Ferracane J (2010) Slumping tendency and rheological properties of flowable composites *Dental Materials* **26(5)** 443-448.
20. Beun S, Bailly C, Dabin A, Vreven J, Devaux J, & Leloup G (2009) Rheological properties of experimental Bis-GMA/TEGDMA flowable resin composites with various macrofiller/microfiller ratio *Dental Materials* **25(2)** 198-205.
21. Yu P, Yap A, & Wang XY (2017) Degree of conversion and polymerization shrinkage of bulk-fill resin-based composites *Operative Dentistry* **42(1)** 82-89.
22. Braga RR, Ballester RY, & Ferracane JL (2005) Factors involved in the development of polymerization shrinkage stress in resin-composites: A systematic review *Dental Materials* **21(10)** 962-970.
23. Itota T, Carrick TE, Yoshiyama M, & McCabe JF (2004) Fluoride release and recharge in giomer, compomer and resin composite *Dental Materials* **20(9)** 789-795.
24. Han B, Dong YM, Wang XY, Tian FC, & Gao XJ (2010) Effect of filler content of composite resins on polymerization shrinkage measured by a video imaging apparatus (Acuvol) *Beijing Da Xue Xue Bao* **42(5)** 582-585.

25. Kwon YH, Kang SI, Hur B, Park JK, & Kim HI (2006) Effect of irradiation mode on polymerization of dental composite resins *Journal of Biomedical Materials Research Part B: Applied Biomaterials* **78(2)** 253-258.

26. Ellakwa A, Cho N, & Lee IB (2007) The effect of resin matrix composition on the polymerization shrinkage and rheological properties of experimental dental composites *Dental Materials* **23(10)** 1229-1235.

27. Yap AU, Pandya M, & Toh WS (2016) Depth of cure of contemporary bulk-fill resin-based composites *Dental Materials Journal* **35(3)** 503-510.

28. Carrera CA, Lan C, Escobar-Sanabria D, Li Y, Rudney J, Aparicio C, & Fok A (2015) The use of micro-CT with image segmentation to quantify leakage in dental restorations *Dental Materials* **31(4)** 382-390.

29. Reddy SN, Jayashankar DN, Nainan M, & Shivanna V (2013) The effect of flowable composite lining thickness with various curing techniques on microleakage in class II composite restorations: An in vitro study *Journal of Contemporary Dental Practice* **14(1)** 56-60.

30. Braga RR, & Ferracane JL (2004) Alternatives in polymerization contraction stress management *Critical Reviews in Oral Biology and Medicine* **15(3)** 176-184.

31. Labella R, Lambrechts P, Van Meerbeek B, & Vanherle G (1999) Polymerization shrinkage and elasticity of flowable composites and filled adhesives *Dental Materials* **15(2)** 128-137.

32. Unterbrink GL, & Liebenberg WH (1999) Flowable resin composites as "filled adhesives": Literature review and clinical recommendations *Quintessence International* **30(4)** 249-257.

33. Gordan VV, Blaser PK, Watson RE, Mjor IA, McEdward DL, Sensi LG, & Riley JR (2014) A clinical evaluation of a giomer restorative system containing surface prereacted glass ionomer filler: Results from a 13-year recall examination *Journal of the American Dental Association* **145(10)** 1036-1043.

34. Zanatta RF, Lungova M, Borges AB, Torres C, Sydow HG, & Wiegand A (2017) Microleakage and shear bond strength of composite restorations under cycling conditions *Operative Dentistry* **42(2)** E71-E80.

35. Sadeghi M, & Lynch CD (2009) The effect of flowable materials on the microleakage of class II composite restorations that extend apical to the cemento-enamel junction *Operative Dentistry* **34(3)** 306-311.

36. Kasraei S, Azarsina M, & Majidi S (2011) In vitro comparison of microleakage of posterior resin composites with and without liner using two-step etch-and-rinse and self-etch dentin adhesive systems *Operative Dentistry* **36(2)** 213-221.

37. Atash BYL, Seyed TE, & Mohammadi BM (2015) Bonding durability of four adhesive systems *Journal of Dentistry (Tehran)* **12(8)** 563-570.

38. Korkmaz Y, Gurgan S, Firat E, & Nathanson D (2010) Effect of adhesives and thermocycling on the shear bond strength of a nano-composite to coronal and root dentin *Operative Dentistry* **35(5)** 522-529.

39. Reis A, Loguercio AD, Manso AP, Grande RH, Schiltz-Taing M, Suh B, Chen L, & Carvalho RM (2013) Microtensile bond strengths for six 2-step and two 1-step self-etch adhesive systems to enamel and dentin *American Journal of Dentistry* **26(1)** 44-50.

©Operative Dentistry, 2018, **43-6,** 665-673

Microshear Bond Strength of High-viscosity Glass-ionomer to Normal and Caries-affected Dentin Under Simulated Intrapulpal Pressure

HA El-Deeb • EH Mobarak

Clinical Relevance

Current versions of high-viscosity glass-ionomer cements used with atraumatic restorative treatment show comparable bonding to normal and caries-affected dentin.

SUMMARY

Objectives: The use of high-viscosity glass-ionomer cements (HVGICs) for atraumatic restorative treatment (ART) restorations is widely practiced with the advent of various HVGICs. However, the bonding of the latter to caries-affected dentin (CAD) should be validated, especially because it is the common substrate left after conservative caries removal following the ART approach. Hence, this study was carried out to evaluate the microshear bond strength (μSBS) of three HVGICs to normal dentin (ND) and CAD under intrapulpal pressure (IPP) simulation.

Methods and Materials: The occlusal enamel of 90 molars with mid-coronal caries was cut to expose flat dentin surfaces containing both ND and CAD. Dentin substrates (ND and CAD) were differentiated using visual, tactile, caries-detecting dye, and dye-permeability methods. Prepared crown segments were equally divided (n=30) according to the tested HVGICs into GC Fuji IX GP Fast, Fuji IX GP containing chlorhexidine, and zinc-reinforced ChemFil Rock HVGIC. Microcylinders of tested HVGICs were built up on both dentin substrates (n=30 for each tested HVGIC per each substrate) using starch tubes while the specimens were subjected to simulated IPP of 15 mm Hg. The μSBS test was conducted using a universal testing machine, and failure modes were determined using a scanning electron microscope. Data were statistically analyzed using two-way analysis of variance (ANOVA) with repeated measures, one-way ANOVA, and Bonferroni *post hoc* tests (α=0.05).

Results: For both dentin substrates (ND and CAD), the μSBS values of ChemFil Rock were significantly higher than those recorded for the other HVGICs. The μSBS values of each tested HVGIC to ND and CAD were not statistically different. Failure modes were mainly mixed.

Heba Ahmed El-Deeb, associate professor, BDS, MDS, DDSc, Conservative Dentistry Department, Faculty of Dentistry, Cairo University, Cairo, Egypt

*Enas Hussein Mobarak, professor, BDS, MDS, DDSc, Conservative Dentistry Department, Faculty of Dentistry, Cairo University, Cairo, Egypt

*Corresponding author: 14 ElAnsar St., Cairo 12311, Egypt; e-mail: enasmobarak@hotmail.com

DOI: 10.2341/17-154-L

Conclusions: Zinc-reinforced HVGIC ChemFil Rock showed superior bonding to ND and CAD compared to the GC Fuji IX GP Fast and Fuji IX with chlorhexidine. However, each of the tested HVGICs showed comparable bonding to both dentin substrates (ND and CAD).

INTRODUCTION

After more than 20 years of scientific studies, the atraumatic restorative treatment (ART) approach has become a cornerstone in global oral health.[1] ART involves the removal of soft completely demineralized carious tooth tissues with hand instruments, leaving hard, discolored caries-affected dentin (CAD), followed by the restoration of the cavity with an adhesive dental material that simultaneously seals the remaining caries-risk pits and fissures. Because of their biocompatibility, adhesive potential to tooth structure, compatibility of their coefficient of thermal expansion with that of the tooth structure, and the potential for fluoride releasing and recharging, glass-ionomer cements (GICs) are considered "smart" restorative materials to be used with ART. Despite of these outstanding advantages, GICs still suffer from shortcomings, such as early weakening of strength properties compared to resin composites, lack of command set, and moisture sensitivity.[2] Therefore, improvements were needed to overcome the above-stated drawbacks.[3]

Attempts to enhance the mechanical properties of GICs by increasing the powder/liquid ratios[4] came up with newer brands of HVGICs that were recommended for use with ART. Meta-analytic studies proved that HVGICs can be used with remarkable success in single-surface cavities; however, it fails to be routinely used in multiple-surface cavities in posterior teeth.[5-7]

Additionally, the properties of these materials can be strengthened via alteration of the glass powder composition, thus increasing the hydrolytic stability as well as the reactivity. Furthermore, the use of multicomponent fluorophosphoaluminosilicate glasses supplemented with zinc oxide particles could improve the setting reactivity and thus the material properties.[3,8]

From another aspect, researchers tried to gain a therapeutic benefit from the HVGICs through incorporating antibacterial agents, such as chlorhexidine (CHX), with glass-ionomer materials. Achieving the optimal amount of concomitant antibacterial agent without jeopardizing the basic properties of the parent materials was indeed a prime challenge. So far, various studies[9-11] have been conducted on the physical and mechanical properties of the recent types of HVGICs. Nevertheless, to date, limited studies have been focused on the bonding performance of these newer materials.

Using caries-free substrates to investigate restorative material bonding does not fully reproduce the clinical situation, where the remaining substrate after caries removal includes CAD and normal non–caries affected dentin (ND).[5] Notably, there is no published literature that deals with the bond strength of the recently introduced HVGICs to the naturally occurring CAD substrate while intrapulpal pressure (IPP) is simulated. Therefore, this study was carried out to test the μSBS of HVGICs to ND and CAD under IPP simulation.

The null hypotheses were that 1) there is no difference in the lSBS among the different HVGICs and 2) there is no difference between lSBS values of any of the tested HVGIC to both dentin substrates: ND and CAD.

METHODS AND MATERIALS

Specimen Preparation

Carious lower posterior molars were collected for the present study. From these, a total of 90 molars having occlusal caries with moderate involvement in dentin, classified according to Mount's classification as (site [1] and size [2] = 1.2) and according to ICDAS II classification (0.5), were used. Teeth were collected according to the research ethical committee guidelines.

The collected teeth were stored in phosphate-buffered saline containing 0.2% sodium azide at 4°C for a couple of weeks, during which time they were used.[12]

To expose flat dentin surfaces with ND and CAD, the occlusal enamel was trimmed perpendicularly to the long axis of each tooth using a slow-speed diamond-saw sectioning machine (Buehler Isomet, Lake Bluff, IL, USA) under water coolant. Ground dentin surfaces showing any signs of early exposure or cracks were not included in this study. To expose the pulp chamber, another cut was made parallel to the occlusal surface 2 mm apical to the cemento-enamel junction. The remnants of pulp tissue were removed from the pulp chamber using a discoid excavator (Carl Martin GmbH, Solingen, Germany) without touching its walls.[13] Each crown segment was mounted on a polymethacrylate plate containing a 19-gauge needle in the center using cyanoacrylate adhesive (Rocket Heavy, Dental Ventures of Amer-

Table 1: *Materials, Batch Numbers, Manufacturers, and Chemical Compositions of the Tested High-Viscosity Glass-Ionomer Cements*

Material/Batch Number	Manufacturer	Composition
GC Fuji IX GP Fast (Radiopaque posterior glass-ionomer restorative cement in capsules) (0804141)	GC Corp (Tokyo, Japan)	Powder 0.40 g/liquid 0.11 g (0.09 mL) per capsule
		Alumino-fluoro-silicate glass, polyacrylic acid, distilled water, polybasic carboxylic acid
Fuji IX GP containing chlorhexidine HVGIC (Radiopaque posterior glass-ionomer trial restorative cement in powder/liquid)	GC Corp	Powder: alumino-fluoro-silicate glass to which 1% chlorhexidine diacetate (Sigma Aldrich, Steinheim, Germany) was incorporated
		Liquid: polyacrylic acid, distilled water, polybasic carboxylic acid
ChemFil Rock (advanced glass-ionomer restorative material) (K79200030-03)	Dentsply De-Trey GmbH (Konstanz, Germany)	Predosed mixing capsule with a minimal dispensable amount of 0.1 mL (280 mg).
		Calcium-aluminum-zinc-fluoro-phosphor-silicate glass, polycarboxylic acid, iron oxide pigments, titanium dioxide pigments, tartaric acid, itaconic acid, water
Dentin Conditioner (GC) (280739GC)	GC Corp	20% polyacrylic acid; 3% aluminum chloride hexahydrate component

ica, Corona, CA, USA) and subsequently embedded in a chemically cured polyester resin (polyester resin #2121, Eternal Chemical Co Ltd, Hsein, Taiwan) up to the level of the cemento-enamel junction.[13]

CAD Identification

Different dentin substrates were detected with the aid of visual and tactile methods. To allow precise identification between ND and CAD, caries-detecting dye[14] and the dye permeability tests[15] were used. Red caries detector dye (Seek, Ultradent, South Jordan, UT, USA) was flooded on the flat dentin surface for 10 seconds, rinsed for five seconds, and then air-dried thoroughly for five seconds. Three different colors were revealed after drying: dark red denoting caries-infected dentin, pink color denoting CAD, and yellow color considered as ND. Partial removal of dark red–stained caries-infected dentin was carried out using a sharp spoon excavator (KLS Martin, Jacksonville, FL, USA). In the dye permeability test,[15] a 19-gauge stainless-steel butterfly needle was centrally fitted to the polymethacrylate plate and cemented to the prepared crown segment, and 10% methylene blue was permeated into the tooth through the pulp chamber under pressure. The selective staining of ND with methylene blue was attributed to the decline in the permeability of CAD compared to ND due to the presence of peritubular and intertubular crystal formation into the dentinal tubules. Therefore, the ND was stained blue, whereas the CAD was stained pale pink. The dentin surface was flattened using a rotary grinding machine and hand polished using 600-grit silicon carbide paper (MicroCut, 8 inch, Buehler) for 10 seconds to produce a standardized smear layer.[15]

Restorative Procedures

The crown segments (n=90) with ND and CAD were randomly and equally divided (n=30) according to the type of the tested HVGICs: GC Fuji IX GP Fast HVGIC (GC Corporation, Tokyo, Japan), Fuji IX GP GIC containing chlorhexidine (GC Corporation), and ChemFil Rock zinc-reinforced HVGIC (Dentsply De-Trey GmbH, Konstanz, Germany). Table 1 shows materials, batch numbers, manufacturers, and chemical compositions. All the specimens were connected to the IPP assembly under 20 mm Hg 30 minutes before and during HVGIC application. The tested HVGICs were applied according to the manufacturers' recommendations.

For the application of Fuji IX GP HVGIC (with and without chlorhexidine), the prepared dentin surface was conditioned with GC dentin conditioner (GC Corporation) for 10 seconds, rinsed thoroughly with distilled water, and blot dried. ChemFil Rock zinc-reinforced HVGIC was applied as per the manufacturer's instructions without surface conditioning. The Fuji IX GP HVGIC (containing CHX) was mixed according to the manufacturer's instructions as follows; 1 scoop (3.6 g) of powder + 1 drop (1 g) of liquid (powder/liquid ratio=1:1) were mixed manually until obtaining a homogeneous consistency. The GC Fuji IX GP Fast and ChemFil Rock capsules were activated and immediately mixed for 10 and 15 seconds, respectively, using an amalgamator (Cap-Mix, Capsule mixing device, 3M ESPE, Seefeld,

Germany). Starch tubes (pasta ZARA, Brescia, Italy) of 0.96-mm internal diameter were cut to 1-mm height to be used to build up the HVGIC microcylinders on different dentin substrates.[16]

A periodontal probe (Primadent International, Frankfurt, Germany) was used to condense the glass ionomer into the starch tubes. For each crown segment, two of the filled starch tubes were applied, one for each dentin substrate (ND and CAD) with slight finger pressure (n=30 for each tested HVGIC per each substrate). Microcylinders were coated with petroleum jelly from their top surfaces and left to set in an incubator at 37°C and a relative humidity of 100% for one hour. After the glass ionomer set, specimens were immersed in artificial saliva[17] at 37°C for four hours to soften the starch tubes. The dissolved starch tubes were carefully removed using a lancet (No. 11, Wuxi Xinda Medical Device Co, Wuxi, Jiangsu, China) leaving the HVGIC microcylinders bonded to the dentin substrates. Glass-ionomer microcylinders with interfacial gaps, bubble inclusions, or other defects were discarded and replaced. The specimens were then stored in artificial saliva at 37°C while the IPP was maintained for 24 hours in a specially constructed large incubator before testing.

Microshear Bond Strength Testing

To avoid data collection bias, blinding was considered during testing of the specimens. A specially designed attachment jig was constructed to hold the specimens to the testing machine.[15] Each specimen with its bonded glass-ionomer microcylinders was secured with four tightening bolts to the lower part of the specially designed attachment jig. The attachment jig was in turn screwed into the lower fixed and the upper movable compartments of the testing machine (Model LRX-plus, Lloyd Instruments Ltd, Ferham, UK) with a 5 KN load cell. A wire loop prepared from an orthodontic stainless-steel ligature wire 180 μm (G&H Orthodontics, Franklin, IN, USA) was wrapped around the bonded microcylinder as close as possible to its base and touching the tooth surface. A tensile load was applied at a crosshead speed of 0.5 mm/min. Data were recorded using computer software (Nexygen-MT, Lloyd Instruments).

The microshear bond strength value was calculated through dividing the load at failure by the bonding area to express the bond strength in MPa according to the following equation: $S = P/\pi r^2$, where S = microshear bond strength (in MPa), P = load at failure (in newtons), $\pi = 3.14$, and r = radius of composite microcylinder (in mm).

Statistical Analysis

Data were blindly analyzed and statistically described in terms of mean ± standard deviation. In the present study, the bond strengths to different dentin substrates were considered as the dependent variables, while the HVGICs were the independent variables. Normal distribution of the data was verified with the Kolmogorov-Smirnov test. The data were found to be normally distributed, and there was homogeneity of variance among the groups. Thus, the statistical evaluation was performed using parametric tests. Two-way analysis of variance (ANOVA) was used to determine the effect of dentin substrates and the HVGICs. It was also used to detect any significant interactions between these two variables. One-way ANOVA was employed to indicate the significant difference among the μSBS values of the tested HVGICs bonded to ND or CAD. The Bonferroni test was used for pairwise comparisons. The significance level was set at $\alpha = 0.05$. To compare the μSBS values of each HVGIC to ND and CAD, Student t-test was used. All statistical calculations were performed using SPSS (Statistical Package for the Social Sciences, SPSS Inc, Chicago, IL, USA) version 15 for Microsoft Windows.

Failure Mode Analysis

After measuring the bond strength, each fractured specimen was inspected using an environmental scanning electron microscope (Quanta 200, FEI Company, Philips, Eindhoven, The Netherlands) at 25 KV to determine its mode of failure. The failure mode was allocated into the following types:

Type I: Adhesive failure (failure at the interface between dentin and HVGIC)
Type II: Cohesive failure (failure in the HVGIC material)
Type III: Mixed failure (involving both adhesive and cohesive failures)

Representative photomicrographs of each type of failure were captured at various magnifications.

RESULTS

The mean and standard deviation for each experimental group are listed in Table 2. Two-way ANOVA showed a significant effect for the tested materials ($p<0.001$) but not for the dentin substrates ($p=0.150$) and their interactions ($p=0.757$).

Table 2: *Microshear Bond Strength μSBS Values (Mean [SD]) in MPa of the Tested High-Viscosity Glass-Ionomer Restorative Materials (HVGICs)*[a]

Dentin Substrates	HVGICs			
	GC Fuji IX GP Fast	Fuji IX GP- CHX	ChemFil Rock	*p*-Value
ND	6.59(2.8) aA (Ptf/tnt=0/30)	6.95(2.9) aA (Ptf/tnt=0/30)	10.51(3.9) aB (Ptf/tnt=0/30)	<0.0001
CAD	7.56(3.1) aA (Ptf/tnt=0/30)	7.27(3.2) aA (Ptf/tnt=0/30)	11.01(3.2) aB (Ptf/tnt=0/30)	<0.0001
p-value	0.20	0.69	0.59	

[a] *Different capital letters denote significant differences within rows, whereas different small letters denote significant differences within a column for each HVGIC. Abbreviations: CHX, chlorhexidine; ND, normal dentin; CAD, caries-affected dentin; Ptf/tnt, pretest failures/total number of tested microcylinders.*

Based on this, the first null hypothesis was rejected, while the second null hypothesis failed to be rejected.

For each dentin substrate (ND or CAD), one-way ANOVA revealed a significant difference among the three HVGIC values ($p>0.0001$). ChemFil Rock, a zinc-reinforced HVGIC, recorded significantly higher μSBS values than GC Fuji IX GP Fast and Fuji IX GP containing chlorhexidine, which were not statistically different from each other (Table 2). Despite that, each tested HVGIC type recorded higher mean μSBS values when bonded to CAD rather than those values when bonded to ND; *t*-test revealed no statistically significant differences between them (Table 2).

Regarding the failure modes, the tested HVGICs bonded to ND and CAD showed predominantly mixed failure (adhesive at dentin side/cohesive in glass ionomer). Figure 1 shows the percentages of the recorded failure modes. Representative SEM micrographs for some failure modes of tested specimens bonded to either ND or CAD are presented in Figure 2.

DISCUSSION

In the current study, the term "normal dentin" is used to describe caries-free dentin. This term has been used by many other authors[18-22] who believe that the term "sound dentin"[23-26] should indicate virgin dentin not subjected to any stimulus, not even an occlusal force, as in the case of an impacted third molar. A nomenclature that defines the type of dentin compared with CAD through discussions among the scientific community is still required.

Differentiation between normal and CAD substrates was carried out using caries-detecting dye and a dye permeability test. Despite the fact that the use of caries-detecting dye is popular,[14] its staining ability, which relies neither on chemical reaction with CAD tissue nor on bacterial staining, could lead to overexcavation. Thus, the dye permeability test, which was found to be a nondestructive, reliable method,[15] was used as an adjunctive way for differentiation between both dentin substrates.

Several studies were conducted to compare bond strength of both substrates (ND and CAD) for adhesive systems and resin composite[15,18,27-29] Nevertheless, few researchers tested bonding of HVGICs to ND and CAD.[30,31] In the current study, all tested HVGICs revealed no significant difference in their bonding to ND and CAD. Alves and others[30] reported equal bonding of Ketac Molar Easy Mix to ND and simulated CAD. Lenzi and others[31] confirmed these

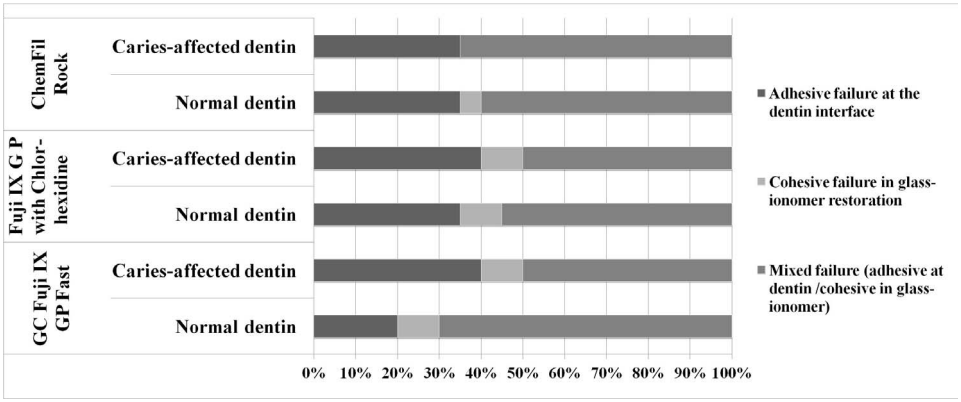

Figure 1. *The percentages of the recorded modes of failure in the tested groups.*

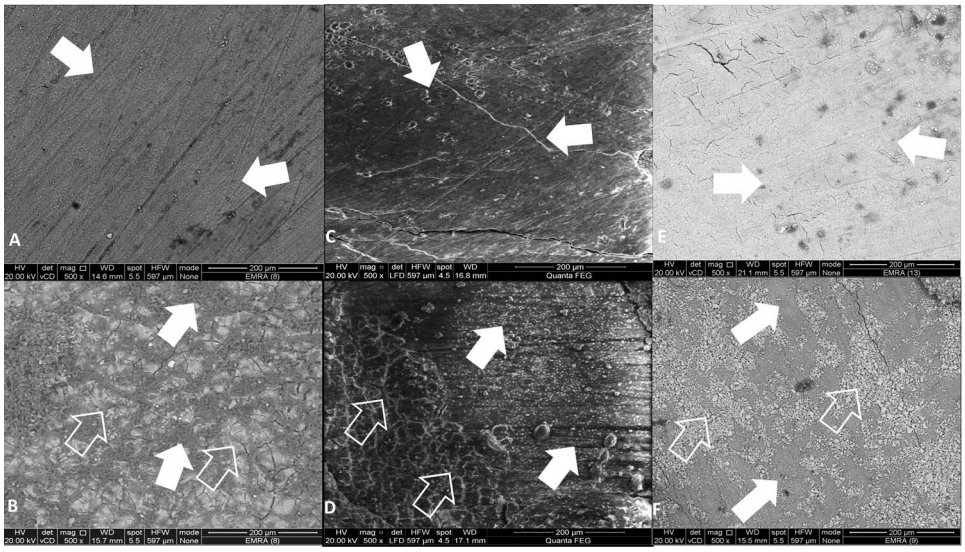

Figure 2. *SEM photomicrographs showing the predominant failure modes of GC Fuji IX GP Fast (A and B), Fuji IX GP containing chlorhexidine (C and D), and ChemFil Rock (E and F). (A, C, and E):Type I: adhesive failure (failure at the interface between dentin and GIC). (B, D, and F) Type III: mixed failure (involving both adhesive and cohesive failures). Filled arrows point to dentin, and hollow arrows point to HVGIC remnants. SEM, scanning electron micrography; GIC, glass-ionomer cement; HVGIC, high-viscosity glass-ionomer cement.*

results when they bonded Fuji IX to ND and artificially induced CAD in primary teeth.

The mechanism of GIC bonding to dentin is not precisely identified. Bonding of GICs is assumed to be a twofold mechanism, chemical interaction and micromechanical interlocking to a lesser degree. The chemical reaction is attributed to the ionic interaction between carboxylic groups from polyacids and the hydroxyapatite from the tooth surface, displacing calcium and phosphate ions from the latter. The micromechanical infiltration, which is expected to have a minor role in comparison with adhesive systems used with resin composite, may be due to the retention provided by surface irregularity of dentin and the porosity formed by the GIC self-etching property.[32]

The higher mean μSBS values obtained for all tested HVGICs bonded with CAD rather than with ND might be due to the presence of the large amount of calcium phosphate crystals occluding the dentinal tubules; these deposits favor the chemical bonding of the GICs. The histological variation between ND and CAD among carious teeth may explain why authors recorded different bond strengths of some cements to ND and CAD.

Similar to GC Fuji IX GP Fast, Fuji IX GP containing chlorhexidine HVGIC showed nonsignificant μSBS values when bonded to both dentin substrates. Previous studies showed that application of GICs to CHX-conditioned dentin surfaces has no significant effect on the bond strength.[33,34] Inclusion of 1.25% of CHX in HVGIC powder showed an antibacterial effect without causing adverse effects on mechanical properties or bond strength to ND,[10] especially when CHX diacetate was used. The tested Fuji IX contains 1% CHX diacetate,[35] which proved to be a stable material, and being a powdery component, it can be easily mixed and blended with glass-ionomer powder.[10,11] On the other hand, CHX digluconate cannot be easily separated into a powder form or even kept stable in this form. In the Fuji IX GP trial material, the concentration of CHX was kept as low as possible as was recommended. This is because CHX is not involved in the formation of the glass-ionomer matrix. A high amount of CHX would affect the network formation and the properties of the glass ionomer. This study is the first to give an idea about the bond of HVGIC containing CHX to CAD.

Generally, the setting process in Fuji IX GP HVGIC, whether containing CHX or not, like other glass-ionomer resin matrices, is developed through an acid-base reaction between the polyacid liquid and the glass powder.[36] The buildup of aluminum polyalkenoate follows the initial formation of calcium polyalkenoate. This arises in a stepwise reaction characterized mainly by an increase in strength properties over the initial 24 hours. In the reaction, precipitation of the matrix goes on until almost no ions remain in insoluble form.[37] Nevertheless, the formation of zinc-polycarboxylate complexes during the setting of ChemFil Rock GIC enhances the strength more than other complexes consisting of bivalent ions, such as calcium and strontium.[37] A new high-molecular-weight acrylic acid copolymer was also integrated in the ChemFil Rock powder, which could be another reason for the recorded increase of its strength properties[38] besides its filler modifications. In addition, the increment of itaconic

acid in the liquid of ChemFil Rock as a comonomer might play a role in its strength properties. It was reported that incorporation of itaconic acid in the conventional commercial GIC could improve the bond strength compared to compositions without copolymer.[39] Bonding under IPP simulation done in the present study might cause changes in the bonding performance of the tested materials, and this might lead to a difference in the obtained results compared with other studies. The dentin surface was conditioned with polyacrylic acid (20%) prior to the application of GC Fuji IX GP Fast and Fuji IX GP containing chlorhexidine. ChemFil Rock HVGIC was applied, as recommended by the manufacturer's instructions, without preconditioning of the dentin surface. Yet ChemFil Rock HVGIC recorded significantly higher bonding values than that of both other types of Fuji IX GP. The smear-covered dentin surface in the case of ChemFil Rock HVGIC could have reduced the dentin permeability compared to that of preconditioned dentin with the other types. This could be the reason for superior bonding of ChemFil Rock HVGIC, as the wetter surface possibly led to weaker bond for Fuji IX HVGICs.

Mode of failure analysis using SEM has been a compulsory part of bond strength studies. The predominant mode of failure in the present study was mixed, and this finding is consistent in part with Choi and others[40] despite differences in methodology. Nevertheless, a higher percentage of adhesive failure was recorded in the present study. This may be due to the specially constructed attachment used for μSBS testing that permitted the applied force to be directed at the interface. In the current study, there was no difference among the obtained failure modes of any of the tested materials with ND and CAD that supports the bond strength results.

Conclusively, the values of the μSBS of the tested brands of the HVGICs showed that these types can be recommended to restore dentin carious cavities in cases where the ART approach is applied, as their bonding to ND and CAD were comparable. While ChemFil Rock was superior in its bonding compared to the other tested HVGICs, the clinical performance of these HVGICs in stress-bearing areas still needs to be investigated.

CONCLUSIONS

Zinc-reinforced high-viscosity glass-ionomer ChemFil Rock showed superior bonding to ND and CAD compared to GC Fuji IX GP Fast and Fuji IX with chlorhexidine. However, the bonding of each of the tested HVGICs showed comparable bonding to both dentin substrates.

Regulatory Statement

This study was conducted in accordance with all the provisions of the local human subjects oversight committee guidelines and policies of Faculty of Dentistry. The approval code for this study is FDCU-05082013-EM03.

Conflict of Interest

The authors of this article certify that they have no proprietary, financial, or other personal interest of any nature or kind in any product, service, and/or company that is presented in this article.

(Accepted 14 October 2017)

REFERENCES

1. Holmgren CJ, & Frencken JE (2009) Conclusions from the symposium: Two decades of ART: Success through research *Journal of Applied Oral Science* **17(Supplement 17)** 134-136.
2. Bonifacio CC, Kleverlaan CJ, Raggio DP, Werner A, de Carvalho RC, & van Amerongen WE (2009) Physical-mechanical properties of glass ionomer cements indicated for atraumatic restorative treatment *Australian Dental Journal* **54(3)** 233-237.
3. Baig MS, Fleming GJ (2015) Conventional glass-ionomer materials: A review of the developments in glass powder, polyacid liquid and the strategies of reinforcement *Journal of Dentistry* **43(8)** 897-912.
4. Yap AU, Pek YS, & Cheang P (2003) Physico-mechanical properties of a fast-set highly viscous GIC restorative *Journal of Oral Rehabilitation* **30(1)** 1-8.
5. de Almeida Neves A, Coutinho E, Cardoso MV, Lambrechts P, & Van Meerbeek B (2011) Current concepts and techniques for caries excavation and adhesion to residual dentin *Journal of Adhesive Dentistry* **13(1)** 7-22.
6. Frencken JE, Leal SC, & Navarro MF (2012) Twenty-five-year atraumatic restorative treatment (ART) approach: a comprehensive overview *Clinical Oral Investigations* **16(5)** 1337-1346.
7. van 't Hof MA, Frencken JE, van Palenstein Helderman WH, & Holmgren CJ (2006) The atraumatic restorative treatment (ART) approach for managing dental caries: A meta-analysis *International Dental Journal* **56(6)** 345-351.
8. Molina GF, Cabral RJ, Mazzola I, Lascano LB, & Frencken JE (2013) Mechanical performance of encapsulated restorative glass-ionomer cements for use with atraumatic restorative treatment (ART) *Journal of Applied Oral Science* **21(3)** 243-249.
9. Palmer G, Jones FH, Billington RW, & Pearson GJ (2004) Chlorhexidine release from an experimental glass ionomer cement *Biomaterials* **25(23)** 5423-5431.
10. Takahashi Y, Imazato S, Kaneshiro AV, Ebisu S, Frencken JE, & Tay FR (2006) Antibacterial effects and physical properties of glass-ionomer cements containing

chlorhexidine for the ART approach *Dental Materials* **22(7)** 647-652.

11. Turkun LS, Turkun M, Ertugrul F, Ates M, & Brugger S (2008) Long-term antibacterial effects and physical properties of a chlorhexidine-containing glass ionomer cement *Journal of Esthetic Restorative Dentistry* **20(1)** 29-44.
12. Mobarak EH, El-Badrawy W, Pashley DH, & Jamjoom H (2010) Effect of pretest storage conditions of extracted teeth on their dentin bond strengths *Journal Prosthetic Dentistry* **104(2)** 92-97.
13. El-Deeb HA, Al Sherbiney HH, & Mobarak EH (2013) Bond durability of adhesives containing modified-monomer with/without-fluoride after aging in artificial saliva and under intrapulpal pressure simulation *Operative Dentistry* **38(1)** 48-56.
14. Nakajima M, Sano H, Zheng L, Tagami J, & Pashley DH (1999) Effect of moist vs. dry bonding to normal vs. caries-affected dentin with Scotchbond Multi-Purpose Plus *Journal of Dental Research* **78(7)** 1298-1303.
15. Mobarak EH, & El-Badrawy WH (2012) Microshear bond strength of self-etching adhesives to caries-affected dentin identified using the dye permeability test *Journal of Adhesive Dentistry* **14(3)** 245-250.
16. Tedesco TK, Montagner AF, Skupien JA, Soares FZ, Susin AH, & Rocha RO (2013) Starch tubing: An alternative method to build up microshear bond test specimens *Journal of Adhesive Dentisry* **15(4)** 311-315.
17. Carrilho MR, Carvalho RM, de Goes MF, di Hipolito V, Geraldeli S, Tay FR, Pashley DH, & Tjaderhane L (2007) Chlorhexidine preserves dentin bond in vitro *Journal of Dental Research* **86(1)** 90-94.
18. Pereira PN, Nunes MF, Miguez PA, & Swift EJ Jr (2006) Bond strengths of a 1-step self-etching system to caries-affected and normal dentin *Operative Dentistry* **31(6)** 677-681.
19. Komori PC, Pashley DH, Tjaderhane L, Breschi L, Mazzoni A, de Goes MF, Wang L, & Carrilho MR (2009) Effect of 2% chlorhexidine digluconate on the bond strength to normal versus caries-affected dentin *Operative Dentistry* **34(2)** 157-165.
20. Mobarak EH, El-Korashy DI, & Pashley DH (2010) Effect of chlorhexidine concentrations on micro-shear bond strength of self-etch adhesive to normal and caries-affected dentin *American Journal of Dentistry* **23(4)** 217-222.
21. Nakajima M, Kitasako Y, Okuda M, Foxton RM, & Tagami J (2005) Elemental distributions and microtensile bond strength of the adhesive interface to normal and caries-affected dentin *Journal of Biomedical Materials Research Part B: Applied Biomaterials* **72(2)** 268-275.
22. Shibata S, Vieira LC, Baratieri LN, Fu J, Hoshika S, Matsuda Y, & Sano H (2016) Evaluation of microtensile bond strength of self-etching adhesives on normal and caries-affected dentin *Dental Materials Journal* **35(2)** 166-173.
23. Kucukyilmaz E, Savas S, Akcay M, & Bolukbasi B (2016) Effect of silver diamine fluoride and ammonium hexafluorosilicate applications with and without Er:YAG laser irradiation on the microtensile bond strength in sound and caries-affected dentin *Lasers in Surgery and Medicine* **48(1)** 62-69.
24. Zanchi CH, Lund RG, Perrone LR, Ribeiro GA, del Pino FA, Pinto MB, & Demarco FF (2010) Microtensile bond strength of two-step etch-and-rinse adhesive systems on sound and artificial caries-affected dentin *American Journal of Dentistry* **23(3)** 152-156.
25. Ergucu Z, Celik EU, Unlu N, Turkun M, & Ozer F (2009) Effect of Er,Cr:YSGG laser on the microtensile bond strength of two different adhesives to the sound and caries-affected dentin *Operative Dentistry* **34(4)** 460-466.
26. Hosoya Y, Kawada E, Ushigome T, Oda Y, & Garcia-Godoy F (2006) Micro-tensile bond strength of sound and caries-affected primary tooth dentin measured with original designed jig *Journal of Biomedical Materials Research Part B: Applied Biomaterials* **77(2)** 241-248.
27. Mobarak EH (2011) Effect of chlorhexidine pretreatment on bond strength durability of caries-affected dentin over 2-year aging in artificial saliva and under simulated intrapulpal pressure *Operative Dentistry* **36(6)** 649-660.
28. Mohamed MF, El Deeb HA, Gomaa IE, & Mobarak EH (2015) Bond durability of different resin cements to caries-affected dentin under simulated intrapulpal pressure *Operative Dentistry* **40(3)** 293-303.
29. Wei S, Sadr A, Shimada Y, & Tagami J (2008) Effect of caries-affected dentin hardness on the shear bond strength of current adhesives *Journal of Adhesive Dentisry* **10(6)** 431-440.
30. Alves FB, Hesse D, Lenzi TL, Guglielmi Cde A, Reis A, Loguercio AD, Carvalho TS, & Raggio DP (2013) The bonding of glass ionomer cements to caries-affected primary tooth dentin *Pediatric Dentistry* **35(4)** 320-324.
31. Lenzi TL, Bonifacio CC, Bonecker M, Amerongen WE, Nogueira FN, & Raggio DP (2013) Flowable glass ionomer cement layer bonding to sound and carious primary dentin *Journal of Dentistry for Children* **80(1)** 20-24.
32. Yoshida Y, Van Meerbeek B, Nakayama Y, Snauwaert J, Hellemans L, Lambrechts P, Vanherle G, & Wakasa K (2000) Evidence of chemical bonding at biomaterial-hard tissue interfaces *Journal of Dental Research* **79(2)** 709-714.
33. Czarnecka B, Deregowska-Nosowicz P, Limanowska-Shaw H, & Nicholson JW (2007) Shear bond strengths of glass-ionomer cements to sound and to prepared carious dentine *Journal of Materials Science: Materials in Medicine* **18(5)** 845-849.
34. Botelho MG (2005) The microtensile bond strength of Fuji IX glass ionomer cement to antibacterial conditioned dentin *Operative Dentistry* **30(3)** 311-317.
35. Cunningham MP, & Meiers JC (1997) The effect of dentin disinfectants on shear bond strength of resin-modified glass-ionomer materials *Quintessence International* **28(8)** 545-551.
36. Frencken JE, Imazato S, Toi C, Mulder J, Mickenautsch S, Takahashi Y, & Ebisu S (2007) Antibacterial effect of chlorhexidine-containing glass ionomer cement in vivo: A pilot study *Caries Research* **41(2)** 102-107.

37. Wilson AD, & Mclean JW (1988). *Glass-Ionomer Cement* Quintessence Publishing Chicago.

38. Zoergiebel J, & Ilie N (2013) Evaluation of a conventional glass ionomer cement with new zinc formulation: Effect of coating, aging and storage agents *Clinical Oral Investigations* **17(2)** 619-626.

39. Boyd D, & Towler MR (2005) The processing, mechanical properties and bioactivity of zinc based glass ionomer cements *Journal of Materials Science: Materials in Medicine* **16(9)** 843-850.

40. Moshaverinia A, Roohpour N, Darr JA, & Rehman IU (2009) Synthesis and characterization of a novel N-vinylcaprolactam-containing acrylic acid terpolymer for applications in glass-ionomer dental cements *Acta Biomaterials* **5(6)** 2101-2108.

41. Choi K, Oshida Y, Platt JA, Cochran MA, Matis BA, & Yi K (2006) Microtensile bond strength of glass ionomer cements to artificially created carious dentin *Operative Dentistry* **31(5)** 590-597.

Departments

Faculty Positions

THE UNIVERSITY OF IOWA
COLLEGE OF DENTISTRY & DENTAL CLINICS

IOWA – OPERATIVE DENTISTRY - DEO

The University of Iowa's College of Dentistry is conducting a search for the **Department Executive Officer (DEO) for the Department of Operative Dentistry**. This is a full-time tenure-track position. Available July 1, 2019. Must have: DDS/DMD degree or equivalent; completion of advanced education in degree-based graduate training program in Operative Dentistry, or related field, from CODA-accredited dental school; substantial record of scholarship, e.g. history of research funding and scholarly publications; evidence of current relevant teaching experience; and demonstrated experience working effectively in diverse environment. Desirable: relevant administrative experience; extensive clinical experience; and active research program w/demonstrated funding by NIH or equivalent agencies. Academic rank/salary commensurate with qualifications/experience. Learn more and/or apply at Jobs@UIowa at https://jobs.uiowa.edu/faculty/view/73518, reference **Req #73518**. *The University of Iowa is an equal opportunity/affirmative action employer. All qualified applicants are encouraged to apply and will receive consideration for employment free from discrimination on the basis of race, creed, color, national origin, age, sex, pregnancy, sexual orientation, gender identity, genetic information, religion, associational preference, status as a qualified individual with a disability, or status as a protected veteran*.

Online Only Articles

On occasion we receive manuscripts that we would like to publish, but do not have the page room to include in the print journal. For the full article, please go to www.jopdentonline.org or enter the provided address into your address bar.

Direct Posterior Restorations: A 13-Year Survey of Teaching Trends and Use of Materials

A Zabrovsky • R Mahmoud • N Beyth • G Ben-Gal

Clinical Relevance: The increasing trend toward composite posterior restorations in an educational environment during a 13-year period may reflect movement toward an amalgam-free era.

doi: https://doi.org/10.2341/17-361-C

Effect of Irradiance and Exposure Duration on Temperature and Degree of Conversion of Dual-Cure Resin Cement for Ceramic Restorations

JS Shim • SH Han • N Jha • ST Hwang • W Ahn • JY Lee • JJ Ryu

Clinical Relevance: Providing longer exposure durations can be an efficient strategy to compensate for attenuated light through ceramic restorative materials in order to achieve a high degree of conversion. However, continuous irradiation with high irradiances for long durations will yield a higher temperature. Providing pauses in the irradiation to avoid continuous accumulation of energy that increases the temperature is recommended.

doi: https://doi.org/10.2341/17-283-L

Benefits of Nonthermal Atmospheric Plasma Treatment on Dentin Adhesion

AP Ayres • PH Freitas • J De Munck • A Vananroye C Clasen • CT dos Santos Dias • M Giannini • B Van Meerbeek

Clinical Relevance: After two years of water aging, the application of nonthermal atmospheric plasma onto dentin for 30 s showed higher microtensile bond strength of a multimode adhesive applied in etch-and-rinse mode. Plasma-treated dentin also resulted in higher nanohardness and Young's modulus of the hybrid layer in immediate evaluation and greater hydrophilicity.

doi: https://doi.org/10.2341/17-123-L

Cuspal Flexure and Stress in Restored Teeth Caused by Amalgam Expansion

BT Danley • BN Hamilton • D Tantbirojn • RE Goldstein • A Versluis

Clinical Relevance: Although amalgam is being phased out, existing amalgam fillings will still be present for many years. Clinicians should be aware that amalgam expansion may create stress conditions that accelerate tooth cracking.

doi: https://doi.org/10.2341/17-329-L

Comparison of the Efficacy of Different Fluoride Varnishes on Dentin Remineralization During a Critical pH Exposure Using Quantitative X-Ray Microtomography

A Sleibi • A Tappuni • D Mills • GR Davis • A Baysan

Clinical Relevance: The application of dental varnish containing fluoride on demineralized dentin can remineralize and protect dentin lesions, but there might be no additional benefit to incorporating calcium and phosphate to enhance the remineralization of dentin caries.

doi: https://doi.org/10.2341/18-014-L

This page was intentionally left blank.

©Operative Dentistry, 2018, **43-6,** E273-E279

Direct Posterior Restorations: A 13-Year Survey of Teaching Trends and Use of Materials

A Zabrovsky • R Mahmoud • N Beyth • G Ben-Gal

Clinical Relevance

The increasing trend toward composite posterior restorations in an educational environment during a 13-year period may reflect movement toward an amalgam-free era.

SUMMARY

Objective: The study aimed to evaluate teaching trends and use of materials in direct posterior restorations during a 13-year period in an Israeli dental school.

Methods: Data registered in computerized files, relating to posterior restorations performed in the student clinic during the past 13 years (2004-2016), were collected. The restorative materials used (ie, amalgam vs composite), the type of tooth, and the number of surfaces restored were analyzed.

Results: Data analysis included 26,925 restorations performed during 13 years. The number of one-surface composite restorations increased from 54.7% (n=330) to 81.9% (n=873). Two-surface restorations increased from 33.3% (n=254) to 64.3% (n=721). The percentage of amalgam restorations in three-surface restorations decreased from 72.08% to 51.34% (n=173). Analysis of tooth type showed that in 2016, the number of composite restorations performed in premolars reached 80.87% (n=723) and in molars 63.50% (n=1035). The percentage of composite restorations in the mandible and the maxilla was virtually equal.

Conclusions: A clear trend in favor of composite resin restorations is evident in the 13-year survey and suggests a move toward an amalgam-free era.

†Asher Zabrovsky, DMD, Department of Prosthodontics, Hadassah School of Dental Medicine, Hebrew University, Jerusalem, Israel

*†Reema Mahmoud, Department of Prosthodontics, Hadassah School of Dental Medicine, Hebrew University, Jerusalem, Israel

Nurit Beyth, DMD, PhD, Department of Prosthodontics, Hadassah School of Dental Medicine, Hebrew University, Jerusalem, Israel

Gilad Ben-Gal, DMD, MSc, PhD, Department of Prosthodontics, Hadassah School of Dental Medicine, Hebrew University, Jerusalem, Israel

*Corresponding author: PO Box 12272, Jerusalem 91120 Israel; e-mail: reema.mahmoud@mail.huji.ac.il

†Authors contributed equally to this work.

DOI: 10.2341/17-361-C

INTRODUCTION

For more than 150 years, amalgam was the primary material used for dental restorations.[1] Today, composite resin materials, due to their esthetic and adhesive properties, are overtaking amalgam. The significant improvements in their physical properties in recent years have increased their prevalence, making them the material of choice in various clinical applications.[2]

Composite resin restorations were first used as anterior restorations. By the late 1990s, it was recommended that the principal use of direct composite resin restorations also include posterior restorations but be limited to permanent teeth with conservative small class 1 and class 2 restorations. This recommendation included preferably premolar teeth with little, if any, occlusal function, and mainly in patients maintaining a high standard of oral hygiene.[3]

Similar trends were observed in dental education. In the course of 25 years, there has been a steady increase in the use of composite resin materials for posterior tooth restoration. Whereas in the mid-1980s 90% of the dental school curricula did not include any consistent teaching of posterior composite resins, the percentage dropped to 4% in the late 1990s and to 0% by the early 2000s. Moreover, today some universities teach composite restoration before introducing amalgam.[4,5]

A comprehensive study compared three schools in three countries (Sweden, Wales, and Ireland) differing in their health care systems, financial remuneration schemes, and regulatory bodies. It found a direct relationship between the number of hours allocated to teaching the placement of posterior resin composites and the students' own perception of the adequacy of their learning combined with confidence in using these materials in clinical procedures. It is conceivable that students who are not confident in performing certain procedures may steer away from using these techniques in the future and may even remain incompetent in these specific procedures for some time.[4]

Guidelines of the Association for Dental Education in Europe maintained that new dentists must be competent "to restore the tooth appropriately to form, function and esthetics with different appropriate materials." Similarly, the UK General Dental Council recommends that new graduates should be qualified in "completing a wide range of procedures in restorative dentistry, including the use of amalgam alloy restorations and tooth-colored restorations."[6]

The present study aimed to evaluate current teaching trends, including the methods and materials used for direct restoration of posterior teeth and to evaluate whether the types of restoration performed by undergraduate students could serve as a predictive tool, with emphasis on the preference for composite materials over amalgam.

METHODS

All direct restorations performed by graduate students at the Hebrew University of Jerusalem's Hadassah School of Dental Medicine between 2004 and 2016 were registered and evaluated. The Faculty of Dental Medicine runs a six-year program in which students treat patients from the fourth year. Treatments were performed in the student clinic by students in their fourth, fifth, and sixth year of studies and supervised by experienced instructors. The duration of the clinic differs between clinical years. Fourth-year students have a six-hour clinic per week, while fifth- and sixth-year students have a 10- and 11- hour clinic, respectively.

Clinical decisions, including material choice, were supervised by instructors from the Department of Prosthodontics. The instructors' experience varied, ranging from one to 40 years.

Each treatment was documented in a computerized file. The medical records were signed by the instructors for every procedure for medical, legal, and monitoring purposes.

Data relating to tooth type, number of surfaces restored, and restoration material (amalgam/composite) were included.

For comparison, the types of restorative materials used were divided into three groups, according to the number of surfaces restored (one, two, and three), type of tooth (molars vs premolars), and jaw (maxilla vs mandible).

The data were arranged and displayed according to frequency tables and scatter charts.

RESULTS

A total of 26,925 restorations were performed in posterior teeth by undergraduate students at the Hadassah School of Dental Medicine from 2004 to 2016. During this 13-year period, the restorative material distribution was almost equal; that is, 49.54% (n=13,338) of the restorations performed were amalgam, and 50.46% (n=13,587) were composite resin. The shift in material choice may be seen in Figure 1. From 2004 to 2008, the material of choice was amalgam. From 2008 to 2012, a similar number of amalgam and composite restorations were performed. The year 2012 marked a turning point, composite resin becoming the dominant material, its use steadily rising.

The results were analyzed further on the basis of surface number (Figure 2). The predominance of one-surface composite restorations was clear, increasing from 54.7% (n=330) in 2004 to 81.9% (n=873) in 2016, whereas amalgam restorations dropped to 18.11% (n=193). The situation was slightly different

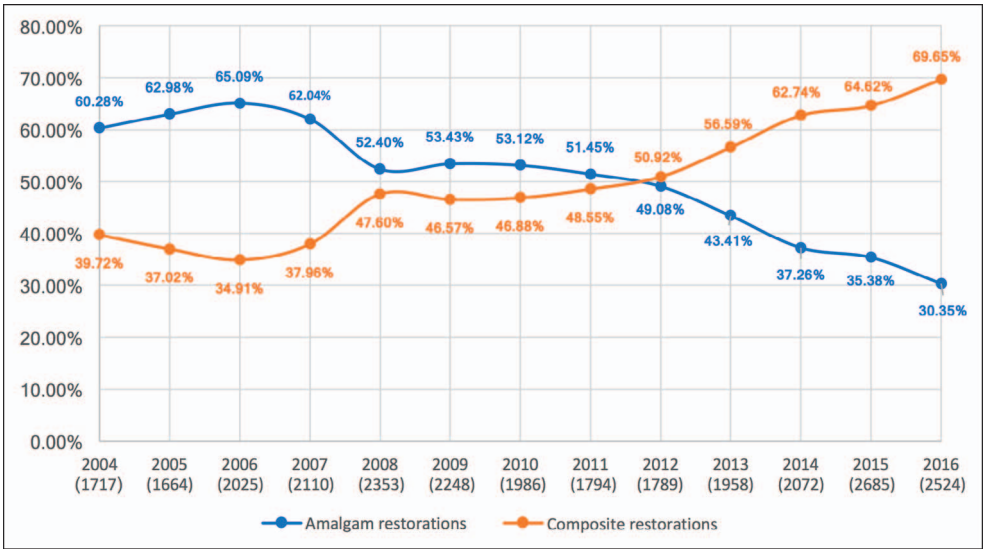

Figure 1. *Percentage of amalgam and composite restorations placed in posterior teeth by graduate students from 2004 to 2016. Numbers in parentheses indicate the number of restorations performed in the same year.*

regarding two-surface restorations. The number of amalgam restorations exceeded the number of composite restorations until 2013. After that, composite restorations were preferred over amalgam. The trend during the study period was clear: from one-third, 33.3% (n=254), of the two-surface restorations in 2004 to almost two-thirds, 64.3% (n=721), in 2016. Three-surface restorations showed a similar trend. Whereas in 2004 amalgam restorations were of significantly higher proportion than composite restorations, 72.08% vs 27.92% (n=253 vs n=98), in 2016 the percentage of amalgam restorations dropped to 51.34% (n=173).

The percentage of restorations in the premolar and molar groups is depicted in Figure 3. As can be seen, since 2010, at the expense of amalgam restorations, there has been a steady and constant increase in the percentage of composite restorations in premolars,

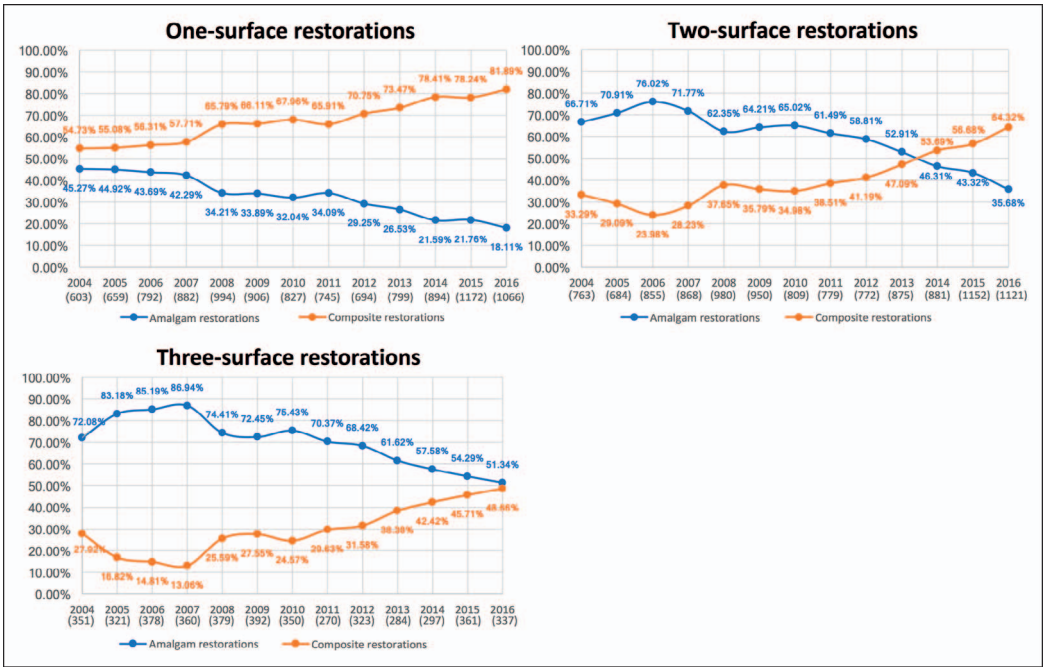

Figure 2. *Percentage of amalgam and composite restorations placed by undergraduate students from 2004 to 2016, divided by surface number.*

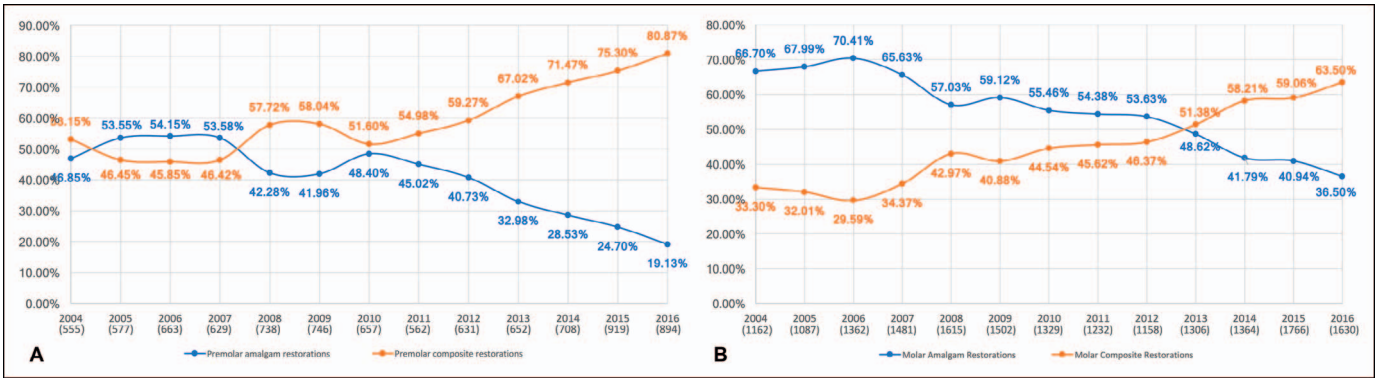

Figure 3. *(A): Percentage of amalgam and composite restorations placed in premolars by graduate students from 2004 to 2016. (B): Percentage of amalgam and composite restorations placed in molars by graduate students from 2004 to 2016.*

which by 2016 reached 80.87% (Figure 3A). In molars, as shown in Figure 3B, the percentage of amalgam restorations in 2004 was 66.70% (n=775) and that of composite restorations 33.30% (n=387). The shift toward composite restorations was gradual, the balance tilting to 63.5% (n = 1035) by 2016.

Restorations in relation to tooth location (first premolar, second premolar, first molar, second molar, and third molar) in both jaws showed a decreasing percentage of composite resin restorations with distal advance (Figure 4.)

A comparison between the maxilla and the mandible shows no noticeable differences between the trends (Figure 5.)

DISCUSSION

During the 13-year period of the study, composite resin became the dominant restorative material, the turning point evident in 2008. A growing transition toward composite resin restorations and a continuous reduction in amalgam shifted the ratio in favor of composite resin restorations in 2012 with a steady linear increase in one-, two-, and three-surface restorations, both in molars and in premolars, regardless of jaw. The shift in trend of the premolar group preceded that of the molar group. This is most likely related to esthetic considerations. Nonetheless, in three-surface restorations, slightly larger amounts of amalgam restorations were observed. It is likely that the overall trend, as in other worldwide dental faculties,[4,7] is adapting itself to the global trend toward an amalgam-free era.

The shift in treatment can be accounted for by numerous reasons. Composite materials have the ability to bond mechanically to the remaining tooth tissues, thereby strengthening the tooth's structure, restoring its original physical integrity and biomechanical properties.[9] Yet the main reason is most likely the increased awareness of the advantage of a minimally invasive approach in treating caries.[2,8] Recent developments in restorative dentistry show that the "extension for prevention" traditional guideline should be avoided and "minimally invasive dentistry" techniques promoted instead. This would avoid unnecessary excessive removal of healthy dental tissue as part of the treatment, leaving the restored teeth with a better overall prognosis and a greater ability to withstand loading in function.[1,8]

Another reason for the increase in composite use may be the sectional matrix systems that were introduced in 2008.[9] These include not only advanced anatomic wave-like wedges but also redesigned bands and grooved, V-shaped tine rings covered with silicone, allowing proper anatomy and tight proximal contact areas,[10] formerly considered problematic, in composite restorations.

Furthermore, the unceasing development of new materials and instruments, as well as improved composite resin material properties and performance, advocated more frequent use of such materials in the posterior area. For one, the new bulk-fill materials (like SDR from Dentsply and Filtek Bulk-Fill from 3M ESPE) probably contributed to favoring composite materials by reducing technique sensitivity[11] and procedure duration.[12] Other contributing factors may be newer, advanced adhesive systems, self-etch, and 10-methacryloyloxydecyl dihydrogen-phosphate–containing materials.[13] In addition, practitioners have had several years of experience with these materials, mastering the techniques required to handle them and perfect their use.[4] This probably also plays a major role in relying on composite materials and abandoning amalgam.

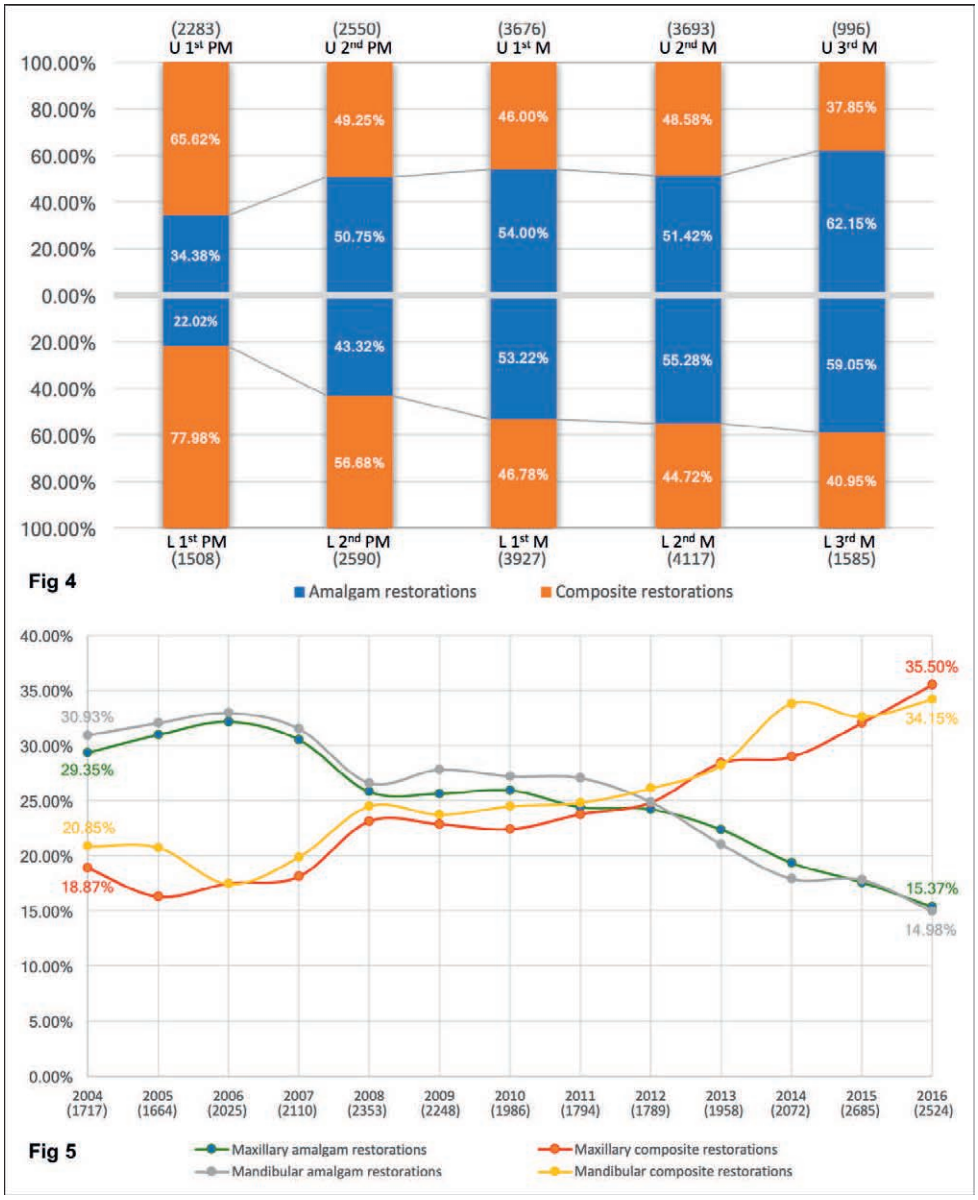

Figure 4. *Percentage of amalgam and composite restorations placed from 2004 to 2016 according to tooth order. U, upper; L, lower; M, molar; PM, premolar.*

Figure 5. *Percentage of amalgam and composite restorations placed in the maxilla and the mandible by graduate students from 2004 to 2016.*

Another contributing factor is the accumulating evidence that the overall performance of the posterior composite resin restorations is high[14] and at least comparable to that of amalgam restorations in many clinical settings.[15,16] Although the annual failure rate of composite restorations is still slightly higher than that of amalgam restorations, it is likely that in future studies the annual failure rate of posterior composite resins will be lower than those found in the present reviews.[14,17,18]

Patients also play an important role in these changes. The awareness and demand for an esthetic outcome, as well as the controversy over amalgam safety, have increased patient preference for composite resin restorations.

The amalgam debate is a driving force in the shift. Environmental pollution caused by medical waste containing mercury is a political issue in some countries. In Norway, for example, the use of amalgam has been banned from 2008,[19] and it appears that similar bills, based mostly on this environmental background, are being promoted in other European countries.[20] In 2013, the Minamata Convention (a World Health Organization committee dealing with the effects of mercury on the environment) committed itself to reducing and limiting the use and production of a range of mercury-containing products, including dental amalgam.[2]

In March 2017, the European Parliament agreed to prohibit by July 2018 the general use of amalgam

in children under 15 years of age and pregnant or breast-feeding women and required member states to draft national plans for phasing down the use of dental amalgam by July 2019, aiming to phase it out by 2022.[21]

These decisions, especially that of the Minamata Convention, have encouraged the production of alternatives to amalgam, causing an irrevocable change of what is customary in restorative dentistry,[1] as reflected also in the present study.

The present findings express the confidence and trust of clinical instructors in using composite resin materials to restore posterior teeth. Moreover, the young generation of instructors who has joined the more experienced ones may also have contributed to the increasing use of composite restorations due to their clear preference for esthetic materials.[22]

It is apparent that the change in trend observed over the past 13 years is on the rise. This change seems consistent with what is happening in other schools of dentistry worldwide.

Although few studies addressed the changes, data from 2011 in the United States showed that posterior composite restorations (for both one and two surfaces) exceeded amalgam restorations in number. In three- and four-surface restorations, similar to our study, amalgam was still the material of choice.[5] In Ireland and the United Kingdom, in the period between 2005 and 2010, a 33% drop in the number of amalgam restorations performed by students was recorded, whereas the number of posterior composite resin restorations increased by 180%.[7]

It is reasonable to assume that the change in trend observed within the faculty will be further reflected in the choices the young graduates will make. It should be emphasized that clinical instructors pass on their own practice methods to their students and that the educational experiences students accumulate throughout their studies contribute to their competency and determine the techniques they will use in their postgraduate practices as independent dentists. Students who graduated in 2008 and thereafter will be practicing dentistry for many decades in the future, making them the leading dentists of the global trend of the shift toward composite resin materials.

CONCLUSIONS

In conclusion, a clear trend in favor of composite resin restorations is evident in this 13-year survey. These results may suggest that the next generation of dentists will favor resin composite restoration, thus moving toward an amalgam-free era.

Regulatory Statement

This study was conducted in accordance with all the provisions of the local human subjects oversight committee guidelines and policies of approval of the Helsinki Ethics Committee. The approval code for this study is 0488-16-HMO.

Conflict of Interest

The authors of this manuscript certify that they have no proprietary, financial, or other personal interest of any nature or kind in any product, service, and/or company that is presented in this article. This research did not receive any specific grant from funding agencies in the public, commercial, or nonprofit sectors.

(Accepted 8 March 2018)

REFERENCES

1. Lynch CD, & Wilson NH (2013) Managing the phase-down of amalgam: Part I. Educational and training issues *British Dental Journal* **215(3)** 109-113.
2. Alexander G, Hopcraft MS, Tyas MJ, & Wong RHK (2014) Dentists' restorative decision-making and implications for an "amalgamless" profession. Part 1: A review *Australian Dental Journal* **59(4)** 408-419.
3. Wilson NH, Dunne SM, & Gainsford ID (1997) Current materials and techniques for direct restorations in posterior teeth. Part 2: Resin composite systems *International Dental Journal* **47(4)** 185-193.
4. Lynch CF, Guillem SE, Nagrani B, Gilmour AS, & Ericson D (2010) Attitudes of some European dental undergraduate students to the placement of direct restorative materials in posterior teeth *Journal of Oral Rehabilitation* **37(12)** 916-926.
5. Rey R, Nimmo S, Childs GS, & Behar-Horenstein LS (2015) Curriculum time compared to clinical procedures in amalgam and composite posterior restorations in U.S. dental schools: A preliminary study *Journal of Dental Education* **79(3)** 331-336.
6. Plasschaert AJM, Holbrook WP, Delap E, Martinez C, & Walmsley AD (2005) Profile and competences for the graduating European *European Journal of Dental Education* **9(3)** 98-107.
7. Lynch CD, Frazier KB, McConnell RJ, Blum IR, & Wilson NH (2010) State-of-the-art techniques in operative dentistry: Contemporary teaching of posterior composites in UK and Irish dental schools *British Dental Journal* **209(3)** 129-136.
8. Wilson NH, & Lynch CD (2014) The teaching of posterior resin composites: Planning for the future based on 25 years of research *Journal of Dentistry* **42(3)** 503-516.
9. Owens BM, & Phebus JG (2016) An evidence-based review of dental matrix systems *General Dentistry* **64(5)** 64-70.
10. Freedman GA (2012) Posterior direct composites In: *Contemporary Esthetic Dentistry* Mosby, St Louis MO 244-266.
11. Van Dijken JWV, & Pallesen U (2014) A randomized controlled three year evaluation of bulk-filled posterior

resin restorations based on stress decreasing resin technology *Dental Materials* **30(9)** 245-251.

12. Flury S, Peutzfeldt A, & Lussi A (2014) Influence of increment thickness on microhardness and dentin bond strength of bulk fill resin composite *Dental Materials* **30(10)** 1104-1112.
13. The Dental Advisor (2012) 3M ESPE Scotchbond Universal Adhesive; Retrieved online May 13, 2017 from https://www.dentaladvisor.com/evaluations/3m-espe-scotchbond-universal-adhesive
14. Ástvaldsdóttir Á, Dagerhamn J, Van Dijken JWV, Naimi-Akbar A, Sandborgh-Englund G, Tranæus S, & Nilsson M (2015) Longevity of posterior resin composite restorations in adults—A systematic review *Journal of Dentistry* **43(8)** 934-954.
15. Opdam NJ, Bronkhorst EM, Roeters JM, & Loomans BA (2007) A retrospective clinical study on longevity of posterior composite and amalgam restorations *Dental Materials* **23(1)** 2-8.
16. Opdam NJ, Bronkhorst EM, Loomans BA, & Huysmans MC (2010) 12-year survival of composite vs. amalgam restorations *Journal of Dental Research* **89(10)** 1063-1067.
17. Demarco FF, Corrêa MB, Cenci MS, Moraes RR, & Opdam NJ (2012) Longevity of posterior composite restorations: Not only a matter of materials *Dental Materials* **28(1)** 87-101.
18. Moraschini V, Fai CK, Alto RM, & Dos Santos GO (2015) Amalgam and resin composite longevity of posterior restorations: A systematic review and meta-analysis *Journal of Dentistry* **43(9)** 1043-1050.
19. Norwegian Ministry of the Environment (2007) Amendment of regulations of 1 June 2004 no 922 relating to restrictions on the use of chemicals and other products hazardous to health and the environment (product regulations) *Oslo: Norwegian Ministry for the Environment*.
20. Lynch CD, & Wilson NH (2013) Managing the phase-down of amalgam: Part II. Implications for practising arrangements and lessons from Norway *British Dental Journal* **215(4)** 159-162.
21. Bourguignon D (2017) Mercury: Aligning EU legislation with Minamata. EPRS European Parliamentary Research Service. Retrieved online May 13, 2017 from: http://www.europarl.europa.eu/RegData/etudes/BRIE/2017/595887/EPRS_BRI(2017)595887_EN.pdf
22. Ben-Gal G, & Weiss EI (2011) Trends in material choice for posterior restorations in an Israeli dental school: Composite resin versus amalgam *Journal of Dental Education* **75(12)** 1590-1595.

©Operative Dentistry, 2018, **43-6,** E280-E287

Effect of Irradiance and Exposure Duration on Temperature and Degree of Conversion of Dual-Cure Resin Cement for Ceramic Restorations

JS Shim • SH Han • N Jha • ST Hwang • W Ahn • JY Lee • JJ Ryu

Clinical Relevance

Providing longer exposure durations can be an efficient strategy to compensate for attenuated light through ceramic restorative materials in order to achieve a high degree of conversion. However, continuous irradiation with high irradiances for long durations will yield a higher temperature. Providing pauses in the irradiation to avoid continuous accumulation of energy that increases the temperature is recommended.

SUMMARY

This study investigated the effects of irradiance and exposure duration on dual-cured resin cements irradiated through ceramic restorative materials. A single light-curing unit was calibrated to three different irradiances (500, 1000, and 1500 mW/cm^2) and irradiated to three different attenuating materials (transparent acryl, lithium disilicate, zirconia) with 1-mm thicknesses for 20 or 60 seconds. The changes in irradiance and temperature were measured with a radiometer (or digital thermometer) under the attenuating materials. The degree of conversion (DC) of dual-cure resin cement after irradiation at different irradiances and exposure durations was measured with Fourier transform near infrared spectroscopy. Two-way analysis of variance revealed that irradiance ($p<0.001$) and exposure duration ($p<0.001$) significantly affected temperature and DC. All groups showed higher DCs with increased exposure times ($p<0.05$),

†Ji Suk Shim, DDS, MSD, Korea University Ansan Hospital, Prosthodontics, Gyeonggi-do, Republic of Korea

†Seok Hwan Han, DDS, MSD, Korea University Graduate School, Medicine, Seoul, Republic of Korea

Nayansi Jha, BDS, Korea University Graduate School, Medicine, Seoul, Republic of Korea

Sung Taek Hwang, Korea University Graduate School, Medicine, Seoul, Republic of Korea

Woobeam Ahn, Korea University Graduate School, Medicine, Seoul, Republic of Korea

Jeong Yol Lee, DDS, PhD, Korea University Guro Hospital, Prosthodontics, Seoul, Republic of Korea

*Jae Jun Ryu, DDS, PhD, Korea University Anam Hospital, Prosthodontics, Seoul, Republic of Korea

*Corresponding author: 73, Inchon-ro, Seongbuk-gu, Seoul 02841, Republic of Korea; e-mail: koprosth@unitel.co.kr

†Authors Shim and Han contributed equally to this work.

DOI: 10.2341/17-283-L

but there were no statistically significant differences between the groups irradiated with 1000 mW/cm^2 and 1500 mW/cm^2 ($p>0.05$). Higher-intensity irradiances yielded higher temperatures ($p<0.05$), but exposure time did not affect temperature when materials were irradiated at 500 mW/cm^2 ($p>0.05$).

INTRODUCTION

Dual-cure resin composite uses both light and chemical initiation to activate polymerization. Adequate light curing is essential to achieve the sufficient polymerization rates of dual-cure resins, as autopolymerization without photopolymerization yields lower polymerization rates compared with dual polymerization.[1,2] Moreover, adequate initial polymerization through light curing is critical for the success of restorations, given that restorations are exposed to masticatory force, saliva, and foods before autopolymerization is sufficiently processed, and these clinical circumstances may lead to material resorption and degradation.[3,4]

Dual-cure resin cements are commonly used to cement ceramic restorative materials, given their color stability and sufficient working times.[5] In this case, initial polymerization of dual-cure resin cements depends on the curing light that reaches luting materials after passage through the ceramics.[6] The irradiance from curing lights is attenuated by ceramics, and clinical trials to compensate for the lack of degree of conversion (DC) are necessary. Using higher irradiances or providing longer exposure durations may be the solution.[7,8]

Currently, light-emitting diode (LED) units are popularly applied in clinical practice. LED units are smaller and wireless[9] and have a longer lifetime (1000 hours with constant light output).[10] Although first-generation LED units have a limited output with an irradiance less than 400 mW/cm^2,[11] LED units recently released on the market can deliver much higher light irradiances (greater than 2000 mW/cm^2), facilitating reduced exposure times. Previous studies evaluating the effects of curing light irradiance on polymerization modes of resin composites used different light sources; quartz tungsten halogen and LED were used as lower-irradiance light sources, and plasma-arc lamps and argon-ion laser were used as higher-irradiance light sources. Each light source has typical wavelengths and characteristics,[12] and comparing the effects of irradiance with different light sources cannot be accurately indicative of the relation between irradiance and polymerization because polymerization aspects can be affected by the spectral emission of light sources.[13,14]

Temperature can be a critical factor affecting polymerization kinetics and the biologic homeostasis of pulp. Increasing temperatures during polymerization promote free radical and monomer mobility[15] and lead to higher polymerization rates and elevated DCs. In addition, external thermal irritation may cause irreversible changes of pulp tissue,[16] and temperature increases in restorative materials have substantial effects because a thinner dentin wall remains between the restorative material and pulp after tooth preparation. Increasing irradiance and exposure duration causes temperatures to rise,[17] and measuring temperature changes, as a result of irradiating at various irradiances and exposure durations, is significant to the clinical outcome.

The purpose of this study was to evaluate the effects of irradiance and exposure duration on the DCs of dual-cure resin cements and temperature changes of restorative materials. For this, three irradiances (500, 1000, 1500 mW/cm^2) were simulated with a single LED light-curing unit (LCU) by combining various ceramic restorations and exposure times, and the degrees of conversion and changes to temperature were evaluated. The null hypothesis was that irradiance and exposure duration have no effect on DC or temperature.

METHODS AND MATERIALS

Specimen Preparation

Figure 1 shows the methods for preparing specimens and irradiating with attenuating materials. A glass slide was positioned at the center of an infrared spectroscopy measuring block and fixed with cellulose tape. Mixed resin cements were applied to the center, and a second glass slide was used to cover the resin cement. The thickness of resin cement was determined by the thickness of the cellular tape (40 μm). A dual-cure resin cement, G-CEM LinkAce (GC Corporation, Tokyo, Japan; Lot 1604071), was used with Automix mixing tips.

Light Curing With Various Materials and Measuring Irradiance and Temperature

A single LED light LCU (Dr's Light, Good Doctors Co, Incheon, Korea) was used in this study. The output of the LCU was manually calibrated, varying the pulse width of LED using a microcontroller controlling the duty cycle of LED. The pulse width modulation is the efficient method to control the output of LED with high resolution.[18] The calibrated

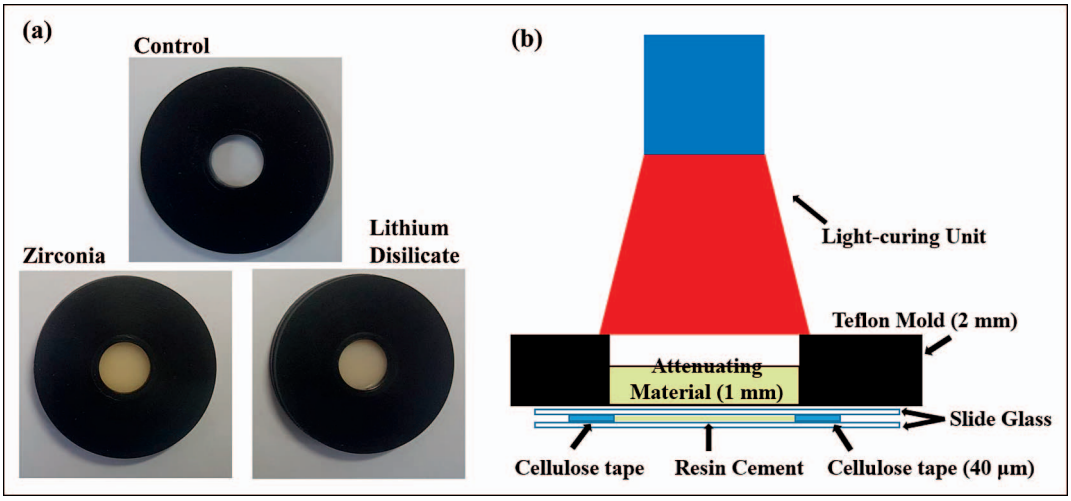

Figure 1. *(a): Teflon molds with different attenuating materials. (b): An illustration of the methods for specimen preparation and irradiation (sagittal view). Measuring irradiance (or temperature) was performed with the same molds, not specimens, overlying a radiometer (or digital thermometer).*

irradiances were confirmed with a radiometer (LED radiometer; Good Doctors Co). The LCU was set up to emit three different light irradiances: low (≈500 mW/cm^2), medium (≈1000 mW/cm^2), and high (≈1500 mW/cm^2). Temperature changes after irradiation were measured with a contact-type digital thermometer (digital thermometer 367DN, TPI, Inchon, Korea) contacting the tip of the thermometer under the center of attenuating material. The temperature was measured at room temperature (24°C), and irradiance and temperature were measured six times each. Light curing was always performed with Teflon molds, and a 2-mm distance from the curing unit tip to each object was provided.

As the three light irradiances were exposed to specimens for 20 or 60 seconds, six different irradiating methods were used in this study. Twenty-seven specimens were prepared for each irradiation method, divided into three groups (n=9) depending on the materials overlying the specimens during light exposure: control, zirconia, and lithium disilicate (Table 1). The control group specimens were light cured through a transparent acrylic plate. For the zirconia and lithium disilicate groups, light curing was applied through the discs with A2 shades composed of translucent zirconia (LAVA Plus, 3M Deutschland GmbH, Neuss, Germany) or lithium disilicate (IPS e.max Press HT ingots, Ivoclar-Vivadent AG, Schaan, Liechtenstein). All attenuating materials had a thickness of 1 mm.

Infrared Spectroscopy Measurements

The DC of the resin cement was evaluated using Fourier transform near infrared spectroscopy (NIR-Solutions, BUCHI, Flawil, Switzerland). Absorbance spectrums were examined by scanning the specimens 10 times over a 10,000- to 4000-cm^{-1} range, with a resolution of 4 cm^{-1}. To calculate DCs, the area of the peak corresponding to vinyl stretching at 6165 cm^{-1} was used.[19] The DCs were calculated from the ratio of the peak area in the monomeric to polymeric states, using the following formula:

$$DC(\%) = (1 - \text{area}_{\text{polymer}}/\text{area}_{\text{monomer}}) \times 100$$

Statistical Analysis

The mean and standard deviation (SD) temperatures and DCs were acquired for each group. Data were evaluated for homogeneity of variance based on

Table 1: *Experiment Study Design*[a]

Attenuating Materials\ Irradiating Methods	Low Irradiance (500 mW/cm^2)		Medium Irradiance (1000 mW/cm^2)		High Irradiance (1500 mW/cm^2)	
	20 s	60 s	20 s	60 s	20 s	60 s
Transparent acryl (control)	C-L20 (n=9)	C-L60 (n=9)	C-M20 (n=9)	C-M60 (n=9)	C-H20 (n=9)	C-H60 (n=9)
Lithium disilicate	L-L20 (n=9)	L-L60 (n=9)	L-M20 (n=9)	L-M60 (n=9)	L-H20 (n=9)	L-H60 (n=9)
Zirconia	Z-L20 (n=9)	Z-L60 (n=9)	Z-M20 (n=9)	Z-M60 (n=9)	Z-H20 (n=9)	Z-H60 (n=9)

[a] *n indicates the number of specimens.*

Table 2: *Irradiance Reaching Sensor for Light Curing Through Different Attenuating Materials (Mean [SD]), and the Reduction of Irradiance by Ceramic Materials*

Attenuating Material	Irradiance, mW/cm^2					
	Low Irradiance		Medium Irradiance		High Irradiance	
Control	494.2 (15.1)	Reduction, %[a]	1034.6 (11.9)	Reduction, %[a]	1486.2 (9.7)	Reduction, %[a]
Lithium disilicate	135.5 (2.1)	27.4	329.3 (3.1)	31.8	484.7 (5.8)	32.6
Zirconia	92.5 (1.8)	18.7	225.8 (10.5)	21.8	322.3 (2.7)	21.7

[a] *Reduction values are calculated compared to control.*

Levene's tests (α=0.05). The influences of independent variables, including irradiance and exposure duration, to temperature and DC were analyzed using two-way analyses of variance (ANOVAs; α=0.001). Between-group comparisons of temperatures and DCs were conducted using one-way ANOVA and Tukey's multiple-comparison tests (α=0.05). All statistical analyses were conducted using SPSS for Windows (release 12.01; SPSS Inc, Chicago, IL, USA).

RESULTS

Table 2 shows the mean and SD irradiances with different light-curing methods, and Table 4 provides calculated radiant exposures. Temperature and DC results, including means, SDs, and statistical significances, are given in Tables 4 and 5, respectively. Two-way ANOVA revealed significant differences in temperature and DC due to irradiance and exposure duration ($p<0.001$; Table 3).

Light irradiance was reduced by lithium disilicate and zirconia, to 26.4%, 31.8%, and 32.6% and 19.7%, 21.8%, and 21.7% at low, medium, and high irradiances, respectively. Temperatures with control, lithium disilicate, and zirconia were increased to 47.1°C, 39.2°C, and 42.2°C, respectively, at room temperature (24°C) by irradiation for 60 seconds at high irradiance (1500 mW/cm^2). Higher irradiance led to significantly higher temperatures, regardless of exposure duration and attenuating materials ($p<0.05$). Longer exposure durations caused higher temperatures at medium (1000 mW/cm^2) and high (1500 mW/cm^2) irradiances ($p<0.05$), but exposure duration did not affect temperature when materials were irradiated with low irradiance (500 mW/cm^2; $p>0.05$).

Groups irradiated for 60 seconds had significantly higher DCs compared with groups irradiated for 20 seconds, regardless of the irradiance and attenuating material ($p<0.05$). In the control groups, statistical differences in DC were as follows: C-L20 < C-M20 = C-H20; C-L60 = C-M60 = C-H60 ($p<0.05$). In the lithium disilicate groups, statistical differences in DC were as follows: L-L20 < L-M20 = L-H20 = L-L60 < L-M60 = L-H60 ($p<0.05$). In the zirconia groups, statistical differences in DC were as follows: Z-L20 < Z-M20 = Z-H20 = Z-L60 < Z-M60 = Z-H60 ($p<0.05$).

Irradiating with low irradiance for 20 seconds caused statistically different DCs in the attenuating materials; higher DCs occurred in the following order: C-L20 > L-L20 > Z-L20 ($p<0.05$). The control group (C-L60) showed higher DCs compared with other attenuating material groups (L-L60 and Z-L60) when they were irradiated with low-intensity irradiance for 60 seconds ($p<0.05$). Irradiating with medium or high irradiance for 60 seconds caused no differences between the attenuating materials ($p>0.05$).

DISCUSSION

The present study aimed to determine the effect of LED light-curing methods on dual-cure resin cement under different restorative materials. To determine the effects of irradiance and exposure duration to DC and temperature, a single LCU was used and irradiance was manually calibrated with a radiometer. Two-way ANOVA showed that irradiance and exposure duration affected both DCs and temperature changes and the null hypothesis was rejected. The results of this study show that irradiating with higher than 1000 mW/cm^2 irradiance for 60 seconds can achieve sufficient DCs despite the attenuating effect of ceramics with 1-mm thickness. Interestingly, DCs and temperatures were affected by irradiance and exposure duration in different ways. All groups showed higher DCs with increased exposure times, but there were no statistically significant

Table 3: *Results of the Two-Way Analysis of Variance for Each Attenuating Material*

Independent Variable	Significance	
	Degree of Conversion	Temperature
Irradiance	$p<0.001$	$p<0.001$
Exposure duration	$p<0.001$	$p<0.001$

Table 4: *Radiant Exposure of Each Group and the Means (SD) and Statistical Differences Between Groups for Temperature*[a]

	Low Irradiance (500 mW/cm^2)			Medium Irradiance (1000 mW/cm^2)			High Irradiance (1500 mW/cm^2)		
	Group	Radiant Exposure, mJ/cm^2	Temperature, °C	Group	Radiant Exposure, mJ/cm^2	Temperature, °C	Group	Radiant Exposure, mJ/cm^2	Temperature, °C
Control									
20 s	C-L20	9884	28.4 (0.3)^{A,a}	C-M20	29,724	32,6 (0.8)^{A,b}	C-H20	29,724	39.3 (2.1) $^{A, c}$
60 s	C-L60	29,652	28.4 (0.6)^{A,a}	C-M60	89,172	39.3 (2.3)^{B,b}	C-H60	89,172	47.1 (2.3) $^{B, c}$
Lithium disilicate									
20 s	L-L20	2710	27.8 (0.7)^{A,a}	L-M20	9694	29.5 (0.3)^{A,b}	L-H20	9694	31.4 (0.3) $^{A, c}$
60 s	L-L60	8130	28.2 (1.1)^{A,a}	L-M60	29,082	33.2 (1.4)^{B,b}	L-H60	29,082	39.2 (1.2) $^{B, c}$
Zirconia									
20 s	Z-L20	1850	27.3 (1.1)^{A,a}	Z-M20	6446	29.3 (0.2)^{A,b}	Z-H20	6446	34.5(1.7) $^{A, c}$
60 s	Z-L60	5550	28.2 (1.3)^{A,a}	Z-M60	19,338	34.2 (3.0)^{B,b}	Z-H60	19,338	42.2(2.7) $^{B, c}$

[a] *Temperature was measured at room temperature (24°C). Similar superscript letters (uppercase for columns and lowercase for rows) indicate homogenous subsets among the experimental groups (*$p>0.05$*).*

differences between the groups irradiated with 1000 mW/cm^2 and 1500 mW/cm^2. Thus, 1000 mW/cm^2 of irradiance was sufficient to achieve DCs through ceramics if sufficient exposure durations were provided. In conclusion, sufficient exposure duration was prerequisite to achieve a high DC. On the other hand, longer exposure durations, with 500 mW/cm^2 of irradiance, did not cause increases in temperature, although higher irradiance caused higher temperature changes. Thus, exposure durations, at low irradiances, did not affect temperatures, and irradiance was more critical to temperature changes than exposure duration.

The concept of the law of reciprocity, that high-irradiance exposure for short durations and low-irradiance exposure for long durations cause similar polymerization to resin composites,[20] is controversial.[21-23] In this study, similar to previous experiments,[24,25] exposure duration was more critical than irradiance. The results, that C-L60 showed a statistically higher DC compared with C-H20, despite both groups providing the same radiant exposure, confirm this. Total radiant exposure is indicated by the number of photons reaching the light beam area,[12] and excessive photons delivered in a short time is not necessary to activate photo-initiators and free radicals.[26,27] Fast saturation of a photo-initiating system restricts the available monomers causing lower DCs and increases the frequency of crosslinking and short polymeric chains, causing the lower mechanical properties of resin composites.[28] Restorative materials attenuate irradiance in certain proportions (lithium disilicate: about 70%; zirconia: about 80%); for example, only 322 mW/cm^2 of irradiance reached the specimens through zirconia when they were exposed to an irradiance of 1500 mW/cm^2. Therefore, there is a limit to the amount of photons that may be delivered to resin composites through ceramics, despite increases in irradiance,

Table 5: *Mean (SD) Degrees of Conversion and Statistical Differences Between the Groups*[a]

	Low Irradiance	Medium Irradiance	High Irradiance
Control			
20 s	58.25 (1.35)^{A,c}	62.87 (3.62)^{B,b}	64.35 (1.84)^{B,a}
60 s	70.07 (0.83)^{C,b}	70.80 (1.29)^{C,a}	69.88 (0.51)^{C,a}
Lithium disilicate			
20 s	54.52 (1.93)^{A,b}	60.71 (5.47)^{B,ab}	62.88 (7.26)^{B,a}
60 s	59.62 (3.43)^{B,a}	70.87 (1.90)^{C,a}	70.23 (2.42)^{C,a}
Zirconia			
20 s	51.84 (2.76)^{A,a}	56.96 (5.48)^{B,a}	60.08 (4.48)^{B,a}
60 s	58.68 (1.57)^{B,a}	68.75 (3.73)^{C,a}	69.47 (2.16)^{C,a}

[a] *Similar superscript letters (uppercase: statistical differences in irradiance and exposure times; lowercase: statistical differences in attenuating materials) indicate homogenous subsets among the experimental groups (*$p>0.05$*).*

because of the limited output of LCUs and the possibility of curing light burns.[29]

Although increasing radiant exposure is necessary to compensate for the attenuating effect of restorative materials, higher radiant exposure may cause temperature rises.[30] In this study, exposure times did not statistically affect temperatures with low irradiances (500 mW/cm^2), but longer exposure durations caused higher temperatures when materials were irradiated with higher than medium irradiance (1000 and 1500 mW/cm^2). Especially, irradiation with 1500 mW/cm^2 for 60 seconds to zirconia caused temperature rises of 18.2°C. The thermal stimulus generated by LCU can cause the thermal response of the dentin-pulp complex.[31] The physiological change of pulp by external heat depends on the intensity and duration of the thermal stimulus to pulp, the fluid motion of the dentinal tubule, the thickness of enamel and dentin, and intervening substrates between heat and tooth, including composite resins. Intrapulpal temperature rise of more than 5.5°C can cause irreversible pulp damage,[32] and thermal stimulus for 60 seconds with increasing temperature of 5°C is critical for the vital pulp.[33] The fluid of the dentinal tubule transmits the sensation to pulp, and the intimate stimuli to the dentinal tubule can cause more physiological changes of the dentin-pulp complex.[34] As the thermal diffusivity of dentin (1.87×10^{-3} cm^2/s) and enamel (4.79×10^{-3} cm^2/s) is relatively low,[35] the intrapulpal temperature change by external heat is less to the tooth that has thicker dentin and enamel walls. Similarly, composite resin acts as an insulator rather than heat container,[30] and thinner composite resins cause higher temperature rises of pulp.[16,36] A previous *in vivo* study showed that LED irradiation with 1200 mW/cm^2 for 60 seconds on a human tooth with a 3-mm-thick enamel-dentin wall caused a temperature rise over the threshold of 5.5°C in the pulp chamber.[37] The results of this study represent the temperature rise of resin cements during cementation of a ceramic crown. In clinical situations, a relatively thin dentin wall remains, dentinal tubules may be exposed, and a comparatively thin resin composite intervenes between the restoration and tooth. Therefore, the results of this study show that lengthy light curing with high irradiance for the polymerization of resin cement under ceramic restorations may cause harmful effects to the pulp. To avoid unfavorable effects, alternative curing techniques, such as providing interrupted light exposure (dividing total exposure duration) is recommended; for example, three periods of interrupted irradiation at 1500 mW/cm^2 for 20 seconds to zirconia (Z-H20) can decrease temperatures by 7.7°C compared with irradiation at 1500 mW/cm^2 for 60 seconds to zirconia (Z-H60).

In this study, a single LED light LCU was used, and the output of the LCU was manually adjusted with a radiometer. Using a single light source and LCU is important to draw concise conclusions for evaluating the effects of light intensity. Despite similar irradiances among different LCUs, polymerization kinetics can be affected by the type of LCU.[12,38] Irradiating kinetics are affected by the design of the LCU; for example, tip diameter affects light dispersion distances from the light tip,[38] and collimating irradiance with distance was different due to commercial differences in LCUs. Moreover, the time to peak output irradiance or homogeneity of irradiance also can differ according to the type of LCU.[12] In addition, the radiant to active light beam area is less than the LCU tip area,[39,40] and measuring the irradiance of light simulating the experimental situation may prevent errors. In this study, all experimental procedures of light exposure were performed with Teflon molds, providing determined distances from curing unit tips to objects. A control group was necessary in this study to provide comparable data and to evaluate the effects of ceramic materials on the resin cement. Measuring temperature on the surface of objects and in the air is technically different; a different thermometer should be used, and measuring temperature in the air is much more sensitive. To use the same method for measuring temperature, transparent acryl was used as a control group instead of direct irradiation, although it is not used in clinical situations.

However, the limitations of this study were the differences in experimental conditions compared with the patients' intraoral conditions. Flat attenuating materials were used, and the irradiation angles and distances in this study may be different from those through anatomic fixed prostheses. Therefore, laboratory research with anatomic crowns or clinical research may be necessary to verify these results. Although irradiating with 500 mW/cm^2 achieved lower DC than the control group and did not affect the temperature in this study design, providing longer exposure durations can derive different results as they provide more energy. More studies with various exposure times may be beneficial to verify the results.

CONCLUSIONS

1. Providing longer exposure durations is more efficient to achieve higher DC compared to irradiating with higher irradiances.
2. While longer exposure durations with 500 mW/cm^2 of irradiance do not cause temperature rises, an irradiance with greater than 1000 mW/cm^2 for longer exposure yields higher temperature changes, which can cause clinically unfavorable results.
3. LED irradiance with 1000 mW/cm^2 for 60 seconds achieves appropriate DC of dual-cure resin cement underlying lithium disilicate or zirconia crown with 1-mm thickness, but providing a pause between irradiances may be necessary to prevent temperature rise.

Regulatory Statement

This study was conducted in accordance with all the provisions of the local human subjects oversight committee guidelines and policies of approval of the Korea University Anam Hospital.

Conflict of Interest

The authors of this manuscript certify that they have no proprietary, financial, or other personal interest of any nature or kind in any product, service, and/or company that is presented in this article.

(Accepted 28 February 2018)

REFERENCES

1. Aguiar TR, Francescantonio M, Arrais CA, Ambrosano GMB, Davanzo C, & Giannini M (2010) Influence of curing mode and time on degree of conversion of one conventional and two self-adhesive resin cements *Operative Dentistry* **35(3)** 295-299.
2. Shim JS, Kang JK, Jha N, & Ryu JJ (2017) Polymerization mode of self-adhesive, dual-cured dental resin cements light cured through various restorative materials *Journal of Esthetic and Restorative Dentistry* **29(3)** 209-214.
3. Price RB, Shortall AC, & Palin WM (2014) Contemporary issues in light curing *Operative Dentistry* **39(1)** 4-14.
4. Dall'Magro E, Sinhoreti MA, Correr AB, Correr-Sobrinho L, Consani S, & Puppin-Rontani RM (2007) Effect of different initial light intensity by the soft-start photoactivation on the bond strength and Knoop hardness of a dental composite *Brazilian Dental Journal* **18(2)** 107-112.
5. Jung H, Friedl K-H, Hiller K-A, Haller A, & Schmalz G (2001) Curing efficiency of different polymerization methods through ceramic restorations *Clinical Oral Investigations* **5(3)** 156-161.
6. Lee IB, An W, Chang J, & Um CM (2008) Influence of ceramic thickness and curing mode on the polymerization shrinkage kinetics of dual-cured resin cements *Dental Materials* **24(8)** 1141-1147.
7. Alexander Tarimo S, Mabula Machibya F, & Zhi Min Z (2017) Influence of tooth thickness on degree of conversion of photo-activated resin composite irradiated through the tooth *International Journal of Dentistry and Oral Science* **4(3)** 450-456.
8. Santos G, El-Mowafy O, Rubo JH, & Santos M (2004) Hardening of dual-cure resin cements and a resin composite restorative cured with QTH and LED curing units *Journal of the Canadian Dental Association* **70(5)** 323-327.
9. Dunn WJ, & Bush AC (2002) A comparison of polymerization by light-emitting diode and halogen-based light-curing units *Journal of the American Dental Association* **133(3)** 335-341.
10. Shortall A, & Harrington E (1997) Effectiveness of battery powered light activation units *British Dental Journal* **183(3)** 95-100.
11. Shortall A, & Harrington E (1996) Guidelines for the selection, use, and maintenance of visible light activation units *British Dental Journal* **181(10)** 383-387.
12. Price R, Ferracane J, & Shortall A (2015) Light-curing units: a review of what we need to know *Journal of Dental Research* **94(9)** 1179-1186.
13. Nomoto R (1997) Effect of light wavelength on polymerization of light-cured resins *Dental Materials* **16(1)** 60-73.
14. Price RB, & Felix CA (2009) Effect of delivering light in specific narrow bandwidths from 394 to 515nm on the micro-hardness of resin composites *Dental Materials* **25(7)** 899-908.
15. Cook WD (1992) Thermal aspects of the kinetics of dimethacrylate photopolymerization *Polymer* **33(10)** 2152-2161.
16. Matalon S, Slutzky H, Wassersprung N, Goldberg-Slutzky I, & Ben-Amar A (2010) Temperature rises beneath resin composite restorations during curing *American Journal of Dentistry* **23(4)** 223-226.
17. Hannig M, & Bott B (1999) *In-vitro* pulp chamber temperature rise during composite resin polymerization with various light-curing sources *Dental Materials* **15(4)** 275-281.
18. Huang TK, Hung CC, & Tsai CC (2006) Reducing, by pulse width modulation, the curing temperature of a prototype high-power LED light curing unit *Dental Materials Journal* **25(2)** 309-315.
19. Stansbury J, & Dickens SH (2001) Determination of double bond conversion in dental resins by near infrared spectroscopy *Dental Materials* **17(1)** 71-79.
20. Musanje L, & Darvell B (2003) Polymerization of resin composite restorative materials: exposure reciprocity *Dental Materials* **19(6)** 531-541.
21. Halvorson RH, Erickson RL, & Davidson CL (2002) Energy dependent polymerization of resin-based composite *Dental Materials* **18(6)** 463-469.
22. Lindberg A, Peutzfeldt A, & van Dijken JW (2005) Effect of power density of curing unit, exposure duration, and

light guide distance on composite depth of cure *Clinical Oral Investigations* **9(2)** 71-76.

23. Peutzfeldt A, & Asmussen E (2005) Resin composite properties and energy density of light cure *Journal of Dental Research* **84(7)** 659-662.
24. Faria-e-Silva AL, & Pfeifer CS (2017) Effectiveness of high-power LEDs to polymerize resin cements through ceramics: an *in vitro* study *Journal of Prosthetic Dentistry* **118(5)** 631-636.
25. Jang Y, Ferracane J, Pfeifer C, Park J, Shin Y, & Roh B (2017) Effect of insufficient light exposure on polymerization kinetics of conventional and self-adhesive dual-cure resin cements *Operative Dentistry* **42(1)** E1-E9.
26. Feng L, Carvalho R, & Suh BI (2009) Insufficient cure under the condition of high irradiance and short irradiation time *Dental Materials* **25(3)** 283-289.
27. Feng L, & Suh BI (2007) Exposure reciprocity law in photopolymerization of multi-functional acrylates and methacrylates *Macromolecular Chemistry and Physics* **208(3)** 295-306.
28. Aguiar F, Braceiro A, Lima D, Ambrosano G, & Lovadino JR (2007) Effect of light curing modes and light curing time on the microhardness of a hybrid composite resin. *Journal of Contemporary Dental Practice* **8(6)** 1-8.
29. Spranley TJ, Winkler M, Dagate J, Oncale D, & Strother E (2012) Curing light burns *General Dentistry* **60(4)** e210-e214.
30. Kwon SJ, Park YJ, Jun SH, Ahn JS, Lee IB, Cho BH, Son HH, & Seo DG. (2013) Thermal irritation of teeth during dental treatment procedures *Restorative Dentistry & Endodontics* **38(3)** 105-112.
31. Jakubinek MB, O'Neill C, Felix C, Price RB, & White MA (2008) Temperature excursions at the pulp–dentin junction during the curing of light-activated dental restorations *Dental Materials* **24(11)** 1468-1476.
32. Zach L, & Cohen G (1965) Pulp response to externally applied heat *Oral Surgery, Oral Medicine, Oral Pathology* **19(4)** 515-530.
33. Eriksson A, Albrektsson T, Grane B, & McQueen D (1982) Thermal injury to bone: a vital-microscopic description of heat effects *International Journal of Oral Surgery* **11(2)** 115-121.
34. Ramoglu SI, Karamehmetoglu H, Sari T, & Usumez S (2015) Temperature rise caused in the pulp chamber under simulated intrapulpal microcirculation with different light-curing modes *Angle Orthodontist* **85(3)** 381-385.
35. Brown WS, Dewey WA, & Jacobs HR (1970) Thermal properties of teeth. *Journal of Dental Research* **49(4)** 752-755.
36. Al-Qudah A, Mitchell C, Biagioni P, & Hussey D (2007) Effect of composite shade, increment thickness and curing light on temperature rise during photocuring *Journal of Dentistry* **35(3)** 238-245.
37. Runnacles P, Arrais CA, Pochapski MT, Dos Santos FA, Coelho U, Gomes JC, De Goes MF, Gomes OM, & Rueggeberg FA (2015) *In vivo* temperature rise in anesthetized human pulp during exposure to a polywave LED light curing unit *Dental Materials* **31(5)** 505-513.
38. Shortall A, Price R, MacKenzie L, & Burke F (2016) Guidelines for the selection, use, and maintenance of LED light-curing units—part 1 *British Dental Journal* **221(8)** 453-460.
39. Price RB, Rueggeberg FA, Labrie D, & Felix CM (2010) Irradiance uniformity and distribution from dental light curing units *Journal of Esthetic and Restorative Dentistry* **22(2)** 86-101.
40. Michaud PL, Price RB, Labrie D, Rueggeberg FA, & Sullivan B (2014) Localised irradiance distribution found in dental light curing units *Journal of Dentistry* **42(2)** 129-139.

©Operative Dentistry, 2018, **43-6,** E288-E299

Benefits of Nonthermal Atmospheric Plasma Treatment on Dentin Adhesion

AP Ayres • PH Freitas • J De Munck • A Vananroye • C Clasen
CT dos Santos Dias • M Giannini • B Van Meerbeek

Clinical Relevance

After two years of water aging, the application of nonthermal atmospheric plasma onto dentin for 30 s showed higher microtensile bond strength of a multimode adhesive applied in etch-and-rinse mode. Plasma-treated dentin also resulted in higher nanohardness and Young's modulus of the hybrid layer in immediate evaluation and greater hydrophilicity.

SUMMARY

Objectives: This study aimed to evaluate the influence of two nonthermal atmospheric plasma (NTAP) application times and two storage times on the microtensile bond strength (μTBS) to dentin. The influence of NTAP on the mechanical properties of the dentin-resin interface was studied by analyzing nanohardness (NH) and Young's modulus (YM). Water contact angles of pretreated dentin and hydroxyapatite blocks were also measured to assess possible alterations in the surface hydrophilicity upon NTAP.

Methods and Materials: Forty-eight human molars were used in a split-tooth design (n=8). Midcoronal exposed dentin was flattened by a 600-grit SiC paper. One-half of each dentin surface received phosphoric acid conditioning, while the other half was covered with a metallic barrier and remained unetched. Afterward, NTAP was applied on the entire dentin surface (etched or not) for 10 or 30 seconds. The control groups did not receive NTAP treatment. Scotchbond Universal (SBU; 3M ESPE) and a resin-based composite were applied to dentin following the manufacturer's

*Ana Paula Ayres, DDS, MSc, PhD, KU Leuven (University of Leuven), Department of Oral Health Sciences, BIOMAT & UZ Leuven (University Hospitals Leuven), Dentistry, Leuven, Belgium

Pedro Henrique Freitas, DDS, MSc, PhD, Department of Restorative Dentistry, College of Dentistry, Faculty of Health Sciences, University of Manitoba, Winnipeg, MB, Canada

Jan De Munck, DDS, MSc, PhD. KU Leuven (University of Leuven), Department of Oral Health Sciences, BIOMAT & UZ Leuven (University Hospitals Leuven), Dentistry, Leuven, Belgium

Anja Vananroye, MSc, PhD, Chemical Engineering Department, Soft Matter, Rheology and Technology, KU Leuven, University of Leuven, Leuven, Belgium.

Christian Clasen, MSc, PhD, Chemical Engineering Department, Soft Matter, Rheology and Technology, KU Leuven, University of Leuven, Leuven, Belgium

Carlos Tadeu dos Santos Dias, MSc, PhD, Exact Sciences Department, Luiz de Queiroz College of Agriculture, University of São Paulo, Piracicaba, SP, Brazil

Marcelo Giannini, DDS, MSc, PhD, Department of Restorative Dentistry, Piracicaba Dental School, State University of Campinas, Piracicaba, SP, Brazil

Bart Van Meerbeek, DDS, MSc, PhD, KU Leuven (University of Leuven), Department of Oral Health Sciences, BIOMAT & UZ Leuven (University Hospitals Leuven), Dentistry, Leuven, Belgium

*Corresponding author: Av. Nenê Sabino, 1801, Uberaba-MG 38055-500, Brazil; e-mail: anapaulaayres4@gmail.com

DOI: 10.2341/17-123-L

instructions. After 24 hours of water storage at 37°C, the specimens were sectioned perpendicular to the interface to obtain approximately six specimens or bonded beams (approximately 0.9 mm^2 in cross-sectional area) representing the etch-and-rinse (ER) approach and another six specimens representing the self-etch (SE) approach. Half of the μTBS specimens were immediately loaded until failure, while the other half were first stored in deionized water for two years. Three other bonded teeth were selected from each group (n=3) for NH and YM evaluation. Water contact-angle analysis was conducted using a CAM200 (KSV Nima) goniometer. Droplet images of dentin and hydroxyapatite surfaces with or without 10 or 30 seconds of plasma treatment were captured at different water-deposition times (5 to 55 seconds).

Results: Two-way analysis of variance revealed significant differences in μTBS of SBU to dentin after two years of water storage in the SE approach, without differences among treatments. After two years of water aging, the ER control and ER NTAP 10-second groups showed lower μTBS means compared with the ER NTAP 30-second treated group. Nonthermal atmospheric plasma resulted in higher NH and YM for the hybrid layer. The influence of plasma treatment in hydrophilicity was more evident in the hydroxyapatite samples. Dentin hydrophilicity increased slightly after 10 seconds of NTAP, but the difference was higher when the plasma was used for 30 seconds.

Conclusions: Dentin NTAP treatment for 30 seconds contributed to higher μTBS after two years of water storage in the ER approach, while no difference was observed among treatments in the SE evaluation. This result might be correlated to the increase in nanohardness and Young's modulus of the hybrid layer and to better adhesive infiltration, since dentin hydrophilicity was also improved. Although some effects were observed using NTAP for 10 seconds, the results suggest that 30 seconds is the most indicated treatment time.

INTRODUCTION

One of the most recent innovations in adhesive dentistry involves the treatment of different dental surfaces using nonthermal atmospheric plasma (NTAP), a novel technology that delivers highly reactive species in a gaseous medium at or below physiologic temperature. This technology tries to solve challenges commonly associated with hybridization of dentin during bonding procedures, therefore influencing the quality and longevity of the tooth-resin interface. A recently published review collected and summarized the current advances of NTAP in improving the durability of dentin bonding.[1] The studies have demonstrated that NTAP applied on the dentin surface enhanced the bond strength of etch-and-rinse (ER) adhesives,[2-4] but the results were more product dependent when employed to self-etch (SE) adhesives.[5,6]

Overall, NTAP has demonstrated efficacy in improving different properties of dental bonding because it provides higher wettability of the dentin surface,[2,6-9] improves resin polymerization,[10,11] and allows deeper adhesive penetration.[2,4,11] For the ER bonding technique, it was reported that a short plasma treatment could change the chemical structure of the exposed collagen fibrils and increase the hydrophilicity of the dentin surface, which allows better adhesive penetration into the dental collagen fibrils and enhances the dentin bond strength.[11]

A complex biomechanical entity is formed in the adhesive dental restoration that consists of the tooth substrate and the biomaterial. To predict the long-term performance of dental adhesives, it is necessary to understand their mechanical properties. The bonding area between the restorative resin composite and the dentinal cavity wall presents a gradual transition of different components, resulting in a heterogeneous gradient of physico-mechanical properties.[12] Nevertheless, acid pretreatment modifies the hardness of the dentin surface, and the bonded interface zone might allow some flexibility with the hybridization process after resin polymerization. Such an elastic bonding area might have a strain capacity sufficient to relieve stresses between the composite shrinkage and the rigid dentin substrate,[12,13] thereby preserving the integrity of marginal adaptation and consequently increasing the durability of the restoration.

The influence of the NTAP application on the mechanical properties of the adhesive-dentin interface is not established yet. The NTAP effect depends on treatment time, working gas, input power, pulse frequency of the plasma device, and also on other factors related to the substrate.[1] Some investigations relate wettability enhancement associated with the NTAP treatment in different dental substrates.[2,6-9] The plasma device of the present study (Surface Plasma Tool Model SAP; Surface–Engineering and Plasma Solution, Campinas, Brazil) improved the

Table 1: *Number of Specimens (n) and Repetitions (r) per Specimen Analyzed in Each of the Assays*

Etching	NTAP	μTBS		Nanohardness	Young's Modulus	Contact Angle: Dentin	Contact Angle: Hydroxyapatite
		1-wk	2-y				
None		n/r	n/r	n/r	n/r	n/r	n/r
	None	8/6	8/6	3/5	3/5	5/1-3	5/1-3
	10 s	8/6	8/6	3/5	3/5	5/1-3	5/1-3
	30 s	8/6	8/6	3/5	3/5	5/1-3	5/1-3
Phosphoric acid	None	8/6	8/6	3/5	3/5	—	—
	10 s	8/6	8/6	3/5	3/5	—	—
	30 s	8/6	8/6	3/5	3/5	—	—

wettability of the zirconia surface, decreasing the contact angle (CA) by approximately 50%.[14] There is still a lack of information of the influence of this specific equipment and settings on the hydrophilicity of dentin tissue.

Therefore, this study aimed to assess the extent two application times of NTAP, 10 and 30 seconds, affect the long-term microtensile bond strength (μTBS) of one commercial multimode adhesive system. The influence of NTAP on the mechanical properties of the dentin-resin interface was studied by analyzing nanohardness, Young's modulus, and CA. The following null hypotheses were tested: 1) plasma treatment does not affect the dentin-bond strength tested immediately or after two years of aging, 2) NTAP treatment does not produce differences in the nanohardness and Young's modulus of the resin-dentin interface's structures (dentin, hybrid layer, and adhesive layer), and 3) the CA of the dentin and hydroxyapatite surfaces is not affected by the NTAP treatment.

METHODS AND MATERIALS

The distribution of specimens for each research subproject is detailed in Table 1. All statistical testing was performed at a preset alpha of 0.05, and the values were calculated using SAS 9.3 Software (SAS Institute, Cary, NC, USA). Kolmogorov-Smirnov and Cramer–von Mises tests were used to verify normal distribution, and the Brown-Forsythe test was applied to homoscedasticity analysis.

μTBS

Forty-eight noncarious human third molars (two groups per tooth; n=8 per experimental group) were stored in 0.5% chloramine/water immediately after extraction, then cleaned and stored in distilled water at 4°C to be used within three months. The occlusal third of the crowns was removed with a diamond saw, exposing the occlusal dentin surface (Isomet 100, Buehler, Lake Bluff, IL, USA). A standardized smear layer was produced under water irrigation using 600-grit SiC paper (Buehler-Met II, Buehler), and the flat surface was divided into two parts with similar areas using a thin diamond blade. One-half of each dentin surface was demineralized for 15 seconds with 34% phosphoric acid (Scotchbond Etchant, 3M ESPE, St Paul, MN, USA) in an ER approach, while the other half was covered with metallic paper and not etched in the SE approach. Afterward, NTAP was applied on the entire dentin surface (etched or not) for 10 or 30 seconds.

The plasma equipment used in this study (Surface Plasma Tool Model SAP, Surface–Engineering and Plasma Solution) consisted of a handheld unit using argon as the operating gas at a flow rate of 5.0 L/min. The plasma torch emerging at the exit nozzle was about 1.0 mm in diameter and was operated at room temperature (22°C). A mobile base allowed keeping a distance of 10 mm between the nozzle and the dentin surface. Control groups did not receive NTAP treatment. Thus, the following groups were investigated (n=8):

1. SE control (unetched dentin, NTAP untreated)
2. SE NTAP 10 seconds
3. SE NTAP 30 seconds
4. ER control (etched dentin, NTAP untreated)
5. ER NTAP 10 seconds
6. ER NTAP 30 seconds

After the respective treatments, a multimode adhesive system (Scotchbond Universal, 3M ESPE; Table 2) was applied following the manufacturer's instructions and light-cured with a multiwavelength LED unit (VALO, Ultradent Products Inc, South Jordan, UT, USA) in standard mode with an output of about 1200 mW/cm^2, as measured by the MARC Patient Simulator (BlueLight Analytics, Halifax, NS, Canada).

Table 2: *Composition of Scotchbond Universal (3M ESPE) and Its Application Modes*

Composition (Batch No.)	Adhesive Mode	Application Method
Scotchbond Universal Etchant: 34% phosphoric acid, water, synthetic amorphous silica, polyethylene glycol, aluminum oxide (N489165)	Two-step etch and rinse (ER)	Application of phosphoric acid gel etchant on dentin for 15 s and gentle air drying; rubbed application of the adhesive for 20 s, followed by 5-s gentle air-drying and 10-s light curing
Scotchbond Universal: 10-MDP, dimethacrylate resins, HEMA, methacrylate-modified polyalkenoic acid copolymer, filler, ethanol, water, initiators, and silane (621418), pH = 2.7	One-step self-etch (SE)	Rubbed application of the adhesive for 20 s, followed by 5-s gentle air drying and 10-s light curing

Abbreviations: 10-MDP, 10-methacryloyloxydecyl dihydrogen phosphate; HEMA, 2-hydroxyethyl methacrylate.

A composite buildup (Filtek Supreme Ultra, shade A2 enamel, 3M ESPE) was made in layers (6-mm high), and each 2-mm layer was light-cured for 20 seconds with the VALO. The tooth root was removed 4 mm below the adhesive-dentin interface. After 24 hours of storage in deionized water (37°C), the specimens were sectioned perpendicular to the interface into 0.9-mm-thick bonded beams with a diamond saw under water cooling (Isomet, Buehler).

Approximately six specimens representing the ER approach and another six specimens representing the SE approach were obtained after sectioning the teeth. After one week, the beams were attached to a BIOMAT jig[15] with cyanoacrylate glue (Model Repair II Blue; Dentsply-Sankin, Tochigiken, Japan) and tested in tension at a crosshead speed of 1 mm/min until failure in a universal testing machine (LRX, Lloyd, Hampshire, UK). The specimens from the other 24 teeth were stored in deionized water for two years. The storage medium was replaced every 15 days by deionized water at room temperature, and then the samples were kept at 37°C until the next water replacement.

A single failure stress value was calculated for each half of the tooth by averaging all beams obtained from that half tooth. The μTBS (MPa) was derived from dividing the force (Newton) applied at the time of fracture by the bonded area, of which the cross-sectional area was measured with a digital caliper (Starrett, Itu, SP, Brazil). The bond strength data (MPa) was then analyzed by two-way analysis of variance (ANOVA) and Tukey's multiple comparison test for each adhesive technique (SE and ER).

After failure, the specimens were mounted on brass stubs and observed using a digital microscope system (Hirox KH-8700, Tokyo, Japan). The failure mode of each beam was classified into one of the following categories: cohesive failure in composite resin (C), cohesive failure in dentin (D), adhesive failure (A), or mixed failure of composite resin, adhesive, and dentin (M). Representative areas were photographed at 200× magnification. Data were submitted to chi-square analysis to demonstrate the effect of the factor "time" on failure mode.

Nanohardness and Young's Modulus

The same groups were used in this part of the study. Three bonded teeth from each group (n=3) were longitudinally sectioned through the sample center with a diamond saw, under water cooling (Isomet, Buehler), to obtain two 1.5-mm-thick bonded slices. Each central slab was individually embedded in an epoxy resin (EpoxiCure, Buehler) and manually polished under water irrigation using SiC paper (Buehler-Met II, Buehler) with decreasing abrasiveness (600, 1000, 1200, 1500, and 2000). Special soft discs (Apex Diamond Grinding Disks, Buehler) were associated with diamond polishing suspensions (MetaDi, Buehler) of 9-, 6-, 3-, 1-, and 0.5-μm grit size. Samples were ultrasonically cleaned with distilled water for five minutes between each polishing step.

The computer-controlled nano-indenter Hysitron Custom Triboindenter (Hysitron, Minneapolis, MN, USA) was used with a cell Berkovich point for the nanohardness and Young's modulus evaluation. Samples were individually placed on a computer-controlled X-Y table and were kept hydrated during the test. To ensure a precise transfer of the preprogrammed positions to the nanoindenter, an accurate calibration of the probe was performed on the standard fused quartz sample before the test's start. Five equally spaced (10-μm) indentations were preprogrammed and performed on the dentin, hybrid layer, and adhesive layer, totaling 15 per specimen (n=3, representing three specimens per group) with a load of 1000 μN and a standard trapezoidal load function of 5-2-5 s. The nanohardness and Young's modulus of each area were computed as described elsewhere.[16] Data were analyzed using one-way ANOVA (dentin treatment as factor; dentin, hybrid

layer, and adhesive as levels) and Tukey's test for the SE and ER approaches.

CA by Sessile Drop Method

Human Teeth—Ten noncarious human third molars (n=5) were selected and stored in 0.5% chloramine/water (4°C) immediately after extraction, then cleaned and stored in distilled water at 4°C to be used within three months after extraction. The teeth had their root and occlusal third removed using a diamond wafering blade (Buehler-Series 15HC Diamond, Buehler) on an automated sectioning device (Isomet 2000, Buehler) under running water. The exposed surface was ground with 600-grit SiC paper (Buehler-Met II, Buehler) under water irrigation. All surfaces of the dentin slices were carefully verified by stereomicroscopy for the absence of enamel/pulp tissue (Wild M5A, Wild, Heerbrugg, Switzerland).

Half of each tooth was treated with an NTAP brush for 10 or 30 seconds while a blade was used to separate and protect the other half, which was used as the untreated same-tooth control. This split of the sample was considered important since the standard deviation within dentin is large as it depends on different factors such as depth, age of the teeth, and number of tubules.[17]

Hydroxyapatite Plate—A commercially available hydroxyapatite plate (10 × 10 × 2 mm; APP100, Hoya, Tokyo, Japan) with a total area similar to an entire dentin flat slice dimension was prepared for CA evaluation. The purpose was to analyze an inorganic material present in dentin with and without the NTAP application. Comparing the results with dentin hydrophilicity should then estimate the plasma's influence on total and partial inorganic material. The blocks were also divided into two halves, and a blade protected one-half (control) from plasma treatment during the 10- or 30-second application.

CA Measurement: Three Repetitions in the Same Spot—Excess water on the dentin surfaces was gently blot dried with Kimwipes tissues (Kimberly-Clark, Roswell, GA, USA) before water CA measurement. Hydroxyapatite blocks were air-blown clean and kept dried before the experiment. The CA of distilled water was measured by the sessile drop technique with the use of a CAM200 goniometer (KSV Nima, Espoo, Finland), and the samples were kept in a 100% humidity chamber during measurement.

A drop of water (approximately 1.0 μL) was placed on one of the halves of the dentin surface (n=3), and the image was immediately sent via the camera to the computer for analysis. Images were captured every five seconds at different water-deposition times (5-55 seconds).

The specimen images were analyzed by a computer program (Image J software) with an angular dimension tool to measure the static CA. Right and left angles were measured to obtain a mean CA value. One drop of water was applied on each half of the sample surface: treated side and control side. After the first CA measurement, the sample was kept in position and blot-dried, and another drop of water was applied in the same spot following the same protocol. All measurements were done in triplicate.

CA Measurement: Immediate Analysis (Unrepeated)—The intriguing results of CA data after three repetitions led us to the decision to perform another test, recording the CA immediately after the plasma treatment, evaluating only one drop of water. In this way, it was possible to better assess the surface hydrophilicity change upon the treatment, without water intake interference. Therefore, 10 dentin and hydroxyapatite samples (n=5) were prepared as described before, and the CA was individually evaluated in each half of the specimens.

RESULTS

μTBS

All assumptions related to normal distribution and homoscedasticity were attended. No significant difference was found for the evaluation time factor ($p=0.22$) in the ER approach, while the treatment factor ($p=0.02$) and the interaction between the "evaluation time" and "treatment" ($p<0.0001$) showed statistical differences. In the SE approach, the evaluation time factor was statically significant ($p<0.0001$), while no difference was found for the treatment factor ($p=0.20$) or the interaction between the "evaluation time" and "treatment" ($p=0.17$). At the one-week evaluation, no differences among the treatments were found in either adhesive technique (Table 3). After two years of water storage in the ER evaluation, the NTAP 30-second group presented a higher mean μTBS compared with the other groups. There were no pretest failures.

Cohesive failure within the composite resin was the most predominant failure pattern observed in all groups at both evaluation times (Figure 1). However, after aging, the incidence of adhesive and mixed failure increased, regardless of whether or not there was a plasma application. The factor "time" caused a

Table 3: *Microtensile Bond Strength (MPa) as a Function of Dentin Treatment and Storage Time for Each Adhesive Mode*[a]

Treatment	Storage Time	
	1 wk	2 y
SE Control	49.5 (10.0) Aa	35.14 (10.5) Ba
SE NTAP 10 s	48.5 (9.0) Aa	42.09 (4.2) Ba
SE NTAP 30 s	47.1 (8.3) Aa	46.47 (10.7) Ba
ER Control	48.8 (6.4) Aa	38.7 (8.0) Ab
ER NTAP 10 s	53.9 (11.2) Aa	44.9 (7.9) Ab
ER NTAP 30 s	46.7 (7.0) Aa	59.0 (11.6) Aa

[a] *Values are given as mean (SD). Different uppercase letters indicate significant differences ($p \leq 0.05$) between different storage times within the same treatment, and different lowercase letters indicate significant differences ($p \leq 0.05$) between different treatments within the same aging condition, for the same adhesive mode (self-etch [SE] or etch and rinse [ER]). NTAP, nonthermal atmospheric plasma.*

statistically significant difference in failure mode distribution ($p<0.0001$). After 24 hours of storage, adhesive failures ranged between 7% and 15%, increasing to between 20% and 46% after two years, whereas cohesive failures ranged from 65% to 85% at 24 hours, decreasing to 32% to 50% after aging. These higher ratios of adhesive failure after direct water exposure for a long time indicates degradation of the interfacial area, although the 30-second NTAP-treated groups did not show a significant statistical μTBS reduction after two years of aging in ER mode.

Nanohardness and Young's Modulus

All assumptions related to normal distribution and homoscedasticity were attended. The mean values and standard deviation of nanohardness and Young's modulus are shown in Tables 4 and 5, respectively. The nanohardness of adhesive layer ($p=0.181$) did not show significant differences among the groups. In the hybrid layer, the control groups showed lower nanohardness than their corresponding experimental groups. Lower dentin nanohardness was reported for NTAP 30-second groups.

The lowest dentin Young's modulus was recorded for the NTAP 30-second SE and ER groups, although it did not differ from the NTAP 10-second SE group. For both approaches (ER and SE), the groups treated with NTAP (10 and 30 seconds) showed a higher Young's modulus in the hybrid layer than their respective controls. There was no statistical difference among groups in the "adhesive layer" evaluation ($p=0.062$).

CA by Sessile Drop Method

CA Measurement: Three Consecutives Repetitions in the Same Spot—The CAs of specimens treated with NTAP for 30-seconds were significantly lower than those on the untreated dentin/hydroxyapatite surfaces (Figures 2 and 3). The dentin hydrophilicity slightly decreased after the 10-second plasma treat-

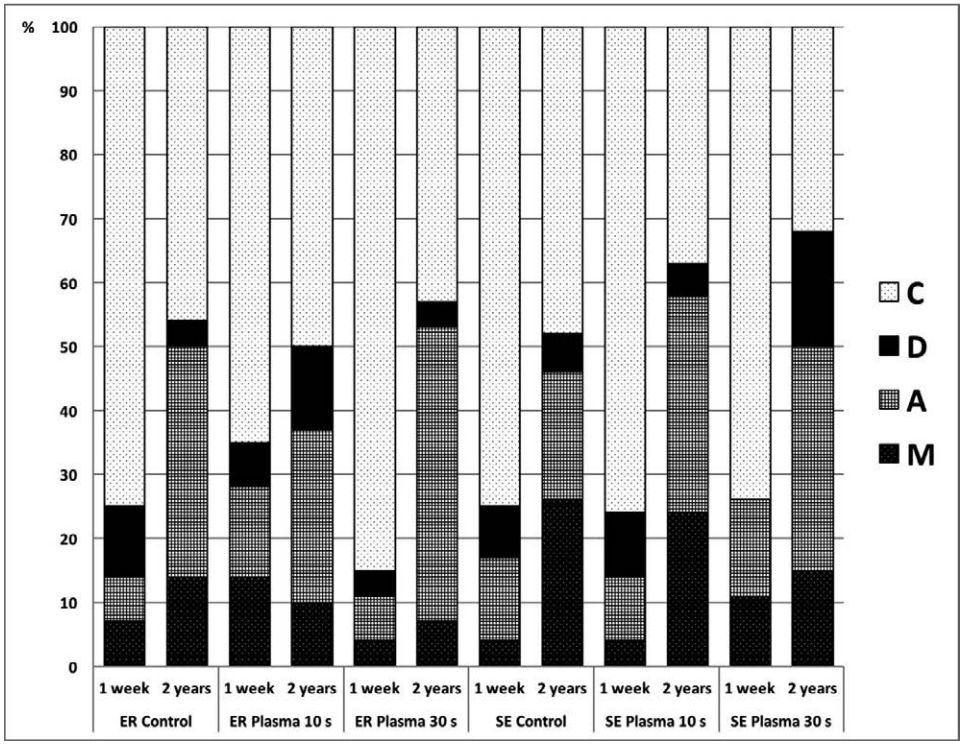

Figure 1. *Distribution (%) of failure modes of the groups tested after one week and two years of water storage. C, cohesive failure in composite resin; D, cohesive failure in dentin; A, adhesive failure; M, mixed failure of composite resin, adhesive, and dentin.*

Table 4: *Nanohardness (GPa) Means (Confidence Interval) of the Dentin, Hybrid Layer, and Adhesive Layer (n=3) of a Multimode Adhesive*[a]

Treatment	Dentin	Hybrid Layer	Adhesive Layer
Control SE	2.5 (2.5-2.6) **a**	1.4 (1.3-1.5) **b**	1.3 (1.2-1.3) **a**
SE NTAP 10 s	2.4 (2.4-2.5) **ab**	1.6 (1.5-1.7) **a**	1.3 (1.3-1.3) **a**
SE NTAP 30 s	2.3 (2.2-2.4) **b**	1.6 (1.5-1.8) **a**	1.4 (1.3-1.4) **a**
Control ER	2.5 (2.4-2.5) **a**	1.2 (1.2-1.3) **b**	1.3 (1.3-1.3) **a**
ER NTAP 10 s	2.6 (2.5-2.7) **a**	1.5 (1.5-1.6) **a**	1.3 (1.3-1.4) **a**
ER NTAP 30 s	2.0 (2.0-2.1) **b**	1.4 (1.4-1.5) **a**	1.3 (1.3-1.4) **a**

[a] *The dentin was either plasma treated (NTAP 10 or 30 seconds) or untreated (control) in self-etch and etch-and-rinse approaches. Identical letters in the same column did not differ by Tukey test (p>0.05). control ER, etch-and-rinse dentin specimens without NTAP; control SE, self-etch dentin specimens without NTAP; NTAP, nonthermal atmospheric plasma.*

ment time, but the difference from the dentin control group was higher when the plasma was used for 30 seconds (Figure 2). The influence of the NTAP treatment in hydrophilicity was more evident in the hydroxyapatite samples (Figure 3), in which the CA deeply decreased even with just 10 seconds of the NTAP application. In CA measurement repetitions, the dentin/hydroxyapatite control groups remained close to the first CA means, while the NTAP 30-second groups showed gradually higher CA results, both in the dentin and the hydroxyapatite.

CA Measurement: Immediate Analysis (Unrepeated)—Figure 4 shows the CA means of dentin and hydroxyapatite of the immediate plasma-treated and untreated (control) surfaces. In dentin, the discrepancy between the NTAP 30-second group and the control group was greater than the difference between the NTAP 10-second group and its control group. However, for the hydroxyapatite substrate, both treatment times produced a large difference in CA compared with the means in the control groups.

DISCUSSION

The benefits of applying plasma to dentin tissue are expected to act primarily on the longevity of adhesive restoration. Therefore, it is necessary to evaluate such effects as the function of the aging of the tooth-restoration interface. The first null hypothesis was partially accepted because the μTBS of the plasma-treated dentin differed from the untreated group only in the evaluation of two years of aging when plasma was applied for 30 seconds in etched dentin.

Regarding the multimode adhesive evaluated in the present study, two years of water aging did not produce a statistically significant μTBS reduction in values in the ER approach; however, the evaluation time factor was significant in the SE evaluation. Scotchbond Universal (SBU) adhesive's long-term effectiveness presents some conflicting results in the literature,[6,18-21] although none of them evaluated such a long period of aging. The differences in the test design might explain such controversies; however, this multimode adhesive showed great durability under the present study conditions, especially in the ER approach, and no pretest failures were recorded for both times of evaluation.

On the contrary, unlike most investigations using plasma,[2-6,11] in this study the NTAP treatment did not cause any difference in the immediate (one-week) results of μTBS. In the SE approach, no

Table 5: *Young's Modulus (GPa) Mean Values (Confidence Interval) of the Dentin, Hybrid Layer, and Adhesive Layer (n=3) of a Multimode Adhesive*[a]

Treatment	Dentin	Hybrid Layer	Adhesive Layer
Control SE	36.7 (34.0-39.4) **a**	15.6 (14.5-16.8) **b**	9.9 (9.6-10.3) **a**
NTAP 10 s	35.5 (33.0-38.0) **ab**	20.1 (19.3-21.0) **a**	10.1 (9.8-10.5) **a**
NTAP 30 s	31.4 (28.3-34.5) **b**	20.1 (19.3-21.0) **a**	10.1 (9.6-10.7) **a**
Control ER	37.3 (35.9-38.7) **a**	12.2 (11.9-12.4) **b**	10.1 (10.0-10.3) **a**
NTAP 10 s	37.7 (36.5-38.9) **a**	15.1 (14.0-16.1) **a**	10.4 (10.4-10.5) **a**
NTAP 30 s	33.4 (31.1-35.6) **b**	14.7 (14.0-15.3) **a**	10.7 (10.0-11.4) **a**

[a] *The dentin was either plasma treated (NTAP 10 or 30 seconds) or untreated (control) in self-etch (SE) and etch-and-rinse (ER) approaches. Identical letters in the same column did not differ by Tukey test (p>0.05). control ER, etch-and-rinse dentin specimens without NTAP; control SE, self-etch dentin specimens without NTAP; NTAP, nonthermal atmospheric plasma.*

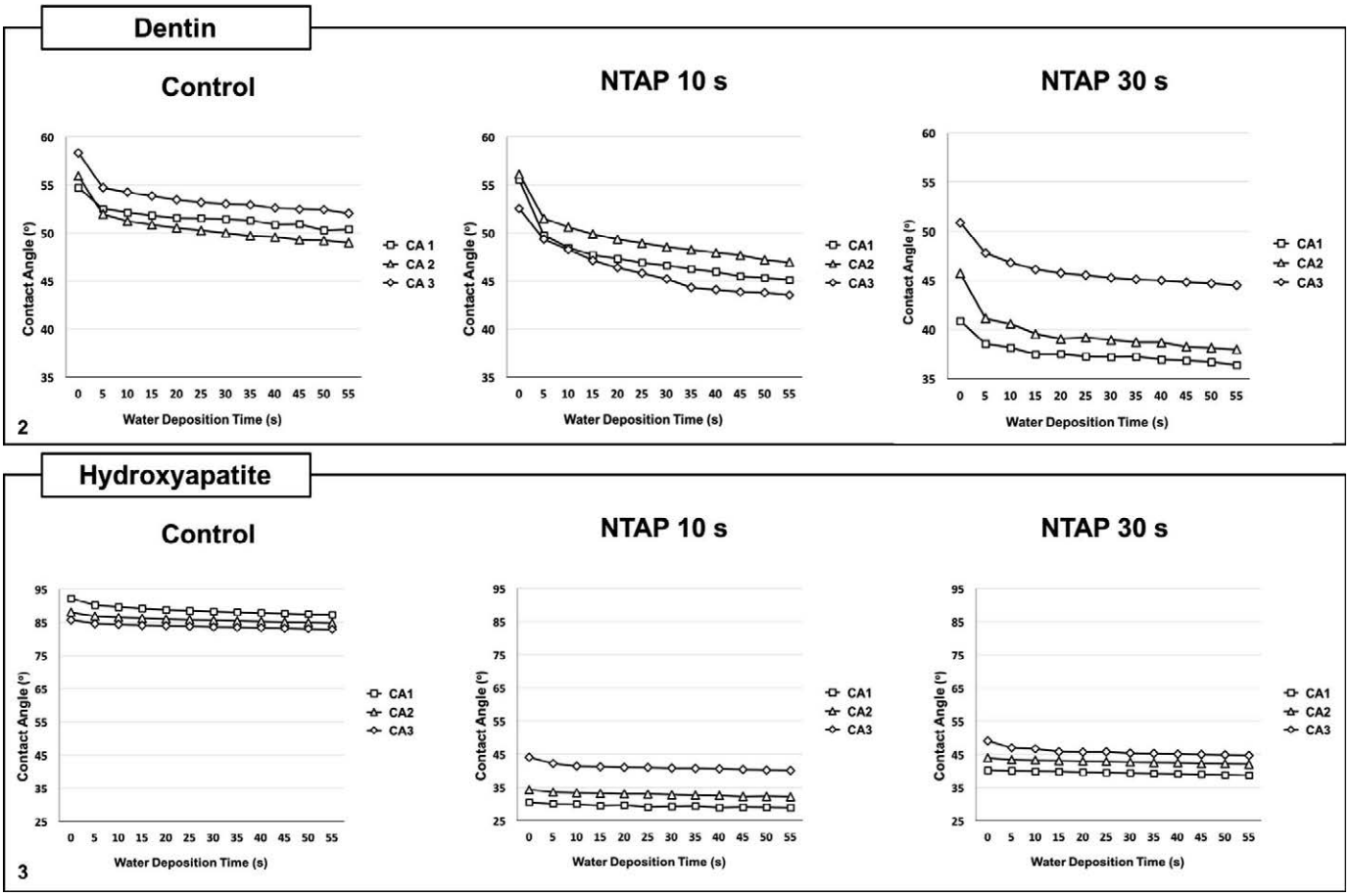

Figure 2. *Means of water contact angle on dentin treated with NTAP for 10 or 30 seconds and compared with those on untreated dentin (control). CA1, CA2, CA3 = first, second, and third contact angle measurements, respectively.*

Figure 3. *Means of water contact angle on hydroxyapatite treated with NTAP for 10 or 30 seconds and compared with those on untreated hydroxyapatite (control). CA1, CA2, CA3 = first, second, and third contact angle measurements, respectively.*

statistical differences among treatments were observed after two years of water storage. Hirata and others[6] also found the same performance in one-year aged plasma-treated groups associated with SBU in the SE approach.

In the present study, two years of water storage did not decrease dentin μTBS for ER groups, and the two-year aged control group and NTAP 10-second group presented significantly lower μTBS when compared with the NTAP 30-second group. There is today no clear consensus about the potential beneficial effects of NTAP, especially because most of the investigations did not evaluate long-term results. Different factors, such as specifications of the plasma device and the adhesive system used, makes it difficult to draw a direct comparison with other plasma studies, and this fact justifies the evaluation of a longer aging using the same parameters (adhesive system, direct water storage, NTAP application time/specifications).

However, studies from our research group using the SBU adhesive associated with the same plasma equipment (Surface Plasma Tool Model SAP) in standard specifications were recently published. SBU maintained its μTBS strength to dentin after one year of direct water exposure and exposure to simulated pulpal pressure, although remarkable statistical differences between treatments were observed depending on the aging condition.[22] A more recent method, mini-interfacial fracture toughness, showed no difference among plasma-treated and -untreated groups upon 6 months of aging, which could be explained by the short-time aging evaluation, once SBU also showed bonding stability in the present study even after two years of water aging.[23]

Although nanohardness and Young's modulus assessments were performed only one week after

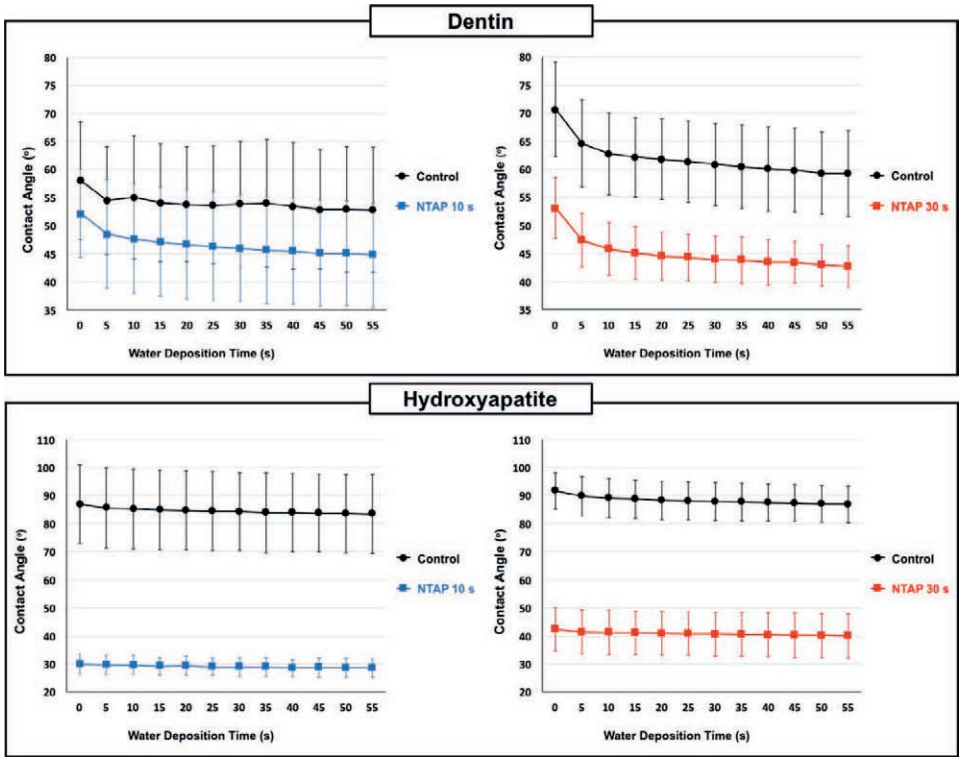

Figure 4. *Means of water contact angle immediately after NTAP application for 10 or 30 seconds on the surfaces of dentin and hydroxyapatite surfaces compared with those on untreated (control) substrates.*

applying NTAP, adhesives, and composite, they provided consistent and very rich information to explain the beneficial effects of NTAP on resin/dentin-treated interfaces. When evaluating the hybrid layer, both application times of NTAP (10 seconds and 30 seconds) presented values of nanohardness and Young's modulus that were statistically higher than the respective untreated (control) groups. Thus, the second hypothesis was rejected because NTAP produced significant stiffening of the hybrid layer.

Another important observation was that no difference in nanohardness or Young's modulus was found in the adhesive layer (Tables 4 and 5). This result was also expected since the same adhesive resin was used in all the groups. However, the differences found in the hybrid layer raise the question about what caused the hardness increase in the specific area where the adhesive was in intimate contact with the plasma-modified surface.

The findings in the mechanical properties of the resin-dentin interface might be related to two possible alterations promoted by the NTAP application. One is the possible promotion of a higher cross-link density of the adhesive system, which may have originated from a greater number of chemical reactions, promoting the breaking of carbon chains. The plasma-treated dentin receives a jet of electrons, free radicals, and ions and therefore produces a more reactive surface, which can trigger more chemical reactions of the monomer components of the adhesive system. Chen and others[10] applied a plasma brush in a model adhesive under different water/HEMA mass ratios and demonstrated the plasma's effectiveness in inducing polymerization. Conversion values of the plasma-cured groups were higher than those of light-cured samples with the same mass ratio and water content.

Another possible explanation is that the adhesive system is able to interact strongly with partially demineralized dentin (in the SE mode) and fully demineralized dentin (in the ER technique), leaving less voids or water-filled spaces. An *in situ* zymography assay showed a progressive decline of enzymatic activity with increase of NTAP exposure time.[22] Application of NTAP apparently inhibited the enzymatic activity in the ER specimens, especially in the hybrid layer area. The NTAP-treated dentin should demonstrate better infiltration and polymerization of resin monomers, corroborating the present findings of mechanical properties in the hybrid layer.

These theories might be confirmed by additional evaluations, such as transmission electron microscopy and Fourier transform infrared spectroscopy, in which the ultramorphology interaction between the

adhesive and plasma-treated dentin can be observed as well as the degree of conversion of resin-based materials, respectively. In addition, long-term aging evaluation of nanohardness and Young's modulus of the resin-dentin interface's structures are incentivized. The correlation between μTBS and nanomechanical properties of the resin-adhesive interface might be controversial. According to Freitas and others, this correlation was reported as inverse, suggesting that a lower Young's modulus for the adhesive layer offers more adequate resistance of the adhesive to elastic deformation under stress, although the difference was statistically significant only for the adhesive layer and the SBU adhesive was not evaluated.[24] In the present study, the higher nanohardness and Young's modulus were related to the NTAP application effect on the hybrid layer, which also presented the highest μTBS absolute means when applied for 30 seconds in dentin, indicating a positive correlation.

The supposition of a higher interaction of the adhesive system with the plasma-treated substrate was corroborated by the findings in the CA analysis by the sessile drop method. The NTAP treatment had a much stronger influence on the hydrophilicity of hydroxyapatite than of dentin. This finding indicates that the plasma effect is stronger on the inorganic content of the substrate. However, it is worth mentioning that the hydroxyapatite arrangement in the dentin substrate is much more complex, involving tubules with different distributions and diameters.[16] In dentin, the NTAP application time of 10 seconds promoted a slightly lower CA mean than the control group, while the application for 30 seconds showed a more significant difference. Thus, the third hypothesis was also rejected.

In the triplicate test, every time that the application of the water droplet was repeated, the hydrophilicity decreased in the NTAP 30-second groups. Apparently, the presence of moisture on a surface after the NTAP application is likely to decrease the hydrophilicity potential. The highly reactive particles produced on the surface by NTAP can cross-link rapidly to form various chemical functional groups.[10] The authors hypothesize that the droplets of water molecules may have acted as a contaminant, preventing the new water droplets from reacting with the plasma-modified surface, jeopardizing the wettability. This would also explain why the NTAP effect was more evident in the hydroxyapatite dry sample than in the partially wet dentin.

Therefore, it seems reasonable to counteract rehydration of the dentin after the NTAP application and to avoid contamination by water/saliva, letting only the adhesive system have direct contact with the plasma-treated substrate, allowing for a good infiltration. The NTAP application for longer time (30 seconds) produced higher hydrophilicity in dentin than the shorter time (10 second) in the first CA assessment and was more negatively affected in the third water droplet application. But it is worth noting that even after three water drop exposures, the NTAP treatment still maintained a higher hydrophilicity than the control groups in all water deposition times, especially on the hydroxyapatite substrate, which indicates the partial maintenance of hydrophilic properties.

Aiming to evaluate only the immediate effect of the NTAP treatment on surface hydrophilicity, the sessile drop CA method was performed again on new samples, but with only one measurement per spot. A larger number of samples were prepared to obtain a more representative mean since there were no repetitions. Once again, the NTAP effect on hydroxyapatite's hydrophilicity was much stronger than on the dentin's, even using the shorter treatment time (10 seconds), whose effect did not differ from the longer treatment time (30 seconds) in this particular substrate. In dentin, the application time for 30 seconds produced a more significant difference in the CA comparison with the control group.

Besides adhesion by contact, the presence of the 10-MDP monomer in the composition of the multimode adhesive tested in this study produces chemical reactions with calcium from hydroxyapatite, forming a hydrolytic stable dentin-resin interaction.[25] Yoshida and others revealed Ca-salt formation and nanolayering within the hybrid layer; however, this additional bonding mechanism was not always equally consistent for SBU nor Clearfil SE Bond (Kuraray Noritake).[26] According to those authors, more intense nanolayering was found in the areas with more demineralization. Because the dentin is a moist substrate, the preexisting and/or remaining water may result in more ionization of the acidic functional monomer once intense nanolayering is observed in the neighborhood of the dentin tubules.

Regarding the chemical surface characterization of NTAP-treated dentin surfaces, a study using Raman confocal microscopy showed no statistical difference in carbonate and collagen type I spectra in etched and unetched dentin groups after plasma application.[22] They also reported no remarkable topographical alteration at the dentin surface when character-

ized by atomic force microscopy. One could expect that the NTAP effect on surface hydrophilicity, especially on inorganic substrate, could also influence the chemical interaction potential of 10-MDP with hydroxyapatite. A dense nanolayered structure with a hydrophobic nature would help in protecting the resin-dentin interface against hydrolytic degradation effects.

CONCLUSIONS

Dentin NTAP treatment for 30 seconds influences the μTBS of the multimode SBU adhesive in the ER approach after two years of water aging. This positive result might be correlated with the increase in nanohardness and Young's modulus of the hybrid layer and to the greater dentin hydrophilicity, two phenomena observed in short-time evaluation. Although some effects were observed using a plasma application for 10 seconds, the results suggest that 30 seconds is the most indicated treatment time.

Acknowledgement

The authors acknowledge the State of São Paulo Research Foundation (FAPESP) for financial support (2013/15952-7 and 2015/05939-9) of this study.

Regulatory Statement

This study was conducted in accordance with all the provisions of the local human subjects oversight committee guidelines and policies of the Commission for Medical Ethics of KU Leuven. The approval code for this study is: S57622.

Conflict of Interest

The authors of this article certify that they have no proprietary, financial, or other personal interest of any nature or kind in any product, service, and/or company that is presented in this article.

(Accepted 17 May 2018)

REFERENCES

1. Liu Y, Liu Q, Yu QS, & Wang Y (2016) Nonthermal atmospheric plasmas in dental restoration *Journal of Dental Research* **95(5)** 496-505.
2. Han GJ, Kim JH, Chung SN, Chun BH, Kim CK, Seo DG, Son HH, & Cho BH (2014) Effects of non-thermal atmospheric pressure pulsed plasma on the adhesion and durability of resin composite to dentin *European Journal of Oral Science* **122(6)** 417-423.
3. Dong X, Ritts AC, Staller C, Yu Q, Chen M, & Wang Y (2013) Evaluation of plasma treatment effects on improving adhesive-dentin bonding by using the same tooth controls and varying cross-sectional surface areas *European Journal of Oral Science* **121(4)** 355-362.
4. Ritts AC, Li H, Yu Q, Xu C, Yao X, Hong L, & Wang Y (2010) Dentin surface treatment using a non-thermal argon plasma brush for interfacial bonding improvement in composite restoration *European Journal of Oral Science* **118(5)** 510-516.
5. Dong X, Li H, Chen M, Wang Y, & Yu Q (2015) Plasma treatment of dentin surfaces for improving self-etching adhesive/dentin interface bonding *Clinical Plasma Medicine* **3(1)** 10-16.
6. Hirata R, Teixeira H, Ayres AP, Machado LS, Coelho PG, Thompson VP, & Giannini M (2015) Long-term adhesion study of self-etching systems to plasma-treated dentin *Journal of Adhesive Dentistry* **17(3)** 227-233.
7. Koban I, Duske K, Jablonowski L, Schröder K, Nebe B, Sietmann R, Weltmann KD, Hübner NO, Kramer A, & Kocher T (2011) Atmospheric plasma enhances wettability and osteoblast spreading on dentin *in vitro*: proof-of-principle *Plasma Processes and Polymers* **8(10)** 975-982.
8. Chen M, Zhang Y, Sky Driver M, Caruso AN, Yu Q, & Wang Y (2013) Surface modification of several dental substrates by non-thermal, atmospheric plasma brush. *Dental Materials* **29(8)** 871-880.
9. Lehmann A, Rueppell A, Schindler A, Zylla I-M, Seifert HJ, Nothdurft F, Hannig M, & Rupf S (2013) Modification of enamel and dentin surfaces by non-thermal atmospheric plasma *Plasma Processes and Polymers* **10(3)** 262-270.
10. Chen M, Zhang Y, Yao X, Li H, Yu Q, & Wang Y (2012) Effect of a non-thermal, atmospheric-pressure, plasma brush on conversion of model self-etch adhesive formulations compared to conventional photo-polymerization *Dental Materials* **28(12)** 1232-1239.
11. Zhang Y, Yu Q, & Wang Y (2014) Non-thermal atmospheric plasmas in dental restoration: improved resin adhesive penetration *Journal of Dentistry* **42(8)** 1033-1042.
12. Van Meerbeek B, Willems G, Celis JP, Roos JR, Braem M, Lambrechts P, & Vanherle G (1993) Assessment by nano-indentation of the hardness and elasticity of the resin-dentin bonding area *Journal of Dental Research* **72(10)** 1434-1442.
13. Sadr A, Shimada Y, Lu H, & Tagami J (2009) The viscoelastic behavior of dental adhesives: a nanoindentation study *Dental Materials* **25(1)** 13-19.
14. Lopes B, Ayres AP, Lopes L, Negreiros W, & Giannini M (2014) The effect of atmospheric plasma treatment of dental zirconia ceramics on the contact angle of water *Applied Adhesion Science* **2(1)** 1-8.
15. Poitevin A, De Munck J, Van Landuyt K, Coutinho E, Peumans M, Lambrechts P, & Van Meerbeek B (2007) Influence of three specimen fixation modes on the microtensile bond strength of adhesives to dentin *Dental Materials Journal* **26(5)** 694-699.
16. Oliver W & Pharr G (1992) An improved technique for determining hardness and elastic modulus using load and displacement-sensing indentation systems *Journal of Materials Research* **7(6)** 1564-1583.
17. Tjäderhane L, Carrilho MR, Breschi L, Tay FR, & Pashley DH (2009) Dentin basic structure and composition-an overview *Endodontic Topics* 2009 **20(1)** 3-29.

18. Marchesi G, Frassetto A, Mazzoni A, Apolonio F, Diolosà M, Cadenaro M, Di Lenarda R, Pashley DH, Tay F, & Breschi L (2014) Adhesive performance of a multi-mode adhesive system: 1-year *in vitro* study *Journal of Dentistry* **42(5)** 603-612.
19. Rosa WL, Piva E, & Silva AF (2015) Bond strength of universal adhesives: a systematic review and meta-analysis *Journal of Dentistry* **43(7)** 765-776.
20. Muñoz MA, Luque-Martinez I, Malaquias P, Hass V, Reis A, Campanha NH, & Loguercio AD (2015) *In vitro* longevity of bonding properties of universal adhesives to dentin *Operative Dentistry* **40(3)** 282-292.
21. Vermelho PM, Reis AF, Ambrosano GM, & Giannini M (2017) Adhesion of multimode adhesives to enamel and dentin after one year of water storage *Clinical Oral Investigations* **21(5)** 1707-1715.
22. Ayres AP, Bonvent JJ, Mogilevych B, Soares LES, Martin AA, Ambrosano GM, Nascimento FD, Van Meerbeek B, & Giannini M (2017) Effect of non-thermal atmospheric plasma on the dentin-surface topography and composition and on the bond strength of a universal adhesive *European Journal of Oral Sciences* **126(1)** 53-65.
23. Ayres APA, Pongprueksa P, De Munck J, Gré CP, Nascimento FD, Giannini M, & Van Meerbeek B (2017) Mini-interfacial fracture toughness of a multimode adhesive bonded to plasma-treated dentin *Journal of Adhesive Dentistry* **19(5)** 409-416.
24. Freitas PH, Giannini M, França R, Correr AB, Correr-Sobrinho L, & Consani S (2016) Correlation between bond strength and nanomechanical properties of adhesive interface *Clinical Oral Investigations* **21(4)** 1055-1062.
25. Yoshida Y, Van Meerbeek B, Nakayama Y, Yoshioka M, Snauwaert J, Abe Y, Lambrechts P, Vanherle G, & Okazaki M (2001) Adhesion to and decalcification of hydroxyapatite by carboxylic acids *Journal of Dental Research* **80(6)** 1565-1569.
26. Yoshida Y, Nagakane K, Fukuda R, Nakayama Y, Okazaki M, Shintani H, Inoue S, Tagawa Y, Suzuki K, De Munck J, & Van Meerbeek B (2004) Comparative study on adhesive performance of functional monomers *Journal of Dental Research* **83(6)** 454-458.

©Operative Dentistry, 2018, **43-6,** E300-E307

Cuspal Flexure and Stress in Restored Teeth Caused by Amalgam Expansion

BT Danley • BN Hamilton • D Tantbirojn • RE Goldstein • A Versluis

Clinical Relevance

Although amalgam is being phased out, existing amalgam fillings will still be present for many years. Clinicians should be aware that amalgam expansion may create stress conditions that accelerate tooth cracking.

SUMMARY

Objective: Cracks in amalgam-filled teeth may be related to amalgam expansion. This study measured cuspal flexure and used finite element analysis to assess associated stress levels in amalgam-filled teeth.

Methods and Materials: External surfaces of 18 extracted molars were scanned in three dimensions. Nine molars were restored with mesio-occluso-distal amalgam fillings; the other teeth were left intact as controls. All teeth were stored in saline and scanned after two, four, and eight weeks. Cuspal flexure and restoration expansion were determined by calculating the difference between scanned surfaces. Stresses in a flexed tooth were calculated using finite element analysis.

Results: Cusps of amalgam-filled teeth flexed outward approximately 3 μm, and restoration surfaces expanded 4 to 8 μm during storage. Cuspal flexure was significantly higher in the amalgam group (multivariate tests, $p<0.05$), but storage time had no significant effect (repeated measures, $p>0.05$). Expansion caused stress concentrations at the cavity line angles. These stress concentrations increased stresses due to mastication 44% to 178%.

Conclusions: Amalgam expansion pushed cavity walls outward, which created stress concentrations at the cavity line angles. Expansion stresses can raise stresses in amalgam-filled teeth and contribute to incidentally observed cracks.

Brent T Danley, BS, College of Dentistry, University of Tennessee Health Science Center, Memphis, TN, USA

Bruce N Hamilton, MS, DDS, Department of Restorative Dentistry, College of Dentistry, University of Tennessee Health Science Center, Memphis, TN, USA

Daranee Tantbirojn, DDS, MS, PhD, Department of Restorative Dentistry, College of Dentistry, University of Tennessee Health Science Center, Memphis, TN, USA

Ronald E Goldstein, DDS, private practice, Atlanta, and clinical professor of Oral Rehabilitation, Dental College of Georgia, Augusta University, Augusta, GA, USA

*Antheunis Versluis, PhD, College of Dentistry, Department of Bioscience Research, College of Dentistry, University of Tennessee Health Science Center, Memphis, TN, USA

*Corresponding author: 875 Union Ave, Memphis, TN 38163; e-mail: antheun@uthsc.edu

DOI: 10.2341/17-329-L

INTRODUCTION

Dental amalgam was introduced in dentistry in the early 1800s and has accumulated an impressive

Figure 1. *Cracks on marginal ridges and triangular ridges next to amalgam restorations.*

record as a tooth-filling material. However, because of environmental, health, and esthetic concerns, amalgam is being replaced by resin-based alternatives as the material of choice for direct restorations. In 2005, an estimated 52 million amalgam fillings were placed in the United States versus approximately 96 million in 1990.[1,2] According to a projection from the United States Food and Drug Administration, more than 30 million amalgam restorations are expected to be placed up to the year 2023.[3] Although the use of amalgam is thus declining, millions of amalgam-restored teeth are still in function today and will be for many years depending on their durability.

Despite the respectable life span of amalgam fillings, often surpassing that of resin-based composite restorations,[4-6] their ultimate failure can have serious consequences for the longevity of a tooth. Common reasons for restoration failures are secondary caries, fracture of the filling, or tooth fracture.[6-8] Secondary caries or fractured fillings can be treated by replacing the filling, but a fractured tooth will require complex or costly indirect restoration or even become unrestorable.

Cracks are a common sight in teeth. Dental practitioners often observe cracks developing at a marginal ridge or radiating from amalgam fillings, as shown in Figure 1. Fractures are the final stage of crack propagation. Teeth restored with nonbonded amalgam were found to be more likely to have cracks or fractured tooth structures than adhesive composite restorations.[6,8,9] Restoration, cavity design, excursive occlusal interference, and age have all been identified as factors that predispose a tooth to cracking.[9-11]

Another factor that may also play a role is expansion of the amalgam restoration, which would introduce stresses in a restored tooth. Amalgam is known to expand due to phase changes and corrosion.[12,13] Expansion of amalgam in a confined cavity coupled with creep and corrosion products has been proposed to close the interfacial gap and cause the amalgam extrusion that can be observed after years of service.[14] The observation of creep implies the presence of continuous pressure imposed on the restoration by the confining tooth structure, which in turn implies the presence of stresses in the tooth structure. It is conceivable that the presence of such stresses has consequences for the longevity of teeth with amalgam fillings if it elevates stress levels in the tooth structure.

Considering the large pool of aging amalgam restorations present in the population, understanding how they may affect stresses in a tooth will remain a clinical concern for many years. The objective of this study was to investigate whether amalgam fillings could add stresses in the tooth-restoration complex and, if so, how significant those stresses could be. To verify that an amalgam restoration can stress a tooth, we measured cuspal flexure of teeth with an amalgam filling. The significance of expansion on stress levels was assessed by evaluating restored teeth with similar cuspal flexure in a finite element analysis.

METHODS AND MATERIALS

Cuspal Flexure and Restoration Expansion

Eighteen extracted human maxillary and mandibular molars (approved by the Institutional Review Board) were mounted in stainless steel rings with embedded reference spheres (Figure 2). The mean and standard deviation of the buccal-lingual widths, measured at the height of contour, were 10.0 ± 0.6 mm. Nine teeth were filled with amalgam, and the other nine teeth were left intact (no preparation). A sample size of nine had 95% confidence to detect a difference of 0.65 standard deviation between groups. The external enamel surfaces were etched with 37% phosphoric acid solution to obtain dull surfaces. A mesio-occluso-distal (MOD) cavity (4-mm deep, 4-mm wide) was prepared in nine teeth and was restored with zinc-containing amalgam (Permite, SDI, Bayswater, Victoria, Australia). The external tooth surfaces and reference spheres were scanned from eight directions following restoration using a three-dimensional optical scanner (COMET xS, Steinbichler Optotechnik GmbH, Neubeuern, Germany). This scan was used as a baseline. After scanning, the restored teeth were immersed in normal saline solution (0.9% sodium chloride irrigation USP; B. Braun Medical Inc, Bethlehem, PA, USA) for eight weeks and rescanned at two, four, and eight weeks. Nine unprepared teeth were used

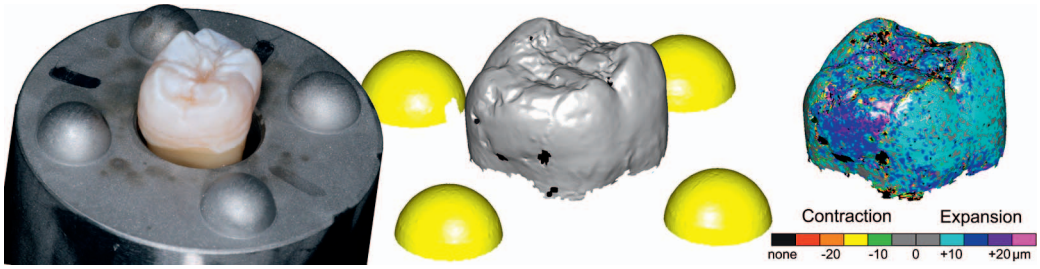

Figure 2. *Teeth were secured in stainless steel rings with embedded reference spheres. The scans were aligned with their baseline using the reference spheres (yellow). Cuspal flexure and expansion of the amalgam restoration on the occlusal, mesial, and distal surfaces are shown according to the color scale.*

as a control. They were scanned and stored using the same procedure as the restored teeth. Scanned surfaces were aligned with the baseline scans by means of the reference spheres on the mounting rings using Cumulus software (Regents of the University of Minnesota; Figure 2). Buccal and lingual tooth surface areas (from height of cavity floor to just below the cuspal ridges) as well as occlusal and proximal amalgam filling surfaces were separately selected on the baseline scans. Custom-developed software compared each of the selected baseline surface areas with the follow-up surface scans. Differences between the baseline and follow-up surfaces, which geometrically constitute a volume, were calculated and divided by the selected surface areas to obtain the buccal and lingual cusp flexure and the occlusal and proximal amalgam filling expansion. Total cuspal flexure was the sum of the buccal and lingual flexure; proximal expansion was the average of the mesial and distal amalgam filling expansion. Effects of amalgam restoration on cuspal flexure were compared with the control group at each time interval with multivariate tests and post hoc multiple comparisons using the Games-Howell test (equal variances not assumed; IBM SPSS Statistics, version 25.0, Armonk, NY, USA). Effects of storage time on cuspal flexure of the amalgam-restored teeth and control teeth were analyzed using general linear model repeated measures (IBM SPSS Statistics).

Finite Element Analysis

Volumetric expansion was applied in a finite element model of an MOD-restored tooth to evaluate the stress distribution associated with experimentally measured cuspal flexure. The finite element model was based on an image of a cross-sectioned tooth. The outlines of the dentin and enamel were traced and imported into a finite element program (Marc/Mentat, MSC Software, Palo Alto, CA, USA). Three cavity shapes were created using the Mentat preprocessor software, with 0°, 5°, or 10° of wall convergence. Each cavity was 4-mm deep and 4-mm wide, as shown in Figure 3. The outlined dentin, enamel, and restoration were meshed manually using quadrilateral elements, using an element relaxation option that maintained optimal element shapes. The root was not modeled because restoration expansion affected only the tooth crown. The tooth models were therefore fixed below the cemento-enamel junction. Amalgam restoration surfaces were free to separate or slide along the surrounding cavity surfaces with an arbitrary 0.5 coefficient of friction.

Material properties were assigned to the dentin, enamel, and restoration elements. The applied elastic moduli (84 GPa for enamel, 18 GPa for dentin, and 28 GPa for amalgam) as well as the Poisson's ratios (0.30 for enamel, 0.24 for dentin, and 0.35 for amalgam) were obtained from the literature.[15] Transverse isotropic conditions were prescribed for the enamel, assuming the 84 GPa elastic modulus value along the principal enamel axis, perpendicular to the enamel-dentin junction, whereas the value was 42 GPa in lateral directions. Since the objective of this analysis was stress in the tooth structure for a specific experimentally measured cuspal deflection value, creep of the amalgam did not need to be modeled.

To produce the specific cuspal deflection, volumetric expansion was prescribed for the modeled amalgam restoration using thermal analogy. This involved increasing notional temperature in the amalgam to induce expansion. The resulting volume change pressed the amalgam restoration against the surrounding cavity floor and walls, generating deformation and stress in the tooth, outward flexure of the cusps, and an elevation of the occlusal surface as it was extruded. In addition, occlusal forces were applied on the lingual or buccal cuspal inclines to simulate a chewing load of 20 N distributed over a 1.5-mm^2 surface area.

Figure 3. *Calculated displacements and stresses in the cross section of an amalgam-filled tooth with 3-μm cuspal flexure due to amalgam expansion. Stress concentrations are seen at the cavity line angles. Stress concentrations intensified when a masticatory load was added on the lingual or buccal cusp (20 N over 1.5 mm^2 area, indicated with arrows).*

Stresses in three directions (cross-sectional plane and perpendicular to the cross section according to plane strain conditions) were collected in the dentin and enamel elements during the simulation of amalgam expansion and cuspal flexure. The combination of these three stress components was expressed in an equivalent stress value according to the modified von Mises criterion. This criterion is based on the common von Mises criterion but modified such that it can account for the higher compressive and lower tensile strengths of enamel, dentin, and amalgam. The modification assigns tensile stresses higher "weight" in the equivalent stress expression than compressive stresses.[16] The compressive/tensile strength ratios used were 384/10 for enamel, 297/99 for dentin, and 388/66 for amalgam.[15]

RESULTS

Displacements were measured across all external surfaces (Figure 2) after two-, four-, and eight-week storage. Mean cuspal flexure and expansion values of the occlusal, mesial, and distal amalgam surfaces were calculated over each affected surface (Table 1). Positive values indicate outward movement (expansion). Multivariate tests showed that the amalgam restoration caused significant cuspal flexure at each time interval. The repeated-measures tests indicated that the storage time had no significant effect on either the amalgam (p=0.202) or control groups (p=0.069). Amalgam on proximal surfaces expanded more than those on the occlusal surface.

To match the experimentally determined cuspal flexure of about 3 μm, a 0.3% volumetric (=0.1% linear) expansion was applied in the finite element analysis. The simulated amalgam expansion caused stresses in the tooth structure, with stress concentrations at the cavity floor and line angles (Figure 3). The occlusal surface extruded 3.5 to 4 μm due to the amalgam expansion. The 5° of wall convergence increased cuspal flexure by 26% compared with a cavity with straight walls and 29% when the wall convergence was 10°. Stress concentrations in dentin

Table 1: *Cuspal Flexure and Amalgam Expansion on Occlusal and Proximal (Averaged From Mesial and Distal) Surfaces (Mean ± Standard Deviation; μm)*[a]

	2 wk	4 wk	8 wk
Cuspal flexure, amalgam	3.18 ± 2.72*	3.55 ± 2.14*	3.70 ± 2.42*
Cuspal flexure, control	−0.40 ± 0.77§	−0.53 ± 1.00§	−0.41 ± 0.49§
Amalgam expansion, occlusal	4.69 ± 1.38	5.05 ± 1.37	5.02 ± 1.35
Amalgam expansion, proximal	8.66 ± 1.40	8.36 ± 1.43	8.40 ± 1.51

[a] *Positive values indicate outward flexure (expansion). The symbols * and § indicate significantly different mean cuspal flexure values between the control and amalgam-restored teeth (multivariate tests, $p=0.002$, $p=0.001$, $p<0.001$ for the two-week, four-week, and eight-week time intervals, respectively).*

due to amalgam expansion were 3% to 14% higher with convergent cavity walls. The expansion of the amalgam filling caused an increase in stress values in dentin at the lingual line angle by 131% to 178% when a 20-N masticatory load was simulated on the lingual cusp and 44% to 45% in the buccal line angle when the load was applied on the buccal cusp. These percentages corresponded with an average stress increase at the cavity line angles of 10 to 15 MPa. Stresses at the opposite cavity line angle decreased during cuspal loading.

DISCUSSION

A study about amalgam fillings may seem obsolete in the 21st century. However, considering the longevity of amalgam fillings, which can be 30 to 40 years, hundreds of millions are currently in function all over the world. In 2009, a meeting convened at World Health Organization headquarters in Geneva, Switzerland, encouraged a global "phase down" of the use of amalgam due to environmental health concerns and in response to global initiatives on mercury reduction from the United Nations Environment Programme.[17] However, complete phase out of amalgam has not yet happened, as it is still the most affordable restorative option.[2,17] Amalgam restorations will therefore have a presence in dentistry for many years to come.

Although it is well-known that amalgam expands and amalgam extrusion is observed at the margins,[12-14] the mechanism of crack initiation by such expansion has not been studied directly. In this study, we explored expansion as one of the mechanisms contributing to the cracks and fractures that are often observed in aging amalgam-filled teeth. Cracks that could be detected with an explorer were found to be twice as likely in teeth restored with amalgam compared with resin-based composites.[9] In 370 patients with cracked tooth syndrome, 82% of those were found in amalgam-filled teeth.[18] In addition, a 12-year survival study reported more than 10% of 1200 amalgam fillings failed because of tooth fracture or cracked tooth.[8] Cracks in the tooth structure are in response to stresses, which can originate from masticatory forces, environmental effects, or pressure exerted by an expanding restoration. Amalgam expansion due to phase changes or corrosion is well documented,[12,13] and cuspal flexure of amalgam-filled teeth has been observed *in vitro*.[19] Under clinical conditions, amalgam expansion is also confirmed by the observation of occlusal extrusion of aging fillings.[14,20,21] Nevertheless, stresses in the tooth structure due to amalgam expansion have been largely dismissed with reference to creep as an alleviating mechanism.[14] Although amalgam creep would lessen stress levels, creep does not occur without the presence of continuous stress.

The most obvious source for continuous stress is pressure imposed on the amalgam filling by the confining tooth structure if amalgam would expand. If amalgam is under pressure from the tooth structure, the tooth must also be under stress. To evaluate the hypothesis that a tooth structure can be stressed by an amalgam filling, we measured cuspal flexure. The experimental method for measuring tooth cusps bending in- or outward is well established for determining the effects of polymerization shrinkage or hygroscopic expansion stresses in restored teeth.[22-24] We used saline storage in an attempt to accelerate the aging of our amalgam fillings because reference surfaces necessary for accurately determining tooth surface changes cannot be kept stable for long. We measured significant cuspal flexure for the amalgam-filled teeth of more than 3 μm after two weeks of storage. This value is comparable to the 2.7 μm previously reported for teeth with 4-mm-wide amalgam MOD fillings after one week.[19] Since unsupported cusps after cavity preparation have been shown to flex in random directions,[25] the consistently outward cuspal flexure supports the hypothesis that the amalgam fillings expanded and stressed the tooth structure. Moreover, we measured 4- μm to 8-μm expansion on the occlusal and proximal amalgam surfaces, which confirmed an expanding amalgam filling and indicated that the reason for the cuspal flexure was likely expansion of the filling.

Amalgam expansion and creep are generally considered positive effects because they close the interfacial gap,[14] thereby tacitly assuming that expansion is an insignificant factor in tooth fractures. In a photoelastic study, cylindrical amalgam fillings caused only minimal stresses in a block of photoelastic material.[26] To test the significance of the measured flexure values, we calculated the stress level associated with 3-μm cuspal flexure of a tooth with MOD filling using finite element analysis. The analysis showed stress concentrations at the cavity line angles. Stress concentrations are areas where stresses are higher compared with surrounding areas (indicated by orange and yellow colors in Figure 3) and therefore identify locations where maximum stress will be exceeded first and crack initiation is thus most likely. The analysis thus confirmed clinical observations that line angles are usually involved in cuspal fractures. Nevertheless, there is no clinical or experimental evidence that amalgam expansion stress is sufficient to cause cusp fracture.[21] In our finite element analysis, the highest (principal) stresses at the cavity line angles were in the range of 10 to 25 MPa, which is well below the tensile strength of dentin and thus supports the notion that amalgam expansion alone is not sufficient to cause tooth fracture.

Cuspal fracture usually occurs during functional or parafunctional loading, often when no excessive forces are applied. Anecdotes of cuspal or tooth fractures when chewing on soft food are very familiar. Such fracture behavior has all the characteristics of fatigue failure, which is a process of crack propagation under repetitive loading that is lower than the original structural strength. Amalgam expansion stresses may not be sufficient to fracture a cusp, but they may accelerate fatigue crack initiation and propagation by raising stress levels in a tooth. We used the finite element analysis to test this hypothesis and found that amalgam expansion stresses associated with a 3-μm cuspal flexure increased stress concentrations at the cavity line angles 44% to 178% compared with a nonexpanding amalgam filling. According to the classic crack growth equation known as Paris' law, the fatigue crack rate is essentially a power function of the stress amplitude.[27] Increases in the level of repetitive stress values could thus result in significant acceleration of crack propagation and in higher incidence of fatigue fractures. The clinical significance of amalgam expansion is therefore not its inability to break a cusp but rather the effect it has on increasing the stress levels.

Stress levels in restored teeth depend on many factors, where each combination of amalgam alloy, cavity configuration, and tooth will affect the stress development and distribution. Not all variations could be covered in this study. The amalgam we used is a high-copper, non-gamma-2 admixed alloy containing 0.2% zinc.[28] High-copper amalgam associated with expansion and low creep is thought to have contributed to an increased incidence and severity of cusp fracture of endodontically treated posterior teeth.[29] Other amalgams, for example, zinc-containing low-copper alloys, could have caused more expansion if contaminated with moisture,[30] or amalgams exhibiting more creep could have resulted in lower cuspal flexure values.[14] We chose the zinc-containing high-copper alloy because it allowed us to accelerate the aging process needed to assess cuspal flexure before reference surfaces became unstable. The controls showed that after eight weeks in saline, the stability of the reference surfaces became unreliable. Note that moisture contamination was not an issue because the fillings were placed in a dry *in vitro* environment.

The choice of cavity configuration also affected our outcomes. A large MOD cavity significantly weakens the tooth structure, which increases the tooth deformation and thus stresses in the tooth. The slot cavity design in this study had a constant 4-mm depth without proximal boxes to achieve maximal cuspal deformation. A small occlusal cavity or conventional Class II cavity is less injurious to the tooth stiffness, which results in less tooth deformation from amalgam expansion and thus lower stresses in the tooth. This may explain the previously mentioned low stresses in a block of photoelastic material with cylindrical cavity.[26] Note, however, that stress concentrations will change depending on the cavity configuration. In occlusal fillings, stress concentrations due to expansion are likely to shift to the occlusal surface where the lower tensile strength and fracture toughness of enamel may predispose occlusal margins to increased risk of crack initiation and propagation. In this study, we considered three levels of convergence for our MOD cavities (0°, 5°, and 10°). Generally, stress concentrations intensified with increasing convergence. However, the value did not only depend on convergence, but also the surrounding, remaining tooth structure. For example, a smaller cavity with higher conversion angle may generate lower stress concentrations than a large cavity with less convergence. Similarly, stress distributions are affected by the location and distribution of occlusal loading. Two load conditions were examined in this study. They

showed that loading of unsupported cusps creates significant stress concentrations at the cavity line angles. Those stress concentrations caused by masticatory loading can be avoided by bonding a filling to the cavity walls.[31] However, stress concentrations at cavity line angles that are generated by restoration expansion will not be prevented by bonding. Note also that expansion stresses differ from more familiar polymerization shrinkage stresses because stresses caused by the expansion of Class II restorations tend to concentrate on internal tooth surfaces, whereas stresses caused by shrinkage tend to concentrate on external tooth surfaces.[31] Restoration expansion stress concentrations thus coincided with the location where stresses generated by masticatory loading also concentrated.

Clearly, predicting stresses is complex and should not be generalized because unique factors of each tooth-restoration complex need to be taken into account. The results of this study should therefore not be applied blindly to other alloys or cavity configurations. The significance of our experiment, however, is the demonstration that amalgam has the potential to significantly raise stress levels in filled teeth. Even though the life span of amalgam fillings is respectable,[4,6,8] cracks in the tooth structure can lead to extensive re-restoration or render a tooth unrestorable.

Clinicians should therefore be aware that cracks associated with amalgam restorations are likely to propagate in a fatigue process that eventually leads to catastrophic fracture. Viewing teeth with amalgam filling up close with an intraoral camera helps to verify the presence of microcracks, especially when using a bright light to transilluminate the tooth. Moreover, clinicians should be aware that higher convergent cavity walls as well as sharp cavity line angles intensify the local stress concentrations, which are likely to accelerate crack propagation, and that bonding an amalgam filling may restore structural integrity but will not eliminate the effect of amalgam expansion stresses. Amalgam fillings have a good track record for longevity and technique insensitivity, but if clinicians are concerned about maintaining tooth integrity, amalgam may not be the best choice. Amalgam fillings may create stress conditions that accelerate tooth cracking. Amalgam fills a cavity but does not restore the tooth.[31]

CONCLUSION

During the eight-week storage in normal saline solution, amalgam fillings expanded and pushed cavity walls outward. Finite element analysis showed that the expansion caused stress concentrations in the tooth structure at the lingual and buccal internal line angles. These expansion stresses added to stresses generated by masticatory loads and were hypothesized to contribute to initiation and propagation of tooth cracks incidentally observed around amalgam restorations. Results from the finite element analysis suggested that cavity convergence may be a contributing factor.

Acknowledgements

This study was supported, in part, by the University of Tennessee Health Science Center College of Dentistry Alumni Endowment Fund, the Tennessee Dental Association Foundation, and by the Alpha Omega Foundation Research Fund. The authors are grateful to Dr Ralph DeLong, University of Minnesota, who developed the Cumulus software.

Regulatory Statement

This study was conducted in accordance with all the provisions of the local human subjects oversight committee guidelines and policies of the University of Tennessee Health Science Center. The approval code for this study is 15-04302-NHSR.

Conflict of Interest

The authors of this article certify that they have no proprietary, financial, or other personal interest of any nature or kind in any product, service, and/or company that is presented in this article.

Note

This study was presented in part at the International Association for Dental Research annual meeting in San Francisco, March 2017.

(Accepted 30 May 2018)

REFERENCES

1. US Public Health Service, Committee to Coordinate Environmental Health and Related Programs (1993) *Dental Amalgam: A Scientific Review and Recommended Public Health Service Strategy for Research, Education and Regulation*: *Final report of the Subcommittee on Risk Management* (PHS publication No. 342-322/60025) US Government Printing Office, Washington, DC.
2. Beazoglou T, Eklund S, Heffley D, Meiers J, Brown LJ, & Bailit H (2007) Economic impact of regulating the use of amalgam restorations *Public Health Reports* **122(5)** 657-663.
3. US Food and Drug Administration (2009) Department of Health and Human Services, 21 CFR Part 872 Docket No. FDA-2008-N-0163 Dental Devices: Classification of Dental Amalgam, Reclassification of Dental Mercury, Designation of Special Controls for Dental Amalgam, Mercury, and Amalgam Alloy; Final Rule. Federal Register Vol. 74, No. 148 August 2009. Retrieved online April 10, 2018 from: https://www.gpo.gov/fdsys/pkg/FR-2009-08-04/pdf/E9-18447.pdf
4. Mjör IA, Dahl JE, & Moorhead JE (2000) Age of restorations at replacement in permanent teeth in

general dental practice *Acta Odontologica Scandinavica* **58(3)** 97-101.

5. Forss H & Widström E (2001) From amalgam to composite: selection of restorative materials and restoration longevity in Finland *Acta Odontologica Scandinavica* **59(2)** 57-62.
6. Van Nieuwenhuysen JP, D'Hoore W, Carvalho J, & Qvist V (2003) Long-term evaluation of extensive restorations in permanent teeth *Journal of Dentistry* **31(6)** 395-405.
7. Forss H & Widström E (2004) Reasons for restorative therapy and the longevity of restorations in adults *Acta Odontologica Scandinavica* **62(2)** 82-86.
8. Opdam NJM, Bronkhorst EM, Loomans BAC, & Huysmans MCDNJM (2010) 12-year survival of composite vs amalgam restorations *Journal of Dental Research* **89(10)** 1063-1067.
9. Ratcliff S, Becker IM, & Quinn L (2001) Type and incidence of cracks in posterior teeth *Journal of Prosthetic Dentistry* **86(2)** 168-172.
10. Kahler B, Kotousov A, & Melkoumian N (2006) On material choice and fracture susceptibility of restored teeth: an asymptotic stress analysis approach *Dental Materials* **22(12)** 1109-1114.
11. Lubisich EB, Hilton TJ, & Ferracane J (2010) Cracked teeth: a review of the literature *Journal of Esthetic and Restorative Dentistry* **22(3)** 158-167.
12. Jensen SJ & Jörgensen KD (1985) Dimensional and phase changes of dental amalgams *Scandinavian Journal of Dental Research* **93(4)** 351-356.
13. Okabe T & Mitchell RJ (1996) Setting reactions in dental amalgam: part 2. The kinetics of amalgamation *Critical Reviews in Oral Biology and Medicine* **7(1)** 23-35.
14. Osborne JW (2006) Creep as a mechanism for sealing amalgams *Operative Dentistry* **31(2)** 161-164.
15. Craig RG & Powers JM (2002) *Restorative Dental Materials* Mosby, St. Louis MO.
16. Versluis A, Tantbirojn D, & Douglas WH (1997) Why do shear bond tests pull out dentin? *Journal of Dental Research* **76(6)** 1298-1307.
17. World Health Organization (2010) *Future Use of Materials for Dental Restoration: Report of the Meeting Convened at WHO HQ, Geneva, Switzerland 16th to 17th November 2009* WHO Document Production Services, Geneva, Switzerland. Retrieved online October 11, 2017 from: http://www.webcitation.org/6sxseUsC7
18. Udoye CI & Jafarzadeh H (2009) Cracked tooth syndrome: characteristics and distribution among adults in a Nigerian teaching hospital *Journal of Endodontics* **35(3)** 334-336.
19. Sheth JJ, Fuller JL, & Jensen ME (1988) Cuspal deformation and fracture resistance of teeth with dentin adhesives and composites *Journal of Prosthetic Dentistry* **60(5)** 560-569.
20. Paffenbarger GC, Rupp NW, & Patel PR (1979) Dimensional change of dental amalgam and a suggested correlation between marginal integrity and creep *Journal of the American Dental Association* **99(1)** 31-37.
21. Jokstad A (1991) Influence of cavity depth on marginal degradation of amalgam restorations *Acta Odontologica Scandinavica* **49(2)** 65-71.
22. Versluis A, Tantbirojn D, Lee MS, Tu LS, & DeLong R (2011) Can hygroscopic expansion compensate polymerization shrinkage? Part I: deformation of restored teeth *Dental Materials* **27(2)** 126-133.
23. Tantbirojn D, Pfeifer CS, Braga RR, & Versluis A (2011) Do low-shrink composites reduce polymerization shrinkage effects? *Journal of Dental Research* **90(5)** 596-601.
24. Suiter EA, Watson LE, Tantbirojn D, Lou JSB, & Versluis A (2016) Effective expansion: balance between shrinkage and hygroscopic expansion *Journal of Dental Research* **95(5)** 543-549.
25. Francis AV, Veríssimo C, Braxton AD, Tantbirojn D, Soares CJ, & Versluis A (2014) Cusp flexure caused by cavity preparation *Journal of Dental Research* **93(Special Issue B)** Abstract 949.
26. Osborne JW (1999) Expansion of contaminated amalgams assessed by photoelastic resin *Quintessence International* **30(10)** 673-681.
27. Paris P & Erdogan F (1963) A critical analysis of crack propagation laws *Journal of Basic Engineering* **85(4)** 528-533.
28. SDI (2011) *Pre-dosed Amalgam Capsules Permite, Lojic+ & GS-80; Instructions for Use* Retrieved online October 11, 2017 from: http://www.webcitation.org/6sxsXNlRR
29. Hansen EK & Asmussen E (1993) Cusp fracture of endodontically treated posterior teeth restored with amalgam: teeth restored in Denmark before 1975 versus after 1979 *Acta Odontologica Scandinavica* **51(2)** 73-77.
30. Yamada T & Fusayama T (1981) Effect of moisture contamination on high-copper amalgam *Journal of Dental Research* **60(3)** 716-723.
31. Versluis A & Tantbirojn D (2011) Filling cavities or restoring teeth? *Journal of the Tennessee Dental Association* **91(2)** 36-42.

©Operative Dentistry, 2018, **43-6,** E308-E316

Comparison of the Efficacy of Different Fluoride Varnishes on Dentin Remineralization During a Critical pH Exposure Using Quantitative X-Ray Microtomography

A Sleibi • A Tappuni • D Mills • GR Davis • A Baysan

Clinical Relevance

The application of dental varnish containing fluoride on demineralized dentin can remineralize and protect dentin lesions, but there might be no additional benefit to incorporating calcium and phosphate to enhance the remineralization of dentin caries.

SUMMARY

Objectives: The objective of this *in vitro* study was to quantify the amount of mineral change in demineralized dentin at pH 5.5 after the application of dental varnishes containing fluoride with casein phosphopeptide–amorphous calcium phosphate, fluoride and bioglass, or fluoride alone.

Methods and Materials: A total of 12 extracted human sound mandibular premolar root samples were coated with an acid-resistant varnish, leaving a 2 × 3 mm window at the outer root surface. These root specimens were then randomly divided into four groups and separately subjected to the demineralizing cycle at a pH of 4.8 for five days to create artificial caries-like lesions in dentin. Subsequently, each sample was imaged using quantitative x-ray microtomography (XMT) at a 15-µm voxel size. Each test group then received one of the following treatments: dental varnish contain-

*Ahmed Sleibi, School of Medicine and Dentistry, Queen Mary University of London, Oral Bioengineering, London, United Kingdom

Anwar Tappuni, School of Medicine and Dentistry, Queen Mary University of London, Oral Immunobiology and Regenerative Medicine, London, United Kingdom

David Mills, School of Medicine and Dentistry, Queen Mary University of London, Oral Bioengineering, London, United Kingdom

Graham Davis, School of Medicine and Dentistry, Queen Mary University of London, Oral Bioengineering, London, United Kingdom

Aylin Baysan, The Institute of Dentistry, Barts and the London, Queen Mary's School of Medicine and Dentistry, Centre of Oral Bioengineering, London, United Kingdom

*Corresponding author: Turner Street, London, E1 2AD, UK; e-mail: a.baysan@qmul.ac.uk

DOI: 10.2341/18-014-L

ing casein phosphopeptide–amorphous calcium phosphate and fluoride (CPP-ACP, MI varnish, GC Europe), bioglass and fluoride (BGA, Experimental, Dentsply Sirona), or fluoride alone (NUPRO, Dentsply Sirona), as well as a control group, which received no treatment. These samples were kept in deionized water for 12 hours. The thin layer of varnish was then removed. All samples including the nonvarnish group were subjected to the second demineralizing cycle at pH 5.5 for five days. The final XMT imaging was then carried out following the second demineralizing cycle. XMT scan was also carried out to varnish samples at 25 μm voxel size. The change in mineral concentration in the demineralized teeth was assessed using both qualitative and quantitative image analysis.

Results: There was an increase in radiopacity in the subtracted images of all varnish groups; a significant increase in mineral content, 12% for the CPP-ACP and fluoride ($p \leq 0.05$ and $p \leq 0.001$), 25% BGA ($p \leq 0.001$), and 104% fluoride alone varnish ($p \leq 0.001$). There was an increase in the size of radiolucency in the lesion area with a significant decrease in mineral content in the nonvarnish group, 10% ($p \leq 0.05$ and $p \leq 0.001$).

Conclusions: There was encouraging evidence of a remineralization effect following the application of dental varnish on dentin and also an observed resistance to demineralization during the acidic challenge in all cases. However, a dental varnish containing fluoride alone appeared to have a much greater effect on dentin remineralization when compared with CPP-ACP with fluoride and bioglass with fluoride.

INTRODUCTION

Remineralization is a continuous process of mineral exchange within the demineralized tooth structure. The newly formed crystals ($Ca_{10}(PO_4)_6F_2$) are comparatively more resistant to dissolution.[1] This could be seen in both enamel and dentin and achieved either as part of routine daily plaque control or through the application of various remineralization agents.[2] In this respect, there is considerable evidence supporting the use of fluoride-based treatments to remineralize tooth structure.[3,4] However, the effectiveness of fluoride alone (F) with an inadequate source of calcium (Ca^{+2}) and phosphorous (PO_4^{3-}) could be limited.[5-7]

It has been reported that providing both Ca^{+2} and PO_4^{-3} together with fluoride had a superior impact in preventing dentin caries when compared with F in populations with high caries risk.[8] In this respect, different formulations of calcium phosphate have been incorporated into fluoride products, including casein phosphopeptide–amorphous calcium phosphate (CPP-ACP) and bioglass (calcium sodium phosphosilicate).[5,9] These formulations were recently introduced as part of fluoride varnish where there is a chance to act as slow-release fluoride reservoirs due to adherence to the tooth surface for longer periods of time.[10] A recent *in vitro* study reported a significant remineralization effect using fluoride with CPP-ACP on caries-like lesions in bovine dentin that received no toothbrushing in comparison with a dental varnish containing F.[11]

Despite the promising results from several studies, there was a low level of evidence to suggest either CPP-ACP or bioglass plus fluoride formulation to enhance the remineralizaton on dentin lesions.[12-15] In addition, none of the conducted studies compared these formulations in more challenging conditions, such as a constant demineralizing cycle at pH 5.5. This could be valid for individuals who have an impairment in the salivary function, where saliva is unable to maintain the natural pH during an acidic challenge, or for those with a resting pH of 5.5 combined with a high-caries risk.[16] In addition, the significant drop in salivary pH is more likely to be seen in individuals with excessive sugar and fermentable carbohydrate intake who are metabolized by micro-organisms to produce acids.[17] Therefore, the aim of this study was to compare the mineral deposition of different dental varnishes containing CPP-ACP with fluoride, bioglass with fluoride, and F on dentin-like lesions at a critical pH using quantitative x-ray microtomography (XMT).

METHODS AND MATERIALS

Twelve human sound mandibular premolars that were extracted for orthodontic purposes were collected, cleaned, and polished using nonfluoridated pumice and a slow handpiece. The teeth were then stored in 1% thymol prior to sample preparation.

Preparation of Demineralized Solution

The demineralization buffer solution was prepared using 0.2205 g/L $CaCl_2 \cdot 2H_2O$, 0.1225 g/L KH_2PO_4, and 50 mmol/L acetic acid. The pH was adjusted to 4.8 using 0.05 g/L KOH for the first demineralization cycle, to create artificial-like caries in dentin.[18] An Oakton pH meter (Oakton Instruments, Nijkerk, the Netherlands) was used to measure the pH of the

Table 1: *Dental Varnish Used for the Study*

Group	Varnish Name Company	Active Ingredients	Other Ingredients
CPP-ACP	MI varnish GC, Japan	5% NaF and CPP-ACP	Polyvinyl acetate, hydrogenated rosin, ethanol, silicon dioxide
BGA	Experimental Dentsply Sirona, USA	5% NaF and bioglass	Urethane methacrylate, hydrogenated rosin, resin, alcohol, sodium, sucralose, flavor, titanium dioxide
F	NUPRO White Dentsply Sirona, USA	5% NaF	Urethane methacrylate, hydrogenated rosin, resin, alcohol, sodium, sucralose, flavor, titanium dioxide
NC	Negative control non-varnish	—	—

demineralized solution. All chemical reagents were obtained from Sigma-Aldrich (Gillingham, Dorset, UK). The same buffer solution with pH 5.5 was prepared to immerse the specimens following dental varnish application.

Preparation of Artificial Caries-like Lesions

The crowns of collected teeth were removed 1 mm below the cemento-enamel junction using a 0.3-mm-thick diamond disc under running water at 3000 rpm speed (Struers, Copenhagen, Denmark). Adhesive tapes of 2 × 3 mm were placed coronally 2 mm beyond the cutting side of the root samples, and then an acid-resistant varnish (Revlon, New York, NY, USA) was applied. A dentin window of 2 × 3 mm was then exposed by removing the piece of tape on each sample. These allocated areas represented the lesion sites. The root specimens were separately immersed in 10 mL of demineralizing solution at pH 4.8 and then kept in a shaker incubator for five days at 37°C to simulate body temperature.[18,19] The solution was replaced every 24 hours to keep the demineralization process under fresh solution.[20]

XMT Baseline Scan

Following the first demineralization cycle, each root specimen was washed thoroughly with deionized water and placed vertically inside a clear plastic tube (Sterilin, Newport, UK) and held with soft wax (6969 from Poth Hille & Co Ltd, Rainham, Essex, UK) to prevent any possible movement. The tube was then filled with deionized water to keep the samples hydrated during the scanning procedure. Subsequently, each prepared sample was placed on a movable kinematic stage, ensuring the long axis of the tooth was parallel to the XMT rotational axis. The XMT scanner was set to produce a 15 μm voxel size reconstruction, and the x-ray generator was set to 90 kV and 180 μA. Each XMT scan took around seven hours to complete.[20] A calibration carousel was repeatedly scanned at the end of each tomography scan.[21,22] The baseline XMT scan was subsequently carried out following the first demineralizing cycle at pH 4.8 and before the application of dental varnish.

Dental Varnish Application

Following the baseline scan, the root specimens were randomly divided into four groups (three samples each) to receive one of the allocated treatments (Table 1). The specimens were dried using a three-in-one dental syringe. A thin and uniform layer of dental varnish was applied to each specimen covering the 2 × 3 mm exposed window. The specimens were then kept separately in deionized water (10 mL) and placed in a shaker incubator at 37°C for 12 hours. The thin layer of varnish was then carefully removed using a scalpel blade (Swann-Morton, Sheffield, UK),[23] and each area was visually inspected using a 4× magnification lens to confirm the removal of all varnish remnants.

Second Demineralizing Cycle and the Final XMT Scan

All root specimens, including the nonvarnish group, were subjected to the second demineralizing cycle at pH 5.5 for five days. The specimens were then placed in a shaker incubator in 10 mL of demineralizing solution at 37°C. This solution was changed every 24 hours to keep the lesion area in contact with the fresh demineralizing solution.[20] All root specimens, including the nonvarnish group, were then prepared for the final XMT scan using the same settings as in the baseline scans.

Image Analysis

The obtained 2D images (>1000 projections) from the XMT scan were corrected for beam hardening,[4] and reconstructed to create the three-dimensional (3D) image. The 3D image from the baseline scan of each sample was aligned with the 3D image from the final scan using the in-house–developed alignment software running under International Date Line (IDL, Exelis Visual Information Solutions, Boulder,

Colorado, USA) The initial 3D image was then subtracted from the final 3D image using in-house–developed IDL software. The volumetric subtraction was carried out to detect the mineral gain/loss as visually detected as an increase in the radiopacity/radiolucency in the demineralized area. To quantify mineral change in the demineralized area, the average linear attenuation coefficient (LAC) from a total of 15 points from the baseline scans that were randomly selected from the demineralized area was compared with the corresponding average of 15 points from the final scan. These points were chosen in five slices, with three points in each, and subsequent analyses were carried out separately for each sample.

The obtained LAC value of each point was converted to mineral concentration (g cm^{-3}) using the following equation[15]:

$$c = \frac{\mu - \mu_o}{\mu_m - \mu_o}\rho_m$$

where μ is the measured LAC, μ_o is the LAC of the deionized water and plastic that assumed soft tissue (0.268 cm^{-1}), μ_m is the pure sample material LAC that presumed a pure hydroxyapatite (3.12 cm^{-1}), and P_m is the concentration of the pure hydroxyapatite (3.16 cm^{-3}).

XMT Scan for the Test Varnishes

The contents of each varnish were mixed and placed into small centrifuge tubes and positioned on a movable kinematic stage with the long axis of the tube parallel to the XMT rotational axis. The x-ray generator was set at 90 kV and 180 μA, and to produce 25-μm voxel resolution using the high-definition XMT scanner, each scan took about 60 min.

Power Calculation

Sample size calculation was based on the data from a previous study, where the mean difference between baseline and final scans was 0.32 and the standard deviation of the differences was 0.02.[15] The statistical power was set to 80% at a level of significance of 0.05 (two sided).

Statistical Analysis

One-way analysis of variance (ANOVA) was performed to find the differences in mineral change between the groups. Paired *t*-test was used to analyze the mineral change following the application of varnish for each sample by comparing the 15 points between baseline and final scans. The mean percentages in mineral change of each group were then calculated. Data analysis was performed using IBM SPSS Statistics 24.0 (SPSS Inc, Chicago, IL, USA).

RESULTS

Qualitative Assessment of Mineral Change

The subtracted images of the root specimens that received dental varnishes showed an increase in the radiopacity in the demineralized area, whereas there was an increase in the radiolucency for the negative group (Figure 1).

Quantitative Mineral Concentration Change

One-way ANOVA showed that there was a significant difference between the test groups ($p<0.001$). Paired *t*-test revealed a significant increase in mineral content in all samples for the varnish groups. The mean percentage of mineral gain was higher in samples treated with the dental varnish containing F 104% ($p\leq0.001$) then bioglass and fluoride (BGA) with fluoride 25% ($p\leq0.001$) and finally CPP-ACP with fluoride 12% ($p\leq0.05$ and $p\leq0.001$). There was a significant decrease of 10% ($p\leq0.05$ and $p\leq0.001$) in mineral content for the nonvarnish samples (Table 2).

XMT Scans for Dental Varnishes

The XMT scans of the dental varnish containing CPP-ACP and fluoride showed a homogenous mixture of fine particles with a density of approximately 0.2 to 0.3 LAC. However, the BGA varnish had a non-homogenous mixture and more defined particles that settled on the base of the tube, with a higher density (0.4-0.8 LAC) when compared with the former varnish. The images of the varnish containing F were less homogenous with more defined particles when compared with images of the CPP-ACP varnish. However, the density of the F varnish was higher than the CPP-ACP formulation and lower than the BGA varnish (0.3-0.5 LAC). Most of the defined particles of the dental varnish in the F group accumulated in the apical half of the tube.

DISCUSSION

The results of this laboratory-based study showed that dental varnish containing F had a superior remineralization effect on dentin when compared with other varnishes formulated with either CPP-ACP and fluoride or BGA. A constant demineralizing model at pH 5.5 was carried out instead of

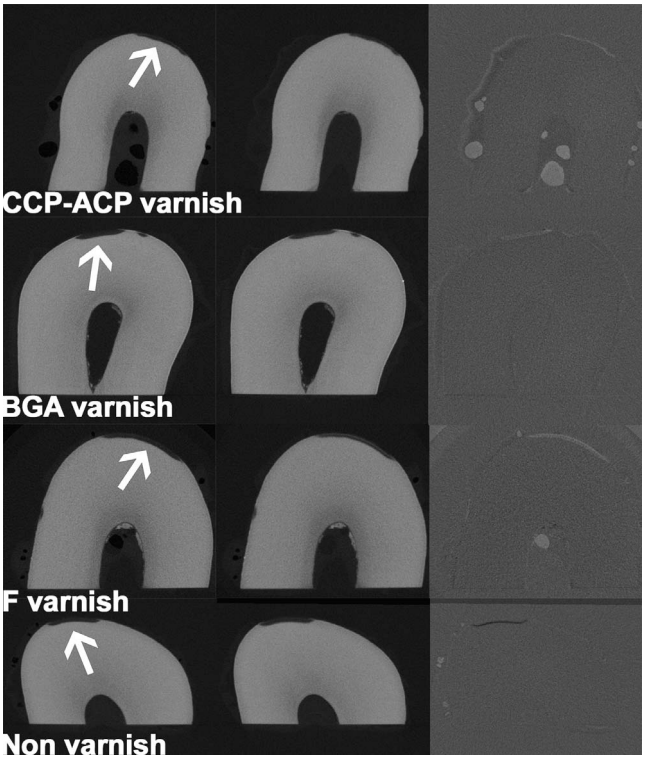

Figure 1. *The baseline XMT scan (left), final XMT scan (middle), and subtracted image (right) of the test groups. The contrast of the subtracted images had been increased by a factor of 8 to show subtle differences in mineral concentration. The arrow refers to the lesion area. The radiopaque area demonstrated an increase in the mineral contents of all varnish samples, whereas the radiolucency in the nonvarnish sample revealed more mineral loss following the second demineralization cycle (bubbles presented in only one image showed as the differences in the content between air and water).*

demineralization/remineralization cycling. The reason for this was to simulate an extreme clinical condition, such as those with a critical saliva pH and exposed dentin surfaces, where there is a risk of mineral loss,[16,17] and thus a periodic application of fluoride varnish is recommended.[2]

In this study, the varnishes were removed after 12 hours to emphasize the chemical effect rather than the mechanical effect and also to simulate the clinical situation in which dental varnish could be retained on the tooth surface prior to removal from regular toothbrushing and mastication.[25-27] In previous studies, it is noted that dental varnishes containing fluoride were removed from the test specimens within a period ranging from 6 to 24 hours following the application.[13,28-30]

The superior remineralization effect of the varnish containing F in comparison to calcium phosphate varnishes could be related to the ability of the latter varnishes to release inorganic phosphorous in addition to calcium and fluoride, thereby decreasing the bioavailability of fluoride ions through the formation of a lower-soluble fluorapatite rather than loosely bonded CaF^+ and CaF_2 in the immersion solution.[13,31,32] In addition, it can be speculated that both dental varnishes (CPP-ACP and BGA) with calcium and phosphate had the ability to form hydroxyapatite crystals on the lesion surface that could restrict infiltration and deposition of fluoride ions in the demineralized region in comparison with the varnish containing F.

The lowest mineral deposition for the varnishes containing CPP-ACP and fluoride could be related to the higher ability of the CPP-ACP compound to dissolve in the aqueous solution.[33] This might assist in releasing calcium, phosphate, and fluoride ions into the aqueous solution rather than retaining them in the demineralized area. This explanation was supported by Sleibi and others, who confirmed that the highest fluoride, calcium, and phosphate ion release was seen in the varnish containing CPP-ACP formulation with fluoride compared with the varnish with BGA.[34] In addition, the varnish containing F showed the lowest fluoride ion release.[34] These results were also consistent with the findings of previous studies that the dental varnish with fluoride and CPP-ACP had the highest calcium and fluoride ion release in comparison with the varnishes with different calcium phosphate formulations.[32,35]

Similarly, bioglass facilitates rapid ionic exchange of sodium ions with hydrogen cations in the aqueous solution, allowing discharge of calcium and phosphate ions from the glass to the immersion solution.[36] Although bioglass has the ability to retract free ions, the time required for completion might be insufficient for this process, since the immersion solution was constantly changed. Therefore, this process possibly then led to disposal of these free ions. In this respect, it can be speculated that the experimental BGA varnish released more ions and had a minimum capability to retain them in the lesion area in comparison to the varnish with F. This explanation, however, should be interpreted with caution, as the samples were immersed in deionized water and then subjected to a constant demineralizing solution that would not simulate natural saliva with regard to compositions and physical properties.

The mineral gain was higher with the BGA varnish when compared with the CPP-ACP technology. This might again be due to the presence of silanols in the BGA structure that remain attached to the tooth structure following release of ions from the BGA. Subsequently, this process would act as a

Table 2: *Mean Mineral Concentrations (g cm^{-3}) at Baseline and Final XMT Scans With Standard Deviations (SD), Mean Differences in Mineral Content,* p-*Value of the Mean Differences for Each Sample, and the Overall Change in the Mean Percentage of Mineral Gain/Loss for Each Test Group*

Varnish Group	Sample	Baseline Scan Mean ±SD	Final Scan Mean ±(SD)	Mean Difference	*p*-Value	Overall Change in Percentage
CPP-ACP	1	0.22 ± 0.08	0.24 ± 0.1	0.02	0.05*	12% increase
	2	0.22 ± 0.05	0.25 ± 0.06	0.03	<0.001**	
	3	0.23 ± 0.02	0.26 ± 0.02	0.03	<0.001**	
BGA	1	0.26 ± 0.04	0.32 ± 0.06	0.07	<0.001**	25% increase
	2	0.2 ± 0.02	0.25 ± 0.04	0.05	<0.001**	
	3	0.23 ± 0.03	0.28 ± 0.07	0.06	<0.001**	
F alone	1	0.25 ± 0.03	0.47 ± 0.05	0.22	<0.001**	104% increase
	2	0.19 ± 0.01	0.45 ± 0.03	0.26	<0.001**	
	3	0.26 ± 0.02	0.49 ± 0.03	0.23	<0.001**	
NC	1	0.36 ± 0.02	0.33 ± 0.02	−0.03	<0.001**	10% decrease
	2	0.33 ± 0.07	0.3 ± 0.03	−0.03	0.03*	
	3	0.2 ± 0.06	0.17 ± 0.04	−0.02	0.01*	

Abbreviations: CPP-ACP, casein phosphopeptideã amorphous calcium phosphate; BGA, Bioglass experimental varnish; F, Fluoride; NC, Negative control (non varnish).
** Significant at* p≤*0.05; ** Highly significant at* p≤*0.001.*

nucleation site on the tooth surface to retract calcium and phosphorous, forming a calcium-phosphate–rich layer that can resist an acidic environment.[37,38] In a previous study, BGA had more favorable remineralization potential than CPP-ACP on the enamel structure. Mehta and others suggested that CPP-ACP failed to be retained for a longer period on the tooth structure, due to its amorphous nature, such that it was unlikely to adhere to the tooth surface when compared with the firmly attached bioglass particles.[39] The superior mineral gain for the BGA formula over CPP-ACP was consistent with the findings of a recent study in which natural dentin caries specimens were assessed under a constant remineralizing condition.[15] Those authors proposed that BGA plus F had a higher remineralization efficacy than the CPP-ACP with F formula not only in the net-demineralizing but also in the net-remineralizing condition.

Regarding the CPP-ACP plus F, the findings of the present study were consistent with the results of Mohd Said and others, who reported that the F had a significant remineralization effect on CPP-ACP with fluoride varnishes on enamel caries.[13] Thereby, within the limitations of this study, it could be assumed that CPP-ACP failed to enhance the remineralization effect of fluoride. However, these results were in contrast to the findings of Shen and others,[35] who reported that CPP-ACP varnish had a superior effect on the F varnish in protecting against enamel demineralization. This could well be due to the fact that the dental varnish in the later study was applied to the area adjacent to the demineralized area, whereas in this study, it was applied directly onto the lesion. It can be speculated that it is better to manage the already formed demineralized lesions with the application of a dental varnish containing F, rather than calcium phosphate–containing fluoride varnishes, considering that the application of the F varnish is in contact with the lesion surface. The superior remineralization effect of the F compared with the CPP-ACP formula was also inconsistent with the findings of Wierichs and others and Pithon and others.[11,40] There was a significant mineral gain observed for the CPP-ACP plus fluoride varnish compared with F on artificial-like enamel and dentin caries.[11,40] However, in these previous studies, the varnishes were not removed from the samples, which might have led to an additional remineralization effect as well as a mechanical effect from the extended retention period.

The decrease in mineral concentration in the lesion area of the nonvarnish samples (negative control) following the second demineralization cycle that was also identified as an increase in the radiolucency in the subtracted image (Figure 1) confirmed the considerable effect of the fluoride varnish application, not only to remineralize dentin but also to prevent these dentin lesions from further demineralization. These results were in agreement with the finding of an *in situ* study by Zaura-Arite and ten Cate, in which the application of a placebo

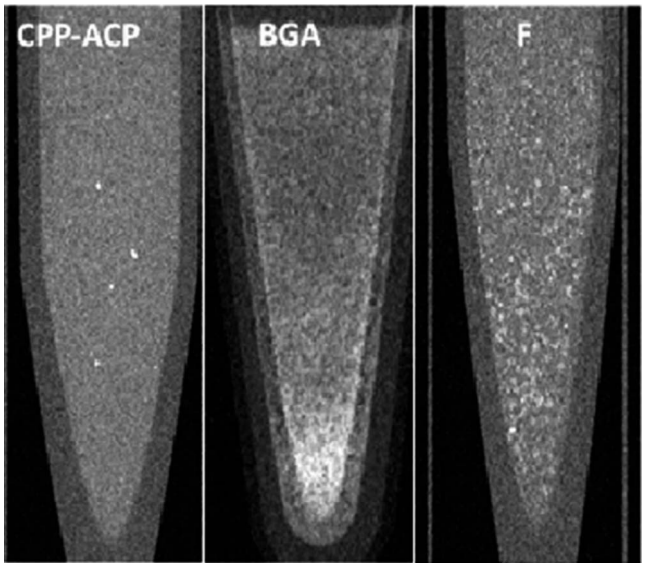

Figure 2. *XMT images of each dental varnish. CPP-ACP = casein phosphopeptide–amorphous calcium phosphate; BGA = Bioglass experimental varnish; F = Fluoride.*

varnish did not inhibit mineral loss in dentin samples compared with fluoride varnish.[41]

Nevertheless, the variances in the physical properties and chemical composition, including the presence of artificial resin in the composition of both BGA and F varnishes, could be the cause of these differences in mineral precipitation.[42-44] In this study, the XMT image of varnish liquid with CPP-ACP showed the most homogenous and small-size particles that could easily be detached from the immersion solution, whereas the large particles of both BGA and F varnishes might assist the ions to be settled (attached) on the tooth structure following the application. This probably led to a decrease in ion detachments of both BGA and F varnishes. The above explanation can be clearly seen in Figure 2, where large defined particles were mostly accumulated on the base and middle half of the bottle in both BGA and F varnishes, whereas there was a homogenous mixture for the CPP-ACP varnish. This explanation could also be applicable in a worse scenario in which the large particles represented the inactive ingredients only. This was due to the possible entrapment of small active particles (ions) underneath the large particles, restricting their release in the aqueous solution.

The small sample size could be a limitation of this study; however, the XMT scanner combined both improved accuracy and contrast sensitivity, and with its noninvasive nature, this scanner enables precise analysis of mineral gain/loss.[21] Each sample was also evaluated and statistically analyzed through comparing 15 different points from the baseline and from the final scans that had the same 3D positions. Each sample took about 14 hours to complete for baseline and finals scans (in total: 28 hours). In addition, the samples were assessed using both qualitative and quantitative measurements with consistent results, which supported these findings. The power calculation was carried out by considering a previous study as a reference, which employed the XMT technique.[15]

CONCLUSIONS

Within the limitation of this study, there was encouraging evidence of a remineralization effect with dental varnish containing fluoride on dentin in all cases, and the ability of this varnish to resist demineralization during the acidic conditions was evident in this laboratory setting. However, a dental varnish containing F seemed to be promising when compared with the dental varnish containing fluoride either with bioglass or CPP-ACP. Without the application of dental varnish containing fluoride, there was a risk of potential mineral loss. Further studies are required to confirm whether these results could be replicated in a clinical situation, particularly for those who are at high risk for caries initiation.

Acknowledgements

This work was financially supported by the Ministry of Higher Education in Iraq as a part of a PhD project. The dental companies GC (Japan) and Dentsply Sirona (USA) are appreciatively acknowledged for providing the materials for this study.

Regulatory Statement

This study was conducted in accordance with all the provisions of the local human subjects oversight committee guidelines and policies of the Research Ethics Committees Northern Ireland. The approval code for this study is ORECNI, 16/NI/0101.

Conflict of Interest

The authors declare no potential conflicts of interest with respect to publication of this article.

(Accepted 30 May 2018)

REFERENCES

1. Cochrane NJ, Cai F, Huq NL, Burrow MF, & Reynolds EC (2010) New approaches to enhanced remineralization of tooth enamel *Journal of Dental Research* **89(11)** 87-97.
2. Longbottom C, Ekstrand K, & Zero D (2009) Traditional preventive treatment options In: Pitts NB (ed) *Detection, Assessment, Diagnosis and Monitoring of Caries. Mono-*

graphs in Oral Science 21 Karger, Basel, Switzerland 149-155.

3. Amaechi BT & van Loveren C (2013) Fluorides and non-fluoride remineralization systems *Monographs in Oral Science* **23** 15-26.
4. Fontana M (2016) Enhancing fluoride: clinical human studies of alternatives or boosters for caries management *Caries Research* **50(Supplement 1)** 22-37.
5. Reynolds EC (2009) Casein phosphopeptide-amorphous calcium phosphate: the scientific evidence *Advances in Dental Research* **21(1)** 25-29.
6. Gao SS, Zhang S, Mei ML, Lo EC, & Chu CH (2016) Caries remineralisation and arresting effect in children by professionally applied fluoride treatment—a systematic review *BMC Oral Health* **16(1)** 12.
7. Vogel GL (2011) Oral fluoride reservoirs and the prevention of dental caries *Monographs in Oral Science* **22** 146-157.
8. Papas A, Russell D, Singh M, Stack K, Kent R, Triol C, & Winston A (1999) Double blind clinical trial of a remineralizing dentifrice in the prevention of caries in a radiation therapy population *Gerodontology* **16(1)** 2-10.
9. Burwell AK, Litkowski LJ, & Greenspan DC (2009) Calcium sodium phosphosilicate (novamin): remineralization potential *Advances in Dental Research* **21(1)** 35-39.
10. Øgaard B, Seppa L, & Rölla G (1994) Professional topical fluoride applications-clinical efficacy and mechanism of action *Advances in Dental Research* **8(2)** 190-201.
11. Wierichs RJ, Stausberg S, Lausch J, Meyer-Lueckel H, & Esteves-Oliveira M (2018) Caries-preventive effect of NaF, NaF+TCP, NaF+CPP-ACP and SDF varnishes on sound dentin and artificial dentin caries *in vitro Caries Research* **52(3)** 199-211.
12. Li J, Xie X, Wang Y, Yin W, Antoun JS, Farella M, & Mei L (2014) Long-term remineralizing effect of casein phosphopeptide-amorphous calcium phosphate (CPP-ACP) on early caries lesions *in vivo*: a systematic review *Journal of Dentistry* **42(7)** 69-77.
13. Mohd Said SN, Ekambaram M, & Yiu CK (2017) Effect of different fluoride varnishes on remineralization of artificial enamel carious lesions *International Journal of Paediatric Dentistry* **27(3)** 163-173.
14. Fernando D, Attik N, Pradelle-Plasse N, Jackson P, Grosgogeat B, & Colon P (2017) Bioactive glass for dentin remineralization: a systematic review *Materials Science and Engineering: C* **76** 1369-1377.
15. Sleibi A, Tappuni AR, Davis GR, Anderson P, & Baysan A (2018) Comparison of efficacy of dental varnish containing fluoride either with CPP-ACP or bioglass on root caries: ex vivo study *Journal of Dentistry* **73** 91-96.
16. Hicks J, Garcia-Godoy F, & Flaitz C (2004) Biological factors in dental caries: role of saliva and dental plaque in the dynamic process of demineralization and remineralization (part 1) *Journal of Clinical Pediatric Dentistry* **28(1)** 47-52.
17. Touger-Decker R, & van Loveren C (2003) Sugars and dental caries *American Journal of Clinical Nutrition* **78(4)** S881-S892.
18. Ten Cate J (2008) Remineralization of deep enamel dentine caries lesions *Australian Dental Journal* **53(3)** 281-285.
19. Qi YP, Li N, Niu LN, Primus CM, Ling JQ, Pashley DH, & Tay FR (2012) Remineralization of artificial dentinal caries lesions by biomimetically modified mineral trioxide aggregate *Acta Biomaterialia* **8(2)** 836-842.
20. Zhi Q, Lo E, & Kwok A (2013) An *in vitro* study of silver and fluoride ions on remineralization of demineralized enamel and dentine *Australian Dental Journal* **58(1)** 50-56.
21. Davis GR, Evershed AN, & Mills D (2013) Quantitative high contrast x-ray microtomography for dental research *Journal of Dentistry* **41(5)** 475-482.
22. Evershed A, Mills D, & Davis G (2012) Multi-species beam hardening calibration device for X-ray microtomography *Proceedings of the SPIE Digital Library* **Viii** 85061N–85061N-2012. https://www.spiedigitallibrary.org/conference-proceedings-of-SPIE/8506.toc?SSO=1
23. Kato MT, Italiani FM, Araújo JJ, Garcia MD, Carvalho Sales-Peres SH, & Buzalaf MAR (2009) Preventive effect of an iron varnish on bovine enamel erosion *in vitro Journal of Dentistry* **37(3)** 233-236.
24. Davis GR & Mills D (2016) 2D beam hardening correction for micro-CT of immersed hard tissue *Proceedings of SPIE Digital Library* **9967**, 996707.
25. Sorvari R, Meurman JH, Alakuijala P, & Frank RM (1994) Effect of fluoride varnish and solution on enamel erosion *in vitro Caries Research* **28(2)** 27-32.
26. Beltrán-Aguilar ED & Goldstein JW (2000) The fluoride varnish: a review of their clinical use, cariostatic mechanism, efficacy and safety scientific evidence *Advances in Dental Research* **21(1)** 25-29.
27. Vivaldi-Rodrigues G, Demito CF, Bowman SJ, & Ramos AL (2006) The effectiveness of a fluoride varnish in preventing the development of white spot lesions *World Journal of Orthodontics* **7(2)** 138-144.
28. Delbem AC, Bergamaschi M, Sassaki KT, & Cunha RF (2006) Effect of fluoridated varnish and silver diamine fluoride solution on enamel demineralization: pH-cycling study *Journal of Applied Oral Science* **14(2)** 88-92.
29. Souza JG, Rochel ID, Pereira AF, Silva TC, Rios D, Machado MA, Buzalaf MA, & Magalhes AC (2010) Effects of experimental xylitol varnishes and solutions on bovine enamel erosion *in vitro Journal of Oral Science* **52(4)** 553-559.
30. Tuloglu N, Bayrak S, Tunc ES, & Ozer F (2016) Effect of fluoride varnish with added casein phosphopeptide-amorphous calcium phosphate on the acid resistance of the primary enamel *BMC Oral Health* **16** 103.
31. Christoffersen J, Christoffersen MR, Kibalczyc W, & Perdok W (1988) Kinetics of dissolution and growth of calcium fluoride and effects of phosphate *Acta Odontologica Scandinavica* **46(6**) 325-336.
32. Cochrane N, Shen P, Yuan Y, & Reynolds E (2014) Ion release from calcium and fluoride containing dental varnishes *Australian Dental Journal* **59(1)** 100-105.

33. Cochrane NJ & Reynolds EC (2009) Casein phosphopeptides in oral health In: Wilson M (ed) *Food Constituents and Oral Health: Current status and Future Prospects* Woodhead, Cambridge, UK.

34. Sleibi A, Tappuni A, Karpukhina N, Hill R, & Baysan A (2018) A comparative evaluation of ion release characteristics of three different fluoride containing dental varnishes *Caries Research* **52(ORCA 65 Abstract)** 468-547, www.karger.com/doi/10.1159/000488302.

35. Shen P, Bagheri R, Walker GD, Yuan Y, Stanton DP, Reynolds C, & Reynolds EC (2016) Effect of calcium phosphate addition to fluoride containing dental varnishes on enamel demineralization *Australian Dental Journal* **61(3)** 357-365.

36. Burwell A, Jennings D, & Greenspan DC (2010) Novamin and dentin hypersensitivity *in vitro* evidence of efficacy *Journal of Clinical Dentistry* **21(3)** 66-71.

37. Hench LL (1991) Bioceramics: from concept to clinic *Journal of the American Ceramic Society* **74(7)** 1487-1510.

38. Gjorgievska E & Nicholson J (2009) A preliminary study of enamel remineralization by dentifrices based on recalden (CPP-ACP) and novamin (calcium-sodium-phosphosilicate) *Acta Odontologica Latino Americana* **23(3)** 234-239.

39. Mehta AB, Veena Kumari RJ, & Izadikhah V (2014) Remineralization potential of bioactive glass and casein phosphopeptide-amorphous calcium phosphate on initial carious lesion: an *in-vitro* pH-cycling study *Journal of Conservative Dentistry* **17(1)** 3-7.

40. Pithon MM, Dos Santos MJ, Andrade CS, Leão Filho JC, Braz AK, de Araujo RE, Tanaka OM, Fidalgo TK, Dos Santos AM, & Maia LC (2015) Effectiveness of varnish with CPP-ACP in prevention of caries lesions around orthodontic brackets: an OCT evaluation *European Journal of Orthodontics* **37(2)** 177-182.

41. Zaura-Arite E & Ten Cate JM (2000) Effects of fluoride- and chlorhexidine-containing varnishes on plaque composition and on demineralization of dentinal grooves *in situ European Journal of Oral Science* **108(2)** 154-161.

42. Castillo JL, Milgrom P, Kharasch E, Izutsu K, & Fey M (2001) Evaluation of fluoride release from commercially available fluoride varnishes *Journal of the American Dental Association* **132(10)** 1389-1392.

43. Delbem ACB, Brighenti FL, Oliveira FAL, Pessan JP, Buzalaf MAR, & Sassaki KT (2009) *In vitro* assessment of an experimental coat applied over fluoride varnishes *Journal of Applied Oral Science* **17(4)** 280-283.

44. Shen C & Autio-gold J (2002) Assessing fluoride concentration uniformity and fluoride release from three varnishes *Journal of the American Dental Association* **133(2)** 176-182.

Founders' Fund

Academy of Operative Dentistry

The Founders' Fund was established in 1986 by the Executive Council of the Academy of Operative Dentistry in honor of the six founding members of the Academy, Drs. José E. Medina, Charles F. Bouschor, Floyd E. Hamstrom, Carl J. Monacelli, James P. Vernetti, and Ralph J. Werner.

PURPOSE OF THE FUND

This Fund has been established exclusively to enhance the art and science of Operative Dentistry by providing financial support to programs including, but not limited to, the following:

- Scientific Dental Research
- Dental Educational Programs
- Support of the Academy to encourage, define and enlarge the role of Operative Dentistry in teaching institutions, private practice and the armed forces.
- Provide aid, encouragement and assistance to graduate dentists, graduate and postdoctoral dental students and pre-dental students.

FUND MEMBERSHIP

Any member of the Academy in good standing is a member of the Fund. The Board of Trustees, elected by the members of the Academy, is actively soliciting funds to build the principal amount. This sum will produce interest to be used to support the purposes of the Fund.

WAYS TO CONTRIBUTE

You may make annual cash donations at any time. Many gifts of cash are made to honor, or in memory of friends or loved ones. Other gifts may be made as wills and bequests, gifts of property, life insurance proceeds or trusts. Please tear/cut and send the attached form with your TAX DEDUCTIBLE contribution.

We thank you for your contribution to the Founders' Fund. Contributions such as yours will enable the ideals of your academy to be sustained through a wide variety of programs and people continuing their quest for the highest quality of dental care possible.

IN HONOR OF:

I/We would like to make a contribution of
$ _____ to the FOUNDERS' FUND
in honor of:
Name: _____
Address: _____
_____
My/Our Name: _____
Address: _____
_____

IN MEMORY OF:

I/We would like to make a contribution of
$ _____ to the FOUNDERS' FUND
in memory of:
Name: _____
Address: _____
_____
My/Our Name: _____
Address: _____
_____

Credit Card# _____
Expiration Date. _____ Code: _____

All checks should be made payable to The Academy of Operative Dentistry All proceeds go to the Founders' Fund.

Please send contributions to:
Dr. Richard G. Stevenson III
P.O. Box 25637
Los Angeles, CA 90025

OPERATIVE DENTISTRY

CORPORATE SPONSORS

These Dental Manufacturers have joined Operative Dentistry in our commitment to publish quality dental literature in a timely manner. We thank them for their support.

OPERATIVE DENTISTRY

Volume 43 / Number 6
November/December 2018

www.jopdent.org
563–676

Reviewer Recognition

Clinical Technique/Case Report

Clinical Research

Laboratory Research

Departments

Online Only Articles